Synthesis and Characterisation of Branched Poly(ethylene terephthalate)s

by

ALAN FINLAY NEILSON

A thesis submitted to the Department of Pure and Applied Chemistry, University of Strathclyde, in accordance with the requirements for the degree of Doctor of Philosophy.

December 1999

Abstract

This report details the work carried out on the synthesis and characterisation of branched polyesters. The experimental effort concentrated on the branching of PET-type polymers with a variety of potential branching agents, such as trimesic acid, and the control of branching with end-capping agents, such as benzyl alcohol. The polymers synthesised were then characterised by solution viscosity, end-group analysis, DSC analysis, rheological analysis and light scattering.

Extensive branching of polymers has been observed and controlled *via* end-capping agents. One group of polyesters synthesised with increasing levels of brancher, were characterised by absolute $\overline{M}_w$ values which increased from ~10K to ~350K. Despite this, all of the macromolecules displayed roughly the same solution viscosity. Though the corresponding melt viscosity increased with $\overline{M}_w$, the values achieved were far below those expected for analogous linear polymers of comparable $\overline{M}_w$.

A second group of polyesters synthesised with a fixed level of brancher and increasing levels of end-capper were characterised by a much narrower range of $\overline{M}_w$ values. These polymers however had melt viscosities lower than those of linear polymers yet had $\overline{M}_w$'s of between ~3 and ~ 15 times greater than those of linear polymers.

Acknowledgements

Firstly, I would like to thank Professor D. C. Sherrington for his helpfulness, kindness, generosity, and support during my *Ph.D.*

I would also like to thank Andy for allowing me to "borrow" his technical knowledge from time to time, and the rest of C405 for putting up with my many failings. In particular I would like to thank Michael and Robert for being on hand for beers (or is it the other way round) when required.

Special thanks to Professor R.W. Richards and the rest of the members of the IRC in Polymer Science and Technology at the University of Durham, for their assistance and the use of their light scattering equipment. Thanks to Professor J. Ferguson and Dr. N. Hudson for all their help, and the use of their melt viscometer. Thanks also to Dr. P.J. Hall for the use of his DSC apparatus.

Finally, I would like to thank Dr. W.A. Macdonald and ICI (now Du Pont) Polyester for their help and financial support throughout this project.

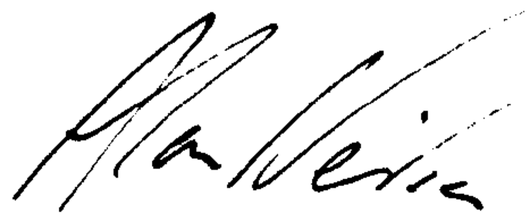

Alan Neilson

List of Abbreviations

2,6 PDCA	2,6-pyridine dicarboxylic acid
4-SPA	4-sulfophthalic acid
5-SIPA	5-sulfoisophthalic acid
9-Anth	9-anthracenemethanol
ADC	analogue / digital converter
B3CA	benzene tricarboxylic acid
B4CA	benzene tetracarboxylic acid
BHET	bis-2-hydroxyethyl terephthalate
BnOH	benzyl alcohol
bs	broad singlet
BTCTC	benzene tricarbonyl trichloride
BzCOOH	benzoic acid
d	doublet
DCA	dichloroacetic acid
DCB	dichlorobenzene
DCM	dichloromethane
DEG	diethylene glycol
DMF	dimethyl formamide
DMS	dynamic mechanical spectroscopy
DMSO	dimethylsulfoxide
DMT	dimethyl terephthalate
DMTA	dynamic mechanical thermal analysis
EG	ethylene glycol
End	End-group Analysis
FTIR	Fourier transform infrared
GPC	gel permeation chromatography
HFIP	1,1,1,3,3,3-hexafluoro *iso*-propanol
MEK	methyl ethyl ketone
MMT	monomethyl terephthalate
NMR	nuclear magnetic resonance
OCP	*ortho*-chlorophenol
Penta	pentaerythritol
PET	poly(ethylene terephthalate)
PPM	parts per million
t	triplet (NMR)
TAME	terephthalic acid monomethyl ester
TCE	1,1,2,2-tetrachloroethane
TFA	trifluoroacetic acid
THF	tetrahydrofuran
s	singlet (NMR)
s	sharp (FTIR)
vss	very strong singlet

Contents

Abstract iii

Acknowledgements iv

List of Abbreviations v

Contents vi

1 Introduction 1

1.1 Polymers 1

1.2 Step-growth Polymerisation 3

1.2.1 Step-growth of Polyesters 3

1.2.2 Assumptions 4

1.2.3 Kinetics of Step-growth Polymerisation 4

1.2.4 Step-growth Polymerisation of Polyfunctional Reagents 6

1.2.5 Molecular Weight Distribution 8

2 Poly(ethylene terephthalate) 10

2.1 PET Production 12

2.1.1 Direct Esterification 12

2.1.2 Ester Interchange 14

2.1.3 Polycondensation 16

2.1.4 Reversibility 17

2.1.5 Catalysts and Stabilisers 18

3 Polymers of Controlled Architecture 21

3.1 Background 22

3.2 Synthetic Strategies 22

4 Methods of Analysis 25

4.1 Gel Permeation Chromatography (GPC) 25

4.2 Vapour Pressure Osmometry 26

4.3 Viscosity 27
4.3.1 Melt Viscosity 27
4.3.2 Solution Viscosity 27
4.4 Differential Scanning Calorimetry (DSC) 29
4.5 Light Scattering 31
4.6 End-group Analysis 35
4.6.1 Extent of Reaction 36
4.6.2 Composition Parameter 36
4.6.3 Branching Coefficient 37
4.6.4 Number-average Degree of Polymerisation 37
4.6.5 Number-average Molecular Weight 38
4.6.6 Weight-average Molecular Weight 38
4.6.7 Number-average Branching Density 38
4.6.8 Intrinsic (Inherent) Viscosity 39
4.7 Dynamic Mechanical Thermal Analysis (DMTA) 39

5 Branched PET 41
5.1 Literature Examples 41
5.2 Project Objectives 44
5.2.1 Core Molecules 44
5.2.2 Pre-formation of Oligomeric Polymer Cores 46
5.2.3 Branching Strategy 46
5.2.4 End-Cappers 48
5.2.5 Characterisation 49

6 Results and Discussion 50
6.1 Initial reactions 50
6.2 Branched BHET Reactions 51
6.2.1 Trimesic acid Branched Polymers 52
6.2.2 Trimesic acid Branched Polymers with Ballmilling 53
6.2.3 Low Level Trimesic acid Branching 55
6.2.4 Effect of Varying Time of Addition of Trimesic Acid Brancher 60

6.2.5 Branched 'Monomer' Reactions 61
6.2.6 Adjusted 'Monomer' Based Reactions 63
6.2.7 Other Branching Monomers 64
6.2.8 End-capped Reactions 74
6.2.9 Flexible Branching Agents 81
6.2.10 Ionomer Branching Agents 82

7 Experimental 87
7.1 Reagents 87
7.2 Analytical Methods 88
7.3 PET Synthesis 88
7.3.1 Polycondensation Rig 89
7.3.2 Poly(ethylene)Terephthalate Production 90
7.3.3 Polycondensation Reactions 93
7.4 Analysis of Polymers 117
7.4.1 FTIR Spectral Analysis 117
7.4.2 ^{1}H NMR and End-group Analysis 117
7.4.3 Solution Viscosity 125
7.4.4 Differential Scanning Calorimetry (DSC) 129
7.4.5 Light Scattering 129
7.4.6 Determination of dn/dc 136
7.4.7 Determination of n, the refractive index 146
7.4.8 Melt Viscosity Measurement 154
7.4.9 Gel Permeation Chromatography 156

8 Conclusions 85

9 Further Work 86

10 Appendix 1 157
10.1 Sample calculation of intrinsic viscosity 157

11 Appendix 2 159
11.1 Calculation of Number of End-Groups (E) of PET 31 from

End-Group Analysis Data 159
11.2 Calculation of Extent of Reaction (P) of PET 31 160
11.3 Branching Coefficient (α) of PET 31 160
11.4 Number Average Degree of Polymerisation ($\overline{X}_n$) of PET 31 161
11.5 Number Average Molecular Weight ($\overline{M}_n$) of PET 31 161
11.6 Weight Average Molecular Weight of PET 31 161
11.7 Number Average Branching Density ($\overline{B}_n$) of PET 31 162
11.8 Weight Average Branching Density ($\overline{B}_w$) of PET 31 162
11.9 Intrinsic (Inherent) Viscosity of PET 31 162
11.10 Viscosity Average Molecular Weight of PET 31 162

12 Appendix 3 163
12.1 Synthesis of Bis-hydroxy-(2-ethyl terephthalate) (BHET) 163

1 Introduction

1.1 Polymers[1, 2]

Polymers are high molecular weight molecules (typically 10^4 - 10^6 Daltons), made up by the repetition of small, simple chemical units. In some cases, the repetition is linear, giving rise to a 'straight' chain molecule.

Figure 1: Straight Chain Polymer

In other cases the chains are branched or interconnected to form three-dimensional networks.

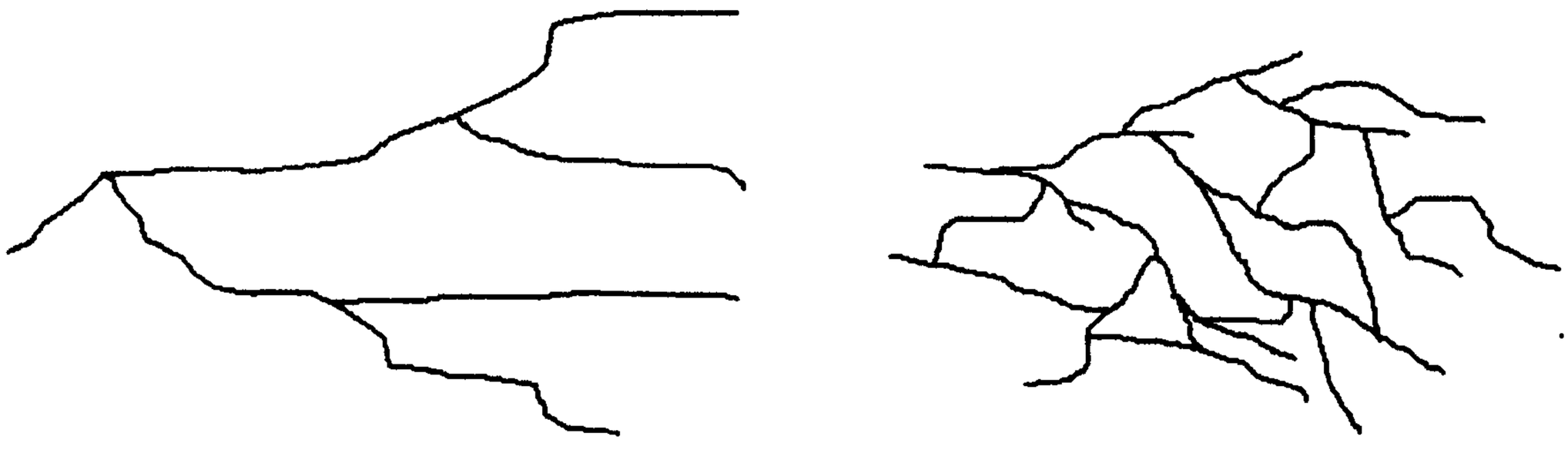

Figure 2: Branched and Crosslinked Polymers

Branched polymers can be further subdivided into three categories; branched, hyperbranched, star polymers, and dendrimers.

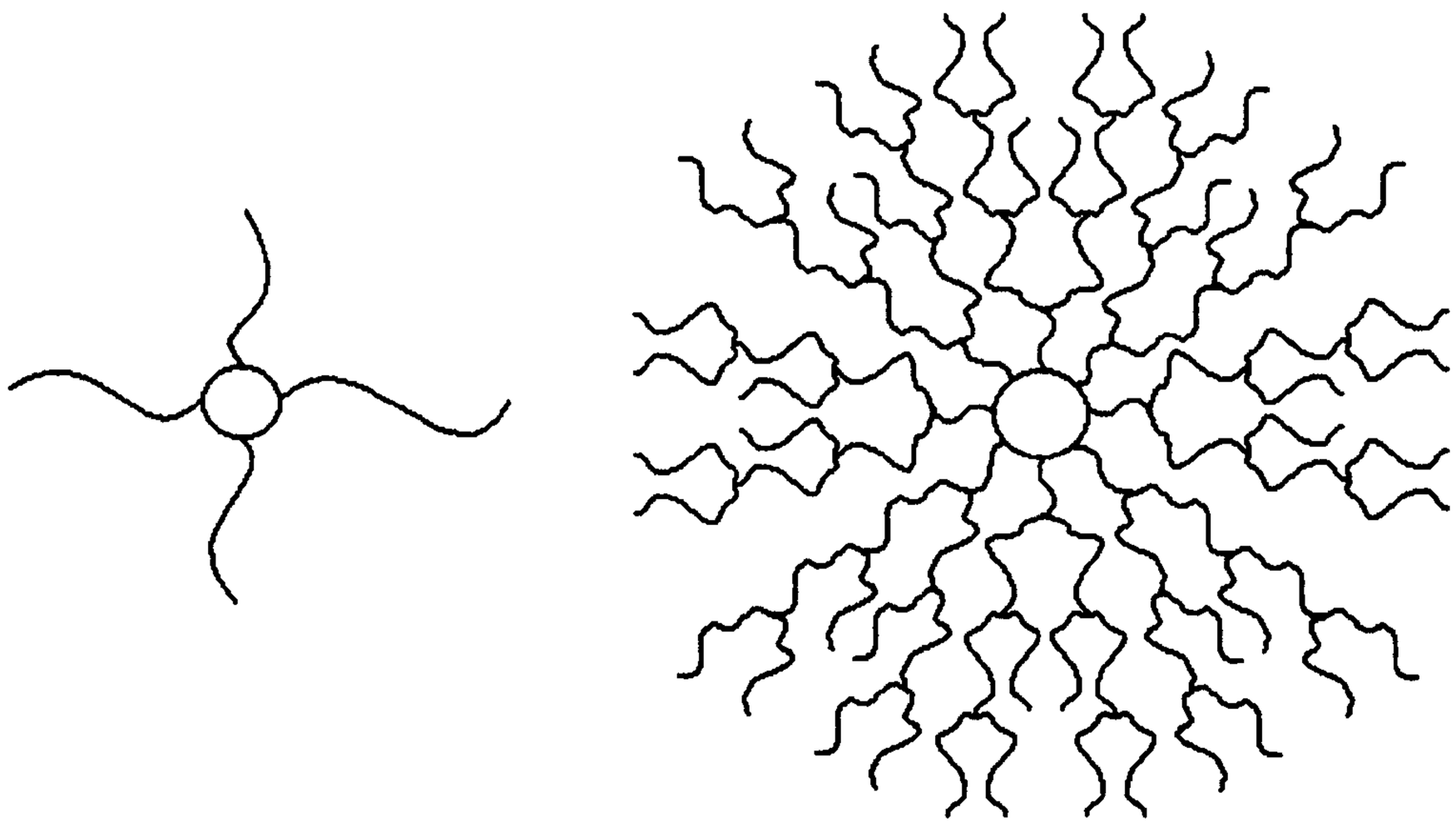

Figure 3: Star and Dendritic Polymers

Branched polymers are generally overall linear in shape with a small amount of branching. Hyperbranched polymers are much more branched in nature and have a topology, which is undefined, but tends to be more globular than linear and branched polymers. Dendrimers are species that have a perfectly branched three-dimensional structure.[3] Star polymers are a special category of dendrimer where they have a star shape, with linear branches radiating out from a central core.

The change in molecular architecture can have an immense impact on the physical properties of the polymer. Linear polystyrene, for example, is a thermoplastic, *i.e.* it softens on heating, and can be processed, whereas its crosslinked analogue is a thermosetting plastic, *i.e.* once formed it can soften if heated, but it cannot be processed, due to the crosslinked network that extends throughout its structure. Therefore the molecular architecture of the polymer can be as important, as the molecular composition of the monomer segments present.

1.2 Step-growth Polymerisation[4,5]

Polymeric species can be made *via* a number of types of reaction: free radical and ionic addition, condensation polymerisation *etc*. In 1929 W.H. Carothers[6] proposed that these reactions should be categorised into two groups.

1. Condensation polymers
2. Addition polymers

Condensation polymers are those that are made by the elimination of a small molecule such as water, in a repeated condensation reaction. Whereas addition polymers are formed in a single chain reaction in which no such loss occurs.

It later became obvious that this definition was inadequate as there were several notable exceptions to the rule; for this reason Flory offered an amendment to the definition.[7] He re-classified the polymers in terms of reaction mechanism rather than the product produced, replacing the term condensation with step-growth. This allowed the inclusion of polymers such as polyurethanes, which grow by a step mechanism without the elimination of a small molecule.[8] Addition reaction polymers were renamed chain reaction polymers. Thus, polymerisations are now classified without regard for the loss of any molecules.

1.2.1 Step-growth of Polyesters

The step-growth polymerisation of polyesters follows the general reaction below.

Scheme 1: General Esterification

This reaction is analogous to the simple esterification of mono-functional acids and alcohols. Removal of water forces the reaction to completion. The molecule formed is also bifunctional and so may react again. In this manner, a polymer of n monomer

units can be built up in n – 1 "steps". The reaction needs no catalyst but can be catalysed by the addition of strong acid or acidic salt. This reaction is termed direct esterification, the same effect can be achieved with an ester interchange reaction (see section 2.1.2).

1.2.2 Assumptions[7,8]

Flory proposed two assumptions, for use when dealing with the kinetics of step-growth reactions. These were that firstly that the rate of reaction of a functional group is independent of the size of the molecule. This assumption has been backed up repeatedly by experimental evidence.

Another basic assumption made by Flory was that all like functional groups can be considered to be equally reactive. This implies that a monomer will react with both monomer and polymer species with equal ease.

1.2.3 Kinetics of Step-growth Polymerisation[2]

The assumption that the functional group reactivity is independent of chain length can be verified experimentally by following the kinetics of a polyesterification reaction.

In the case where the reaction is uncatalysed, the acid will act as its own catalyst. Flory[9] described the kinetics of this uncatalysed reaction as shown in equations 1 – 4. At any time, t, the rate of condensation can be defined as the rate of disappearance of the carboxyl groups.

$$-d[COOH]/dt = k[COOH]^2[OH]$$

Equation 1:Self-catalysed Condensation

If the concentration of acid groups and alcohol groups is equal then

$$-dc/dt = kc^3$$

Equation 2: Self-catalysed Condensation

Where c equals the functional group concentration. Integration of this equation gives the following expression.

$$2kt = 1/c^2 - 1/c_0^2$$

Equation 3: Self-catalysed Condensation

The Carothers equation states that x_n (the number average degree of polymerisation) = 1/(1-p); where p is the extent of reaction.

Since $x_n = c/c_0$ then:-

$$2c_0^2kt = 1/(1 - p)^2 - 1$$

Equation 4: Self-catalysed Condensation

However, in 1979, Amass[10] showed that Flory's substitution of $[H^+]$ with [RCOOH] was incorrect, because terminal carboxyl group of a polymer chain can be expected to be part of a weak acid of which the dissociation is governed by the dissociation constant (K_a). Amass showed that the reaction was in fact of the order 2.5, and not third order as previously shown by Flory (Equation 2).

$$K_a = [RCOO^-][H^+]/[RCOOH]$$

Equation 5: Dissociation Constant

$$K_a = [H^+]^2/[RCOOH]$$

Equation 6: Dissociation Constant

$$[H^+] = (K_a[RCOOH])^{1/2}$$

Equation 7: Proton Concentration in Terms of Carboxyl Concentration

$$-dc/dt = k\,K_a^{1/2}c^{2.5}$$

Equation 8 : Modified Self-catalysed Condensation

For a reaction catalysed by strong acid

$$-d[COOH]/dt = k'[COOH][OH]$$

Equation 9: Acid Catalysed Condensation

(Note k' includes a term involving the concentration of strong acid catalyst)

If the concentration of acid groups and alcohol groups is equal then

$$-dc/dt = k'c^2$$

Equation 10: Acid Catalysed Condensation

Where c equals the functional group concentration. Integration of this equation gives the following expression.

$$c_0k't = 1/c - 1/c_0$$

Equation 11: Acid Catalysed Condensation

Since $x_n = c/c_0$ then:-

$$c_0k't = 1/(1 - p) - 1$$

Equation 12: Acid Catalysed Condensation

These equations were subsequently verified experimentally by Flory[7,11].

1.2.4 Step-growth Polymerisation of Polyfunctional Reagents

Polymerisation of reagents with more than two functional groups per molecule can lead to three-dimensional networks. These polymers are highly complex and their synthesis is complicated by the formation of gels. When gelation sets in the reaction mixture can be divided into two distinct parts: the gel, which is insoluble in non-degrading solvents, and the sol, which remains soluble and can be separated from the gel. As the reaction proceeds the amount of gel increases and the sol. Gelation can

occur at relatively low molecular weight averages, but when it occurs, the molecular weight average becomes infinite.

Gelation[12,13,14]

In order to calculate the point in the reaction when gelation takes place, the branching coefficient α must be defined.

α is defined as the probability that a given functional group on a branch unit is attached to another branch.

The point at which gelation becomes possible is defined by α_c, the critical value of α for gelation.

$$\alpha_c = 1/(f - 1)$$

Equation 13: Critical Branching Coefficient

(Where f is the functionality of the branching agent.)

This can be linked to the extent of reaction (conversion) p via the following expression.

$$\alpha = p\rho/ (- p (1 - \rho))$$

Equation 14: Branching Coefficient

Where ρ, the composition parameter, is defined as -

ρ = No. of groups of initial polyfunctional units/ total No. of initial functional groups

1.2.5 Molecular Weight Distribution

Most methods of synthesising polymers do not give rise to a product that has a uniform mass throughout. The random nature of the synthesis creates chains of various lengths and so we normally say that the polymer sample has a molecular weight distribution. Calculation of the polymer's molecular weight then gives an average value, rather than one unique value. The numerical value of this average depends very much on the method of its calculation. These different definitions, listed below, are all useful tools depending on the situation they are to be used in. Ratios of molar mass averages (typically $\overline{M}_w/\overline{M}_n$) indicate the breadth of the molecular weight distribution or the polydispersity D.

A colligative method, such as osmotic pressure, effectively counts the number of molecules present and provides a number average molar mass, $\overline{M}_n$, defined as: -

$$\overline{M}_n = \sum M_i N_i / \sum N_i = \sum w_i / \sum (w_i/M_i)$$

Equation 15: Number-average Molecular Weight

Where N_i is the number of molecules of species i of molar mass M_i, and $w_i = N_i M_i / N_A$, Where N_A is Avogadro's number.

From light scattering measurements the weight average mass, $\overline{M}_w$, is obtained. This is defined as :-

$$\overline{M}_w = \sum N_i M_i^2 / \sum N_i M_i = \sum w_i M_i / \sum w_i$$

Equation 16: Weight-average Molecular Weight

This method relies on the size (weight) of the molecule rather than the number of molecules. $\overline{M}_n$ and $\overline{M}_w$ are the two main averages encountered, other averages include $\overline{M}_z$ (the z-average), $\overline{M}_{z+1}$ (the z+1-average) and $\overline{M}_v$ (the viscosity average).

$$\overline{M}_z = \sum N_i M_i^3 / \sum N_i M_i^2 = \sum w_i M_i^2 / \sum w_i M_i$$

$$\overline{M}_{z+1} = \sum N_i M_i^4 / \sum N_i M_i^3$$

$$\overline{M}_v = [\sum N_i M_i^{1+v} / \sum N_i M_i]^{1/v}$$

Equation 17: Other Molecular Weight Averages

The diagram below shows a typical molecular weight distribution of a polymer prepared by a random method. It can be seen that the weight average datum is higher than the number average. The M_w value is important as higher molecular weight chains may have a greater influence over the physical properties of a sample than chains of a lower molecular weight. $\bar{M}_w$ takes this into account.

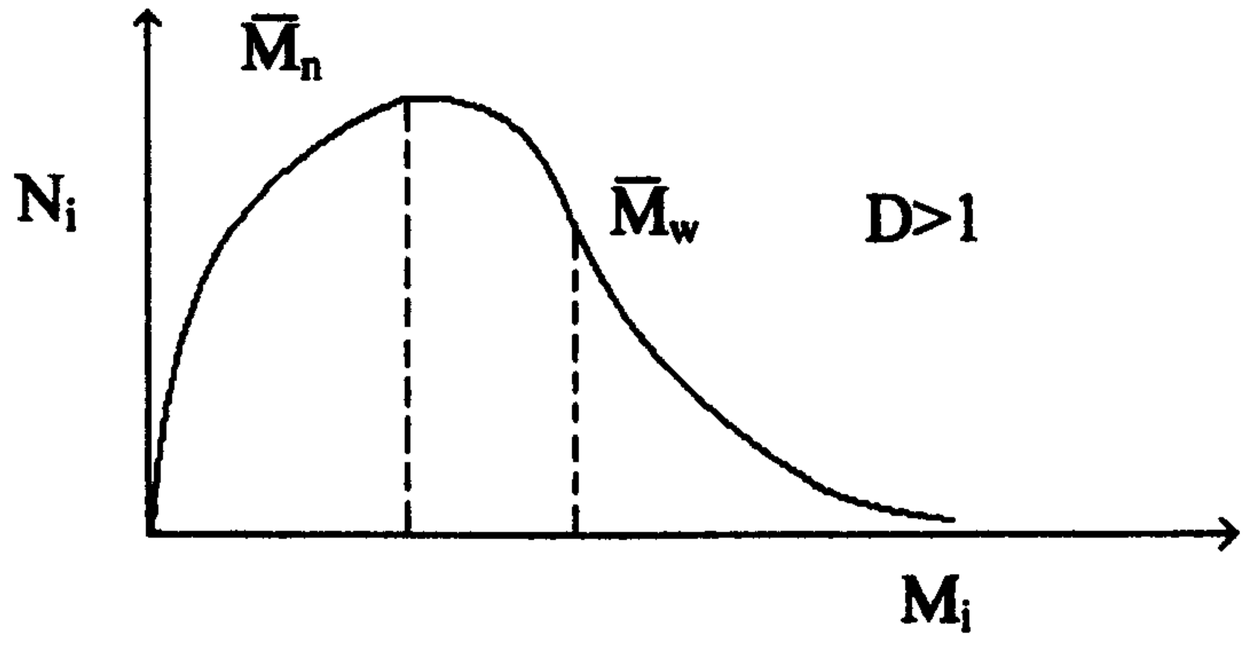

Figure 4: Random Molecular Weight Distribution

Where N_i is the fraction of polymer in each interval of M_i considered.

2 Poly(ethylene terephthalate)[15,16]

Poly(ethylene terephthalate) or PET, was developed in the U.K. by the Calico printer's association (C.P.A.).[21] It was a direct development of work carried out by W.H. Carothers on polyesters.[17,18,19] First patented in 1941,[20] it is now widely used in a variety of industrial and domestic applications. The most easily recognised of these are in fibres (Terylene), in films (Melinex ™), or in moulded products (Melinar ™). The American company Du-Pont, purchased the patent from the C.P.A. and started production in the U.S. in March 1953, at their plant in Kinston, North Carolina, where the fibre was known as 'Dacron'. ICI started full-scale production of polyester fibre in 1955 and the production of polyester film commenced four years later.

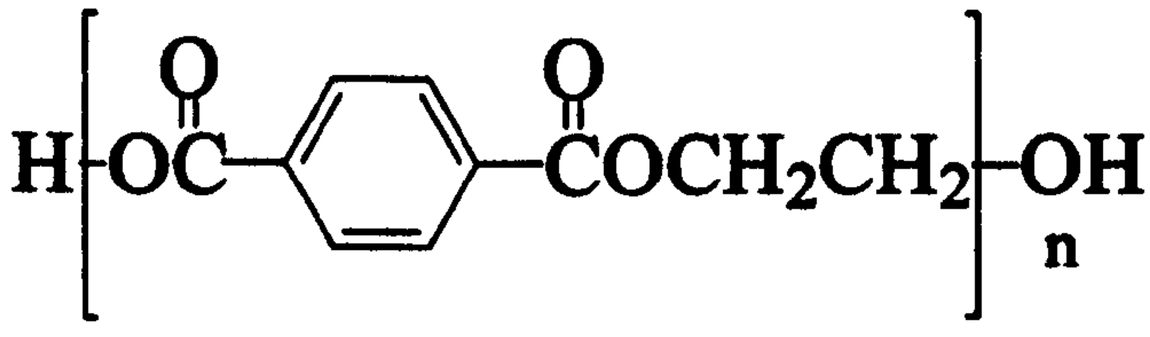

Structure 1: Poly(ethylene terephthalate)

Melinex has many valuable properties and characteristics that make it highly attractive for industrial use, some of which are listed below:[21]

- Outstanding strength
- Dimensional stability
- High resistance to chemicals
- Low water absorption
- Toughness
- Great flexibility
- High gas barrier properties
- High clarity

It is also stable to a wide range of temperature and humidity conditions.

All this adds up to a highly versatile material, which has uses in many different fields, ranging from packaging to printing and photography.

Melinex ™ also has a wide range of applications in the electrical and electronic industries, from slot liners in electrical motors to cable insulation and printed circuit boards that make much of modern communications systems possible. It provides the graphic layer in membrane touch pads for a variety of keyboard applications, such as the control panels on microwave ovens.

The manufacture of Melinex ™ film from ICI-produced raw material proceeds from polymer production through five stages of filming. This produces a flexible, dimensionally stable film, with a wide range of visual characteristics and good mechanical properties. The thermal behaviour of PET film can also be modified to meet the stringent customer demands placed upon it.

PET, when moulded into one of its most easily recognisable forms, a carbonated drinks bottle, takes advantage of one of the polymer's key properties, *i.e.* its good gas barrier properties, to maintain the CO_2 pressure. Using Melinex ™ and Melinar ™ many foods and drinks are packaged and kept fresh and free of contamination. In fact, if PET and other plastics were not used in food packaging, up to 50% of all perishable goods would go to waste.[16]

2.1 PET Production

PET is produced *via* a two-step process. Firstly the reaction of an organic acid with an alcohol followed by a polycondensation reaction. The acid component is usually either terephthalic acid (TPA) itself, or dimethyl terephthalate (DMT), and the alcohol usually (mono)-ethylene glycol (MEG).

2.1.1 Direct Esterification

In large-scale production of PET, ICI uses mostly pure terephthalic acid.[21] Terephthalic acid and ethylene glycol are combined to form the monomer bis-(2-hydroxyethyl) terephthalate (BHET). The process in which these two reactants are combined is called direct esterification. It is carried out at pressures slightly above atmospheric and temperatures above 200 °C, during the reaction water boils off and is discarded.

Terephthalic acid is a solid that is not readily soluble in glycol, even on heating. Due to this, the reaction mixture is in the form of a slurry rather than a low viscosity liquid. The rate of reaction at the boiling point of glycol (197 °C), is very slow and reaction times of around nine hours are typical. The rate of esterification, rather than the low solubility of terephthalic acid, is the rate determining step of the reaction since the addition of a suitable catalyst can reduce the reaction times to three hours or less.[22,23,16]

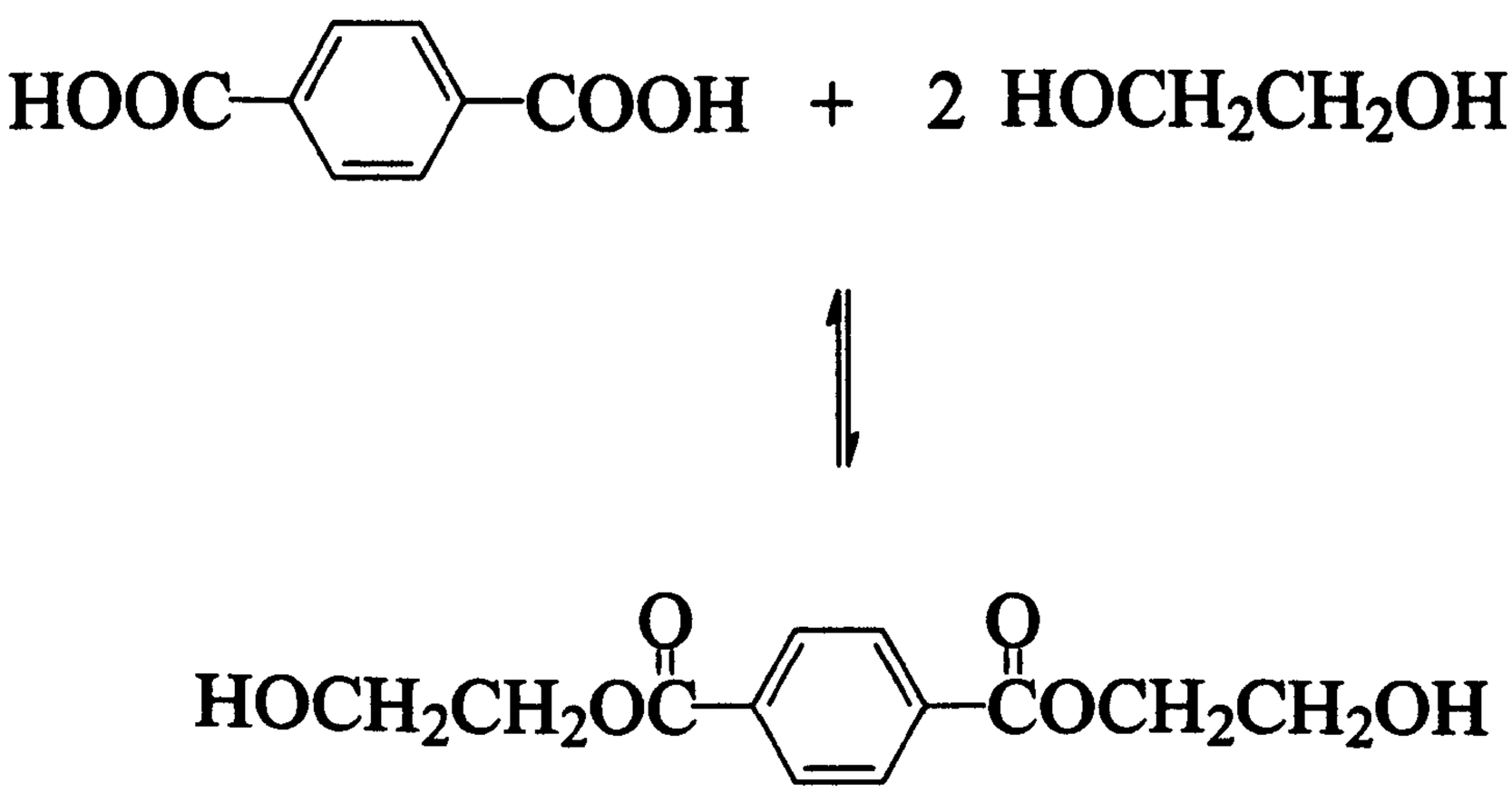

Scheme 2: BHET Production

A better method from the point of view of product quality is to carry out the reaction at elevated pressures of 3-4 atmospheres. This means that the temperature can be raised to 240°C without causing the glycol to boil off. Oxygen must be excluded from the reaction mixture as it could cause oxidation, leading to a yellowing of the monomer and therefore colouring in the polymer and finished product. This process can be carried out without a catalyst. Due to terephthalic acid being an acid, and diethylene glycol (DEG) production being an acid catalysed process, DEG may be formed as a by-product during the reaction. DEG production can be minimised by the addition of a small amount of base to the melt. Sodium hydroxide (50-100 ppm) is frequently used, although ICI Fibres use trimethyl-2-hydroxyethyl ammonium hydroxide in their continuous process. Another method of reducing DEG formation is to increase the ratio of glycol to terephthalic acid, usually to between 1.5:1 and 2:1. When all, or nearly all, of the theoretical amount of water has been distilled off, the pressure is reduced to atmospheric. It is at this time that any remaining water and glycol distils over. A stabiliser is then added to prevent discoloration due to free base in the melt.

Ensuring that the reaction runs to completion is not necessary, since any free carboxyl ends, provided that there are not too many of them, are esterified during the early stages of the polycondensation process. In fact, since under these conditions the esterification process is more rapid than polycondensation, incomplete esterification can actually result in an increase in the overall polymerisation rate with a detectable reduction in cycle time.

With a continuous process it is possible to reduce the ratio of glycol to terephthalic acid further than with a batch process. This means that the vapour pressure of glycol in the melt is lower and the reaction can be carried out at atmospheric pressure.

2.1.2 Ester Interchange

On a laboratory scale, BHET is produced *via* an ester-interchange reaction rather than the direct-esterification route favoured by industry.

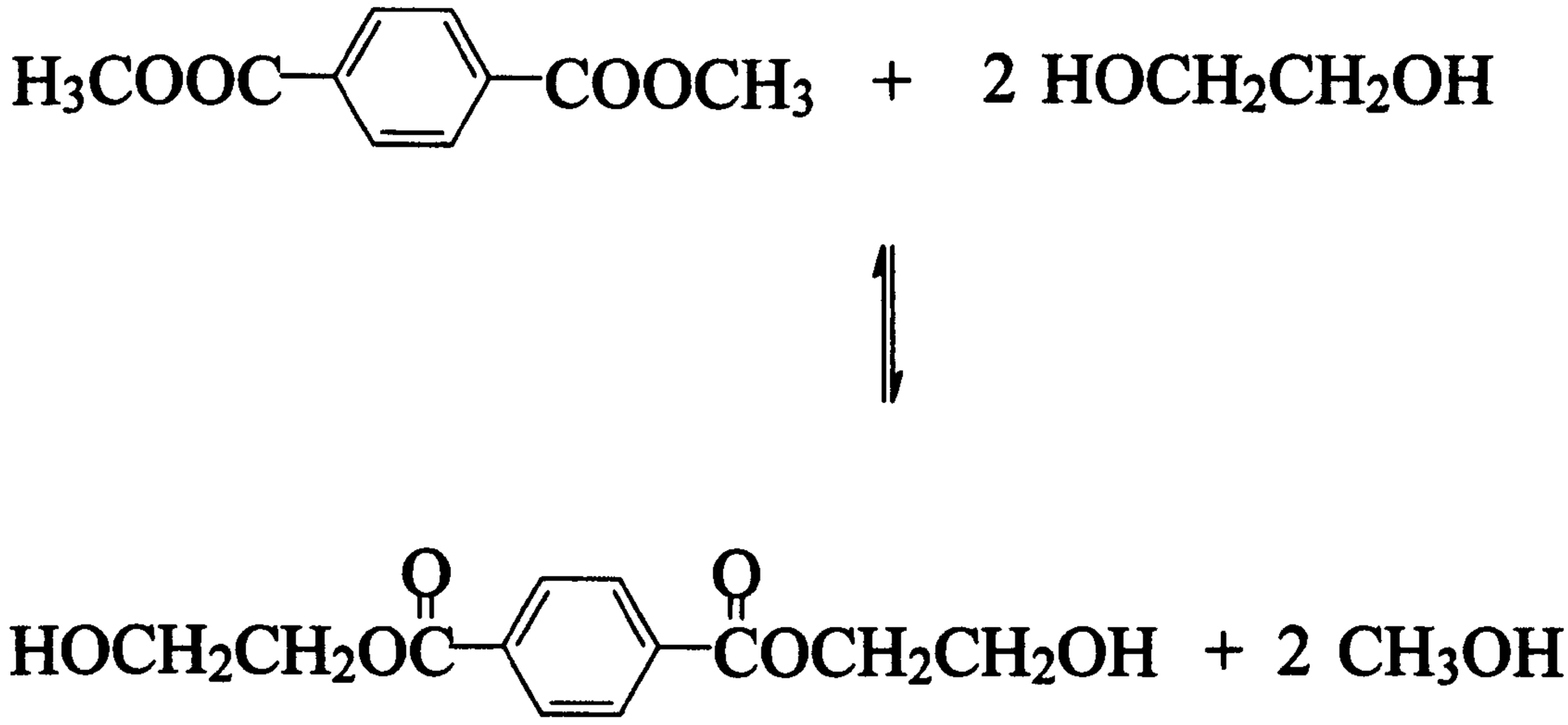

Scheme 3: BHET Production by Ester Interchange

In the ester interchange reaction dimethyl terephthalate (DMT) is heated with glycol to form BHET and methanol. The reaction must be carried out in the presence of a catalyst in a vessel fitted with a separating column, condenser, and receiver. In practice, a 2.1:1 ratio is used instead of the stoichiometric amounts. The reaction mixture is heated to around 140 °C where a clear solution is obtained. The reaction starts at about 150 °C, where, at first, there is a very rapid evolution of methanol.

Superheating can occur very readily at this stage and care must be taken with large-scale reactions in glass to avoid sudden violent evolution of methanol. This can be achieved by the presence of a nucleating agent. Pieces of 'Fluon' or better still a 'Fluon' agitator is excellent for this purpose.

The catalyst must always be added below 150 °C. Overheating at this stage on the plant can also lead to flooding of the ester interchange column and a pressure build up in the ester interchange vessel. This, in turn, can lead to an effect known as "priming" in which the batch erupts violently and the methanol condenser and possibly the column and associated pipe work become blocked with solid DMT.

Once the initial surge is over the rate of heat input is governed by the volatility of glycol and DMT. If too much heat is supplied, DMT can be carried over and again cause condenser blockage. In practice, the batch temperature increases gradually throughout the process until, by the time the theoretical amount of methanol has been distilled off, the temperature is around 210 °C. On the plant scale, when about 95% of the theoretical amount of methanol has been collected no further separation is attempted. As the batch temperature is raised further to 220-230 °C, the total distillate (consisting mainly of ethylene glycol and methanol) is collected. DMT carryover is one of the main problems with conventional ester interchange reactions. An adaptation of this process involves continuous addition of DMT. Instead of all reactants being present and mixed at the start of the reaction, the glycol and catalyst are charged to the reaction vessel and heated to around 180 °C. Molten DMT is added continuously to the system over approximately 30 minutes. This process greatly reduces the cycle time for ester interchange, eliminates priming, is easier to control and simplifies column design. This however is not very practicable on relatively small laboratory scale work.

The product obtained at the end of the ester interchange reaction is not simply the glycol ester of terephthalic acid. As DMT can react with BHET as well as with glycol, and the ester interchange catalysts can also catalyse the polycondensation reaction, the reaction product is an equilibrium mixture of free glycol, BHET and short chain oligomers. The melting point of the mixture varies with composition, being higher the lower the glycol to terephthalate ratio, but it is normally in the region of 150-200 °C. Diethylene glycol is also produced, to some extent. The catalyst employed governs the extent of DEG production. Ester interchange is not as robust a process as direct esterification, where the problem of batch priming does not occur. Unlike direct esterification it is essential that the ester interchange reaction proceeds to completion as unreacted methyl ester ends can act as chainstoppers in the polycondensation. The oligomer produced by this reaction tends to polymerise more slowly than that produced by direct esterification, probably due to its higher glycol content.

2.1.3 Polycondensation

The BHET produced by step one can be forced to polymerise by increasing the reaction temperature from 240 to 290 °C and reducing the pressure to 0.1 mmHg. This removes glycol and causes dimerisation. As the reaction proceeds glycol is eliminated between molecules of oligomer and so the polymer grows in length.

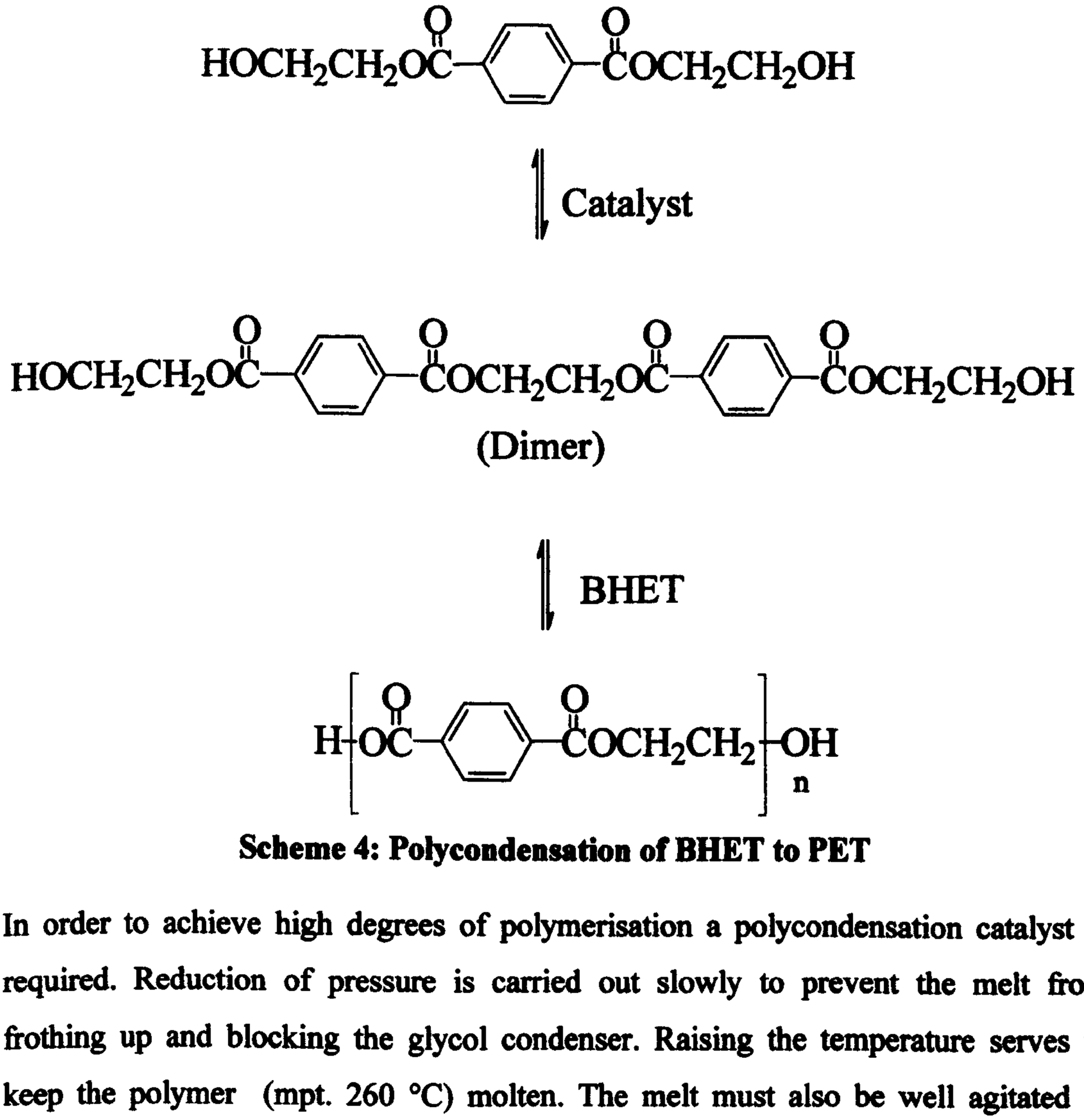

Scheme 4: Polycondensation of BHET to PET

In order to achieve high degrees of polymerisation a polycondensation catalyst is required. Reduction of pressure is carried out slowly to prevent the melt from frothing up and blocking the glycol condenser. Raising the temperature serves to keep the polymer (mpt. 260 °C) molten. The melt must also be well agitated to achieve good polymerisation rates.

2.1.4 Reversibility [24,25,26]

Heating the polymer with excess glycol or water can reverse polycondensation. In the former case, the process is known as glycolysis in the latter it is simple hydrolysis. At temperatures where the polymer is molten, the reaction is very fast, at lower temperatures however, the rate depends on the degree of subdivision of the polymer. In both cases the reaction rate can be increased by the use of a catalyst. Zinc salts are well documented as good catalysts for glycolysis, in particular zinc acetate and zinc stearate.

Below 245 °C the presence of zinc acetate and zinc stearate during PET glycolysis does not effect the glycolysis rate. Below this temperature, the glycolysis reaction occurs between solid PET and liquid ethylene glycol. At temperatures exceeding 245 °C, glycolysis occurs predominately in a single liquid phase allowing catalysis to proceed.

Hydrolysis can also be catalysed by zinc salts, but for best results sodium salts, such as sodium stearate, should be used. The mechanism for this catalysis is thought to involve electrolytic destabilisation of the PET-water interface, resulting in a greater interfacial area exposed to the hydrolysis reaction. Sulfuric acid can also be used as a hydrolysis catalyst however this leads to problems such as corrosion of equipment and difficult separations of liquid products from acid waste.[27]

As a method of recovering scrap polymer, glycolysis has the disadvantage that DEG and other impurities, such as degradation products are not readily removed and so the monomer produced tends to be of an inferior quality.

DEG formation can be avoided by alkaline hydrolysis of PET with sodium or potassium hydroxide.[28] This yields EG and terephthalic salts which can then be protonated easily to TPA.

2.1.5 Catalysts and Stabilisers[16,29,30,31,32]

Direct Esterification

No catalysts are required for direct esterification, however a trace of base is added as a softening point stabiliser, to reduce the amount of DEG produced in the reaction. Quartenary ammonium hydroxides have been found to be useful for this purpose, as they give no insoluble residues in the polymer.

Ester Interchange[33]

Many metal salts have been found to be efficient catalysts in the ester interchange reaction, those, which have been used commercially fall into two main categories.

1. Alkali and alkaline earth metals *e.g.* Li, Ca, and Mg.
2. Transition and group IIB metals *e.g.* Mn, Co, Zn.

The metals are usually added to the reaction in their acetate form. These are crystalline and non-corrosive, and are therefore easy to handle. They are also readily soluble in hot glycol. However, it is not the acetate form that is believed to be the intermediate. When the polymer is heated with glycol and acetate, the glycerol is converted to ethylene oxide and it is this species which is thought to be catalytically active, independent of the species actually added. The acetates used mostly come in the form of hydrates, however the amount of acetate added to the reaction is always calculated from the anhydrous salt.

Although Kodak and Dupont prefer zinc acetate, manganese acetate is used in the production of all ICI polymers.

Stabilisers

Originally, no stabilisers were used in polymer manufacture. The original film polymer recipe was based on zinc acetate/antimony trioxide.

Stabilisers were introduced by ICI when calcium salts were adopted as the ester interchange catalyst for fibre polymer. It was found that terephthalate precipitated in the polycondensation autoclave leading to a form of polymer contamination known as "tea leaves". Adding phosphorous acid at the end of ester interchange solved the problem and subsequently phosphorous acid addition was found to have beneficial effects in film production.

The stabilisers used up to the present have been phosphorous and phosphoric acids and esters thereof. Stabilisers have the following effects.

- Prevention or reduction of the precipitation of insoluble metal terephthalate during polymerisation.
- Destruction of the catalytic activity of ester interchange catalysts.
- Inhibition of the degradative and colour-forming side reactions of metal salt ester interchange catalysts during polycondensation.
- Inhibition of the catalysis of the oxidation of solid polymer by catalyst residues.
- Improvement of the electrical resistivity of the polymer.
- Phosphates tend to reduce antimony trioxide (the subsequent polycondensation catalyst) to the metal thus greying the polymer.

Polycondensation Catalysts[29,30,34]

Polycondensation catalysts also fall broadly into two main categories.

1. Those that are also ester interchange catalysts and which are deactivated by phosphorous stabilisers, *e.g.* zinc, cobalt and magnesium salts. As already mentioned these tend to catalyse thermal degradation as well as polycondensation. Thus, when used alone it is normally difficult to achieve high molecular weights with these catalysts.
2. Those which show little or no ester interchange activation and are relatively unaffected by phosphorous compounds, *e.g.* antimony, titanium and germanium

oxides etc. Commercial catalysts fall into this category. Antimony and germanium are added as their oxides, titanium as an alkoxide. Like the ester interchange catalysts, the active species is the glycol oxide formed *in situ* in the reaction melt.

Antimony Trioxide[35]

Antimony trioxide has been the main choice of catalyst for polyester production since the mid 1950's. It shows quite a high catalytic activity in polycondensation and because it has very little degradative effect it produces polymer of good colour. The main disadvantage is that it tends to be reduced to the metal by glycol at elevated temperatures. The effect is concentration dependent, the higher the level of antimony trioxide, the greyer the polymer. It is also reduced by phosphite stabilisers, giving polymer that has a relatively poor light transmission. For this reason phosphate stabilisers are used in nearly all film polymers.

Antimony trioxide is normally used at a level of 0.02-0.8 weight %.

Germanium Dioxide

Germanium dioxide exists in two crystalline forms. The tetragonal crystalline form, is highly insoluble, while the hexagonal form, is slightly soluble in glycol. Amorphous germanium dioxide is readily soluble in glycol and therefore is the most convenient form to use as a catalyst and gives polymer of exceptional colour and clarity. Although this is the best catalyst known it does have some disadvantages, notably its price, its scarcity (which also means its price is unstable) and the fact that it is appreciably volatile in glycol. Due to the problem of volatility it gives a less robust process than antimony. It is possible, with some difficulty to recover germanium from polycondensation glycol.

Germanium dioxide is normally added at the 0.02% level.

3 Polymers of Controlled Architecture

In recent years polymer synthesis has turned its attention to the preparation of polymers with complex architectures. There has been significant interest in well-defined highly branched species, and the unusual characteristics that can arise as a consequence of their novel topologies and molecular structures.

The synthesis of three-dimensional macromolecular species with a regular hyperbranched architecture was pioneered by Tomalia *et al.*,[3] and Newkome *et al.*,[36] in the early eighties. Since then, there have been many reports of the stepwise synthesis of such families of monodisperse polymeric species. These materials have been termed 'starburst' polymers or dendrimers (from the Greek dendritic, meaning treelike), on account of their highly branched topology.

The preparation of polymers with well-defined forms of branching has posed a challenge to polymer chemists for many years. Branched polymers are formed in polymerisation reactions but it is difficult, in most cases, to define the number of types of branches and thus to correlate the changes in physical properties with molecular architecture. The growing interest in highly branched, three-dimensional macromolecules is reflected in the large number of reports concerning the synthesis and properties of these structures. These materials can be divided into two families - dendritic, and hyperbranched molecules, which differ in their branching sequences.

Due to the growth in interest in dendrimers and their properties over the last 10 years, there has also been an increase in interest shown in hyperbranched polymers that are structurally similar but are generally easier and cheaper to synthesise.

Although there have been numerous suggestions as to how dendrimers might be exploited in speciality applications,[37,38] the laborious iterative procedures necessary for their synthesis will probably stop them from becoming mainstream or commodity species. If some of the more interesting and potentially useful properties of dendrimers were related to their extensively branched geometry rather than their pure structure and monodisperse nature then it may be possible to replicate these properties by employing polydisperse analogues. These hyperbranched molecules would be far easier to make and could hold the key to unlocking the barrier to large-scale production of these products.

3.1 Background

It is now emerging that dendritic and hyperbranched polymers can show enhanced solubility and reduced viscosity (solution and melt) when compared with their linear counterparts; for example some dendrimers are soluble in a wide range of common organic solvents.

Dendritic molecules have highly regular or 'perfect' branching, whereas hyperbranched macromolecules are randomly branched and contain varying amounts of linear segments. Interesting thermal,[39] viscometric,[40] and other properties[41,42,43,44] have been observed for dendritic and hyperbranched macromolecules and in many cases, this behaviour is different from that of linear polymers. Possible reasons for these differences are the unique three-dimensional structure, and the presence of a very large number of chain-ends in dendritic and hyperbranched molecules.

While dendritic molecules contain no linear segments, and have at least one branch point at every repeat unit, the exact branching sequence and structure of hyperbranched macromolecules is unknown. The behaviour of hyperbranched macromolecules lies directly between that of dendritic and linear polymers, in terms of their solubility and viscosity, and they are similar to linear polymers in terms of reactivities, especially with a solid surface. These findings suggest that the more readily available hyperbranched materials may be used in place of the dendritic structures for some applications, especially those involving their unusual physical properties. However, their overall chemical reactivity may be very different.

3.2 Synthetic Strategies

Over the last decade two distinct methods of synthesising dendritic polymers have been developed.

The first of these is known as the divergent route and involves the formation of the dendrimer by proceeding outwards from a central core. It utilises an iterative reaction scheme. The monomers are added to the core in a stepwise fashion, each intermediate being isolated and purified before proceeding to the next step.

This method has however, several problems. The increasing size of the dendrimer as more layers, or generations, of monomers are added leads to practical difficulties

involving, incomplete conversion of terminal groups, as a result of steric congestion. This in turn leads to isolation and purification problems in terms of removing incompletely converted products. Solving this problem involves the use of large excesses of reagents and forcing conditions, which lead to further difficulties in purification. The iterative method is also time consuming, laborious and potentially, very costly.

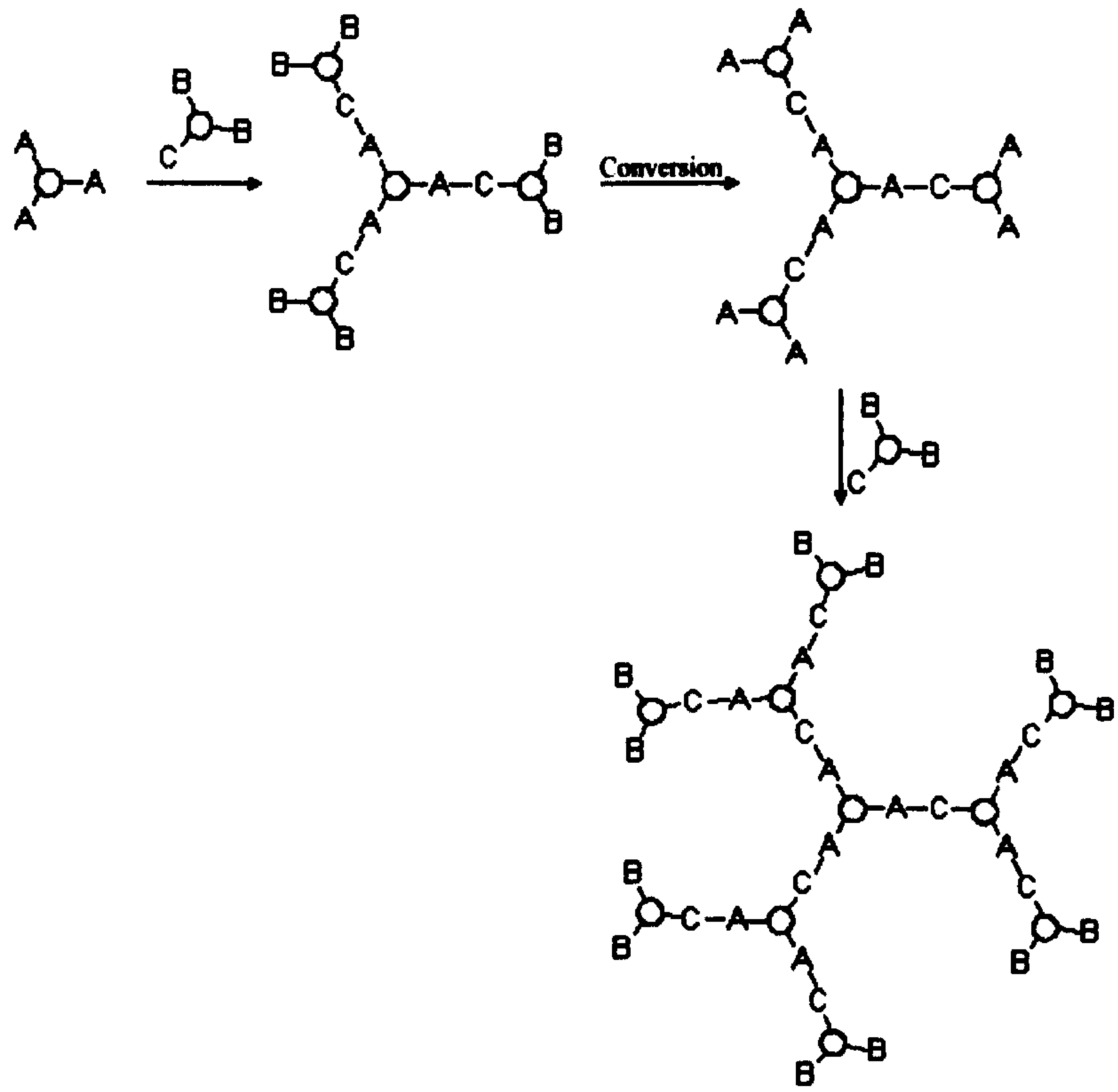

Scheme 5: Divergent Synthesis of Dendritic Polymers

More recently, convergent techniques have been developed, notably by Hawker and Fréchet[45] and have been used by a number of groups working in this field.

In this approach, dendrimer construction commences at what will ultimately end up being the outside of the structure and advances inwards. This is achieved by forming 'dendron wedges'. These wedges are built up by the attachment of a small number (typically two) of smaller wedges to a molecule with two different functional groups A and B. Each wedge has a functional group, C, which will react only with one of the two functional groups, for example A. The reacted functional group on the now larger wedge is now converted to the functional group C, permitting further iteration of the process. Finally the completed dendron wedges are attached to a central core

which has a small number (typically three) of the functional group A.

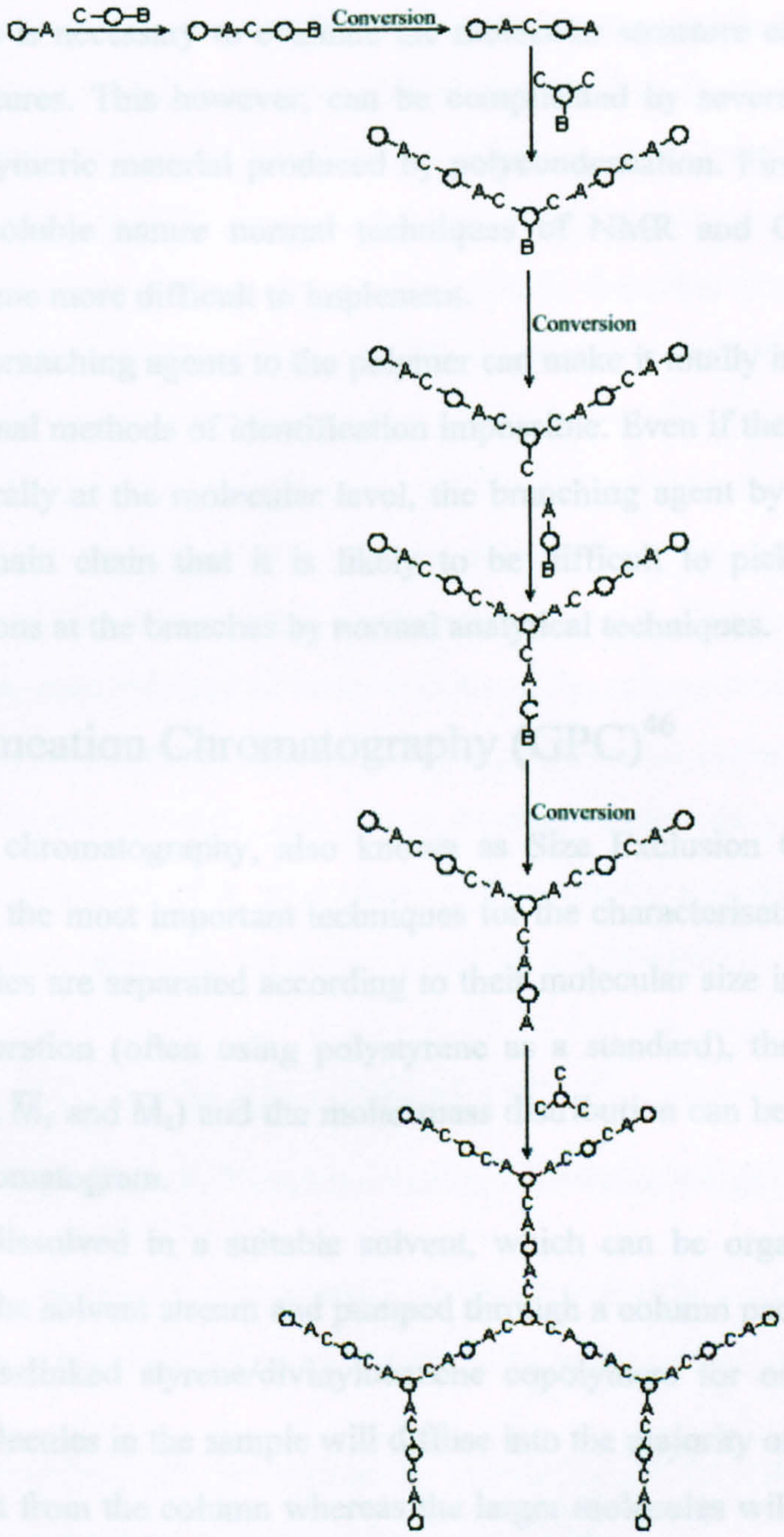

Scheme 6: Convergent Synthesis of Dendritic Polymers

The advantage of this method are that there are fewer steps than in the divergent method, and the number of functional groups to be converted does not increase as the steric bulk of the dendron increases. This gives greater control over the synthesis, minimising the possibility of failure and removing the necessity for large excesses of reagents.

4 Methods of Analysis

Once prepared it is necessary to evaluate the molecular structure of polymers with unusual architectures. This however, can be complicated by several factors, when dealing with polymeric material produced by polycondensation. Firstly due to their often highly insoluble nature normal techniques of NMR and GPC, while not impossible, become more difficult to implement.

The addition of branching agents to the polymer can make it totally insoluble making use of conventional methods of identification impossible. Even if the polymer can be analysed structurally at the molecular level, the branching agent by necessity, is so similar to the main chain that it is likely to be difficult to pick out molecular structural variations at the branches by normal analytical techniques.

4.1 Gel Permeation Chromatography (GPC)[46]

Gel permeation chromatography, also known as Size Exclusion Chromatography (SEC), is one of the most important techniques for the characterisation of polymers. Polymer molecules are separated according to their molecular size in solution. After appropriate calibration (often using polystyrene as a standard), the average molar masses ($\overline{M}_n$, $\overline{M}_w$, $\overline{M}_v$ and $\overline{M}_z$) and the molar mass distribution can be calculated from the resulting chromatogram.

The sample is dissolved in a suitable solvent, which can be organic or aqueous, introduced into the solvent stream and pumped through a column packed with porous gel (usually crosslinked styrene/divinylbenzene copolymers for organic solvents). The smallest molecules in the sample will diffuse into the majority of the pores in the gel and elute last from the column whereas the larger molecules will be increasingly excluded from the pores, will spend a shorter time in the column and hence will be eluted first. Unlike most other chromatographic processes, GPC is a non-interactive, equilibrium process. The separation depending solely on the degree of permeation of the polymer molecules. Therefore, the retention mechanism can be thought of as a physical exclusion of the various sized molecules.

4.2 Vapour Pressure Osmometry[47,48]

This is an indirect method of measuring the number-average molecular weight of a sample. It relies on the small temperature difference resulting from different rates of solvent evaporation from, and condensation onto, droplets of pure solvent and polymer solution maintained in an atmosphere of solvent vapour.

During the experiment two drops, one of pure solvent, the other of polymer solution are dropped onto separate thermistors (capable of detecting temperature differences as low as 10^{-4}K) in a thermostatted chamber, that is saturated with solvent vapour at the temperature of measurement. As there is a difference between the vapour pressure of the drops of solvent and of the solution, solvent from the vapour phase will condense on the solution drop causing its temperature to rise. Due to the large excess of solvent present, evaporation, and hence cooling of the solvent drop is negligible.

At equilibrium the temperature difference, ΔT, is proportional to the vapour-pressure lowering of the polymer solution, and thus to the number-average molecular weight. The thermistors form part of a Wheatstone bridge circuit, and ΔT is recorded as resistance, ΔR. The relationship between ΔR and $\overline{M}_n$ is given below.

$$\Delta R/K^*c = (1/\overline{M}_n)(1 + \tfrac{1}{2}\Gamma_2 c)^2$$

Equation 18: Number-average Molecular weight

Where K^* is the calibration constant, and Γ_2 is the second virial coefficient.

$\overline{M}_n$ is obtained by extrapolating to zero concentration a plot of $(\Delta R/c)^{\frac{1}{2}}$ vs C.

The calibration constant, K^*, is obtained by measuring ΔR for solutions of known concentration, prepared from samples of known mass M_k

$$K^* = M_k(\Delta R/c)_{c \to o}$$

Equation 19: VPO Calibration Equation

4.3 Viscosity

The viscosity of a substance can be measured in many ways and under a number of conditions. These methods can all be divided into two distinct groups: the viscosity of the pure melted polymer, or melt viscosity, and the viscosity of the polymer in solution, or solution viscosity.

4.3.1 Melt Viscosity[49]

The melt viscosity of a polymer is a highly important characteristic with respect to the polymer chemical industry. This attribute is a measure of how easy a molten polymer can flow, and thus indicates how much energy will be required to pump it around a plant as a liquid. It will also effect how easily the polymer can be injection moulded, drawn or melt pressed.

It has been suggested that the melt viscosity of a polymer can be effected by its degree of branching.[50,51] The greater the amount of branches the lower the melt viscosity. The melt viscosity may also be lowered the longer the branches are, up to a critical chain length, Z_c, where the melt viscosity power law changes. Crosslinking has a profound effect on the melt viscosity, as in this case the chain length has become infinite. Addition of low molecular weight species to the melt (plasticisation) reduces the melt viscosity by lowering the average molecular weight, as does the addition of bulky side groups.

Measurement of melt viscosity can be achieved *via* a rotational or a capillary melt viscometer.

4.3.2 Solution Viscosity [52, 53, 54]

When a polymer is dissolved in a liquid, the interaction of the two components stimulates an increase in polymer dimensions over that in the unsolvated state. Because of the vast difference in size between the solvent and solute, the frictional properties of the solvent in the mixture are drastically altered, and an increase in viscosity occurs which should reflect the size and shape of the dissolved solute even

in dilute solutions. This relationship between polymer size and viscosity was first recognised in 1930 by Staudinger.[55]

Measurements of solution viscosity are usually carried out by comparing the flow time of the polymer solution, t, through a capillary with that of the pure solvent, t_o. The ratio of these two measurements gives the relative viscosity, η_r, which is approximately equal to the ratio of the viscosities of the solution and solvent -

$$\eta_r = t/t_o = \eta/\eta_o$$

Equation 20: Relative Viscosity

This can be expressed as the more useful quantity η_{sp}, the specific viscosity.

$$\eta_{sp} = \eta_r - 1 = (t - t_o)/t_o$$

Equation 21: Specific Viscosity

The measurements are carried out using either a Cannon-Fenske or an Ubbelohde viscometer. The viscometer is filled with the polymer solution and placed in a constant temperature bath. The polymer solution is pumped up to specific level and allowed to fall through the viscometer's capillary. The time it takes to fall is recorded. This measurement is taken at different concentrations and with the pure solvent.

When a plot of η_{sp}/c against c is extrapolated to zero concentration we can obtain the intrinsic viscosity (or viscosity limiting number), $[\eta]$, as defined by the relationship -

$$(\eta_{sp}/c) = [\eta] + K'[\eta]^2c$$

Equation 22: Intrinsic Viscosity - Huggins Equation

Where K' is the Huggins constant, a shape dependant factor.

An alternative extrapolation method uses the inherent viscosity -

$$(\log\eta_r/c) = [\eta] + K''[\eta]^2c$$

Equation 23: Intrinsic Viscosity - Kraemer Equation

Where K" is another shape dependant factor.

For a specific polymer - solvent system the intrinsic viscosity can be related to the molecular weight through the Mark-Houwink equation.

$$[\eta] = K' \overline{M}_v^{a}$$

Equation 24: Mark-Houwink Equation

K' and *a* can be established by calibrating with fractions of known narrow-molecular weight, and once calculated [η] alone will give the molecular weight for an unknown fraction.

4.4 Differential Scanning Calorimetry (DSC)[56]

Differential scanning calorimetry or DSC is a method by which measurements can be made of the specific heat and energies of transition of relatively small (10 mg) samples of polymer.

The DSC instrument consists of an average-temperature circuit which heats/cools the sample and its reference to a predetermined time-temperature program. Whilst a temperature-difference circuit keeps the sample and its reference at the same temperature by comparing their temperatures and proportioning power to the heater/cooler so that the temperatures remain equal. When the sample undergoes a thermal transition, power to the two heaters is adjusted to keep the temperature of the sample and reference constant and the power difference is recorded. DSC is accurate to ~ 1-2%. Whilst this is less accurate than a good adiabatic calorimeter (~0.1%) it is more cost effective, and also quicker and easier to use. In addition, its accuracy is more than adequate for most applications.

Below is a representation of a typical DSC plot showing the glass transition temperature (~75°C), the crystallisation temperature (~100°C), and the melting point (~250°C) of PET.

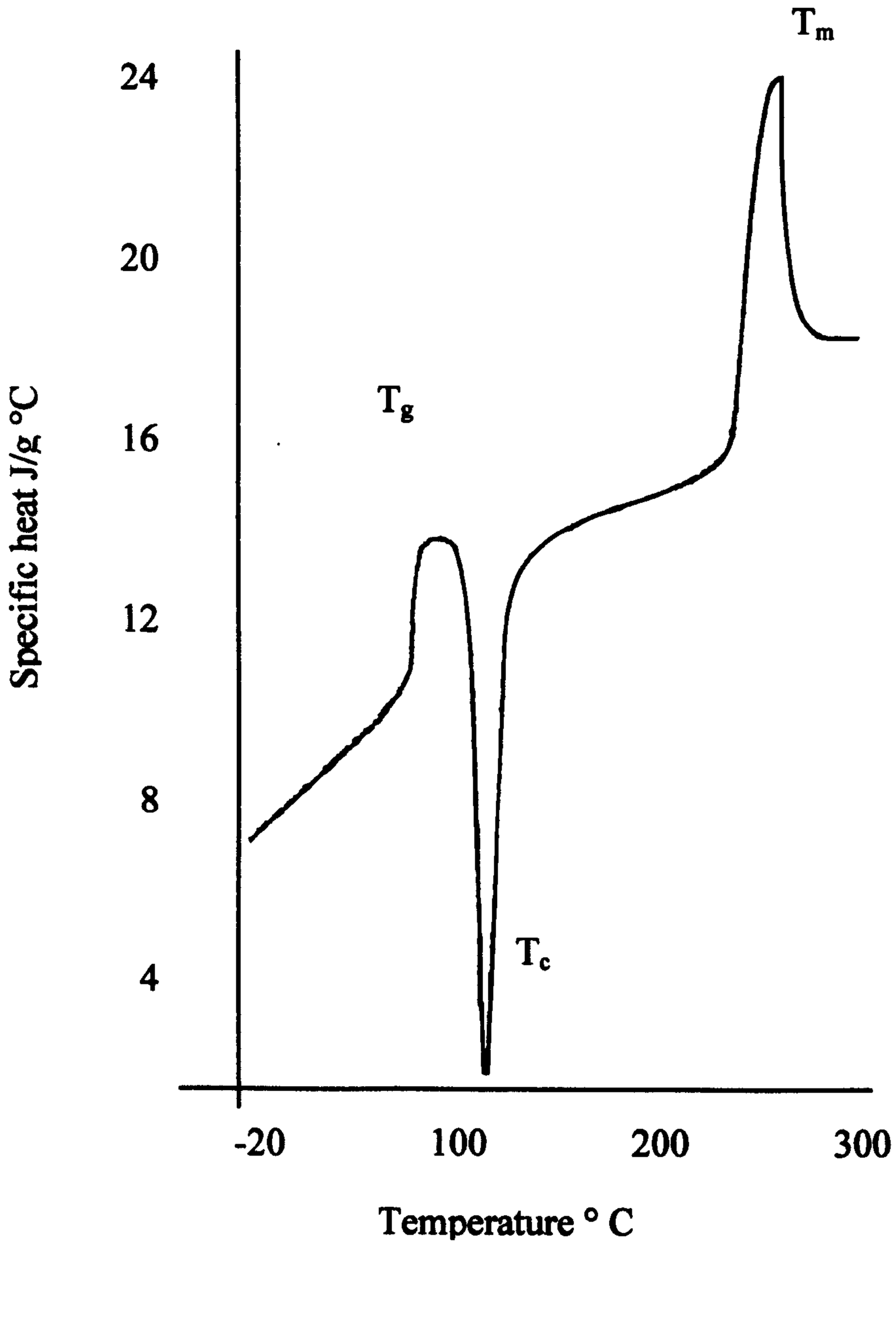

Figure 5: Example of a DSC Curve of PET

4.5 Light Scattering[57,58,59,60]

Light scattering is a useful technique, which is widely used to obtain the absolute molecular weights of polymeric samples. Light scattering occurs whenever a beam of light encounters matter. The nuclei and electrons undergo induced vibrations in phase with the incident light wave and act as sources of light that propagate in all directions. Light may also be scattered whenever it passes through a medium that is 'polarisable', or has a dielectric constant different from unity. The light interacts with the electrons bound in the material and re-radiates the light as scattered light. If the light experiences no energy loss the scattering is termed 'elastic'.

Light may also interact by changing the energy state of an electron in which case it is lost from the system rather than being scattered. This is referred to as absorption. Sometimes light 'lost' in this manner reappears later as light of a different wavelength (fluorescence or phosphoresce) or as heat.

In solutions, additional scattering arises from irregular changes in the density and refractive index due to changes in composition.

Light scattering was first investigated by the Irish physicist Tyndall in 1869.[61] It was not until 1871 however that a coherent theory was put forward by Lord Rayleigh.[62] He applied classical electromagnetic theory to the problem of scattering light in a gas. He showed that ~~the light scattered is inversely proportional to the number of~~ particles per unit volume and the wavelength of the incident light to the fourth power.

Rayleigh's theory assumed that each particle scattered as a point source independent of all others. This is not the case in liquids.

Debye showed in 1944 and 1947[63,64] that the amplitude of scattered light is proportional to the polarisability and hence the mass of the scattered particle.

$$KC/\Delta R_{90} = HC/\Delta\tau = 1/m + 2\,A_2C....$$

Equation 25: The Debye Equation

$$\text{Where } K = 4\pi^2n^2/N_o\lambda^4(dn/dc)^2$$

$$H = 32\pi^3 n^2/3N_o\lambda^4(dn/dc)^2$$

$\Delta\tau$ = Excess turbidity of the solution over the pure solvent

A_2C = The second virial coefficient

M = the mass of particle

ΔR_{90} = The change in Rayleigh ratio at 90°

In a polydisperse sample the heavier molecules contribute more to the scattering than the light ones.

When the size of the scattered particles exceeds $\lambda/20$ light hits different parts of the molecule at different times,

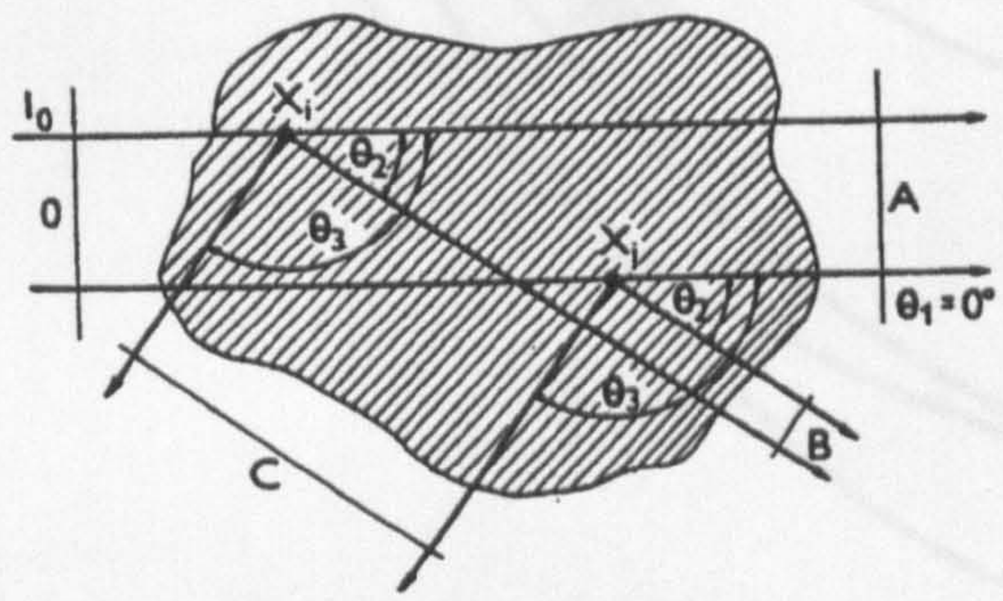

Figure 6: Light Scattering from a large particle

this means that light is striking these areas with different amplitude and phase. Thus the scattered light also has different amplitude and phase. This gives rise to interference between the scattered waves. Consequently the intensity of scattered light varies with the angle, θ.

This has been described by Debye and others as the particle scattering factor $P(\theta)$. This function varies depending on the size parameter.

$$P(\theta) = 1 - 1/3\ (R_G K)^2$$

Equation 26: The Particle Scattering Factor

Where $k = (4\pi n_o/\lambda)(\sin\theta/2)$

R_G= The radius of gyration

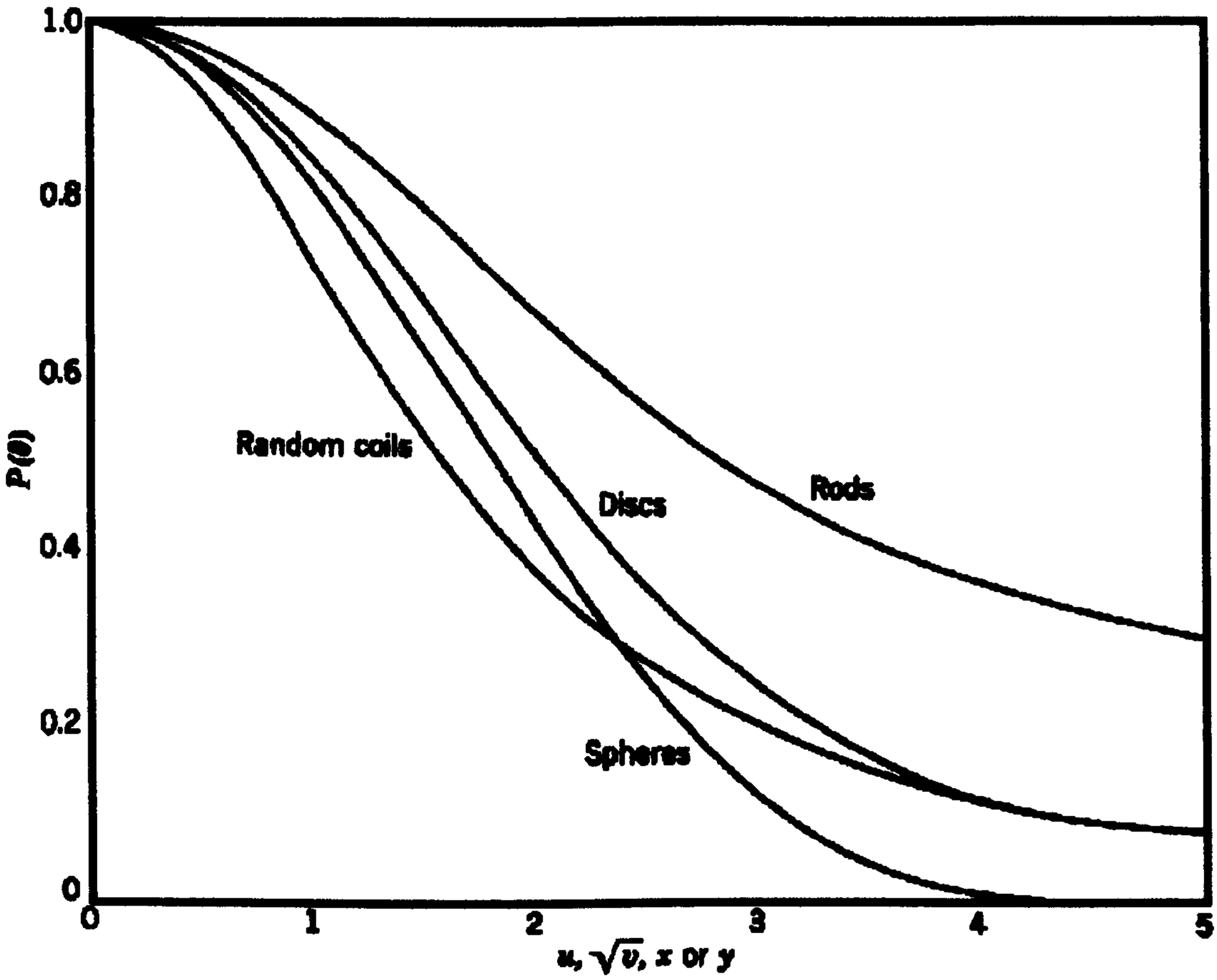

Figure 7: P(θ) as a Function of particle size

In cases where the scattered particles are far greater in size than the wavelength of the incidence light (*e.g.* in polymers) Debye's equation is modified by including P(θ).

$$. KC/\Delta R_{90} = HC/\Delta\tau = 1/mP(\theta) + 2\ A_2C \ldots.$$

Equation 27: Modified Debye Equation

This equation forms the basis for the determination of molecular weight in polymeric samples. For large particles and smaller polymers a simple plot of $KC/\Delta R_{90}$ against concentration of polymer solution, will upon extrapolation to zero concentration yield the reciprocal of the weight average molecular weight as the intercept and the second virial coefficient as the gradient. For larger polymers dissymmetry becomes

prevalent. Scattering is not the same in all directions and so the expression must be modified to take this angular effect into account (as above). Determination of $P(\theta)$ relies on assuming one of the models in Figure 7 above. A more satisfactory method is that put forward by Zimm in 1948.[65,66] This is a double extrapolation method where $KC/\Delta R_{90}$ is plotted against $\sin^2(\theta/2) + K'C$ (where K' is an arbitrary constant chosen to provide a convenient spread of data.) for each concentration at each angle. The plot is extrapolated to zero concentration and zero angle, as in Figure 8 below.

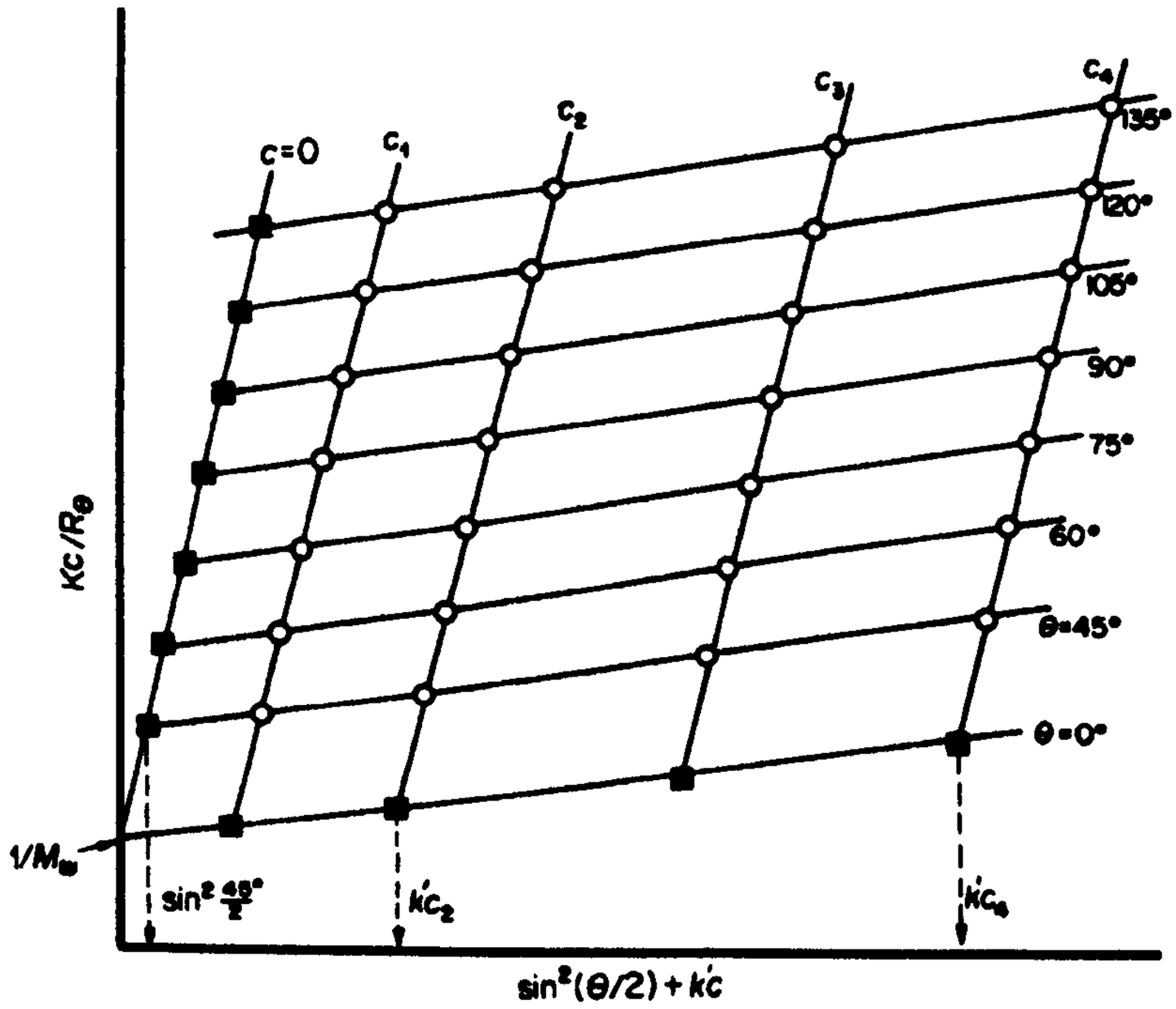

Figure 8: Zimm Plot

The intercept is $1/\overline{M}_w$ and the gradient of the line at zero concentration and zero angle yields the radius of gyration of the polymer.

$$R_g = S_i \overline{M}_w (\lambda'^2/16\pi^2)$$

Equation 28: Radius of Gyration

4.6 End-group Analysis

Many of the properties of branched polymers arise from the fact that there is a marked increase in the number of end-groups, on the polymer, for a specific unit volume. This is not, however, the only reason for using such analysis. End-group analysis opens the doorway to vast amounts of physical data about the branched polymer, including it molecular weight (weight average) and the degree of branching. End-group analysis, when applied to condensation polymers, usually involves chemical methods of analysis for the functional groups. Carboxyl groups in polyesters and polyamides are usually titrated directly with base in an alcoholic or phenolic solvent, whilst amino groups in polyamides are usually titrated with acid under similar conditions. Hydroxyl groups can be detected by I.R. spectroscopy, but a particularly elegant method, devised by Conix,[67] involves the conversion of these groups to carboxyl groups, using succinic anhydride allowing them to be determined by titration. An adaptation of this method, by Zimmerman and Kulbig[68] uses *o*-sulfobenzoic acid instead of the anhydride, and is reported to be far superior in terms of accuracy. The chemical methods used are often limited by the solubility of the polymer in solvents suitable for the titrations. The technique is also limited by the molecular weight of the polymer. Above ~ 25,000, a loss of precision often occurs due to the inability to purify the samples, and a loss of sensitivity, as the fraction of end-groups becomes too small, compared to the vast weight of polymer.

The total number of end-groups is given the symbol *E*. In the case of PET this can be defined as -

$$E = E_{OH} + E_{COOH}$$

Equation 29: Total Number of End-groups

This figure can then be used to calculate the physical parameters listed in the sections below.

4.6.1 Extent of Reaction

Conversion, P, (extent of reaction) can be calculated from knowledge of the number of end-groups present.

For a system containing bifunctional and trifunctional monomers P is given by -

$$P = 1 - E / 10^6 [M_b/2 - \rho(M_b/2 - M_t/3)]$$

Equation 30: Extent of Reaction, with Trifunctional Brancher

Where M_b and M_t are the molecular weights of the bifunctional and trifunctional monomers respectively and ρ is the composition parameter

If a monofunctional group is also present the expression becomes -

$$P = 1 - E / 10^6 [M_b/2 - \rho_t(M_b/2 - M_t/3) + (M_m - M_b/2)\rho_m]$$

Equation 31: Extent of Reaction, with Brancher and Endcapper

Where M_m is the molecular weight of the monofunctional monomer and ρ_t and ρ_m are the composition parameters of the trifunctional and monofunctional components of the system respectively.

4.6.2 Composition Parameter

The composition parameter is defined as the number of groups of initial x-functional units divided by the total initial number of functional units.

In the common case where there are only tri, and bifunctional groups present this is defined as -

$$\rho = 3N_t / (N_t + 2N_b)$$

Equation 32: Composition Parameter

Where N_t and N_b are the initial number of tri, and bifunctional monomers respectively.

If monofunctional groups are present then a series of composition parameters are required, and these are defined as follows:-

$$\rho_t = 3N_t / (3N_t + 2N_b + N_m)$$

$$\rho_b = 2N_b / (3N_t + 2N_b + N_m)$$

$$\rho_m = N_m / (3N_t + 2N_b + N_m)$$

Equation 33: Specific Composition Parameters

Where N_m is the number of monofunctional monomers initially present.

4.6.3 Branching Coefficient

The branching coefficient, α, was elucidated in 1941, by Flory.[12] He assumed that all functional groups have the same reactivity and that intramolecular reactions could be neglected.

$$\alpha = p\rho / 1 - p(1-\rho)$$

Equation 34: Branching Coefficient

At the critical value of branching, α_c, gelation becomes possible. α_c is defined as -

$$\alpha_c = 1/(f-1)$$

Equation 35: Critical Branching Coefficient

(Where f is the functionality of the branching agent)

Therefore, we can see that for a trifunctional branching agent, such as trimesic acid, the critical value would be 0.5.

At this point the extent of reaction, P_C is -

$$P_C = 1 / (1+\rho)$$

Equation 36: Critical Extent of Reaction

4.6.4 Number-average Degree of Polymerisation

The number-average degree of polymerisation, $\bar{X}_n$, can now be defined -

$$\bar{X}_n = (3 - \rho) / (3 - \rho - 3p)$$

Equation 37: Number-average Degree of Polymerisation

4.6.5 Number-average Molecular Weight

The number-average molecular weight, $\overline{M}_n$, is given by -

$$\overline{M}_n = x_n M_o = (3M_b + \rho(2M_t - 3M_b)) / (3 - \rho - 3p)$$

Equation 38: Number-average Molecular Weight

where M_o is the molecular weight of the average monomeric unit, as defined below.

$$M_o = (M_b N_b + M_t N_t) / (N_b + N_t) = (3M_b + \rho(2M_t - 3M_b)) / (3 - \rho)$$

Equation 39: Average Molecular weight of Monomeric Unit

4.6.6 Weight-average Molecular Weight[69, 70,80]

The weight-average molecular weight can now be calculated -

$$\overline{M}_w = \overline{M}_{w,o} + [p f_{n,o} M_o^2] / (\overline{M}_{n,o}[1 - p(f_{w,o} - 1)])$$

Equation 40: Weight-average Molecular Weight

Where $\overline{M}_{w,o} = M_b W_b + M_t W_t + M_m W_m$, is the weight-average molecular mass of the initial monomers and $f_{w,o} = 2\rho_b + 3\rho_t + \rho_m$, is the weight-average functionality of the same mixture, $f_{n,o} = 2(N_b/(N_t+N_b)) + 3(N_t/(N_t+N_b))$ is the number-average functionality and W_b, W_t, and W_m are the initial weight fractions of mono-, bi- and trifunctional monomers respectively.

4.6.7 Number-average Branching Density

In the case of polydisperse polymers with randomly distributed trifunctional and monofunctional units, the number-average degree of branching i.e. the average number of branches per molecule, $\overline{B}_n$, can be calculated as a function of ρ_m and ρ_t and the conversion p:

$$\overline{B}_n = 2\rho / (3 - \rho - 3p)$$

Equation 41: Number-average Branching Density

It is often useful to consider the weight-average branching density, $\overline{B}_w$ -

$$\overline{B}_w = 3\overline{B}_n\overline{M}_w / 2\overline{M}_n$$

Equation 42: Weight-average Branching Density

4.6.8 Intrinsic (Inherent) Viscosity

Three further expressions for the intrinsic viscosity are listed below -

$$(a)\ \log\eta_{o(linear)} = -12.96 + 3.54\log\overline{M}_w$$

$$(b)\ \log\eta_o = 4.36 + 4.78\log[\eta] + 0.037\log\overline{E}_w$$

$$(c)\ \log\eta_o = 2.13 + 4.17\log[\eta] + 0.456\log\overline{M}_w$$

Equation 43: Intrinsic Viscosity Expressions

4.7 Dynamic Mechanical Thermal Analysis (DMTA)[54,56,71]

This is a dynamic mechanical method that assesses the structure and properties of solids and visco-elastic liquids, their dynamic moduli and damping. Changes in these parameters are studied as a function of temperature (DMTA) and the frequency of the applied stress (dynamic mechanical spectrometry, DMS).

The method has great sensitivity in detecting changes in internal molecular mobility and in probing phase structures and morphology. Secondary relaxations in the glassy state can also be studied as well as the glass transition process.

The DMTA imposes a sinusoidal stress on a sample in the bending, shear or tensile mode and determines the sample modulus and tan δ as a function of temperature and/or frequency.

When the stress is applied to a perfectly elastic solid the deformation (and hence the strain) occurs exactly in phase with the applied stress. In the case of a completely viscous material the deformation lies 90° behind the applied stress.

When a sinusoidal stress is applied to a visco-elastic material it behaves neither as a perfectly elastic nor a perfectly viscous body, and the resultant strain lags behind the stress by some angle δ, where $\delta<90°$.

The magnitude of this loss angle is dependent on the amount of internal motion occurring in the same frequency range as the imposed stress.

The complex dynamic modulus (E^* for bending/tensile measurements, G^* for shear measurements) is given by

$$E^* \text{ or } G^* = \frac{\text{Stress Amplitude}}{\text{Strain Amplitude}}$$

Equation 44: Complex Dynamic Modulus

This however does not take phase into account. It is therefore more convenient to define separate elastic and viscous components of the deformations.

The storage or elastic modulus (E' or G') is defined as

$$E' = \frac{\text{Amplitude of in phase stress component}}{\text{Amplitude of in phase strain component}}$$

Equation 45: Storage Modulus

The loss or viscous modulus (E" or G") is defined as

$$E'' = \frac{\text{Amplitude of out of phase stress component}}{\text{Amplitude of out of phase strain component}}$$

Equation 46: Loss Modulus

The storage modulus corresponds to completely recoverable energy where as the loss modulus is the viscous response corresponding to the energy lost through internal motion.

The tangent of the loss angle, tan δ is dimensionless and is equal to the ratio of energy lost (dissipated as heat) to the energy stored per cycle.

$$\text{Tan}\delta = \frac{\text{Loss Modulus}}{\text{Storage Modulus}} = \frac{E''}{E'}$$

Equation 47: Tangent to the Loss Angle

A material may be scanned over a range of temperatures at various imposed frequencies. A loss maximum in the temperature scan is observed when the frequency of a motional process coincides with that of the measured frequency. With increase in measurement frequency the loss process is found at higher temperatures, where the molecular motion is faster.

5 Branched PET

5.1 Literature Examples

With a view to replicating some of the unusual properties of dendrimer molecules whilst avoiding the difficulties associated with their stepwise synthesis, the synthesis of hyperbranched polyesters *via* a single step condensation polymerisation was investigated by Feast, *et al.*[72] The monomer used in this work was derived from 5-hydroxyisophthalic acid (structure 2, page 43) and was polymerised under similar conditions to those used in PET production. In fact prior to this, some work had already been reported on branched PET type structures. However although PET is a very important commodity polymer and has been for a number of years, up until 1976 no data had been published on branched PET. It was then that Manaresi *et al*[73] published a paper examining the relationships between the various viscometric parameters as a function of the extent of reaction and the percentage of branching agent added to the reaction. The agent used in this case was trimethyltrimesate (structure 3, page 43). An ester-interchange reaction was used to synthesise their monomer, followed by a polycondensation reaction under standard conditions. Twenty-eight polymers were made and studied, although in practice these consisted of only 4 types of polymer with 7 repeats of each.

Manaresi found that the intrinsic viscosity, [η], and the Newtonian melt viscosity, [η_o], increased with increasing molecular weight but decreased with increasing branching density, [B_w]. These results were born out by previous findings based on other polymers.[74,75,76] Similar results have been obtained by Peticolas,[77] Schreiber[78] and Ram[79] in the case of polyethylenes with long branches.

However, it was found that if polymers of equal intrinsic viscosity were compared then Newtonian melt viscosity increases with branching density.

Since this paper in 1976 very little has been done in this field, even though PET continues to be a highly marketable commodity.

In 1986 Manaresi continued this work[80] with an investigation into the synthesis and characterisation of highly branched PET. Here he added the monofunctional reagent, methyl 2-benzoylbenzoate (structure 4, page 43) to the reaction melt. It was hoped

that this reagent would act as a chain-stopper and thus prevent gelation. Again the trifunctional reagent trimethyltrimesate was used to generate branches, and again rather few samples (4) were isolated and studied. Nevertheless the work seemed to confirm the theoretical treatment of Flory[8] and Stockmayer,[81,82,83] which predicted that a monofunctional reagent in a system that also contained a trifunctional reagent would shift the critical conversion, p_c, at which gelation occurs, towards higher values. This means that although gelation was still possible, it would only occur after longer periods of time. Manaresi showed that polymers previously produced under normal polycondensation conditions that had gelled did not gel when a monofunctional monomer was added.[80] Investigation of these polymers properties showed them to be consistent with polymers prepared without the monofunctional group, *i.e.* a lowering of the melt and intrinsic viscosities was observed with increasing branching density.

In 1989 Munari[84] extended this work with an investigation into the rheological properties of highly branched PET which had been end-capped with methyl 2-benzoylbenzoate.

More recently, in 1997 Rosu investigated the formation of branched PET using glycerol and pentaerythritol (structure 10, page 45) as the chain branchers, and dodecan-1-ol and benzyl alcohol as chain stoppers.[85]

In 1998, Jayakannan[86] studied the difference in thermal properties between standard linear PET, linear PET whose backbone symmetry is broken by copolymerisation with the chain-extender ethyl-4(2-hydroxyethoxy)benzoate (structure 5, page 43), PET branched with the AB_2 brancher ethyl bis-3,5(2-hydroxyethoxy)benzoate (structure 6, page 43), and PET which had been 'kinked' by the introduction of the bent chain-extender ethyl-3(2-hydroxyethoxy)benzoate (structure 7, page 43). He concluded that the introduction of any comonomer decreases the crystallisation and the melting temperatures. The glass transition temperature is also lowered but to a much lesser extent. Branching has the greatest effect on the polymers thermal properties with 'kinking' and linear disruptions having approximately the same effect.

Overall however the number of branched polymers upon which all of these findings are based is very low (~ 30 samples in total in the literature). There is a need to

examine these systems in much more detail on a laboratory scale, and to provide a methodology for scale-up for more extensive studies at a technical level.

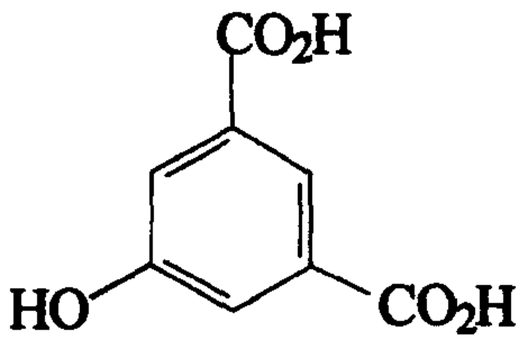

Structure 2:
5-hydroxyisophthalate

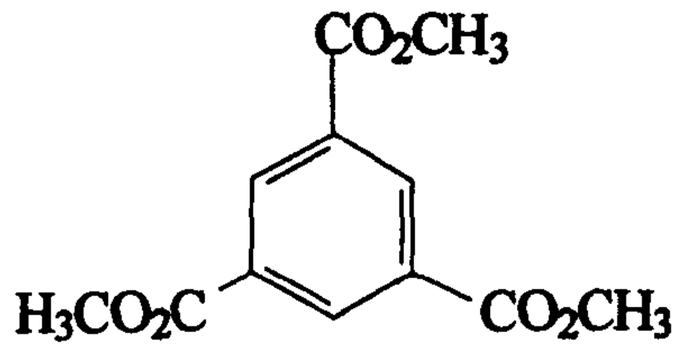

Structure 3:
Trimethyltrimesate

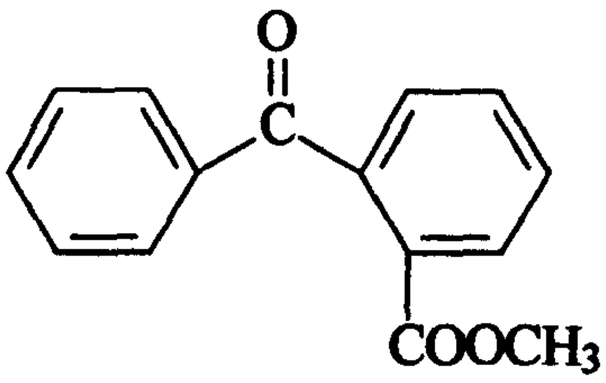

Structure 4:
methyl 2-benzoylbenzoate

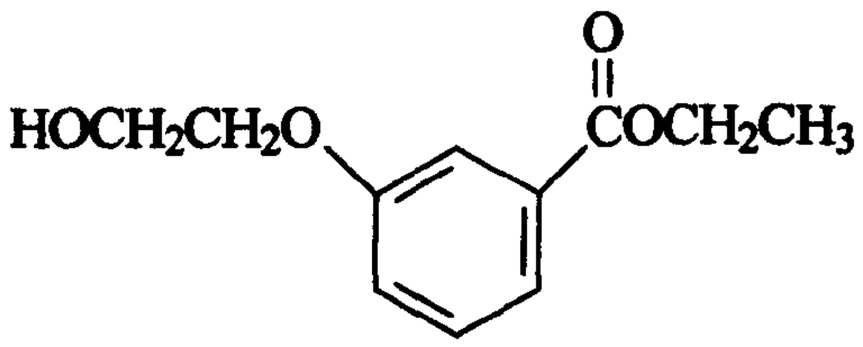

Structure 5:
Ethyl 3(2-hydroxyethoxy)benzoate

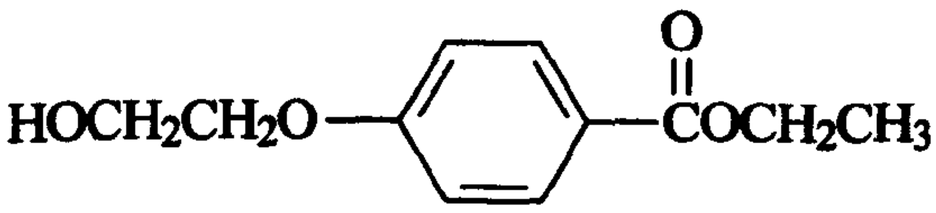

Structure 6:
Ethyl 4(2-hydroxyethoxy)benzoate

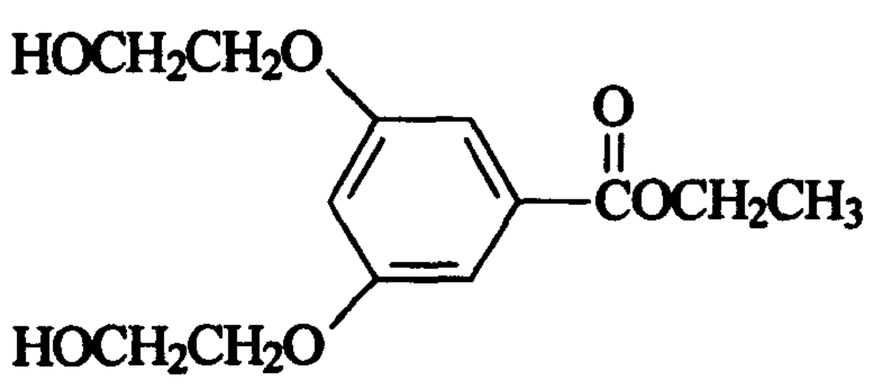

Structure 7:
Ethyl bis-3,5(2-hydroxyethoxy)benzoate

Figure 9: Literature Examples

5.2 Project Objectives

It can be seen from previous work that branched PETs appear to have a number of interesting properties. If such syntheses could be applied on an industrial scale, the modified properties produced could have profound implications in many fields, in particular in polymer coatings. This could provide novel opportunities for the plastics industry.

There is of course a lot of work still to be done before any of the techniques attempted could be applied to plant scale production. This current work will concentrate on trying to move forward towards that goal.

There are a number of modifications that could be applied to PET production, which could result in a mixture of linear and branched polymers. This mixture of polymer architectures may be adequate enough to provide a significant change in the properties of the materials.

5.2.1 Core Molecules

One of the most obvious ways of modifying PET to give branched structures is to simply add a branching agent to the melt, the branching agent would be a polyfunctional molecule with functional groups consistent with those present in the linear reaction. Some of the core molecules that we proposed to investigate in this project are shown in Figure 10.

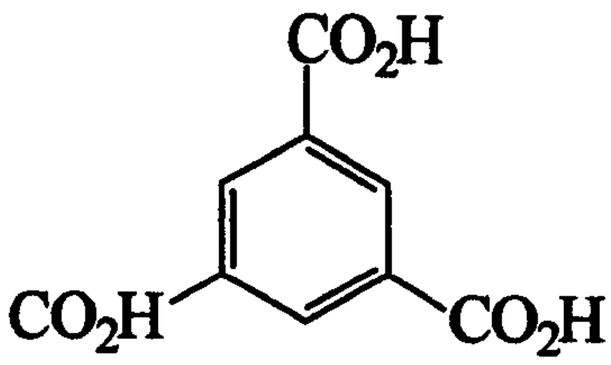

Structure 8:
1,3,5 - benzene tricarboxylic acid
(Trimesic Acid or B3CA)

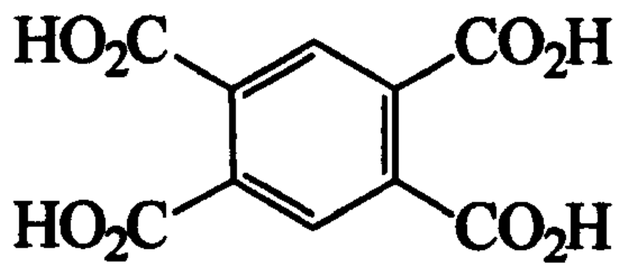

Structure 9:
1,2,4,5 - benzene tetracarboxylic acid
(Pyromellitic Acid or B4CA)

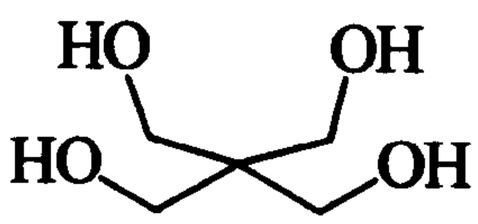

Structure 10:
Pentaerythirol

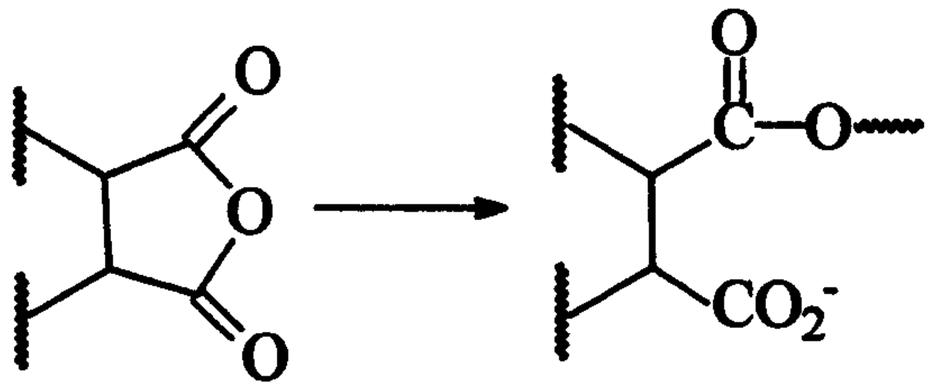

Structure 11:
Anhydrides

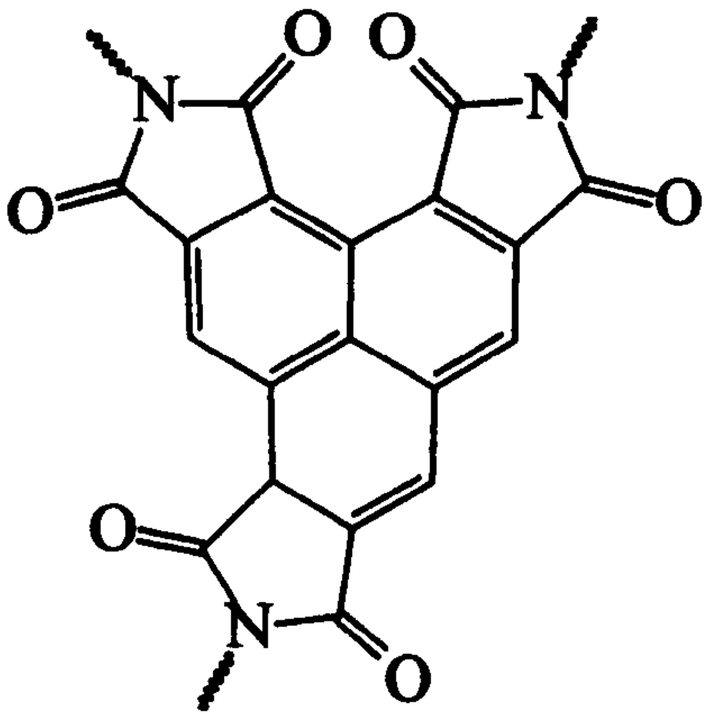

Structure 12:
tris-phthalimide

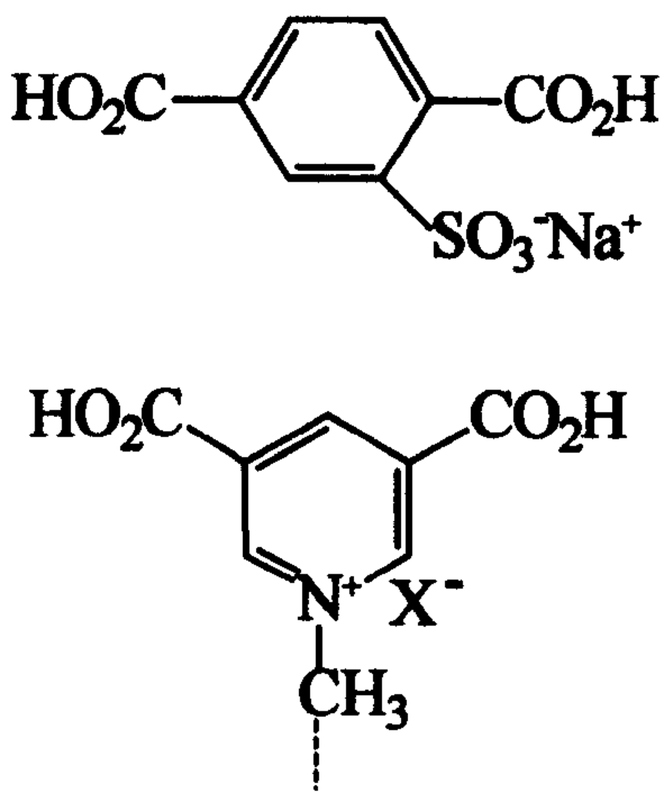

Structure 13:
Ionic branchers

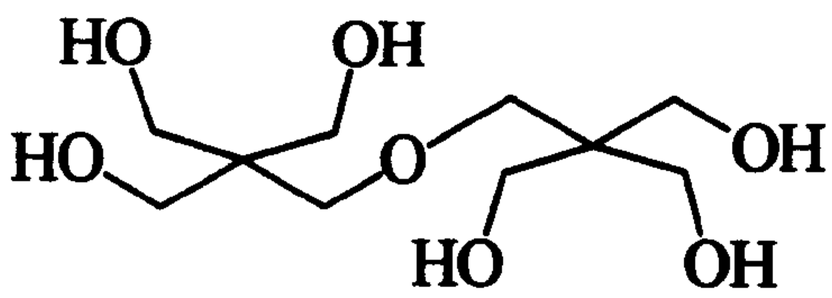

Structure 14:
Di-pentaerythritol

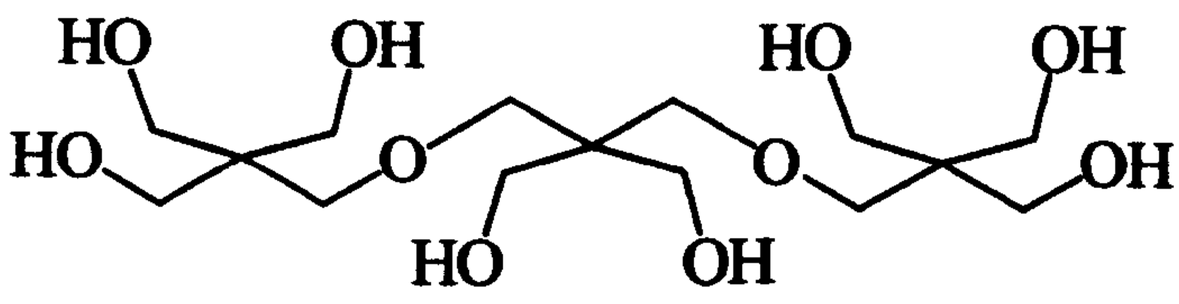

Structure 15:
Tri-pentaerythritol
Figure 10: Branching Agents

Pre-formation of Oligomeric Polymer Cores

A second method for the production of branched PET is to pre-form oligomeric cores, by reaction of the core molecules with oligomeric chains. These oligomers might then be reacted in a standard polycondensation reaction, to give branched PET. A variation of this strategy involves the complete polymerisation of linear PET, isolation of the product and then mixing with a branching agent and further polycondensed to give branched PET. Under normal circumstances it is envisaged that ester interchange may occur in the former example, possibly giving rise to gelation. Investigations of this method therefore, would also involve investigation of additives, which would promote esterification, but would inhibit transesterification.

5.2.2 Branching Strategy

In order to produce a polymer which is sufficiently branched a suitable multi-functional agent must be added to the melt.

There are two possibilities for linear condensations based on monomers with two different functional groups (A and B): -

A-A + B-B monomer systems, and A-B monomer species

A-A + B-B Synthesis

For A-A + B-B reactions to branch a tri-functional, A_3 or AB_2, (or greater) branching agent must be added to the melt. This can lead to problems. As the chains grow cyclisation and crosslinking can occur, causing the melt to gel. This produces a polymer, which is not processable.

For an A_3 brancher -

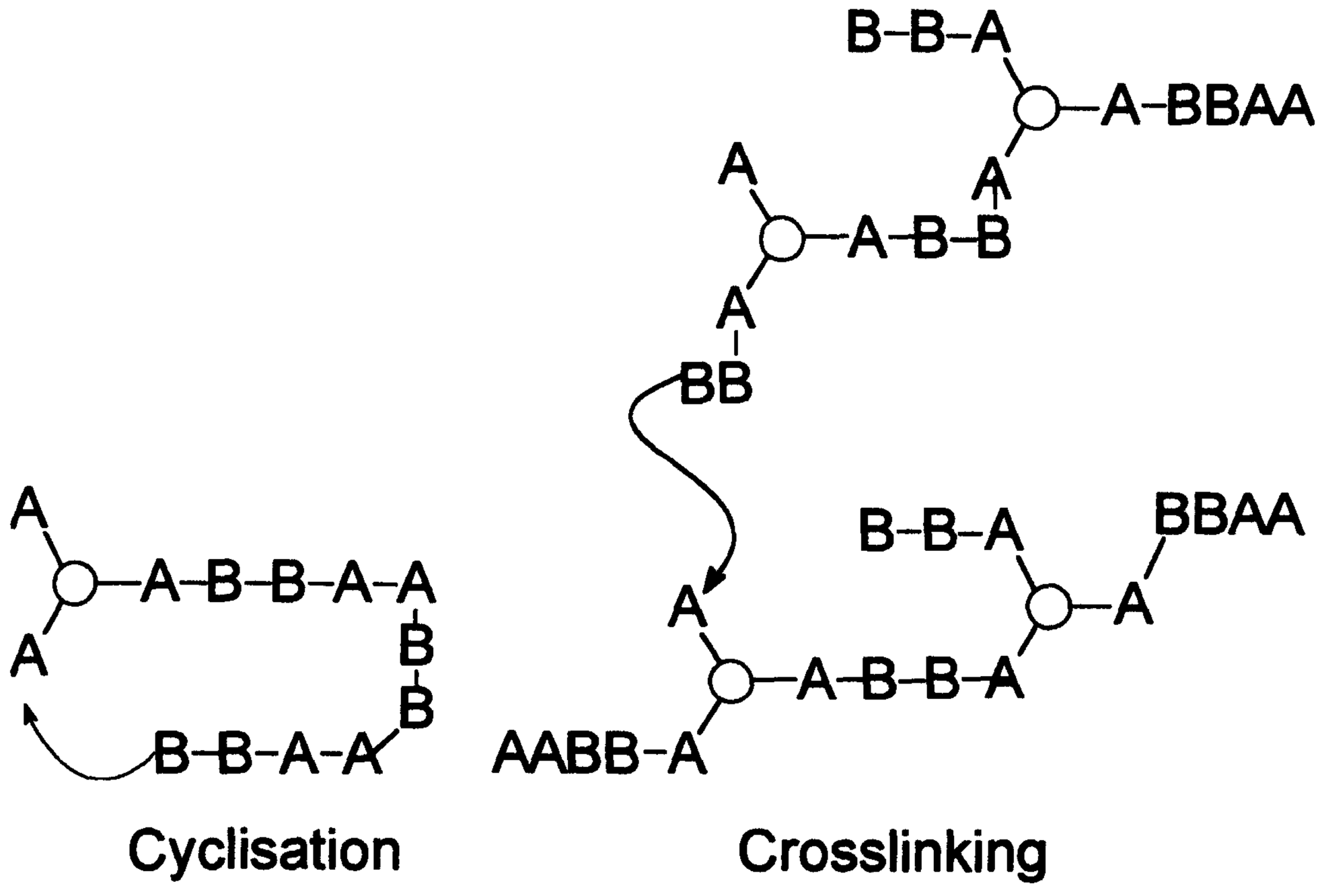

Figure 11: Cyclisation and Crosslinking in A-A + B-B Polymerisation

The standard PET synthesis is a special case of this reaction, where the monomer, BHET, is in a precursor form AA-BB-AA. Under polycondensation conditions this reacts in a concerted manner with another AA-BB-AA molecule, with elimination of AA. This reaction is thus susceptible to the same problems as the standard AA + BB reaction, *i.e.* cyclisation and crosslinking, when *e.g.* A_3 brancher is added.

A-B Synthesis of PET-Type Molecules

A-B type monomers can be reacted with similar branching agents to those used above. If an A_3 brancher is used, cyclisation and cross-linking are not possible due to the sequence of groups in the oligomers formed. As the growing oligomers form, they will always have the same functional group at all chain ends as shown in Figure 12 below. However, cyclisation can still occur if an AB_2 type brancher is used **(Figure 13)**.

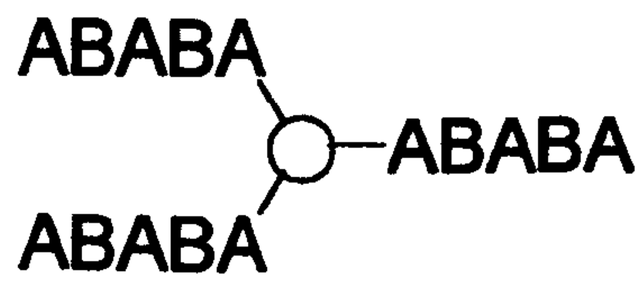

Figure 12:A-B Monomer Branched with A_3 Brancher

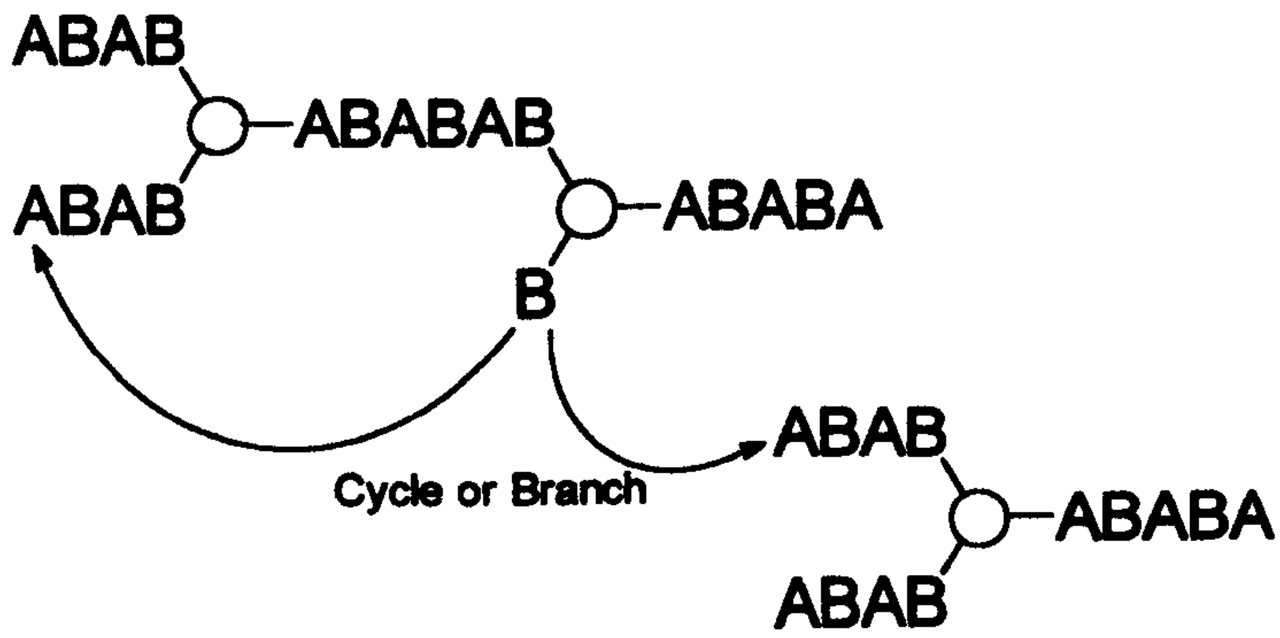

Figure 13:A-B Monomer Branched with AB_2 Brancher

5.2.3 End-Cappers

In any of the above methods of synthesising branched polyesters, the molecular weight can be controlled by the introduction of an end-capper (or chain-stopper) into the melt. The end capper is a monofunctional monomer which, can react with growing chains, but cannot propagate the reaction; thus they limit molecular weight and can avoid gelation.

The end-capper must be involatile if it is to stay in the reaction vessel and not be distilled out during polycondensation. The end-capper must also not interfere with the structure of the resultant polymer. In the case of PET, the most suitable end-capper, from this point of view, is monomethyl terephthalate (MMT); this may, however, be too volatile under polycondensation conditions. Other possible end-cappers include, fatty acids (stearic) and fatty alcohols.

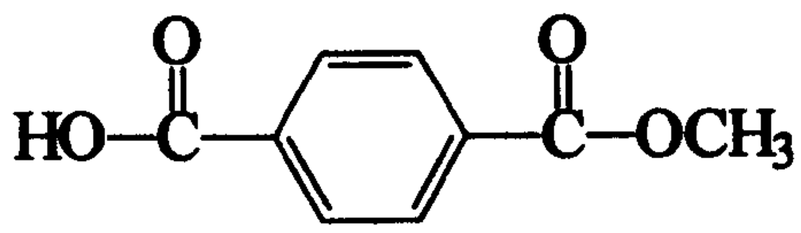

Structure 16: Monomethyl Terephthalate

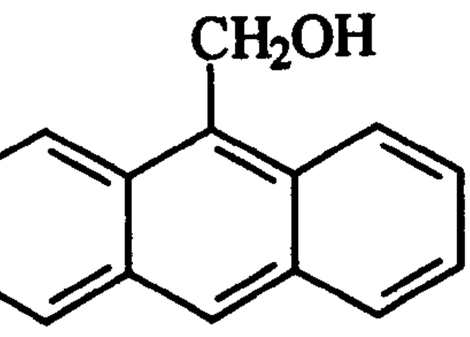

Structure 17: Stearic acid

Structure 18: 9-Anthracene Methanol

5.2.4 Characterisation

It is envisaged that characterisation of the polymers synthesised during this project will be achieved using the following methods: -

1. Reaction Torque:- During the polycondensation reaction the torque exerted on the stirrer by the liquid polymer is monitored. This torque gives some idea of the change in melt viscosity during the reaction.
2. Solution Viscosity:- The viscosity of a range of different concentrations of polymer solution can be is measured to give the intrinsic viscosity. This value can be used to give $\overline{M}_v$ for linear polymers.
3. End-group Analysis:- The conversion of the end-groups of the polymers to acid groups and subsequent potentiometric titration can yield the number of end-groups on the polymer. From this value, theoretical calculations of many branching, molecular weight and viscosity parameters can be determined.
4. Differential Scanning Calorimetry:- This method can be used to define the thermal characteristics of each polymer, in terms of the glass transition, T_g, crystallisation, T_c, and melting point, T_m, temperatures.
5. Melt Viscosity:- The melt viscosity can be investigated in terms of the flow and oscillatory properties of the polymer.
6. Light Scattering:- Light scattering can be used to determine the absolute molecular weight of a polymeric sample. It can also be used to determine the radius of gyration and the diffusion coefficient of the polymeric species.
7. Dynamic Mechanical Thermal Analysis:- This form of analysis can be used to characterise the mechanical properties of a material. The method has great sensitivity in detecting changes in internal molecular mobility and in probing phase structures and morphology. Secondary relaxations in the glassy state can also be studied as well as the glass transition process.

6 Results and Discussion

6.1 Initial reactions

Initially a programme of linear polycondensations using BHET and later ICI's 'monomer' (an oligomeric form of BHET ~ 7 units long) were embarked upon. This study was based on an earlier procedure,[87] which was modified during the course of the test matrix until the current standard procedure was evolved. The rig during this period was still difficult to handle and vacuum leaks were not uncommon. The final vacuum was difficult to obtain and this resulted initially in the production of low molecular weight material. However, at the end of this stage it was thought that the rig was working to its full potential, and that the polymers produced were of a reasonable standard.

Viscometric analysis was carried out only on the last three polymers, as these represented the rig running under what was considered to be standard conditions; no torque data was available for the other initial experiments. Torque differential refers to the difference in torque acting on the reactor's stirrer at end of the reaction, with respect to that at the beginning of the reaction and was provided as a direct read-out from the stirrer's LCD. It was used as a guide to the change in viscosity in the melt during polycondensation reactions.

The tests listed below were all carried out according to conditions set out in ICI's standard operating procedure (S.O.P).[88] Over a 3 hour period, vacuum was slowly applied whilst raising the reactor temperature to 290 °C.

Test code	Starting material	Torque differential (N cm)	I.V.[1] (ml g^{-1})	$\overline{M}_w$ [2] (D)
PET 1	BHET	17.6	0.48	9000
PET 2	BHET	13.1	0.44	8000
PET 3	'Monomer'	11.3	0.59	13000
PET ICI	'Monomer'	-	0.72	17000

Table 1: Linear Polycondensation Reactions

[1] I.V. = Intrinsic Viscosity at 25°C in TFA
[2] $\overline{M}_w$ = Molecular weight average as calculated from Intrinsic Viscosity data

The viscosity data shows that the polymers produced at this stage, particularly those from BHET, were of lower molecular weight than the commercial sample. This is to be expected, due to the sophisticated large-scale equipment used in the industrial set-up. There is however good correlation between the viscosities of like polymers.

A plot of relative torque against reaction time is given in Graph 1.

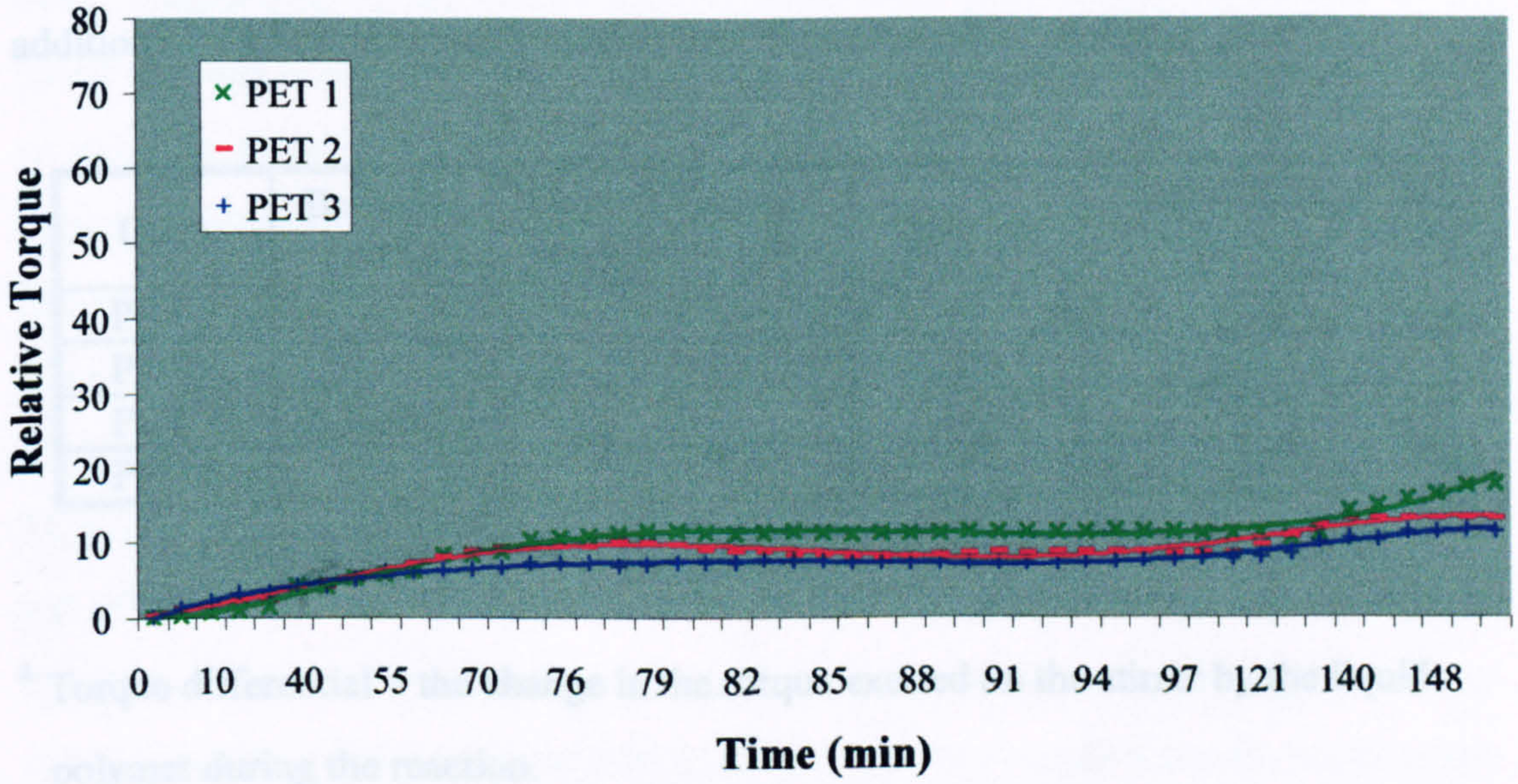

Graph 1: Relative Torque Data During Polymer Synthesis

The torque data illustrates how the viscosity in the melt changed over the course of each experiment. The trends show that the viscosity of the 'monomer' reaction, PET 3, changed less than in the BHET reactions. This is not surprising as the starting 'monomer' units are of longer chain length, and thus in a more condensed state.

6.2 Branched BHET Reactions

PET was branched using a variety of branching agents, in ratios of 1/16 - 2 weight percent (Wt%). Initially experiments concentrated on branching with trimesic acid (Structure 8, Page 45). Later the program was extended to include other multi-functional agents

6.2.1 Trimesic acid Branched Polymers

Based on BHET, these reactions involved the simple addition of varying amounts of trimesic acid (benzene tricarboxylic acid (B3CA)) to the reaction mixture. As before the tests listed below were all carried out according to conditions set out in ICI's standard operating procedure[88] (S.O.P). Vacuum was slowly applied over a 3 hour period whilst raising the reactor temperature to 290 °C. In later reactions the time of addition of the brancher was varied to investigate the effect of this on gelation

Code	Brancher (Wt%)	Time of brancher addition (min)	Gelation	Torque differential (N cm)[a]
PET 5	2	0	✓	76
PET 6	1	0	✓	23.8
PET 7	0.5	0	✓	38.7
PET 8	0.25	0	✓	38.5

Table 2: Trimesic acid Branched Polycondensation Reactions

[a] Torque differential = the change in the torque exerted on the stirrer by the liquid polymer during the reaction.

A plot of relative torque against reaction time is given in Graph 2.

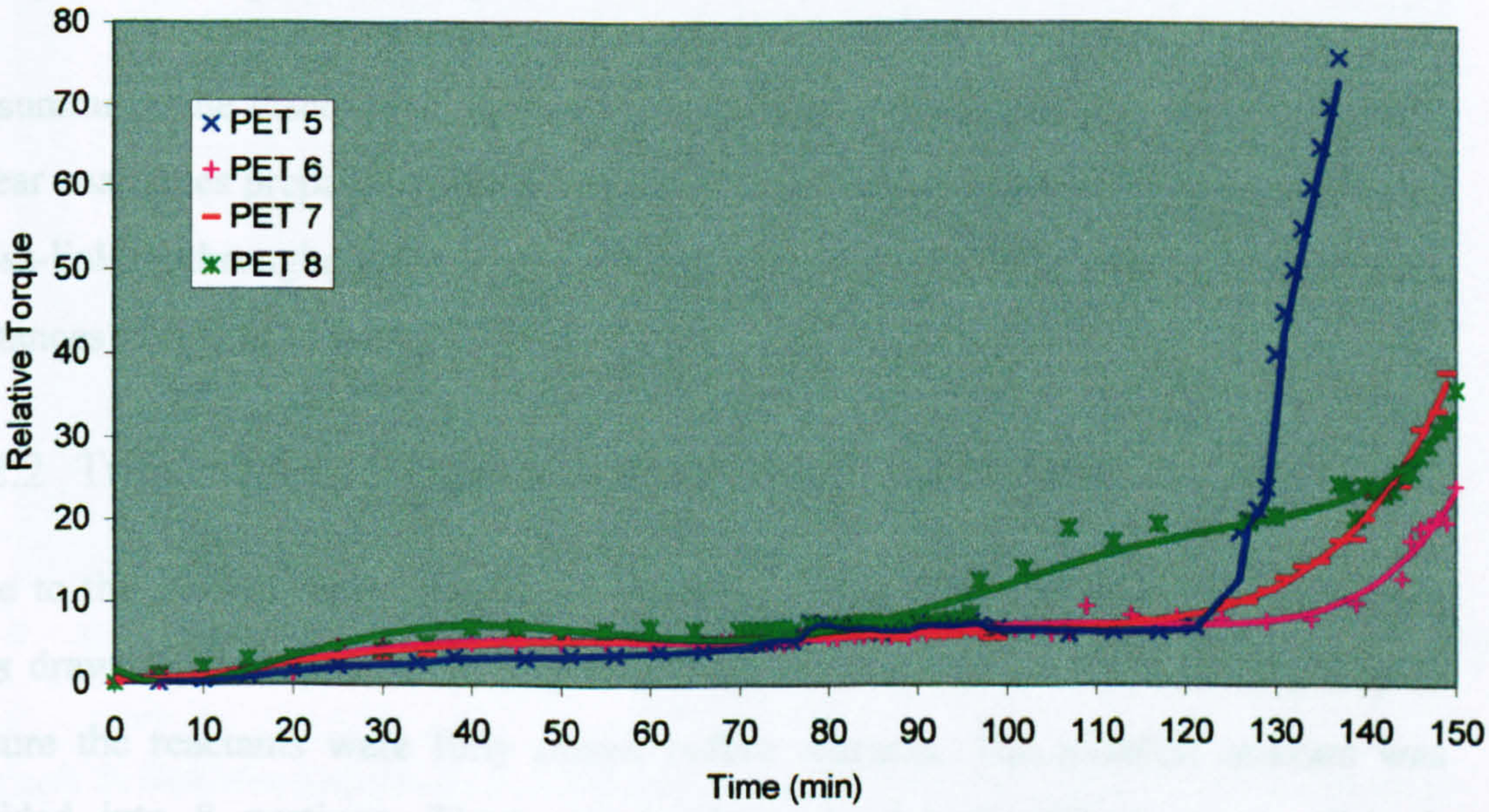

Graph 2: Relative Torque Data for Trimesic acid Branched Polymers

Initial polymers in this series showed signs of gelation to varying extents. PET 5 (2% chain-brancher) was the worst effected. It became so viscous that it wrapped round the stirrer jamming it and forcing the run to be ended 40 minutes early. The isolated polymer appeared as a hard and strong plastic material. It was completely insoluble when added to TFA, and merely swelled. On filtering, 100% of the polymer was recovered as a soft gel. Reactions PET 6, 7 and 8 went to completion and extruded easily. Superficial visual examination showed these polymers to be similar to the linear samples made in the initial tests. However, on dissolution, some small amount of gel was found in each case (< 3%, diminishing in order of percentage chain brancher present). This prevented viscometric measurements from being made. Dissolution was attempted again with different samples from these batches. This time some dissolved completely, whilst some again showed signs of gelation. This shows inconsistency in the sample and the polymer produced was clearly not homogeneous. This may be due to inefficient stirring in the reactor. The reactants were added one on top of the other, leaving all the brancher in one region. The torque data (Graph 2) indicates that after an initial increase, the melt viscosity of the polymers stays approximately constant until the time at which vacuum is applied and the temperature ramped up. This indicates that the major part of the polycondensation occurs beyond this point. In theory, this should give time enough to mix the reactants properly and thus give a homogeneous sample.

In summary, the viscosity in the melt was seen to increase relative to that seen with linear analogues prepared without brancher. Levels of brancher of 2% upwards cause cross-linking throughout the whole polymer sample whilst with lesser amounts some instances of localised gelation occur.

6.2.2 Trimesic acid Branched Polymers with Ballmilling

Due to the inconsistency in gelation observed in the initial reactions, a test matrix was drawn up to repeat these reactions, with the addition of a ball-milling step to ensure the reactants were fully mixed before reaction. The reaction mixture was divided into 8 portions. These were subjected to ball milling in a - Fritsch Pulvetisette®. Each portion was milled for 30 minutes and then combined with the

next portion and milled for a further 30 minutes. This was repeated until 4 portions had been milled together. The mixture was removed and the next 4 portions were mixed. The portions were then combined in the test-vessel before reacting as normal. Reactions PET 9 and 10 were milled in only two portions for 20 minutes each.
In one instance (PET 10) an additional one-hour stirring time was added to the induction period of the polycondensation reaction in an attempt to further guarantee homogeneity.

Code	Wt% Brancher	Induction Period	Torque Differential (N cm)	Gelation	I.V.[1] ($ml\ g^{-1}$)	$\overline{M}_w$[2] (D)
PET 9	1	40	57.9	✓	-	-
PET 10	2	100	61.6	✓	-	-
PET 11	2	40	56.0	✓	-	-
PET 12	1	40	59.5	✓	-	-
PET 13	0.5	40	9.9	×	0.23	3000
PET 14	0.25	40	4.3	×	0.15	1500

Table 3: Ball-Milled Polycondensation Reactions

[1] I.V. = Intrinsic Viscosity at 25 °C in TFA
[2] $\overline{M}_W$ = Molecular weight average as calculated from Intrinsic Viscosity data

Plots of relative torque against reaction time for these reactions are given in Graph 3

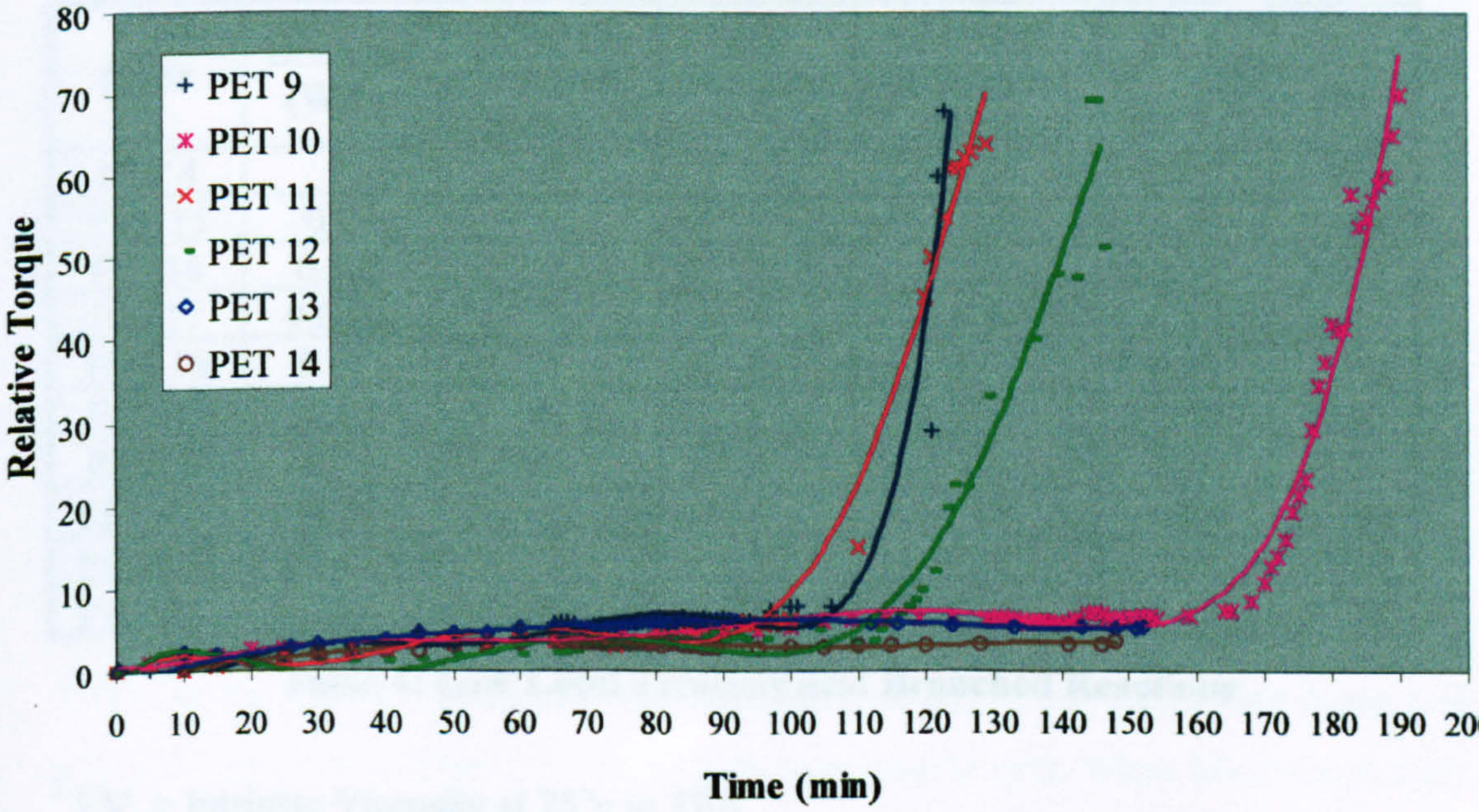

Graph 3: Relative Torque Data for Polymers Prepared from Ball-Milled Precursors

Graph 3 shows that at higher levels of branching agent, *e.g.* 1 and 2 %, the use of ball milling had no effect on the gelation of the polymer. At lower levels, *e.g.* 0.5 %, there appears to have been some effect - *i.e.* no gelation was noted. Extension of the induction period (PET 10) appeared to have a detrimental effect on the polymer, with the rig seizing up 21 minutes before scheduled shutdown. However, this could have just been the result of using 2 % branching agent.

The solution viscosity data (Table 3), for the non-crosslinked samples (PET 13 and 14) is lower than that of commercially available ICI or 'in house' PET. This suggests that branching of the polymer has indeed occurred, although independent $\overline{M}_w$ determination is required to verify this (by elimination of the possibility of the material being merely low molecular weight).

6.2.3 Low Level Trimesic acid Branching

Since higher levels of branching agent caused gelation, a study of the effect of lower levels (0.0625% - 0.25%) of brancher was initiated. The initial four reactions (PET 4, 15–17) followed the standard operating procedure, later reactions (PET 18 -21) varied the time of addition of the branching agent.

Code	Brancher (Wt%)	Time of brancher addition	Gelation	Torque differential (N cm)	I.V.[1] ($ml\ g^{-1}$)	$\overline{M}_w$[2] (D)
PET 4	0	0	×	8.4	0.40	6900
PET 15	0.25	0	×	10.5	0.45	8300
PET16	0.125	0	×	7.2	0.39	6600
PET17	0.0625	0	×	6.4	0.35	5600
PET 18	0.125	0	×	8.0	0.41	7100
PET 19	0.25	40	×	7.0	0.40	7000
PET 20	0.25	85	×	4.8	0.48	9100
PET 21[3]	0.25	150	×	29.8	0.90	24100
PET 33[3]	0.25	0	×	17.5	0.51	10100
PET 34[3]	0	0	×	17.4	0.50	9700

Table 4: Low Level Trimesic acid Branched Reactions

[1] I.V. = Intrinsic Viscosity at 25°c in TFA
[2] $\overline{M}_W$ = Molecular weight average as calculated from Intrinsic Viscosity data
[3] These reactions were run for an additional 30 min after full vacuum was achieved.

A plot of relative torque against reaction time for reactions PET 4, 15 – 17 is given in Graph 4.

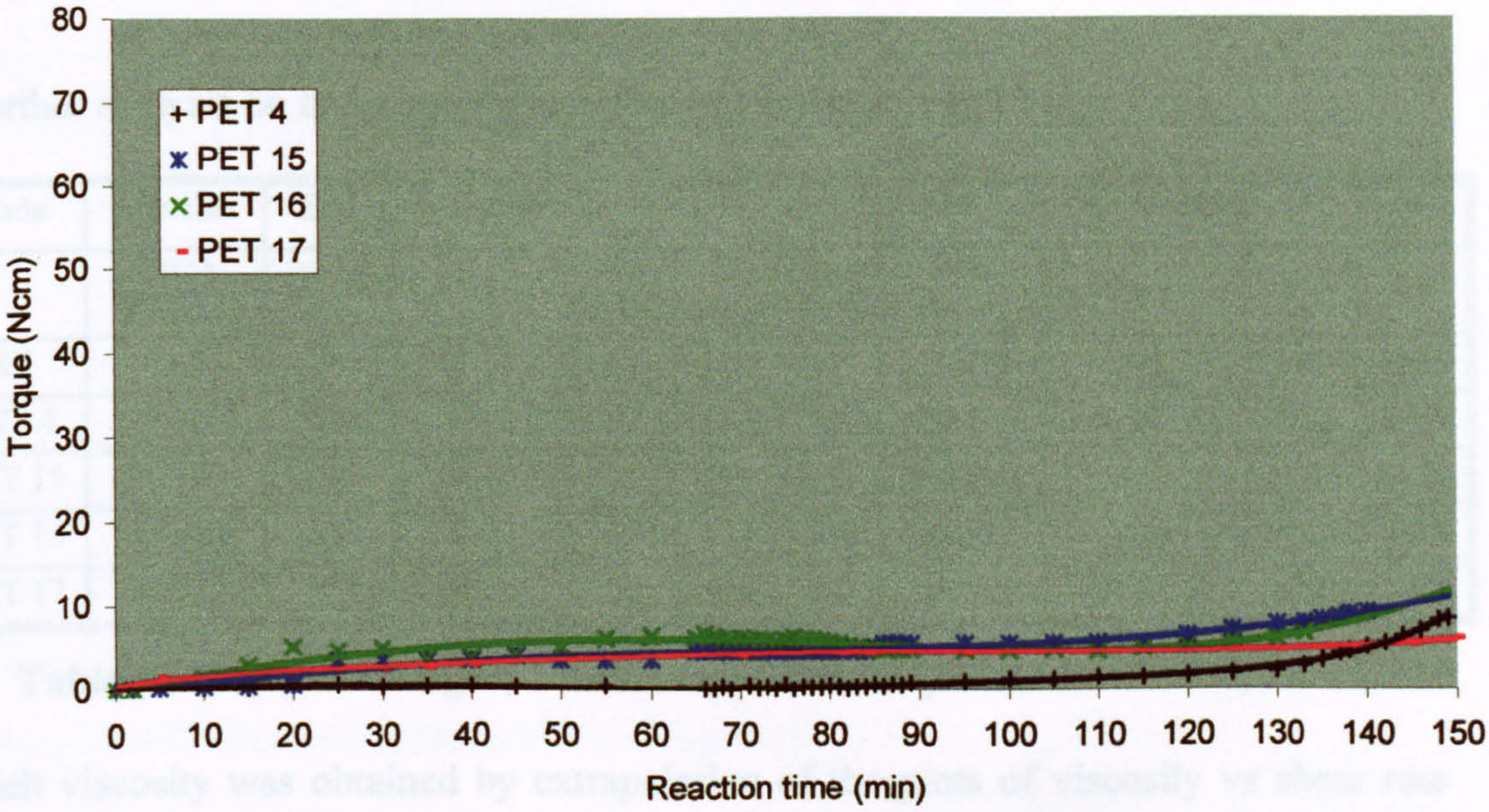

Graph 4: Relative Torque Data for Reactions PET 4, 15 –17

The torque data (Graph 4) shows a similar pattern to linear BHET reactions (Graph 1) an initial increase in torque which levels off for the majority of the reaction increasing slightly around 100-110 minutes where full vacuum is achieved. The final torque levels are on a par with these linear reactions. This is as compared to the highly branched species (Graph 3) where there is a very sharp turn up in torque around 100-110 minutes

The data in Table 4 indicates that there is an initial lowering of solution viscosity with the addition of branching agent. The solution viscosity rises again as more branching agent is added. The latter is a molecular weight effect and is confirmed by the $\overline{M}_W$ data from light scattering (Table 5). The initial fall in solution viscosity is almost certainly a reflection of the globular nature of the branched polymer. This would be expected to have fewer intramolecular entanglements than a free linear coil polymer and hence a lower I.V. for similar molecular weight. When $\overline{M}_W$ rises sharply with branching, the rise in molecular weight then dominates the solution viscosity behaviour. Even with this small increase in solution viscosity with rising $\overline{M}_W$, the

solution viscosity is far lower than would be anticipated. For example PET 15 has a solution viscosity value consistent with a polymer of ~ 10K $\overline{M}_w$, but actually has a $\overline{M}_w$ of ~ 338K.

Further analysis on these polymers is detailed in Table 5 and Table 6.

Code	Brancher	End	Solution	DSC			LS	Melt Visc	G'	G"
	B3CA (Wt%)	/10^6 g	I.V.	Tg (°C)	Tc (°C)	Tm (°C)	$\overline{M}w$ (D)	Pa.s	Pa	Pa
ICI	-	74	0.72	78	169	253	15000	60	580	2565
PET 4	-	78	0.40	73	132	259	8000	80	610	2575
PET 15	0.2500	190	0.45	72	133	254	338000	140	1680	7120
PET 16	0.1250	208	0.39	74	127	258	73000	120	1265	4375
PET 17	0.0625	273	0.35	75	126	260	70000	90	1070	3000

Table 5:Molecular Weight, Thermal and Viscosity Data for PET 4, 15 – 17

Melt viscosity was obtained by extrapolation of the plots of viscosity vs shear rate (typical plots page 149) to zero shear rate. G', the elastic modulus, and G", the loss modulus, were obtained at a frequency of 100 rad s^{-1}.

	PET 15	PET 16	PET 17	PET 4
No. of end-groups, E	190	208	273	78
Extent of conversion, p	0.980	0.979	0.972	0.992
Branching Coefficient, α	0.196	0.100	0.040	0.000
No. Av. Degree of Polymerisation	55.71	48.56	36.06	124.52
No. Av. Mw, $\overline{M}_n$ x10^{-4}	1.15	1.00	0.74	2.57
Weight Av. Mw, $\overline{M}_w$ x10^{-4}	2.76	2.15	1.51	5.11
No. Av. Branching Density, $\overline{B}_n$	0.18	0.08	0.03	0
Weight Av. Branching Density, $\overline{B}_w$	0.65	0.25	0.09	0
Intrinsic Visc., [η]	0.42	0.37	0.29	0.73
Visc. Av. Mw, $\overline{M}_v$ x10^{-4}	0.75	0.61	0.42	1.77
Melt Visc., [η_o] (Pa s)	40	20	10	510

Table 6: Paramenters Derived from Endgroup Analysis Data for PET 4, 15 – 17

In principle similar effects might be expected as well in the melt viscosity behaviour of polymers with the same molecular weight, since intermolecular entanglements would, in theory, be reduced for branched polymers. However this was not immediately obvious. The melt viscosity rises significantly with branching of the polymer (Table 5). Light scattering experiments, however again suggest that this is in fact a molecular weight effect i.e. molecular weight also rises with the degree of

branching, as indeed do the elastic, G', and loss moduli, G"; (Table 5). Data obtained from DSC shows a decrease in the melting point between linear polymer PET 4 and branched polymer PET 15 (Table 5). This seems to go against conventional wisdom, which would say that an increase in molecular weight should be accompanied by an increase in melting point. This is a clear indication of the effect of the globular structure of the branched species. In contrast, the glass transition temperature, T_g, is little affected, it increases slightly with the introduction of branching (PET 17) but then decreases again with increasing molecular weight. This in contrast to the findings of Jayakannan[86] who reports that the T_g is decreased slightly with the introduction of branching. However, no attempt has been made in the latter work to determine the $\overline{M}_W$ of the species and this may have a significant effect on the T_g value. The crystallisation temperature, T_c, decreases with branching but then increases with increasing molecular weight.

End-group analysis confirms that branching densities (weight and number average) both increase with increasing addition of branching agent (Table 6), but use of more than ¼ Wt% B3CA results in formation of a crosslinked polymer. The solution viscosity appears to fall with branching but it is impossible to separate out the effects of increased branching from increased molecular weight especially in the context of melt viscosity. It is difficult to separate molecular weight and branching effects. However, it appears that increased branching increases T_g but decreases T_m and T_c and increasing molecular weight reduces T_m and T_g but increases T_c

It is possible to take the absolute $\overline{M}_W$ data determined by light scattering and place them in the Mark-Houwink equation to predict what solution viscosity a linear polymer of the same molecular weight would have had. Dividing the actual intrinsic viscosity of the sample by this theoretical value gives g, the branching factor for an unentangled system, taking this to the power 2/7 gives the value of g for an entangled system. The g factors for this matrix of polymers are given in Table 7. Where $g \rightarrow 1$ for a linear polymer.

Code	Wt% B3CA	$\overline{M}_w$[1]	I.V.[2]	$\overline{M}_w$[3]	I.V.[4]	g	g
	Brancher	Ls	Back calc.	Soln Visc.	solution	Unentangled	Entangled
PET 4	-	8000	0.44	6900	0.40	0.91	0.97
PET 15	0.25	338000	4.84	8300	0.45	0.09	0.51
PET 16	0.125	73000	1.81	6600	0.39	0.22	0.64
PET 17	0.0625	70000	1.77	5600	0.35	0.20	0.63

Table 7: Branching Factors (g) for Polymers PET 4 and 15 – 17

[1] $\overline{M}_w$, Ls. = Molecular weight calculated from light scattering data

[2] I.V.,Back Calc. = Intrinsic viscosity calculated by substitution of $\overline{M}_w$ found by light scattering into the Mark-Houwink equation.

[3] $\overline{M}_w$, Soln Visc .= Molecular weight calculated from intrinsic viscosity data,

[4] I.V., Solution = Intrinsic viscosity found by solution viscosity experiment

The progressive fall in g confirms that these polymers are very highly branched indeed. Substituting the $\overline{M}_w$ data found by light scattering into Equation 43a (page 39) gives the melt viscosity of a linear polymer of similar molecular weight to the branched one. These back calculations are shown in Table 8, along with the actual melt viscosity found by experiment.

Code	Brancher (Wt% B3CA)	Melt Visc. (Expt.)	Melt Visc. (Back Calculated)
		Pa.s	Pa.s
ICI	-	57	10
PET 4	-	82	10
PET 15	0.25	140	409600
PET 16	0.125	122	1800
PET 17	0.0625	88	1550

Table 8: Back Calculation of Melt Viscosity

The back calculated melt viscosities of the branched polymers are enormously high compared to those found experimentally. This suggests that linear polymers are more viscous in the melt than branched polymers of comparable molecular weight. The experimental data for neither of the linear polymers correlates particularly well to the back-calculated data, but they are of the same order. This shows that the calculations are not particularly precise, however, the deviation observed between the experimental and the back-calculated samples for the branched polymers are so great that the imprecision in the calculation is insignificant.

6.2.4 Effect of Varying Time of Addition of Trimesic Acid Brancher

A plot of relative torque against reaction time for reactions PET 19 – 21 is given in Graph 5.

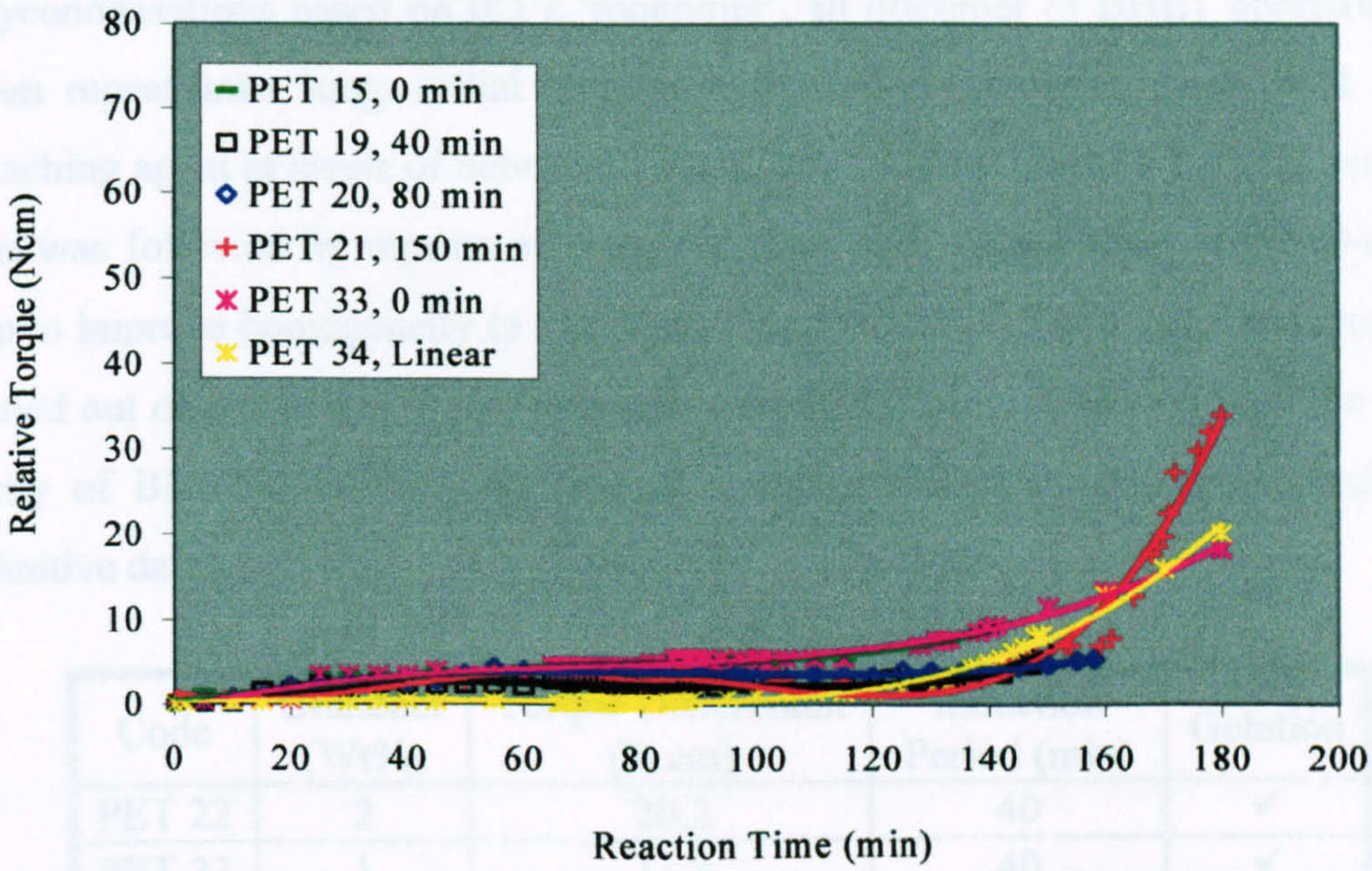

Graph 5: Relative Torque for Reactions with Varied Time of Brancher Addition

These were standard polycondensation reactions with 0.25 Wt% B3CA chain-brancher, where the time of addition of the B3CA was varied. Addition of reactants at 150 min (the usual termination time) as in reaction PET 21 necessitated that this reaction be run 30 minutes longer than normal, so the brancher would have time to react. Reactions PET 33 (standard 0.25 Wt% B3CA branched reaction +30 minutes) and PET 34 (typical linear reaction +30 minutes) are included for comparison. Data for a typical branched polymer, employing 0.25 Wt% B3CA, *e.g.* PET 15 and giving an intrinsic viscosity of ~ 0.45 is also included. Comparison of reaction torque data for reactions PET 15, 19 and 20 appears to indicate that changing the time of addition of the brancher lowers the viscosity in the melt slightly. However, the final solution viscosities (Table 4) are roughly the same. Addition of the brancher at 150 min and extension of the reaction by 30 minutes (PET 21) has a greater effect on the melt. However control experiments PET 33 and 34 show that this effect is due mainly to the increase in reaction time rather than the time of brancher addition.

6.2.5 Branched 'Monomer' Reactions

Running concurrently with the BHET-based programme of reactions was a matrix of polycondensations based on ICI's 'monomer', an oligomer of BHET approximately seven repeat-units long. Initial tests were carried out using trimesic acid as the branching agent at levels of between 0.5 and 2 Wt% (Reactions PET 22, 23, and 24). This was followed by repeats of these reactions with the addition of a ball-milling step to improve homogeneity in the melt (Reactions PET 25 and 26). Less work was carried out on 'monomer' feedstock than with BHET since it was felt that the higher purity of BHET was likely to lead to more reproducible experiments and more definitive data.

Code	Brancher (Wt%)	Torque Differential (N cm)	Induction Period (min)	Gelation
PET 22	2	20.2	40	✓
PET 23	1	11.9	40	✓
PET 24	0.5	9.8	40	✓
PET 25	2	42.7	40	✓
PET 26	2	56.8	100	✓

Table 9: 'Monomer' Based Polycondensation Reactions

All the polymers in this series of reactions gelled, although samples PET 23, and 24 contained only ~2 and ~1 % gel respectively.

The data for the relative torque against reaction time is shown in Graph 6

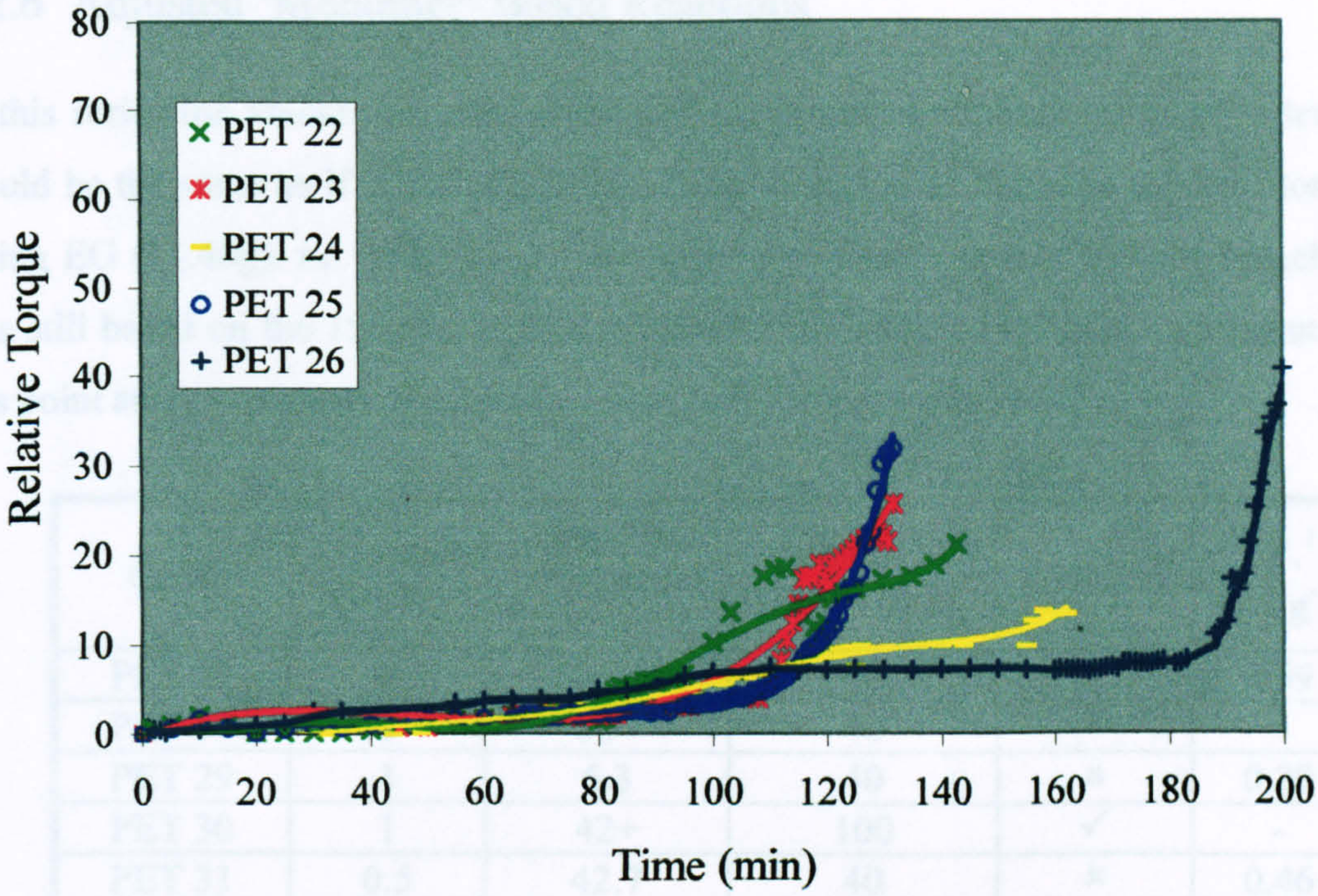

Graph 6: Relative Torque Data for Branched Polymers Prepared from'Monomer'

It is clear that that 'monomer' based reactions follow a similar pattern to the BHET reactions. Addition of the chain brancher at levels of 0.5 – 2 Wt% causes a large increase in viscosity and eventually results in gelation. However, in all cases the relative increase in viscosity is less than in the case of the BHET reactions. This could be attributed to the oligomeric nature of 'monomer'. The torque measurement is not absolute, it is relative to the initial torque on the stirrer. 'Monomer', will by its nature, have a higher viscosity and will undergo fewer condensation reactions than BHET. Thus, the torque will not be expected to rise as much during these reactions. In addition, the brancher segments will be a minimum of seven units apart, giving less chance of local gelation.

The reactions involving 'monomer' could be thought of as BHET reactions, which have been allowed to proceed until the polymer has grown to ~ 7 units long on average, before addition of the chain brancher. Since the reactions are based on added brancher as a Wt% of 'monomer' or BHET, some adjustment for the removal of ethylene glycol (EG) is necessary before a direct comparison can be made. These adjustments were made in following series of reactions.

6.2.6 Adjusted 'Monomer' Based Reactions

In this series the amount of 'monomer' present has been adjusted so that the level would be the same as if BHET (150g) had reacted to form oligomers ~7 units long, losing EG (31.46g). *i.e.* 118.54g of 'monomer' was used, but the Wt% of brancher was still based on the 150g level thus mimicking the addition of branching agent at this point and ensuring the Wt% of brancher to be comparable.

Code	Brancher (Wt%)	Torque Differential (N cm)	Induction Period (min)	Gelation	I.V.[1] (ml g^{-1})
PET 27	0	56.8	40	✖	0.59
PET 28	2	58+	40	✓	-
PET 29	1	6.3	40	✖	0.29
PET 30	1	42+	100	✓	-
PET 31	0.5	42.7	40	✖	0.46
PET 32	1	55.4	40	✓	-

Table 10: Adjusted 'Monomer' Based Reactions

[1] I.V. = Intrinsic Viscosity at 25 °C in TFA

The limited data for this series show that the intrinsic viscosity of branched polymers is again lower than the linear analogue. Reaction PET 29 is an anomaly caused by loss of vacuum during the reaction resulting in polymer of very low molecular weight. Repeat reaction PET 32 confirms this.

Plots of relative torque against reaction time are given in Graph 7.

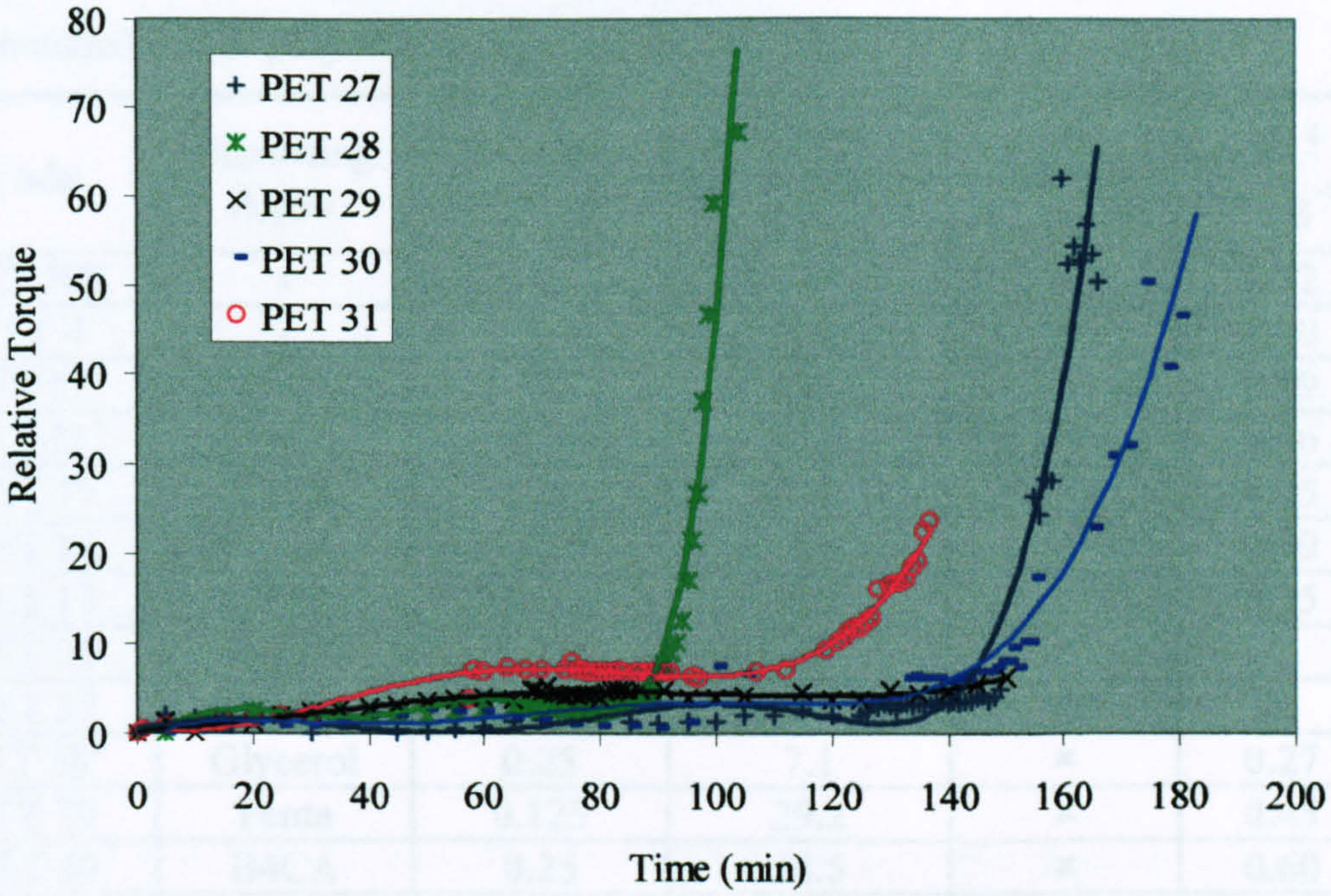

Graph 7: Relative Torque Data for adjusted 'Monomer'Based Polymers

In general the adjustment of 'monomer' levels brought the torque levels in line with those found with BHET reactions, *i.e.* levels of 1 and 2 Wt% brancher caused gelation and lower levels i.e. 0.5 Wt% did not. However, in this case the line is drawn at 0.5 not 0.25 wt%. As expected adjustment of the 'monomer' level increases the tendency for gelation since the proportion of brancher to 'monomer' has increased.

6.2.7 Other Branching Monomers

After investigation of branching with B3CA a comparison was sought by carrying out reactions with other branching agents. The branching agents selected were: -

1. Glycerol
2. 1,2,3,4 –Benzene tetracarboxylic acid (pyromellitic acid or B4CA, structure 9, page 45)
3. Pentaerythritol (penta structure 10, page 45)
4. Di-pentaerythritol (di-penta structure 14, page 45)
5. Tri-pentaerythritol (tri-penta structure 15, page 45)

A summary of the reactions carried out is given in Table 11 along with data for linear and branched B3CA polymers for comparison.

Code	Branching Agent	Brancher (Wt%)	Torque Differential (N cm)	Gelation	I.V.[4] (ml g^{-1})
PET ICI	-	0	-	✖	0.72
PET 4	-	0	8.4	✖	0.40
PET 27[2]	-	0	32.8	✖	0.59
PET 31[2]	B3CA	0.5	23.5	✖	0.46
PET 15	B3CA	0.25[1]	9.4	✖	0.45
PET 16	B3CA	0.125[1]	4.6	✖	0.39
PET 17	B3CA	0.0625[1]	6.1	✖	0.35
PET 36	B4CA	0.25[1]	34	✓	-
PET 37	Penta	0.25[1]	58.9	✓	-
PET 38[3]	Glycerol	0.25	7.1	✖	0.27
PET 39	Penta	0.125	29.2	✖	0.45
PET 40	B4CA	0.25	28.5	✖	0.60
PET 41	Glycerol	0.25	26	✖	0.66
PET 42	Glycerol	0.125	19.4	✖	0.34
PET 43[3]	B4CA	0.25	6.9	✖	0.33
PET 44	Penta	0.125	9.9	✖	0.63
PET 45	Di-penta	0.143	6.5	✖	~0
PET 46	Tri-penta	0.143	5	✖	~0

Table 11: Branched Reaction Data for a Variety of Agents

[1] These reactions contained brancher based on Wt% of BHET

[2] These reactions were based on ICI's 'monomer' feedstock

[3.] These reactions are of lower than expected molecular weight due to loss of vacuum during these reactions

[4] I.V. = Intrinsic Viscosity at 25 °C in TFA

Plots of the change in torque of the stirrer against reaction time are given in Graph 8.

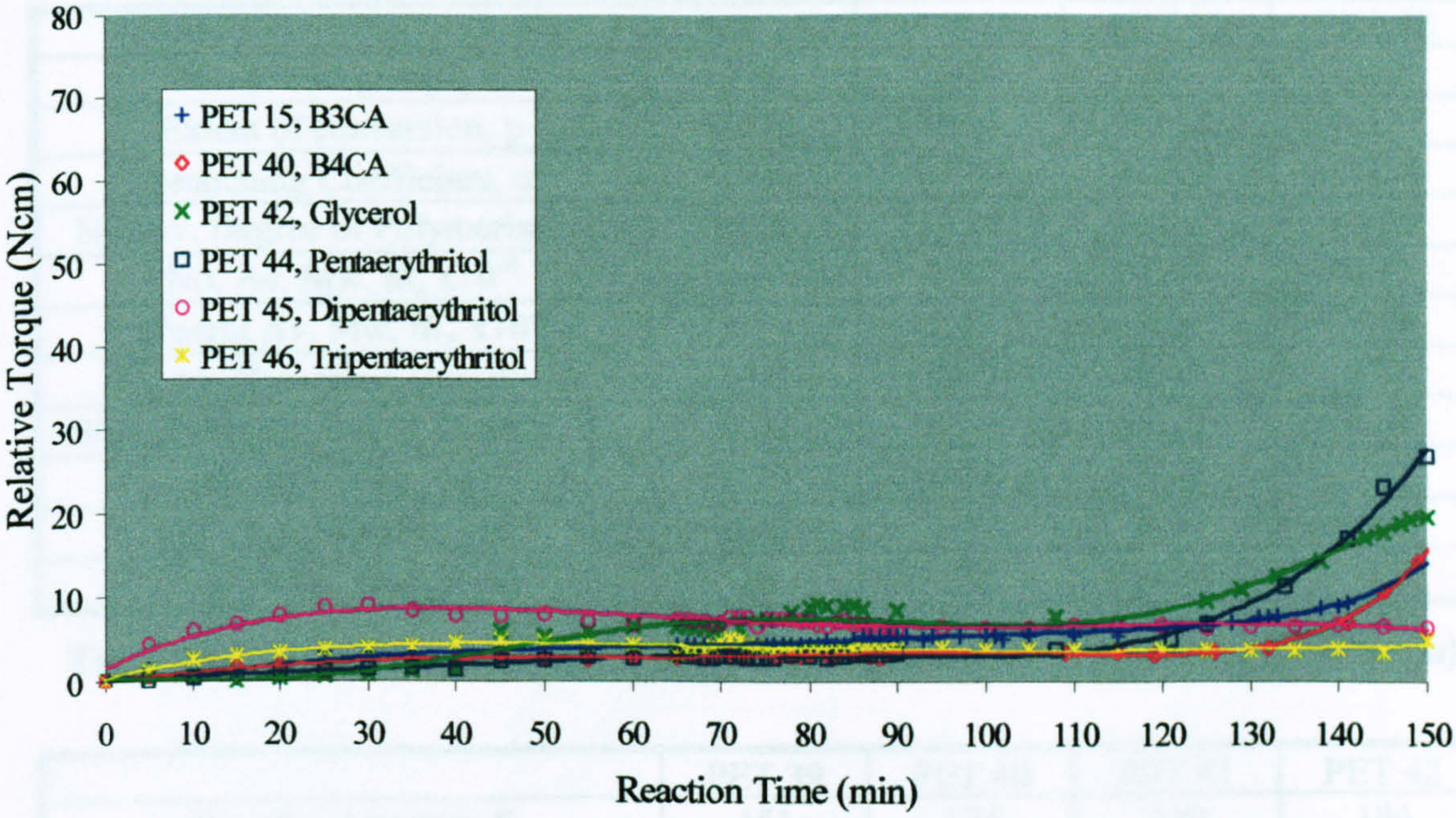

Graph 8: Relative Torque Data for PET Branched with Various Agents

In addition to the torque and solution viscosity data, the non-crosslinked samples were subjected to end-group, DSC, light scattering and rheological analysis. Selected samples were also analysed by GPC at ICI Wilton.

From end-group analysis the parameters shown in Table 12 were calculated.

	PET ICI	PET 4	PET 15	PET 16
No. of end-groups, E	74	78	190	208
Extent of conversion, p	-	0.992	0.980	0.979
Branching Coefficient, α	-	0.000	0.196	0.100
No. Av. Degree of Polymerisation	-	124.52	55.71	48.56
No. Av. Mw, $\overline{M}_n$ x10^{-4}	-	2.57	1.15	1.00
Weight Av. Mw, $\overline{M}_w$ x10^{-4}	-	5.11	2.76	2.15
No. Av. Branching Density, $\overline{B}_n$	-	0	0.18	0.08
Weight Av. Branching Density, $\overline{B}_w$	-	0	0.65	0.25
Intrinsic Visc., [η]	-	0.73	0.42	0.37
Visc. Av. Mw, $\overline{M}_v$ x10^{-4}	-	1.77	0.75	0.61
Melt Visc., [η_o] (Pa s)	-	510	40	20

Table 12: Parameters Derived from End-group Data for Branched PET (Part a)

	PET 17	PET 27	PET 31	PET 38
No. of end-groups, E	273	113	212	269
Extent of conversion, p	0.972	0.923	0.867	0.973
Branching Coefficient, α	0.040	0.000	0.327	0.350
No. Av. Degree of Polymerisation	36.06	13.04	8.96	44.60
No. Av. Mw, $\overline{M}_n$ x10^{-4}	0.74	1.77	1.16	0.91
Weight Av. Mw, $\overline{M}_w$ x10^{-4}	1.51	3.41	3.55	3.19
No. Av. Branching Density, $\overline{B}_n$	0.03	0.00	0.46	0.45
Weight Av. Branching Density, $\overline{B}_w$	0.09	0.00	2.10	2.37
Intrinsic Visc., [η]	0.29	0.54	0.42	0.37
Visc. Av. Mw, $\overline{M}_v$ x10^{-4}	0.42	1.11	0.74	0.61
Melt Visc., [η_o] (Pa s)	10	120	40	25

Table 13: Parameters Derived from End-group Data for Branched PET (Part b)

	PET 39	PET 40	PET 41	PET 42
No. of end-groups, E	151	174	329	184
Extent of conversion, p	0.985	0.982	0.967	0.977
Branching Coefficient, α	0.317	0.171	0.304	0.300
No. Av. Degree of Polymerisation	73.02	58.93	35.06	50.45
No. Av. Mw, $\overline{M}_n$ x10^{-4}	1.50	1.21	0.72	1.28
Weight Av. Mw, $\overline{M}_w$ x10^{-4}	35.98	3.87	2.14	3.78
No. Av. Branching Density, $\overline{B}_n$	0.31	0.16	0.35	0.34
Weight Av. Branching Density, $\overline{B}_w$	14.79	1.03	1.59	1.53
Intrinsic Visc., [η]	0.40	0.52	0.31	0.47
Visc. Av. Mw, $\overline{M}_v$ x10^{-4}	0.69	1.02	0.46	0.90
Melt Visc., [η_o] (Pa s)	100	105	10	70

Table 14: Parameters Derived from End-group Data for Branched PET (Part c)

	PET 43	PET 44	PET 45	PET 46
No. of end-groups, E	270	160	1263	1017
Extent of conversion, p	0.972	0.984	0.666	0.731
Branching Coefficient, α	0.147	0.305	0.015	0.013
No. Av. Degree of Polymerisation	38.27	71.36	3.00	3.72
No. Av. Mw, $\overline{M}_n$ x10^{-4}	0.79	1.46	0.06	0.08
Weight Av. Mw, $\overline{M}_w$ x10^{-4}	2.22	19.94	0.11	0.14
No. Av. Branching Density, $\overline{B}_n$	0.10	0.29	0.40	0.29
Weight Av. Branching Density, $\overline{B}_w$	0.55	7.80	2.11	2.12
Intrinsic Visc., [η]	0.37	0.68	0.03	0.04
Visc. Av. Mw, $\overline{M}_v$ x10^{-4}	0.60	1.58	0.01	0.02
Melt Visc., [η_o] (Pa s)	20	710	~0	~0

Table 15: Parameters Derived from End-group Data for Branched PET (Part d)

The DSC data for these polymers are shown in Table 16.

Code	Brancher (Wt%)	T_g (°C)	T_c (°C)	T_m (°C)
PET ICI	Linear	78.1	169	253.4
PET 4	Linear	73.1	132.3	258.9
PET 27	Linear	72.8	134.7	254.5
PET 31	0.5 B3CA	73.3	134.8	251.9
PET 15	0.25 B3CA	71.7	132.9	253.7
PET 16	0.125 B3CA	73.8	127.1	258.3
PET 17	0.0625 B3CA	75	125.8	260.3
PET 38	0.25 Glycerol	73	129.4	258.5
PET 39	0.125 Penta	74.8	144	254.7
PET 40	0.25 B4CA	72.4	133.4	254.7
PET 41	0.25 Glycerol	72.9	138.7	251.8
PET 42	0.125 Glycerol	73.4	138.7	256.1
PET 43	0.25 B4CA	70.8	113.2	256.5
PET 44	0.125 Penta	68.7	134.8	255.8

Table 16: DSC Termal Transitions For Branched PET

Data obtained from light scattering measurements is shown in Table 17.

Code	Brancher (Wt%)	$\overline{M}_w$(D)
PET ICI	Linear	15000
PET 4	Linear	8000
PET 27	Linear	13000
PET 31	0.5 B3CA	71000
PET 15	0.25 B3CA	338000
PET 16	0.125 B3CA	73000
PET 17	0.0625 B3CA	70000
PET 38	0.25 Glycerol	87000
PET 39	0.125 penta	361000
PET 40	0.25 B4CA	386000
PET 41	0.25 Glycerol	319000
PET 42	0.125 Glycerol	183000
PET 43	0.25 B4CA	48000
PET 44	0.125 Penta	392000
PET 45	0.143 Di-penta	29000
PET 46	0.143 Tri-penta	18000

Table 17: Light Scattering Data for Branched PET

Data obtained from melt rheology experiments are shown in Table 18.

Code	Brancher	Melt Visc.	G'	G"
	Wt%	Pa.s	Pa	Pa
PET ICI	-	60	580	2565
PET 4	-	80	610	2575
PET 15	0.25 B3CA	140	1680	7120
PET 16	0.125 B3CA	120	1265	4375
PET 17	0.0625 B3CA	90	1070	3000
PET 27	-	80	595	1630
PET 31	0.5 B3CA	130	850	4080
PET 38	0.25 Glycerol	65	700	1550
PET 39	0.125 Penta	170	1150	7550
PET 40	0.25 B4CA	260	1150	7860
PET 41	0.25 Glycerol	205	3300	12830
PET 42	0.125 Glycerol	160	2460	7540
PET 43	0.25 B4CA	70	650	635
PET 44	0.125 Penta	360	2100	7900

Table 18:Rheological Data for Branched Polymers

Melt viscosity was obtained by extrapolation of the plots of viscosity vs shear rate (typical plots page 149) to zero shear rate. G', the elastic modulus, and G", the loss modulus, were obtained at a frequency of 100 rad s^{-1}.

Data obtained from GPC analysis are shown in Table 19.

Code	$\bar{M}w$	$\bar{M}n$
PET 16	38800	17800
PET 4	52800	27900
PET 27	59000	31400
PET 39	89700	28100
PET 40	568800	42200
PET 41	69100	26400

Table 19: GPC Data

Branching in these polymers was achieved using two rigid (B3CA and B4CA) and two flexible branchers (glycerol and pentaerythritol) in practice these are two acid and two alcohol functionalised branching agents. These can also be grouped as tri-functional (B3CA and glycerol) and tetra-functional (pentaerythritol and B4CA) agents.

During these reactions the torque exerted on the stirrer stayed relatively constant, sharply increasing towards the end of the reaction as the polymer chain length increases. In reactions PET 42 and PET 44 (glycerol and pentaerythritol), this up-turn occurs significantly earlier (30 min) than in the other reactions. This could be attributed to the smaller, lighter nature of these branchers rendering them more mobile than the other bulkier aromatic branchers or it could be that the alcohol moiety is more reactive under these conditions than carboxylic acid groups. The alcohols can undergo transesterification reactions where as the carboxylic acids have to condense, with loss of water, to esterify. The former reaction is much easier to achieve under the reaction conditions than the latter.

Light scattering analysis of this series of polymers shows much higher $\bar{M}w$ than would be predicted by solution viscosity, and indeed much higher than is possible with linear polymers. This is a good indication that highly branched species have been produced. The light scattering data is at variance with the molecular weights found by GPC. The GPC data however is not absolute and relies entirely on the polystyrene standards with which it was calibrated. Polystyrene however, is a very different polymer from PET and this method of calibration almost certainly invalidates this data.

Analysing the end-group data it is clear that the end-groups present are much higher than would be expected for a linear polymer (PET ICI, 74 end-groups/g, PET 4, 78 end-groups/g) this is consistent with branched polymers. Additionally, no polymer reached the theoretical gel point (α=0.5 for trifunctional branchers, and α=0.33 for tetrafunctional branchers) and so it can be assumed that these polymers are branched but not cross-linked. $\bar{B}_n$, the number average branching density (the average number of branches per molecule) is much larger for the flexible types of brancher (glycerol and pentaerythritol), between 0.29 and 0.45. The more rigid benzene based branchers (B3CA and B4CA) have fewer branches at between 0.03 and 0.18 per repeat unit. PET 31 is the only exception. This polymer is based on the B3CA but has 0.45 branches per repeat unit, more than double the amount of any other polymer of this type. The reason for this is unclear. The only difference between this polymer and the others is that it is based on ICI's 'monomer' feedstock. This molecule corresponds to

a condensate of ~ 7 BHET units and conceivably has more affinity for the branching agent than itself. Whereas BHET may have equal affinity for itself and the brancher, being nearer to the same size than are 'monomer' and brancher. In other words, it is easier to add a small molecule whether it be BHET or brancher, to a growing chain than it is to add a large oligomer like 'monomer'. In the case of the BHET based reactions this could lead to chains of greater linear length than in 'monomer' based reactions where the chain would prefer to add a small branching unit as often as possible.

The number average branching coefficients of polymers PET 42 and 43 ($\bar{B}_n$) are approximately the same even though PET 42 has double the branching agent present in PET 43. However, polymer PET 43 is roughly half the molecular weight of PET 42 and so the branching agent will be more concentrated in the former than in the latter, giving similar branching coefficient.

The intrinsic viscosities of this series of polymers, calculated from end-group analysis (using the Mark-Houwink relationship) and that calculated from experimental solution viscosity are shown in Table 20

Compound	[η] Calc. (end-group)	[η]Calc.(solution)
PET 31	0.42	0.46
PET 15	0.42	0.45
PET 16	0.37	0.39
PET 17	0.29	0.35
PET 04	0.73	0.40
PET 27	0.54	0.59
PET 38	0.37	0.27
PET 39	0.40	0.45
PET 40	0.52	0.6
PET 41	0.31	0.66
PET 42	0.47	0.34
PET 43	0.37	0.33
PET 44	0.68	0.63
PET 45	0.03	~0
PET 46	0.04	~0

Table 21: Comparison of Intrinsic Viscosity Calculated from Solution Viscosity and end-group Data

The error in the solution viscosity values was calculated to be ± 0.08. This means that the data for most of the polymers in Table 21 fall within experimental error, with some notable exceptions: the three glycerol branched polymers (PET 38, 41 and 42) and the linear BHET reaction (PET 4). Why the data for these materials are so far from the predicted values is unclear at this time.

As with B3CA branched polymers, DSC analysis seems to indicate that overall, branching lowers the melting point (T_m) and the crystallisation temperature (T_c) of the polymers whilst the glass transition temperature (T_g) increases with branching. However further work involving a greater number of samples, of varied amounts of brancher are required to clarify this. There is some ambiguity amongst the pentaerythritol derived polymers. Polymers PET 39 and 44 were made to the same specification and are reported to be of similar molecular weight. However, these polymers have very different and inconsistent DSC traces. The lower T_m of PET 39 suggests that this polymer is of lower molecular weight that polymer PET 44 and indeed, it is. The T_c and T_g, however are much higher for PET 39 indicating that although of a lower molecular weight PET 39 is more branched than PET 44.

Reactions PET 45 and 46 (di and tri-pentaerythritol) appear, from their torque data, solution viscosity and their physical appearance, to have yielded products of low molecular weight. However light scattering data suggests that these polymers have molecular weights of a similar level to commercial PET. This variance in result between the two methods can be attributed to the polymers having branched to such an extent that only small 'spherical' molecules of low viscosity have been formed. These molecules would have few intramolecular entanglements and would thus have a much lower solution viscosity than that of a free linear coil polymer. End-group analysis of these polymers supports this theory. $\bar{B}_n$, the number average branching density, for these two polymers is relatively high compared to that for end-capped polymers (PET 50 and 52, see later Table 26) and have a far higher number of end-groups.

Back calculation of intrinsic viscosity and g factors for these branched polymers followed the same procedure as with the trimesic acid branched polymers (page 59).

Code	Brancher	$\bar{M}_w$	I.V.	$\bar{M}_w$	I.V.	g	g
	Wt%	Ls (D)	Back calc. (ml g^{-1})	Soln Visc. (D)	Solution (ml g^{-1})	Unentangled	Entangled
PET 15	0.25 B3CA	338000	4.84	8300	0.45	0.09	0.51
PET 16	0.125 B3CA	73000	1.81	6600	0.39	0.22	0.64
PET 17	0.0625 B3CA	70000	1.77	5600	0.35	0.20	0.63
PET 4	-	8000	0.44	6900	0.40	0.91	0.97
PET 27	-	13000	0.6	13000	0.60	1	1
PET ICI	-	15000	0.66	17000	0.72	1.09	1.03
PET 31[2]	0.5 B3CA	71000	1.78	11000	0.46	0.29	0.70
PET 38[3]	0.25 Glycerol	87000	2.03	3700	0.27	0.13	0.56
PET 39	0.125 Penta	361000	5.05	8300	0.45	0.09	0.50
PET 40	0.25 B4CA	386000	5.27	13000	0.60	0.11	0.54
PET 41	0.25 Glycerol	319000	4.66	15000	0.66	0.14	0.57
PET 42	0.125 Glycerol	183000	3.27	5300	0.34	0.10	0.52
PET 43[3]	0.25 B4CA	48000	1.39	5000	0.33	0.24	0.66
PET 44	0.125 Penta	392000	5.32	14100	0.63	0.12	0.54
PET 45	0.143 Di-penta	29000	1	0	0.01	0.01	0.27
PET 46	0.143 Tri-penta	18000	0.74	0	0.01	0.01	0.29

Table 22: Branching Factors, g, for Branched Polymers

From the g factors, it can be seen that all the polymers are very highly branched. The calculated I.V. values, in accordance with theoretical treatment by Stockmayer[50] and Zimm,[51] and previous work by Manaresi,[73] show that in a comparison of branched and linear polymers of similar molecular weight, the branched polymer will have a lower solution viscosity.

Substituting $\bar{M}w$ data found by light scattering into Equation 43a (page 39) gives the melt viscosity of a linear polymer of similar molecular weight to the branched one. The results of these back calculations are shown in Table 23, along with the actual melt viscosity found by experiment.

Code	Brancher (Wt%)	Expt.Melt Visc. (Pa.s)	Back Calculated Melt Visc. (Pa.s)
PET 27	-	80	10
PET 38	0.25 Glycerol	65	33600
PET 39	0.125 Penta	170	517100
PET 40	0.25 B4CA	260	655400
PET 41	0.25 Glycerol	205	333800
PET 42	0.125 Glycerol	160	47000
PET 43	0.25 B4CA	70	410
PET 44	0.125 Penta	360	692200

Table 23: Back Calculation of Melt Viscosity for Selected Branched Polymers

As with the trimesic acid branched polymers (Table 8, page 59), the data in Table 23 shows that the back calculated melt viscosities of branched polymers are far higher than those found experimentally. Again, this suggests that linear polymers are much more viscous in the melt than branched polymers of comparable molecular weight. These results are borne out by previous findings on PET by Manaresi[73] and similar results on other polymers.[74,75,76]

6.2.8 End-capped Reactions

After investigation of the branching of PET, some attempts to control this branching with end-capping agents was attempted. The aim here was to synthesise branched polymers with an absolute $\overline{M}w$ close to that of model linear PET. This would then allow unambiguous deconvolution of the effect of branching and molecular weight on properties such as solution and melt viscosity. The branching in these polymers was achieved using B3CA and pentaerythritol. Initial experiments were carried out using B3CA, to investigate whether higher levels of branching agent (2 Wt% and greater) that had previously resulted in gelled products, could be safely used when in conjunction with end-capping agents. This investigation was also used to identify the effectiveness of the proposed end-cappers.

The end-capping agents selected were: -

1. Terephthalic acid monomethyl ester; TAME (Structure 16 , page 48)
2. Benzoic acid; BzCOOH
3. Benzyl alcohol; BnOH
4. Stearic acid; Stearic (Structure 17, page 48)
5. 9-Anthracene methanol; 9-Anth (Structure 18, page 48)

A summary of the reactions carried out is given Table 24 along with data for linear and B3CA branched polymer for comparison.

Code	Branching Agent (Wt%)	Endcapper (Wt%)	Torque Differential (N cm)	Gelatio n	I.V. (ml g^{-1})
PET 4	-	-	8.4	×	0.40
PET 15	0.25 B3CA	-	9.4	×	0.45
PET 47	2 B3CA	5 TAME	58.4	✓	-
PET 48	1 B3CA	3 TAME	27.7	✓	-
PET 49	2 B3CA	4 BzCOOH	56.4	✓	-
PET 50	-	2 TAME	14.5	×	0.63
PET 51	2 B3CA	2 BnOH	72.4	✓	
PET 52	-	2 BnOH	3.5	×	0.009
PET 53	2 B3CA	4 BnOH	4.0	×	0.054
PET 54	2 B3CA	4 BnOH	4.1	×	0.24
PET 55	2 B3CA	3 BnOH	13.5	×	0.167
PET 57	-	1 BnOH	6.0	×	-
PET 58	-	5 Stearic	4.3	×	-
PET 59	-	6 9-Anth	3.9	×	-
PET 60	-	1 BzCOOH	14.5	×	-
PET 61	0.125 penta	1 BnOH	4.9	×	0.21
PET 62	0.125 penta	0.5 BnOH	5.0	×	0.21
PET 63	0.125 penta	0.25 BnOH	5.6	×	0.28
PET 64	0.125 penta	0.125 BnOH	3.5	×	0.28
PET 65	0.125 penta	0.0625 BnOH	4.3	×	0.26
PET 66	0.125 penta	0.0312 BnOH	4.9	×	0.27

Table 24: Polycondensations Employing an Endcapper with a Branching Agent

Plots of the change in stirrer torque against reaction time, for end-capped PET reactions are given in graphs 9 - 11.

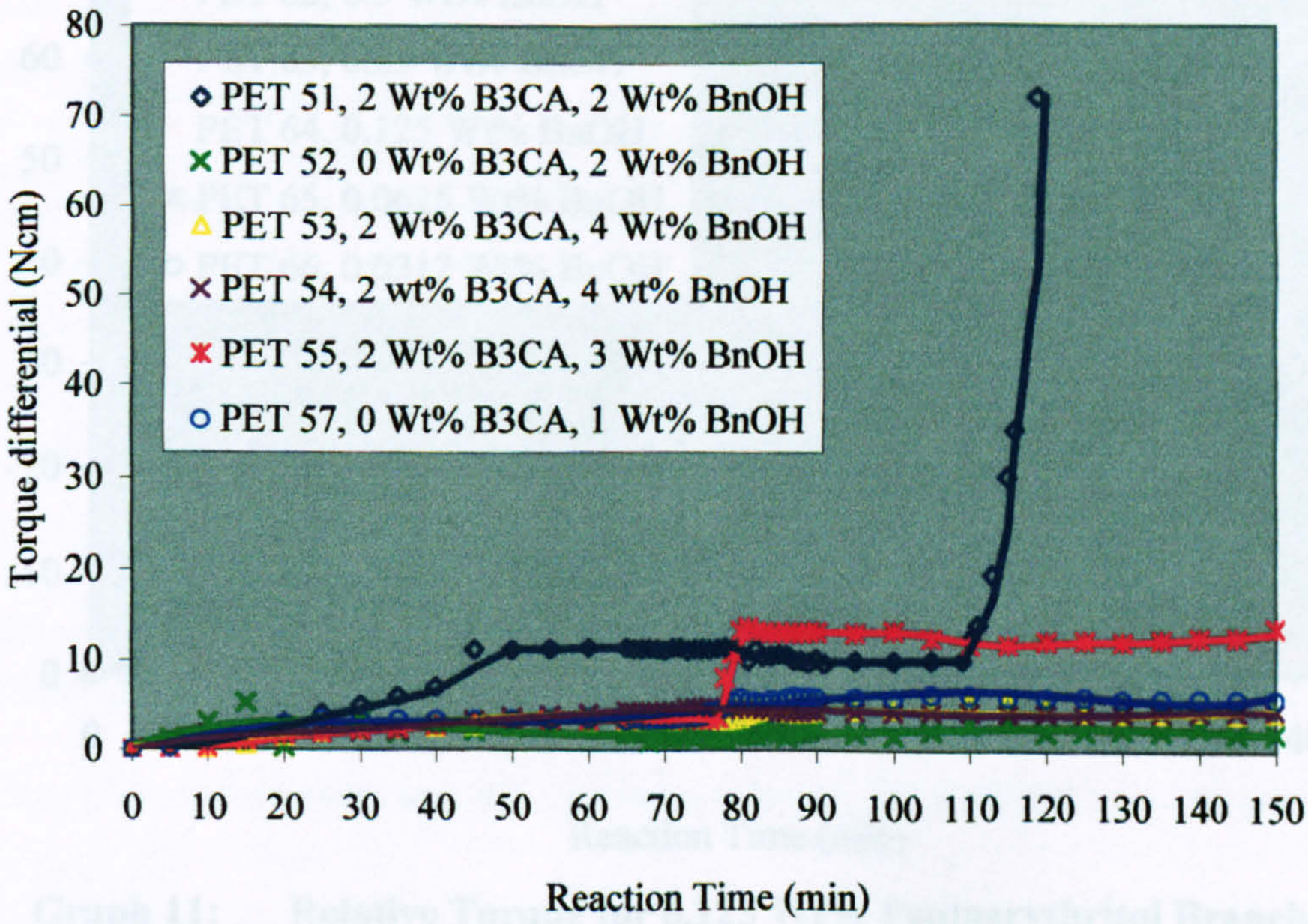

Graph 9: Relative Torque for B3CA Branched Polymers End-capped with BnOH

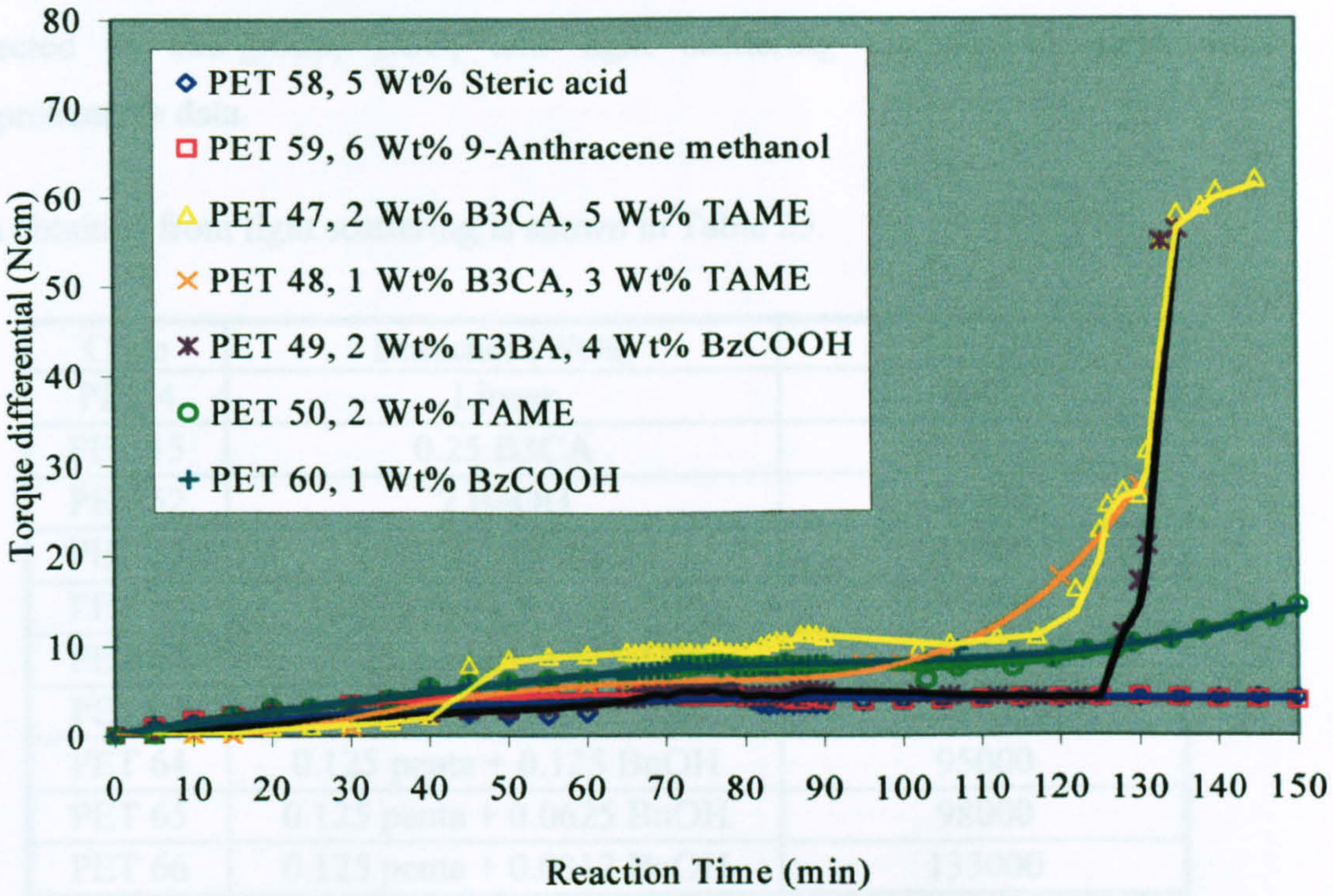

Graph 10: Relative Torque For Other End-capped Reactions

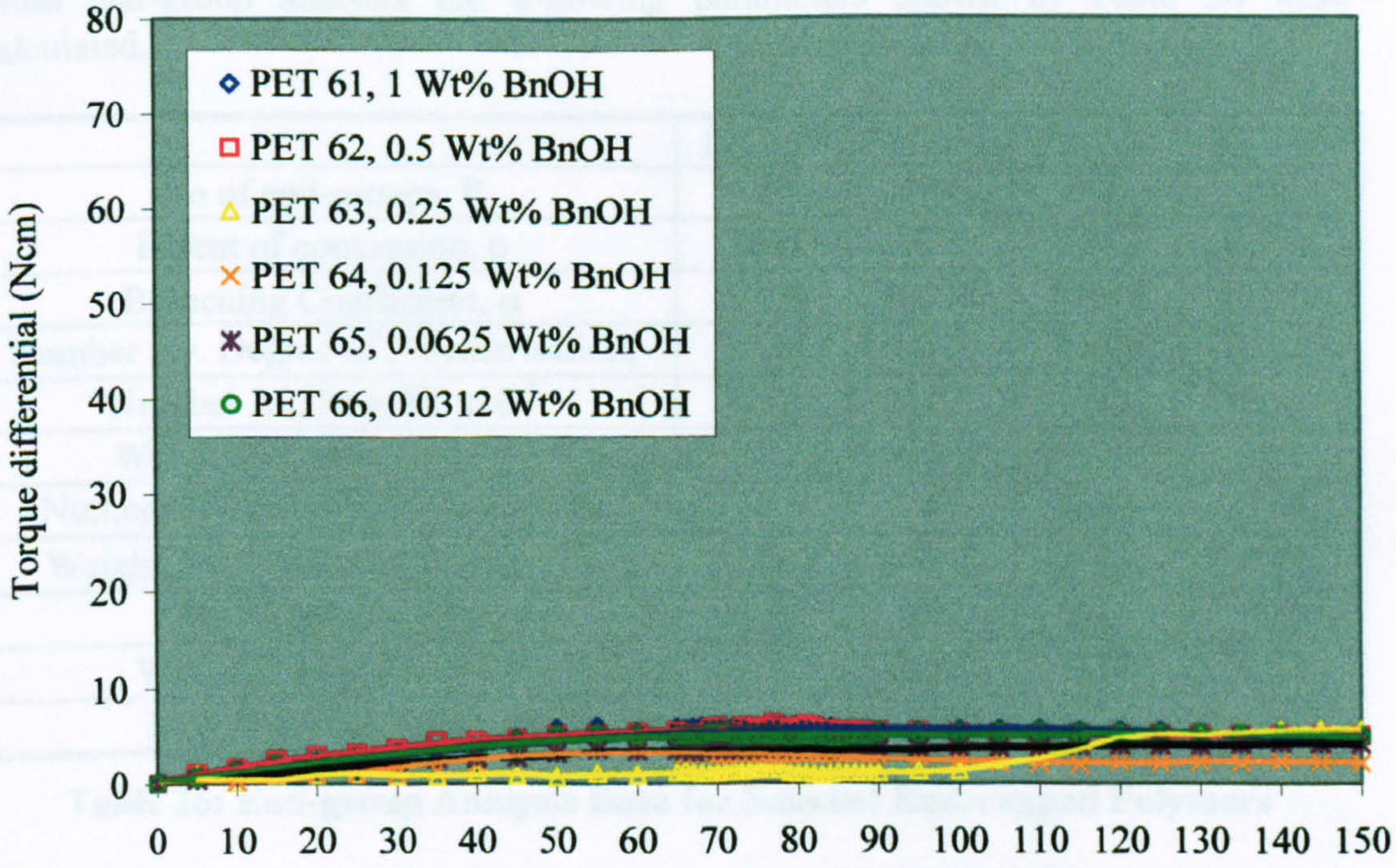

Graph 11: Relative Torque for 0.125 Wt% Pentaerythritol Branched Polymers End-capped with Benzyl Alcohol

In addition to the reaction torque and solution viscosity data, selected samples were subjected to end-group, DSC, and light scattering analysis to yield more comprehensive data.

Data obtained from light scattering is shown in Table 25.

Code	Brancher (Wt%)	$\overline{M}_w$ (D)
PET 4	Linear	8000
PET 15	0.25 B3CA	338000
PET 52	2 BnOH	32000
PET 55	2 B3CA + 3 BnOH	41000
PET 61	0.125 penta + 1 BnOH	36000
PET 62	0.125 penta + 0.5 BnOH	28000
PET 63	0.125 penta + 0.25 BnOH	28000
PET 64	0.125 penta + 0.125 BnOH	95000
PET 65	0.125 penta + 0.0625 BnOH	98000
PET 66	0.125 penta + 0.0312 BnOH	133000

Table 25: Light Scattering Data For Endcapped Polymers

From end-group analysis the following parameters shown in Table 26 were calculated.

	PET 50	PET 52	PET 54	PET 55
No of end-groups, E	109	109	300	207
Extent of conversion, p	0.971	0.971	0.943	0.946
Branching Coefficient, α	0.000	0.000	0.369	0.394
Number Av. Degree of Polymerisation,	34.73	34.73	21.69	23.52
Number Av. Mw, $\overline{M}_n$ x10^{-4}	0.71	0.71	0.42	0.48
Weight Av. Mw, $\overline{M}_w$ x10^{-4}	1.02	0.97	0.56	1.18
Number Av. Branching Density, $\overline{B}_n$	0	0	0.22	0.44
Weight Av. Branching Density, $\overline{B}_w$	0	0	0.43	0.44
Intrinsic Visc., [η]	0.22	0.21	0.13	0.20
Visc. Av. Mw, $\overline{M}_v$ x10^{-4}	0.27	0.26	0.12	0.23
Melt Visc., [η_o] (Pa s)	~0	~0	~0	~0

Table 26: End-group Analysis Data for Selected End-capped Polymers

DSC data for selected end-capped polymers are shown in Table 27 with rheological data in Table 28

Code	Brancher/Endcapper (Wt%)	T_g (°C)	T_c (°C)	T_m (°C)
PET 4	Linear	73.1	132.3	258.9
PET 52	2 BnOH	70.3	112.9	257.2
PET 55	2 B3CA +3 BnOH	67.4	116.5	246.2
PET 61	0.125 penta + 1 BnOH	67.1	114.3	244.1
PET 62	0.125 penta + 0.5 BnOH	67.5	116.1	247.5
PET 63	0.125 penta + 0.25 BnOH	68.3	116.1	247.5
PET 64	0.125 penta + 0.125 BnOH	67.2	115	245.5
PET 65	0.125 penta + 0.0625 BnOH	66	112.4	242.7
PET 66	0.125 penta + 0.0312 BnOH	69.4	124.6	244.9

Table 27: DSC Data For Selected End-capped Polymers

Code	Brancher (Wt%)	Expt Melt Visc. (Pa.s)	Back Calculated Melt Visc.(Pa.s)	G' (Pa)	G" (Pa)
PET 52	2 BnOH	20	100	620	630
PET 55	2B3CA +3 BnOH	15	200	590	230
PET 61	0.125 penta + 1 BnOH	~ 0	150	1650	290
PET 62	0.125 penta + 0.5 BnOH	~ 0	60	1740	190
PET 63	0.125 penta + 0.25 BnOH	~ 0	60	1590	215
PET 64	0.125 penta + 0.125 BnOH	5	4880	1435	350
PET 65	0.125 penta + 0.0625 BnOH	5	5120	1280	300
PET 66	0.125 penta + 0.0312 BnOH	10	15080	990	1100

Table 28:Rheological Data for Selected End-capped Polymers

TAME was proposed by ICI as an end-capper. Its structure is analogous to BHET and so this feature would not effect the properties of the finished polymer. Experiments were carried out using B3CA branching agent and TAME (at ratios of 2:5, 1:3, and 0:2 Wt%). It was found that as with those earlier reactions using only B3CA, levels of 2 and 1 Wt% B3CA caused gelation. The TAME appeared to have no effect. On carrying out a polycondensation with TAME only (PET 50), there appeared to be no significant difference in the torque of the stirrer during the reaction. The appearance and viscosity of the product also seemed the same as those of linear polymer. Indeed, the final product with TAME present had a higher solution viscosity than expected for linear polymer. The end-group analysis of this non-branched control polymer (PET 50) shows a low amount of end-groups consistent with linear PET. This points to no end-capping having occurred. It was concluded that TAME is not suitable for use as an end-capping agent. It could be that the methyl

ester of TAME is able to transesterify with BHET or its oligomers. In response to this fear, benzoic acid was chosen for the next investigation. Similar to TAME it has no second functional group at all, and so there is no risk of transesterification occurring. Experiments were carried out with B3CA as the branching agent and benzoic acid as the end-capper (at ratios of 2:4 and 0:1 Wt%). It was found that like TAME, benzoic acid appeared to have little effect on the branching of the polymer. In the case of the experiment using 2 Wt% B3CA, the benzoic acid failed to prevent gelation. However, the control polymer with no branching agent (PET 50) showed no significant difference in the properties of the final polymer from linear polymer. Although no transesterification can take place it could be that the benzoic acid (b.p. 249 °C) is volatilised off with the ethylene glycol. In any case, this molecule is not suitable for use as an end-capper. The above compounds both have carboxylic acid functionality. It was therefore decided to investigate an end-capper with alcohol functionality. The obvious choice was benzyl alcohol, due to its functional similarity to the PET backbone. Experiments were carried out using B3CA as the branching agent and BnOH as the end-capper (at ratios of 2:2, 2:3, 2:4, 0:2, and 0:1 Wt%). The initial reaction with 2Wt% B3CA and 2 Wt% of BnOH gelled. It was felt on viewing subsequent data that this was an erroneous result, perhaps due to a miscalculation of the mass of end-capper added. In the second reaction, the BnOH content was increased to 3 Wt% and a marked difference in viscosity was noted. Polycondensations with this level of end-capper acted like linear polycondensations, in viscosity terms. There was no marked increase in torque during the reaction and the final product was not gelled. Greater amounts of end-capper (e.g. 4 Wt%) retarded the polycondensation process giving only low molecular weight oligomers. The torque output of the stirrer during these reactions hardly changed at all (~4 Ncm as compared with linear polymer 8 –14 Ncm). The final product was a white crumbly powder. Reactions involving only end-capper gave similar results. DSC data shows thermal transitions at significantly lower temperatures than that found in linear polymers. This can be attributed to the lower molecular weight of these polymers caused by end-capping. Light scattering data indicates that these polymers have higher $\overline{M}_w$ than linear polymers, but have substantially lower $\overline{M}_w$ than polymers with similar branching. Rheological data is lower than for similarly branched or linear

polymers. This may indicate a more globular topology where entanglements, both inter and intramolecular are less likely.

It can be concluded that BnOH can be used to end-cap branched PET and successfully prevent gelation at levels of B3CA brancher where gelation would normally have occurred. This is in line with previous results by Manaresi[80] and Roso[85] where monofunctional agents were also used to stop gelation in highly branched polymers. By changing the amount of end-capper present, this effect can be varied. A second series of benzyl alcohol capped polymers, this time branched with pentaerythritol, showed the control of molecular weight in more detail. The continual addition of BnOH from 0.0312 to 0.25 Wt% decreases the final $\overline{M}_W$ achieved. At this level the polymer seems to be saturated with BnOH and further addition has no additional effect. The melt viscosity data for this series (Table 28, page 78) shows a marked decrease in the melt viscosity of these end-capped polymers. The polymers all exhibit considerably lower melt viscosity that linear PET (PET 4 and PET ICI, Table 18, page 69) even though they have $\overline{M}_W$ values of between 3 and 16 times greater than linear PET (PET 4, Table 25, page 77). The elastic and loss moduli of these polymers is also significantly lower than pentaerythritol branched polymer (PET 44, Table 18) whilst the elastic moduli is significantly higher and the loss moduli significantly lower than linear PET (PET 4, Table 18). The DSC data (Table 27, page 78) shows a reduction in the values of all three thermal parameters. In particular the melting point has notably decreased by between 10 and 15 °C. This again runs contrary to what would be expected for a linear sample of similar $\overline{M}_W$ and seems to indicate a more globular topology where entanglements, both inter and intramolecular are less likely.

Further studies were carried using stearic acid and 9-anthracene methanol as end-cappers. Both of these species are of substantially higher boiling point than the end-cappers used previously and it was unlikely that they would volatilise off. Both reactions were carried out with only end-capper present. Previous experiments containing end-cappers with acid functionality (TAME and benzoic acid) had failed to end-cap their respective reactions. Reasons have been put forward for these failures. The use of stearic acid was an attempt to prove that a molecule with a sufficiently high boiling point and no groups capable of undergoing

transesterification could end-cap reactions and that it was not just the acid group failing to react. The use of 9-anthracene methanol was to see what effect a bulky end-capping group would have. Both of these reactions showed that the molecules under study were capable of end-capping the polymer, although the coloured nature of 9-anthracene methanol containing product is clearly not acceptable in the commercial production of this polymer.

6.2.9 Flexible Branching Agents

All the branching agents discussed thus far have been 'hard' branching agents *i.e.* small molecules with three or greater reactive functional groups.

Larger molecules or polymers might also be used to branch polymers. These could be referred to as 'flexible' branchers as they have long flexible chains along which they could branch.

Investigations into flexible branchers were carried out using polymers based on poly(acrylic acid) (PAA) as branchers. In this work branching was attempted using the flexible branchers shown below and ICI 'monomer' as feedstock.

PAA M_w ~5000

PAA-co-maleic acid M_w ~3000

PAA M_w ~2100

PAA M_w ~1200

The poly(acrylic acid)s were supplied in the sodium salt form and were converted to the acid form for use in polycondensations. The branchers were added at levels of 2, 0.25, 0.125 and 0.0625 Wt% and reacted under standard polycondensation reactions. During each of these reactions, the oligomeric flexible branching agent and the incipient PET were observed to separate into two domains and remain separate during the whole of the polycondensation process. On dissolution in TFA, all the polymers synthesised were observed to contain microgels. These gels prohibited any further analysis of the polymers.

The problem with these reactions seems to be that the two polymers – PET (or ICI's oligomer 'monomer') and PAA are not compatible with each other. Consequently,

the PAA phase separates into a micro-domain minimising reaction with the 'monomer'. Where reaction does occur, gelation results rapidly probably *via* crosslinking of PAA rather than the incipient PET phase

6.2.10 Ionomer Branching Agents

Ionomers are polymers with ionic groups present, which can form pseudo cross-links. These cross-links are more fluid than those of traditional branchers and can continually form and reform. This gives a less rigid structure than normal, but allows the polymer to be processed. Figure 14 shows a schematic representation of ionic crosslinks.

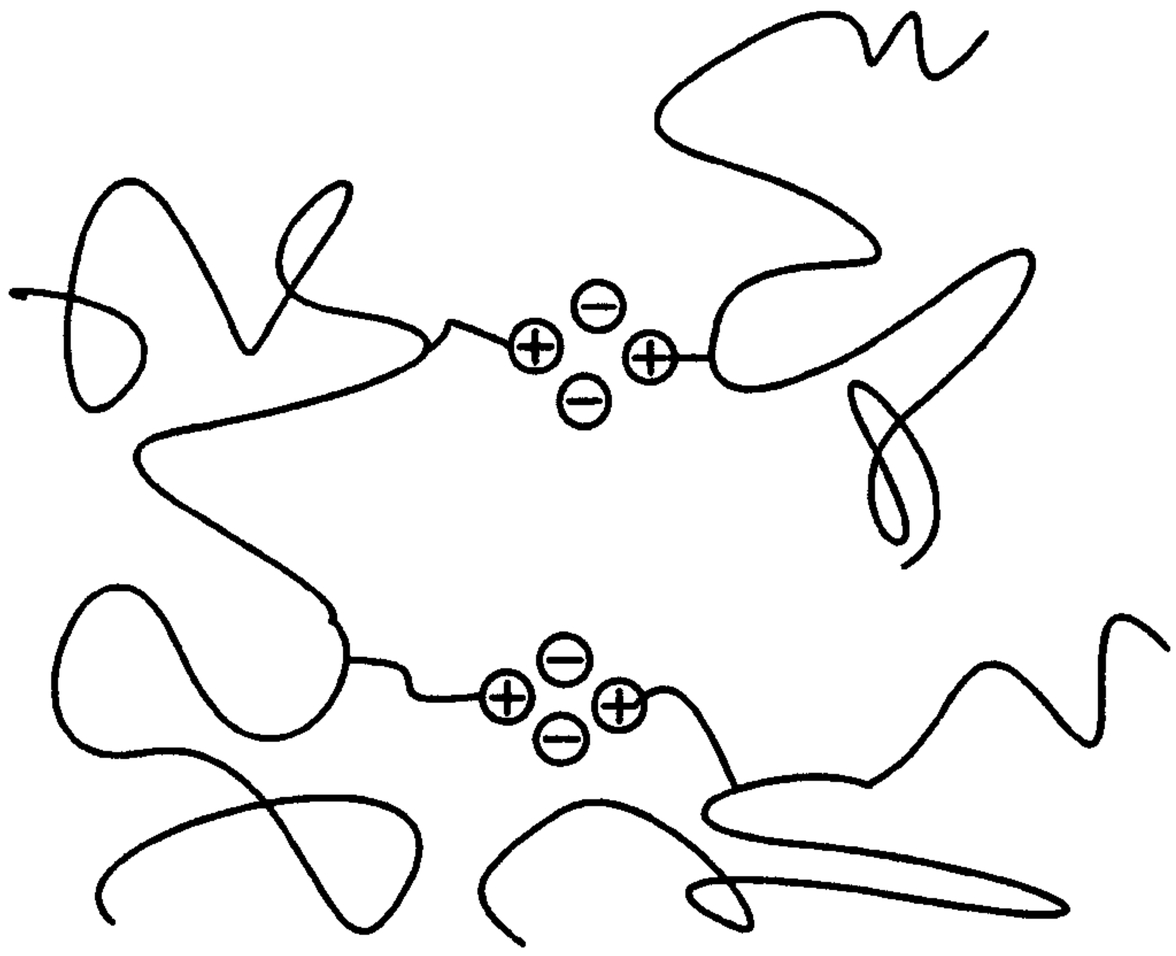

Figure 14: Representation of Ionomer crosslinking

The ionic groups chosen for this work are shown in Figure 15.

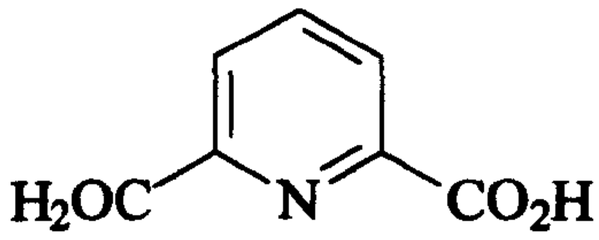

Structure 19:
2, 6-Pyridine Dicarboxylic Acid

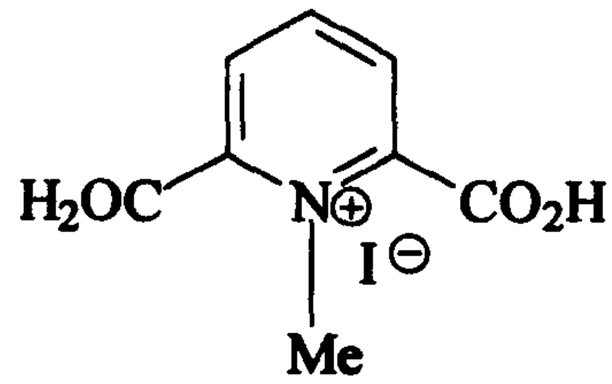

Structure 20:
2, 6, 1-Methyl Pyridine Dicarboxylic Acid

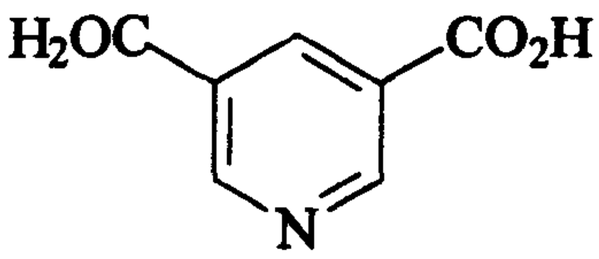

Structure 21:
3, 5-Pyridine Dicarboxylic Acid

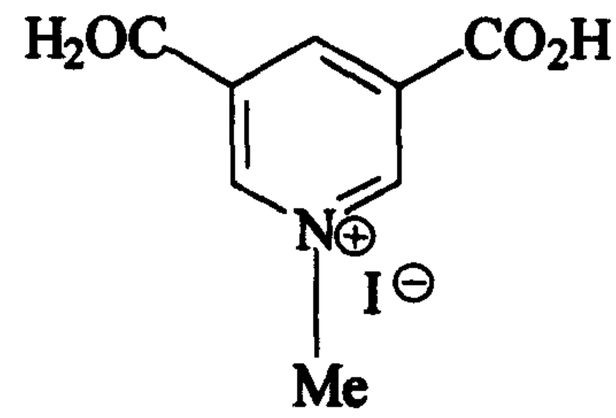

Structure 22:
3, 5, 1-Methyl Pyridine Dicarboxylic Acid

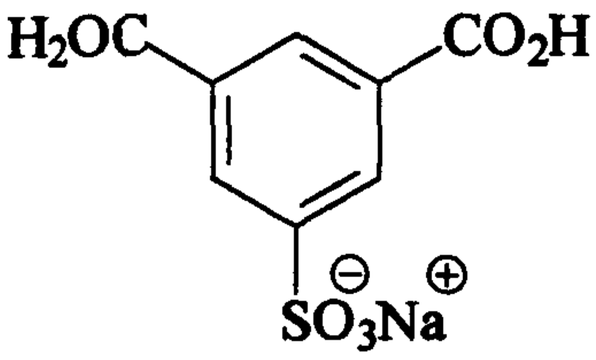

Structure 23:
5-Sulfoisophthalic Acid Sodium Salt

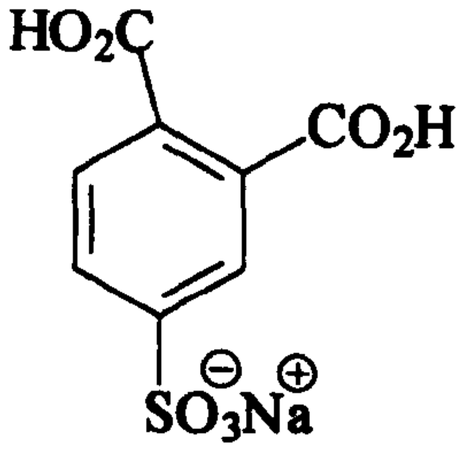

Structure 24:
4-Sulfophthalic Acid Sodium Salt

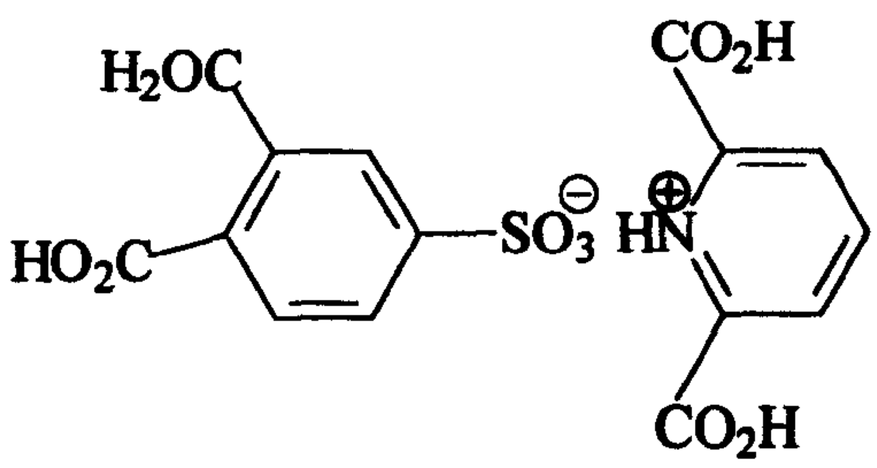

Structure 25:
4-Sulfophthalic Acid 2, 6-Pyridinedicarboxylic Acid Salt and other Isomers

Figure 15: Diacids Potentially Useful as the Bases of Ionic Crosslinking

The branchers were all added at a 2 Wt% level and the reactions carried out as normal

The reactions involving PDCA based branchers all produced purple/black polymer. Gas was evolved during these reactions, and the smell of pyridine was noted. It can be concluded that under the harsh conditions of the polycondensation reaction PDCA breaks down to form carbon dioxide and pyridine. The presence of the purple colour suggested the possibility that some form of complex was forming involving the antimony catalyst. The reactions were repeated without catalyst. This still resulted in the same colour formation; hence ruling out this explanation.

The reactions involving 4-SPA, Na and 5-SIPA, Na appeared to proceed as normal. However, on dissolution in OCP, tiny crystals formed. Microanalytical data indicated that this was unreacted branching agent. It appears that the brancher and the polymer are incompatible and do not react.

7 Conclusions

During the course of this research project, a substantial amount of work has been carried out on the branching of PET by means of standard polycondensation reactions. Substantially branched polyesters were synthesised using a variety of branching agents and their molecular weight was controlled using a range of end-capping agents. The resultant polymers were shown to be of significantly higher molecular weight than the linear polymers produced, and to have both lower solution and melt viscosity than linear polymers of equivalent molecular weight. Branching agents with more flexibility in their backbone, *e.g.* pentaerythritol and glycerol, produced more highly branched species than did the rigid structures of trimesic and pyromellitic acids, although both sets of polymers still grew to equivalent molecular weights. Benzyl alcohol appears to be the most effective end-capping agent of those tested. Small amounts of this agent resulted in very large differences in molecular weight and inhibited gelation in polymers where high levels (>0.25 Wt%) of branching agent were used.

Varying the time of addition of the branching agent had little effect on the branching of the polymer. However higher molecular weight polymers were formed as a direct result of the increases in reaction time that were imposed whilst varying the addition time.

Attempted branching using both flexible and ionomeric branchers failed. In the case of the flexible branchers, this was due to the incompatibility of the chosen brancher (PAA) and the 'monomer' in the melt. The ionomer branchers were too chemically fragile to withstand the harsh conditions of the melt reaction and broke down before any reaction with the 'monomer' took place.

8 Further Work

Very few detailed studies exist where branched polymers have been prepared with careful convolution of absolute molecular weight and degree of branching. Experimentally for melt polycondensations, this is quite difficult to achieve. The results here suggest that indeed branched PET of the same absolute molecular weight as a linear model display both lower solution and melt viscosities. It is important that this result is verified with other polymer systems, particularly those of technological importance. It is also important to follow up the results with the PET system to see how polymers with controlled branching and molecular weight perform in processing and in particular in melt drawing. What is the effect on crystallinity, degree of alignment, toughness, gas permeability etc? Lower melt viscosity for equivalent molecular weights holds out the prospect of lower processing costs but do the products formed have comparable/better/worse properties? Our own rather superficial observations of the bulk form and behaviour of highly branched (globular) PET suggests that key physical properties may indeed be worse than linear PET. It is known that regularly hyperbranched and dendritic polymers do in general have much better solubility characteristics than their linear analogues (*i.e.* tend to dissolve in common organic solvents). Paradoxically this might be an indication that such globular macromolecules will not form the basis of improved 'mechanical' materials, but will have to find a home in more speciality applications. More data is also required on bulk mechanical properties.

9 Experimental

9.1 Reagents

All reagents were obtained from the Aldrich Chemical Co. and used without further purification unless otherwise stated.

Acetone

Acetone was shaken with calcium sulfate (anhydrous), for four hours and was then distilled under nitrogen over fresh calcium sulphate onto more fresh calcium sulphate.

Dichloromethane (DCM)

This was distilled over calcium hydride under nitrogen onto 4Å molecular sieves.

Tetrahydrofuran (THF)

This was distilled over sodium metal and benzophenone under nitrogen onto 4Å molecular sieves.

Methyl ethyl ketone (MEK)

This was distilled over calcium sulfate onto fresh calcium sulphate.

Aniline

This was dried over calcium hydride and distilled under vacuum (0.2 mmHg) at 20 °C. The aniline was then shaken with $SnCl_2$ to remove any sulfurous impurities and was then filtered by gravity.

Nitrobenzene

This was distilled under vacuum (0.05 mmHg) at 40 °C in the presence of dilute sulfuric acid. The liquid was dried over calcium chloride and shaken with fresh calcium chloride. It was then redistilled under vacuum (0.1 mmHg) at ~ 40 °C over phosphorous pentoxide. It was stored over calcium hydride and filtered by gravity before use.

Bis-2-hydroxethyl terephthalate

ICI initially supplied this reagent. However, towards the end of the experimental work supplies were depleted and a method of synthesising sufficient quantities of this feedstock had to be established to finish this programme of work. The synthesis of this is contained in Appendix 3

Succinic Anhydride

Succinic anhydride (10 g) was recrystallised from chloroform. It was then filtered off and washed with diethyl ether (5 x 50ml) and dried in a vacuum oven.

9.2 Analytical Methods

^{1}H and ^{13}C NMR spectra were recorded on a Bruker AMX250, Jeol 270 or Bruker DPX 400 instrument. FTIR spectra were recorded using a Nicolet 400 D spectrometer. Elemental microanalysis was carried out by the Microanalytical Services within the University. DSC data was acquired on a Mettler TA 4000 differential scanning calorimeter and light scattering was carried out on a Malvern 4700 and Brookhaven BI – 9000 RT instruments. Melt rheology measurements were taken on a TA Instruments CSL^{2} controlled stress rheometer.

9.3 PET Synthesis

During this project PET was synthesised using the procedure outlined in section 9.3.2. Linear and branched PET were produced using BHET and ICI's 'monomer' as feedstock and a variety of branching and end-capping agents were used. Experimental details of these reactions are contained in section 9.3.3 below.

9.3.1 Polycondensation Rig

The rig consists of a thick-walled glass reaction tube , with a Quickfit joint at the top and a thin, pre-scored, glass nipple at the bottom. The vessel was suspended in an iron heating block and connected *via* a series of pipes and valves to a vacuum pump and a nitrogen inlet. This allowed both inert and reduced atmospheres as required. All joints were sealed with standard vacuum grease, except for the joint immediately above the heating block. In this case Apizon™ L, specialised vacuum grease, capable of withstanding the high temperatures of the polycondensation process, was used. Two cold traps were employed to collect by-products and protect the vacuum pump; these contain iced water (trap 1) and liquid nitrogen (trap 2). A Eurostar Power Digital overhead stirrer (IKA Labortechnic), was employed to stir the reaction, using a custom-built stirring shaft. Heating was controlled via a MC810 digital temperature controller (Electrothermic Engineering Limited).

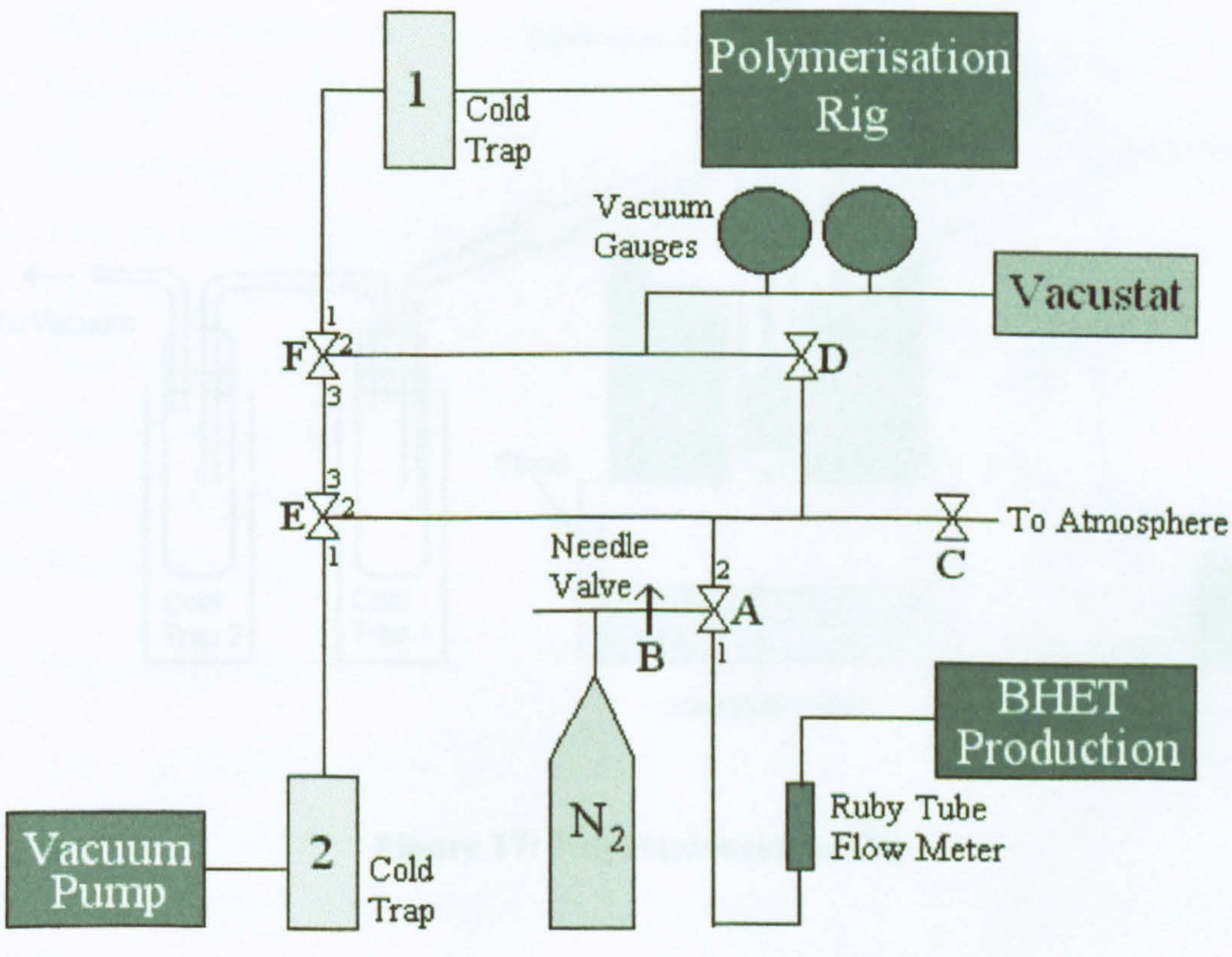

Figure 16: PET Production Apparatus

9.3.2 Poly(ethylene)Terephthalate Production

Synopsis

Briefly, the procedure involves the evacuation of the apparatus interior followed by the introduction of nitrogen. This provides an inert atmosphere for the polycondensation reaction. The temperature is then raised and the pressure of the system is carefully reduced. On completion of the polycondensation reaction, the polymer is extruded, under gravity, into cold water.

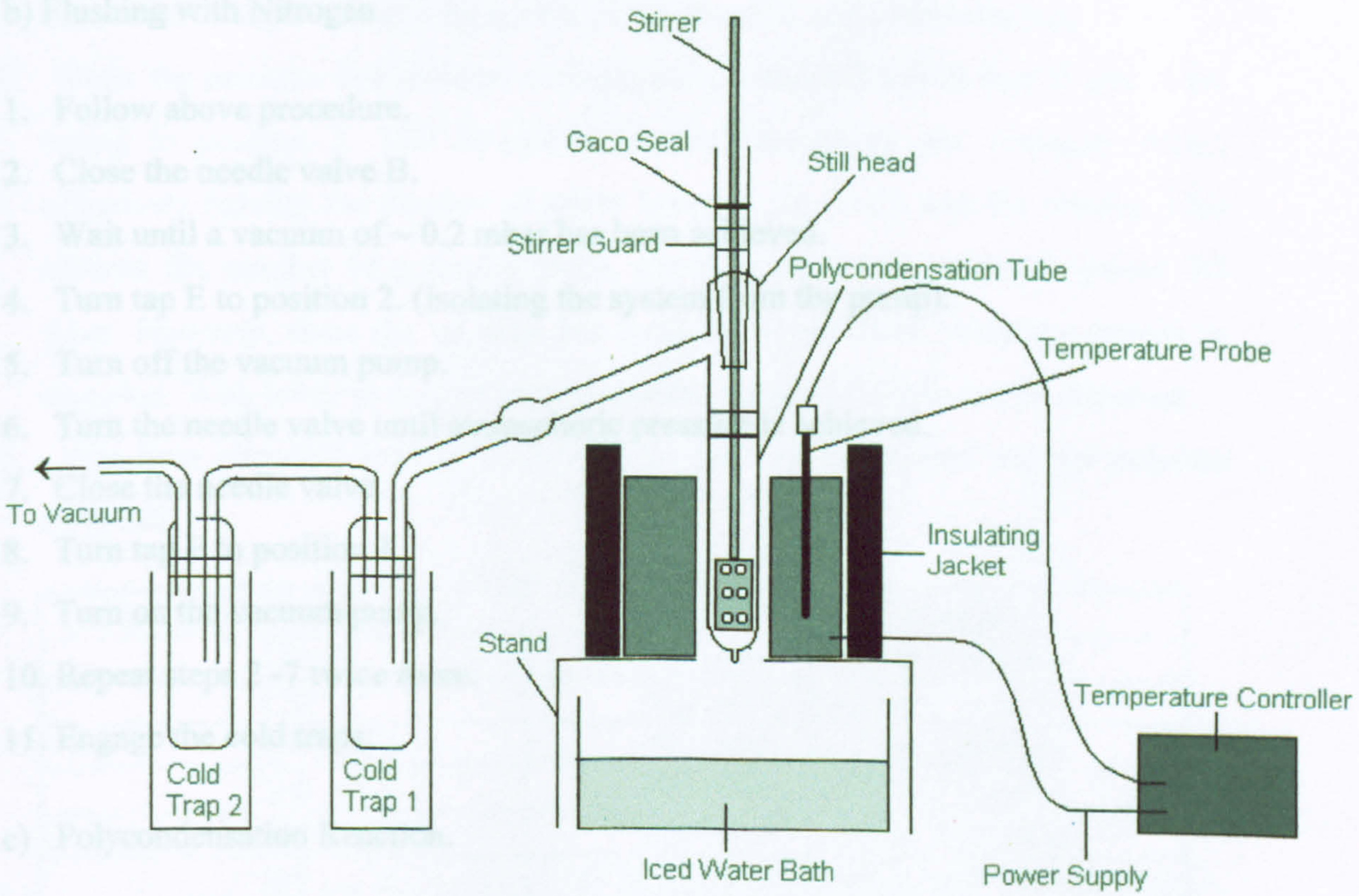

Figure 17: Polycondensation Rig

Experimental Procedure

a) Adjusting the Nitrogen Flow

1. Turn tap A to position 2.
2. Ensure that the needle valve B is fully open.
3. Ensure tap C is closed.
4. Ensure tap D is open.
5. Turn taps E & F to position 1.
6. Turn on the vacuum pump and adjust the nitrogen flow, using the cylinder regulator, so that the nitrogen flow is equal to the pull of the pump - *i.e.* the system remains at atmospheric pressure.

b) Flushing with Nitrogen

1. Follow above procedure.
2. Close the needle valve B.
3. Wait until a vacuum of ~ 0.2 mbar has been achieved.
4. Turn tap E to position 2. (isolating the system from the pump).
5. Turn off the vacuum pump.
6. Turn the needle valve until atmospheric pressure is achieved.
7. Close the needle valve.
8. Turn tap E to position 1.
9. Turn on the vacuum pump.
10. Repeat steps 2 -7 twice more.
11. Engage the cold traps.

c) Polycondensation Reaction.

1. 150 g of BHET, or 'monomer' and 200 ppm of antimony trioxide are weighed into a polycondensation tube.
2. The system is evacuated and a nitrogen atmosphere added *via* procedures a) and b).
3. The thermocouple is inserted in the heating block and the temperature set at 240 °C, for BHET, and 270 °C, for 'monomer'.

4. As soon as the feedstock has melted (usually at the set temperatures) the stirrer is set at 100 RPM, and is then switched to torque mode.
5. Once the heating block has reached the set temperature, it is held there for 40 minutes to allow good mixing of the catalyst and the monomer.
6. The temperature is then slowly increased over a period of ~ 2 hours whilst simultaneously reducing the pressure to ~ 0.2 mbar in accordance with the profile shown in Table 29. It is very important that this is not done too quickly or the melt may become too 'lively' and may be sucked into, and block, the tubes from the reactor.
7. The reaction is monitored visually, and by torque differential readings. Bubbles in the melt show that the viscosity is increasing, as does an increase in torque. There is no need to adjust the stirring speed, as the stirrer is self-compensating.
8. When the pressure has reached a minimum (around 0.2 mbar) taps E and F are turned to position 3. This by-passes the pressure gauge and nitrogen feeder, effectively halving the number of joints between the pump and the reactor. This reduces the number of potential leaks, allowing access to pressures below 0.2 mbar. However, since the vacustat has been by-passed these pressures cannot be recorded. With lower pressures high molecular weight polymer can be achieved.
9. One hour after full vacuum is applied the reaction is stopped and the polymer extruded.

TEMPERATURE (°C)	PRESSURE GAUGE
240 *	500 mbar - held for 5 minutes
250	400 mbar - held for 5 minutes
270	300 mbar - held for 5 minutes
280	200 mbar - held for 5 minutes
290	100 mbar - held for 5 minutes
290	to 50 mbar at the rate of -10 mbar/min
290	to 20 mbar at the rate of -5 mbar/min
290	to 10 mbar at the rate of -2 mbar/min
290	to 0 mbar at the rate of -2 mbar/min

Table 29: Temperature and Pressure profile during Polycondensation

* In the case of 'monomer' this progression starts at 270 °C and increases similarly.

d) Extrusion of Polymer

1. Turn tap E to position 2.
2. Turn off vacuum pump.
3. Open needle valve until atmospheric pressure is achieved. Close needle valve and open tap C to vent to atmosphere (this ensures there is no pressure imbalance in the system).
4. Place a beaker of cold water under the polycondensation tube.
5. Turn off stirrer.
6. Lower test vessel until nipple is clear of heating block.
7. Remove nipple with a spanner or hammer. The polymer will then extrude into the water. Ensure that the polymer is fully quenched on extrusion by swirling the beaker. If the polymer begins to pile up, and swirling does not help, switch to a fresh beaker - all polymer must stay below the water line.

e) Shutdown

1. As soon as all polymer is extruded, switch of the heating block.
2. Switch off the nitrogen supply
3. Remove polycondensation tube from heating block (to prevent sticking)
4. Remove temperature probe (to prevent it becoming welded in position)

Torque Measurements

The stirrer used in the reaction is equipped with a torque meter. This device, although not capable of measuring the torque directly, measures the difference in torque at any given instant, from the initial torque applied to the stirrer. During the reaction, torque readings are recorded throughout, initially by hand and then later by means of an ADC connection to a computer with data logging software.

The torque readings give a guide to changes in the melt viscosity during the reaction, and provide a useful comparison of the said property between different reactions.

9.3.3 Polycondensation Reactions

Initial Reactions

An initial series of fifteen experiments was carried out to ensure that the apparatus was functioning normally. At the end of this series, the evolving operating procedure was then finalised and the test series was begun in earnest

Below is a brief description of the variation from the stated test procedure of each experiment, along with any pertinent comments.

Linear Polymers

PET 1 BHET - 145.23 g

Sb_2O_3 - 0.0299 g

A clear polymer was extruded. It set as a hard white/clear plastic.

PET 2 BHET - 149.3 g

Sb_2O_3 - 0.03 g

The extruded polymer was clear, but set as a hard, white plastic.

PET 3 'Monomer' - 148.39 g

Sb_2O_3 - 0.031 g

As PET 2, but using 'monomer', in place of BHET. The extruded polymer was clear and glassy. It was slightly yellowed in places.

PET 4 BHET - 150.09 g

Sb_2O_3 - 0.0298 g

The extruded polymer was clear and glassy.

The infrared spectra of these linear polymers are very similar, all showing the expected bands below:-

FTIR (Cast film/cm^{-1}) 3550 (OH), 2970 (aliphatic C-H), 1790 (ester carbonyl), 818 (1,4-disubstituted aryl)

Branched BHET Reactions

B3CA Branched Reactions

These reactions were based on BHET, and involved the simple addition of varying amounts of B3CA to the reaction mixture.

PET 5 BHET - 150.7 g

Sb_2O_3 - 0.0299 g

B3CA - 3.01 g (2 Wt%, 0.043 mol eq)

During this reaction the melt became unstable, and began to bubble up. Increasing the pressure temporarily, and re-applying the vacuum more slowly controlled this.
The polymer became so viscous during the reaction that it wrapped itself round the stirrer. It would not extrude. It was rubbery when molten and rock hard when solid.

PET 6 BHET - 150.21 g

Sb_2O_3 - 0.0300 g

B3CA - 1.50 g (1 Wt%, 0.021 mol eq)

A glassy polymer was extruded.

PET 7 BHET - 150.71 g

Sb_2O_3 - 0.0321 g

B3CA - 0.76 g (1/2 Wt%, 0.011 mol eq)

The extruded polymer was glassy and of a good quality.

PET 8 BHET - 150.70 g

Sb_2O_3 - 0.030 g

B3CA - 0.35 g (1/4 Wt%, 0.005 mol eq)

A viscous glassy polymer was extruded.

The infrared spectra of these branched polymers are very similar, all showing the expected bands below: -

FTIR (Cast film/cm^{-1}) 3550 (OH), 2970 (aliphatic C-H), 1790 (ester carbonyl), 925 (1,3,5-trisubstituted aryl), 820 (1,4-disubstituted aryl)

Ball-Milling of B3CA Branched Reactions

This matrix of reactions saw the introduction of a ball-milling procedure to try to mix the reactants better before the reaction.

The reaction mixture was divided into portions each portion being a small proportioned mixture of the total ingredients. These were subjected to ball- milling in a Fritsch Pulvetisette®. The portions were then combined in the test-vessel before reacting as normal. Each portion's individual weight was recorded as well as the final weight in the test-vessel - some mass is lost in the mill.

PET 9	Portion 1	Portion 2
	BHET - 75.01 g	BHET - 75.1 g
	B3CA - 0.75 g	B3CA - 0.76 g
	(1/2 Wt%, 0.011 mol eq)	(1/2 Wt%, 0.011 mol eq)
		Sb_2O_3 - 0.0298 g

Each portion was ball-milled for twenty minutes. The total mass added to the test vessel was 149.91 g.

The system seized up when the polymer became too viscous 26 minutes before the scheduled shutdown.

PET 10	Portion 1	Portion 2
	BHET - 75.11 g	BHET - 75.02 g
	B3CA - 1.55 g	B3CA - 1.52 g
	(1 Wt%, 0.022 mol eq)	(1 Wt%,0.022 mol eq)
		Sb_2O_3 - 0.031 g

Each portion was ball-milled for twenty minutes. The total mass added to the test vessel was 151.36 g.

The reaction was given a further one hour induction, before the implementation of vacuum or temperature rise profiles.

The system seized up when the polymer became too viscous 21 minutes before the scheduled shutdown.

PET 11 Portion 1

BHET - 1.54 g

B3CA - 1.5 g (1 Wt%, 0.021 mol eq)

Sb_2O_3 - 0.0158 g

Ball- milled for 30 minutes and then 14.64 g of BHET was added to the mill. It was milled for a further 30 minutes. 18.64 g of BHET was added and it was ball-milled for a further 30 minutes. 24.31 g of BHET was added and it was ball-milled for a further 40 minutes. 16.65 g of BHET was added and it was ball-milled for a final 30 minutes.

76.00 g was added to the test vessel.

Portion 2

BHET - 1.51 g

B3CA - 1.5 g (1 Wt%, 0.021 mol eq)

Sb_2O_3 - 0.0164 g

Ball- milled for 30 minutes and then 14.86 g of BHET was added to the mill. It was milled for a further 30 minutes. 20.06 g of BHET was added and it was ball-milled for a further 30 minutes. 20.47 g of BHET was added and it was ball-milled for a further 30 minutes. 18.10 g of BHET was added and it was ball-milled for a final 30 minutes.

75.41 g was added to the test vessel.

The system seized up when the polymer became to viscous 18 minutes before the scheduled shutdown

PET 12 Portion 1

BHET - 0.75 g

B3CA - 0.75 g (1/2 Wt%, 0.011 mol eq)

Sb_2O_3 - 0.0145 g

Ball- milled for 30 minutes and then 14.29 g of BHET was added to the mill. It was milled for a further 30 minutes. 20.05 g of BHET was added and it was ball-milled for a further 30 minutes. 19.96 g of BHET was added and it was ball-milled for a

further 30 minutes. 43.97 g of BHET was added and it was ball-milled for a final 30 minutes.

98.21 g was added to the test vessel.

Portion 2

BHET - 5.21 g

B3CA - 0.75 g (1/2 Wt%, 0.011 mol eq)

Sb_2O_3 - 0.0156 g

Ball-milled for 30 minutes and then 14.88 g of BHET was added to the mill. It was milled for a further 30 minutes. 14.96 g of BHET was added and it was ball-milled for a further 30 minutes. 15.9 g of BHET was added and it was ball-milled for a further 30 minutes.

52.66 g was added to the test vessel.

The system seized up when the polymer became to viscous 5 minutes before the scheduled shutdown.

PET 13 Portion 1

BHET - 0.375 g

B3CA - 0.375 g (1/4 Wt%, 0.0054 mol eq)

Sb_2O_3 - 0.015 g

Ball-milled for 30 minutes and then 11.52 g of BHET was added to the mill. It was milled for a further 30 minutes. 19.98 g of BHET was added and it was ball-milled for a further 30 minutes. 20.56 g of BHET was added and it was ball-milled for a further 30 minutes. 28.92 g of BHET was added and it was ball-milled for a final 30 minutes.

80.5 g was added to the test vessel.

Portion 2

BHET - 10.05 g

B3CA - 0.375 g (1/4 Wt%, 0.0054 mol eq)

Sb_2O_3 - 0.015 g

Ball-milled for 30 minutes and then 19.99 g of BHET was added to the mill. It was milled for a further 30 minutes. 20.15 g of BHET was added and it was ball-milled

for a further 30 minutes. 18.75 g of BHET was added and it was ball-milled for a further 30 minutes.

69.4 g was added to the test vessel.

Problems in maintaining vacuum in the early stages of the reaction resulted in a glassy/white in parts polymer which was easily crumbled. This is most likely low molecular weight material. The polymer was extruded easily at the end of reaction.

PET 14 Portion 1

BHET - 10.02 g

B3CA - 0.39 g (1/4 Wt%, 0.0056 mol eq)

Sb_2O_3 - 0.0166 g

Ball-milled for 30 minutes and then 21.35 g of BHET was added to the mill. It was milled for a further 30 minutes. 38.14 g of BHET was added and it was ball-milled for a further 30 minutes. 5.65 g of BHET was added and it was ball-milled for a further 30 minutes.

75.14 g was added to the test vessel.

Portion 2

BHET - 19.13 g

B3CA - 0.364 g (1/4 Wt%, 0.0052 mol eq)

Sb_2O_3 - 0.0144 g

Ball-milled for 30 minutes and then 10.41 g of BHET was added to the mill. It was milled for a further 30 minutes. 20.16 g of BHET was added and it was milled for a further 30 minutes. 15.63 g of BHET was added and it was milled for a further 30 minutes. 9.65 g of BHET was added and it was milled for a further 30 minutes.

75.21 g was added to the test vessel.

The FTIR of these polymers were recorded and showed the following bands: -

FTIR (Cast film/cm^{-1}) 3550 (OH), 2970 (aliphatic C-H), 1790 (ester carbonyl), 925 (1,3,5-trisubstituted aryl), 820 (1,4-disubstituted aryl)

Low Level B3CA Branched Reactions

Below are detailed the reactions involving lower levels of B3CA (1/4Wt% and below) as a branching agent.

PET 15 BHET - 150.05 g
B3CA - 0.376 g (1/4 Wt%, 0.0054 mol eq)
Sb_2O_3 - 0.0310 g

PET 16 BHET - 150.42 g
B3CA - 0.1890 g (1/8 Wt%, 0.0027 mol eq)
Sb_2O_3 - 0.0298 g

PET 17 BHET - 150.56 g
B3CA - 0.0937 g (1/16 Wt%, 0.0013 mol eq)
Sb_2O_3 - 0.0290 g

FTIR and NMR spectral analysis of the above polymers gave the following bands and resonances: -

FTIR (Cast film/cm^{-1}) 3550 (OH), 2970 (aliphatic C-H), 1790 (ester carbonyl), 925 (1,3,5 trisubstituted aryl), 820 (1,4 disubstituted aryl)

^1H NMR ($CDCl_3$/TFA 1:9 v/v /270 MHz): δ8.2 (4H, s, aryl), δ4.8 (4H, s, aliphatic)

^{13}C NMR ($CDCl_3$/ TFA 1:9 270 MHz): δ168.2 (CO), δ133.8 (*p*-aryl), δ130.5 (*m*-aryl), δ64.3 (aliphatic)

PET 18 BHET - 150.13 g
Sb_2O_3 - 0.0299 g
B3CA - 0.1893 g (1/8 Wt%, 0.0027 mol eq)

A repeat of reaction PET 16, clear polymer extruded

PET 19 BHET - 150.15 g
Sb_2O_3 - 0.0296 g
B3CA – 0.3755 g (1/4 Wt%, 0.0054 mol eq)

The B3CA was added to the reaction vessel after the 40 min induction period

PET 20 BHET - 150.13 g

Sb_2O_3 - 0.0303 g

B3CA – 0.3751 g (1/4 Wt%, 0.0054 mol eq)

The B3CA was added to the reaction vessel after full vacuum had been achieved (this means that the B3CA was in the reactor for only 1 hr of the reaction). The polymer produced was white and crumbly.

PET 21 BHET - 150.08 g

Sb_2O_3 - 0.0276 g

B3CA – 0.3750 g (1/4Wt%, 0.0054 mol eq)

The B3CA was added to the reaction vessel 1 hr after full vacuum had been achieved (*i.e.* when the reaction would normally have finished). The reaction was then allowed to run for a further 40 minutes. The polymer gelled and would not extrude from the reactor.

Reactions Based on 'Monomer'

These reactions, based on 'monomer', involve the addition of varied amounts of B3CA to the melt.

PET 22 Monomer - 149.5 g

B3CA - 3.06 g (2 Wt%, 0.044 mol eq)

Sb_2O_3 - 0.030 g

The extruded polymer was extremely viscous and rubbery. It was clear in colour although it set white.

PET 23 Monomer - 153.0 g

B3CA - 1.50 g (1 Wt%, 0.021 mol eq)

Sb_2O_3 - 0.031 g

A glassy clear/yellow polymer was obtained. It was to viscous to extrude. On cooling it turned white.

PET 24 Monomer - 154.0 g

B3CA - 0.76 g (1/2 Wt%, 0.011 mol eq)

Sb_2O_3 - 0.034 g

The polymer extruded and quenched readily, leaving a clear polymer when set.

PET 25

Portion 1	Portion 2
Monomer - 75.07 g	Monomer - 75.15 g
B3CA - 1.54 g	B3CA - 1.47 g
(1 Wt%, 0.022 mol eq)	(1 Wt%, 0.021 mol eq)
	Sb_2O_3 - 0.030 g

Each portion was ball-milled for twenty minutes. The total mass added to the test vessel was 152.13 g.

The system seized up when the polymer became too viscous 7 minutes before the scheduled shutdown.

PET 26

Portion 1	Portion 2
Monomer - 75.11 g	Monomer - 75.00 g
B3CA - 1.64 g	B3CA - 1.39 g
(1 Wt%, 0.023 mol eq)	(1 Wt%, 0.020 mol eq)
	Sb_2O_3 - 0.0298 g

Each portion was ball-milled for twenty minutes. The total mass added to the test vessel was 152.45 g.

The reaction was given an extra 1 hour induction period, before raising the temperature and lowering the pressure.

During the early part of this experiment nitrogen was seen bubbling out of the top of the reaction vessel, and it proved impossible to keep the seal. Nitrogen was therefore allowed to continually bubble through the reactor to try to exclude oxygen.

The system seized up when the polymer became too viscous 38 minutes before the scheduled shutdown.

FTIR spectra were recorded for these polymers and yielded the following bands: -

FTIR (Cast film/cm^{-1}) 3550 (OH), 2970 (aliphatic C-H), 1790 (ester carbonyl), 925 (1,3,5-trisubstituted aryl), 820 (1,4-disubstituted aryl)

Reactions Based on Adjusted 'Monomer' Content

These reactions, based on 'monomer', involve the addition of varied amounts of B3CA to the melt. The amount of 'monomer' present has been adjusted to take account of the difference in mass of the monomer unit and the 7 BHET units that would have to react to make it up (i.e. 6 ethylene glycol molecules).

PET 27 Monomer - 118.66 g

Sb_2O_3 - 0.0300 g

PET 28 Monomer - 118.54 g

B3CA - 3.00 g (2 Wt%, 0.043 mol eq)

Sb_2O_3 - 0.0302 g

The system seized up 55 minutes before the scheduled end.

PET 29 Monomer - 119.39 g

B3CA - 1.50 g (1 Wt%, 0.021 mol eq)

Sb_2O_3 - 0.0300 g

PET 30 Monomer - 119.00 g

B3CA - 1.50 g (1 Wt%, 0.021 mol eq)

Sb_2O_3 - 0.0300 g

This experiment was given an extra hour induction period. During the reaction, vacuum was temporarily lost when the glycol seal failed. The reaction had to be stopped while it was replaced. Air was allowed into the reactor.

PET 31 Monomer - 118.66 g

B3CA - 0.75 g (1/2 Wt%, 0.011 mol eq)

Sb_2O_3 - 0.0297 g

FTIR spectral analysis of the above polymers gave the bands below: -

FTIR (Cast film/cm^{-1}) 3550 (OH), 2970 (aliphatic C-H), 1790 (ester carbonyl), 925 (1,3,5-trisubstituted aryl), 820 (1,4-disubstituted aryl)

PET 32 Monomer - 118.56 g

B3CA - 1.50 g (1 Wt%, 0.021 mol eq)

Sb_2O_3 - 0.0299 g

PET 33 Monomer - 118.80 g

B3CA - 0.375 g (1/4 Wt%, 0.0054 mol eq)

Sb_2O_3 - 0.0310 g

Reaction time was increased by half an hour.

PET 34 Monomer - 118.41 g

Sb_2O_3 - 0.0299 g

Reaction time was extended by half an hour.

PET 35 Monomer - 118.96 g

Sb_2O_3 - 0.0298 g

Penta- 0.1830 g (0.154 Wt%, 0.0054 mol eq)

Pentaerythritol was used as the branching agent instead of B3CA, at a level equivalent to ¼ Wt% B3CA. This is a tetra-functional monomer.

Other Branched Reactions

After investigation of branching with B3CA a comparison was sought by carrying out reactions with other branching agents.

PET 36 BHET - 149.96 g

Sb_2O_3 - 0.0296 g

B4CA – 0.3745 g (1/4 Wt%, 0.0059 mol eq)

The tetra-functional monomer B4CA was used as the branching agent instead of B3CA. Polymer extruded as a clear polymer, subsequently found to be crosslinked.

PET 37 BHET - 149.94 g

Sb_2O_3 - 0.0299 g

Penta - 0.3754 g (1/4Wt%, 0.011 mol eq)

The tetra-functional monomer pentaerythritol was used as the branching agent instead of B3CA. The polymer cross-linked during the reaction.

PET 38 BHET - 150.05 g

Sb_2O_3 - 0.0301 g

Glycerol - 0.3269 g (0.22 Wt%, 0.011 mol eq)

Glycerol was used as the branching agent instead of B3CA. This is a tri-functional monomer. A glassy polymer, of good quality was extruded.

PET 39 BHET - 150.02 g

Sb_2O_3 - 0.0300 g

Penta - 0.1822 g (1/8 Wt%, 0.0054 mol eq)

Pentaerythritol was used as the branching agent instead of B3CA. This is a tetra-functional monomer. The polymer cross-linked during the reaction.

PET 40 BHET - 149.88 g

Sb_2O_3 - 0.030 g

B4CA - 0.3401 g (1/4 Wt%, 0.0054 mol eq)

B4CA was used as the branching agent instead of B3CA. This is a tetra-functional monomer. To ensure a better comparison between this brancher and B3CA the same amount of mole equivalents was used, taking into account the fact that B4CA has 4 functional groups and B3CA only 3. The polymer extruded as a clear polymer.

PET 41 BHET - 150.00 g

Sb_2O_3 - 0.0309 g

Glycerol - 0.3280 g (1/4 Wt%, 0.011 mol eq)

Glycerol was used as the branching agent instead of B3CA. This is a tri-functional monomer. A glassy polymer, of good quality was extruded.

PET 42 BHET - 150.10 g

Sb_2O_3 - 0.0300 g

Glycerol - 0.1780 g (1/8 Wt%, 0.0058 mol eq)

Glycerol was used as the branching agent instead of B3CA. This is a tri-functional monomer. A glassy polymer, of good quality was extruded.

PET 43 BHET - 151.64 g

Sb_2O_3 - 0.0320 g

B4CA - 0.3369 g (1/4 Wt%, 0.0053 mol eq)

B4CA was used as the branching agent instead of B3CA. This is a tetra-functional monomer. The polymer extruded as a clear polymer.

PET 44 BHET - 150.13 g

Sb_2O_3 - 0.0298 g

Penta - 0.1827 g (1/8 Wt%, 0.0054 mol eq)

Pentaerythritol was used as the branching agent instead of B3CA. This is a tetra-functional monomer. The polymer cross-linked during the reaction.

PET 45 BHET - 149.68 g

Sb_2O_3 - 0.0304 g

Dipenta - 0.228 g (1/7 Wt%, 0.0054 mol eq)

Dipentaerythritol was added as a branching agent. The polymer produced was white and crumbly.

PET 46 BHET - 150.43 g

Sb_2O_3 - 0.0304 g

Tripenta - 0.2492 g (1/6 Wt%, 0.0054 mol eq)

Tripentaerythritol branching agent was added, giving rise to a white, crumbly polymer.

NMR spectra of the above polymers showed the following peaks:-

^1H NMR ($CDCl_3$/TFA 1:9 v/v /270 MHz): δ8.2 (4H, s, aryl), δ4.8 (4H, s, Aliphatic)

^{13}C NMR ($CDCl_3$/TFA 1:9 v/v 270 MHz): δ168.2 (CO), δ133.8 (*p*-aryl), δ130.5 (*m*-aryl), δ64.3 (Aliphatic)

Branched Reactions with End-cappers

PET 47 BHET - 149.68 g

Sb_2O_3 - 0.0308 g

B3CA - 3.0052 g (2 Wt%, 0.043 mol eq)

TAME - 7.7227 g (5 Wt%, 0.043 mol)

As well as the B3CA branching agent, TAME end-capper was also added. The TAME was added at a level equivalent to the number of functional groups in 2 Wt% of BC3A. *i.e.* enough was added to be able to react with every acid group in B3CA. The polymer gelled and could not be extruded from the reaction vessel

PET 48 BHET - 150.04 g

Sb_2O_3 - 0.0300 g

B3CA - 1.5000 g (1 Wt%, 0.021 mol eq)

TAME - 3.8612 g (3 Wt%, 0.021 mol)

Recording of torque data was unfortunately interrupted in this case. TAME was used as an end- capper. The polymer gelled and could not be extruded.

PET 49 BHET - 150.30 g

Sb_2O_3 - 0.0296 g

B3CA - 3.0046 g (2Wt%, 0.043 mol eq)

BzCOOH - 5.2273 g (4Wt%, 0.043 mol)

As well as the B3CA branching agent, BzCOOH end-capper was also added. The polymer gelled and could not be extruded from the reaction vessel

PET 50 BHET - 150.01 g

Sb_2O_3 - 0.0301 g

TAME - 2.5788 g (2 Wt%, 0.014 mol)

TAME end-capper (1Wt% equ) was added, but no branching agent.

PET 51 BHET - 150.71 g

Sb_2O_3 - 0.0299 g

B3CA - 3.0005 g (2 Wt%, 0.043 mol eq)

BnOH - 3.1094 g (2 Wt%, 0.029 mol)

As well as the B3CA branching agent, BnOH end-capper was also added. The polymer gelled and could not be extruded from the reaction vessel

PET 52 BHET - 150.10 g

Sb_2O_3 - 0.0298 g

BnOH - 3.100 g (2 Wt%, 0.029 mol)

BnOH end-capper was added. The polymer produced was crumbly and white. It appeared very low molecular weight. A computer was attached to the reactor stirrer *via* an ADC (analogue to digital converter) during this reaction so that the torque could be recorded automatically.

NMR spectral analysis gave the following peaks:-

^{1}H NMR ($CDCl_3$/TFA 1:9 v/v /270 MHz): δ8.2 (4H, s, aryl), δ4.8 (4H, s, aliphatic)

^{13}C NMR ($CDCl_3$/ TFA 1:9 v/v 270 MHz): δ168.8 (CO), δ133.8 (*p*-aryl), δ130.5 (*m*-aryl), δ64.5 (aliphatic)

PET 53 BHET - 150.14 g

Sb_2O_3 - 0.0300 g

B3CA - 3.0000 g (2 Wt%, 0.043 mol eq)

BnOH - 6.2000 g (4 Wt%, 0.057 mol)

BnOH end-capper was added. The polymer produced was white and crumbly.

PET 54 BHET - 150.40 g

Sb_2O_3 - 0.0300 g

B3CA - 3.0010 g (2 Wt%, 0.043 mol eq)

BnOH - 6.2000 g (4 Wt%, 0.057 mol)

BnOH end-capper was added. The polymer produced was white and crumbly.

PET 55 BHET - 150.10 g

Sb_2O_3 - 0.0301 g

B3CA - 3.0004 g (2 Wt%, 0.043 mol eq)

BnOH - 4.6000 g (3 Wt%, 0.043 mol)

As well as the B3CA branching agent, BnOH end-capper was also added. The polymer produced was white and crumbly.

NMR spectral analysis gave the following resonances:-

^{1}H NMR ($CDCl_3$/TFA 1:9 v/v /270 MHz): δ8.2 (4H, s, aryl), δ4.8 (4H, s, aliphatic)

^{13}C NMR ($CDCl_3$/ TFA 1:9 v/v 270 MHz): δ169 (CO), δ133.9 (*p*-aryl), δ130.6 (*m*-aryl), δ64.6 (aliphatic)

PET 56 BHET - 150.13 g

Sb_2O_3 - 0.0300 g

A linear polymer produced using BHET produced 'in house'. On heating to induction temperature (240°C). More ethylene glycol than normal was produced.

PET 57 BHET - 150.14 g

Sb_2O_3 - 0.0300 g

BnOH – 1.5330g (1 Wt%, 0.014 mol)

BnOH end-capper was added to the melt. The polymer produced was white and crumbly.

PET 58 BHET - 150.10 g

Sb_2O_3 - 0.0304 g

Stearic acid - 8.19 g (5 Wt% 0.029 mol)

Stearic acid end-capper was added to the reaction mixture. The polymer produced was white and crumbly.

PET 59 BHET - 149.68 g

Sb_2O_3 - 0.0303 g

9-Anthracene methanol – 8.92 g (6 Wt% 0.043 mol)

9-Anth. end-capper was added to the reaction mixture. The polymer produced was black and crumbly.

PET 60 BHET - 150.50 g

Sb_2O_3 - 0.0298 g

BzCOOH - 1.7431 g (1 Wt%, 0.014 mol)

For comparison BzCOOH end-capper used on its own with no brancher.

PET 61 Monomer - 118.99 g

Sb_2O_3 - 0.0300 g

Penta- 0.1849 g (1/8 Wt%, 0.0054 mol eq)

BnOH - 1.1689 g (1 Wt%, 0.0108 mol)

As well as the Penta branching agent, BnOH end-capper was also added. The polymer produced was white and crumbly.

PET 62 Monomer - 118.71 g

Sb_2O_3 - 0.0304 g

Penta- 0.1835 g (1/8 Wt%, 0.0054 mol eq)

BnOH - 0.5800 g (1/2 Wt%, 0.0054 mol)

The polymer produced was brittle and crystalline.

PET 63 Monomer - 118.72 g

Sb_2O_3 - 0.0307 g

Penta- 0.1827 g (1/8 Wt%, 0.0054 mol eq)

BnOH - 0.2900 g (1/4 Wt%, 0.0027 mol)

The polymer extruded was brittle.

PET 64 Monomer - 118.71 g
Sb_2O_3 - 0.0314 g
Penta- 0.1825 g (1/8 Wt%, 0.0054 mol eq)
BnOH - 0.1451 g (1/8 Wt%, 0.0013 mol)

The polymer extruded was crystalline and brittle.

PET 65 Monomer - 118.73 g
Sb_2O_3 - 0.0303 g
Penta- 0.1834 g (1/8 Wt%, 0.0054 mol eq)
BnOH - 0.0726 g (1/16 Wt%, 0.00067 mol)

Again the polymer synthesised was white and crumbly.

PET 66 Monomer - 119.00 g
Sb_2O_3 - 0.0300 g
Penta- 0.1829 g (1/8 Wt%, 0.0054 mol eq)
BnOH - 0.0363 g (1/32 Wt%, 0.00034 mol)

Again the BnOH had a significant effect. The resultant polymer was of low tensile strength and very crystalline.

Flexible Branching agents

The branching agents used to this point can be described as 'hard' branching agents. These are small molecules. In principle, larger molecules or polymers might also be used as branching agents. These are referred to as 'flexible' branchers, where branching is along a long flexible chain. In this work branching was attempted using the following flexible branchers with ICI 'monomer' as the feedstock.

	$\overline{M}_w$
Poly(acrylic acid) [PAA]	5000
	2100
	1200
Poly(acrylic acid)-co-(Maleic acid) [PAA-co-MA]	3000

The poly (acrylic acid)s were supplied in the sodium salt form and were converted to the acid form.

Conversion of Poly(acrylic acid) Sodium salts to Acid Form

The polymer was dissolved in water, and hydrochloric acid (2M) was added in 10:1 excess and left to stir overnight. The water was then removed under vacuum and the reaction mixture redissolved in methanol. Sodium chloride was filtered off. Molecular sieves (4 Å) were added and the solution was left for 24 hours. The methanol was then removed and the product freeze-dried.

Flexible Brancher Reactions

Polycondensations of this type utilised the standard procedure outlined in section 9.3.2. During all reactions, the two polymers were observed to withdraw into two separate phases.

Code	Mass of 'monomer' (g)	Mass of Brancher (g)	Mass of Catalyst (g)	Wt% Brancher
PET 67	118.92	3.08	0.0308	2.6
PET 68	118.40	0.385	0.0309	0.33
PET 69	118.41	0.211	0.0295	0.20
PET 70	118.29	0.385	0.0298	0.33
PET 71	118.10	0.1926	0.0299	0.167
PET 72	118.29	0.310	0.0299	2.6
PET 73	118.09	0.0956	0.0289	0.083
PET 74	118.50	0.3855	0.0305	0.33
PET 75	118.91	0.0961	0.0324	0.083

Ionomers

Ionomers are polymers with ionic groups present, which can form pseudo cross-links. These cross-links are more fluid than those of traditional branchers and can continually form and reform. This gives a less rigid structure than normal.

The ionic groups chosen for this work are listed below. There structures can be found in Figure 15 (page 83).

2,6-methylpyridine dicarboxylic acid (2,6 methyl PDCA)

2,6-pyridine dicarboxylic acid (2,6 PDCA)

3,5-pyridine dicarboxylic acid (3,5 PDCA)

5-sulfoisophthalic acid sodium salt (5-SIPA,Na)

4-sulfophthalic acid sodium salt (4-SPA, Na)

Methylation of 2,6-Pyridinedicarboxylic acid (2,6 PDCA)

2,6 PDCA (10 g) was dissolved in acetone (150 ml) and methyl iodide (2 mole equivalents, 17 g, 7.4 ml) was added. The solution was then stirred for 72 hours.

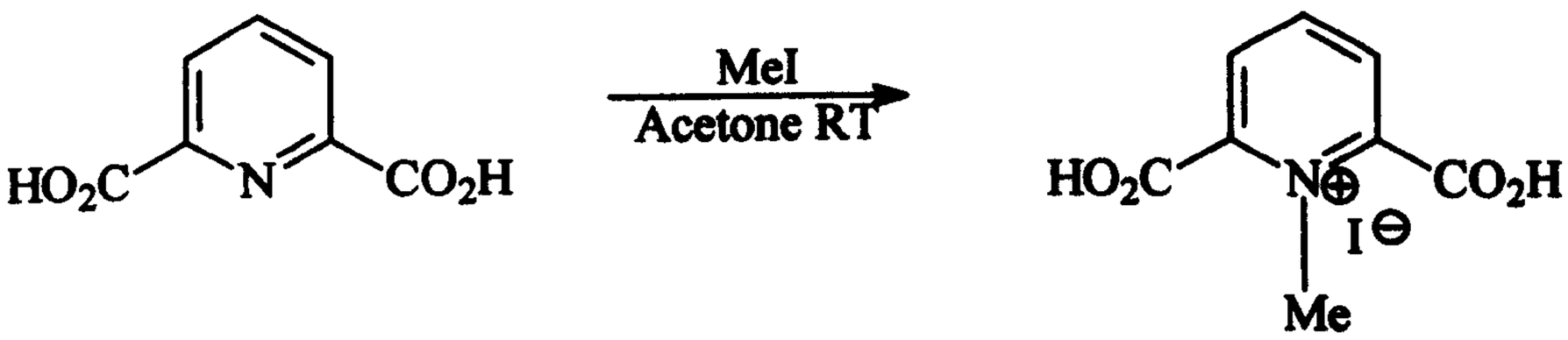

Scheme 7: Methylation of 2,6-Pyridinedicarboxylic acid

The resulting powder was filtered off and washed with acetone (5 x 20 ml) and then dried to constant weight. 10.43 g were recovered. Elemental microanalysis and an FTIR spectrum were obtained on the product.

Microanalytical Data	(Calculated)	C: 31.1% H: 2.6% N: 4.5% I: 41.1%
	(Found)	C: 34.4% H: 3.7% N: 5.0% I: 45.4%

FTIR (KBr/cm^{-1}) 3465 (OH), 3070 (pyridine C=C-H), 1701 (aryl acid, C=O), 1578 (pyridine C=C), 770 (2,6-disubstituted pyridine) 750 (2,6-disubstituted pyridine)

Neutralisation of 4-Sulfophthalic acid (4SPA)

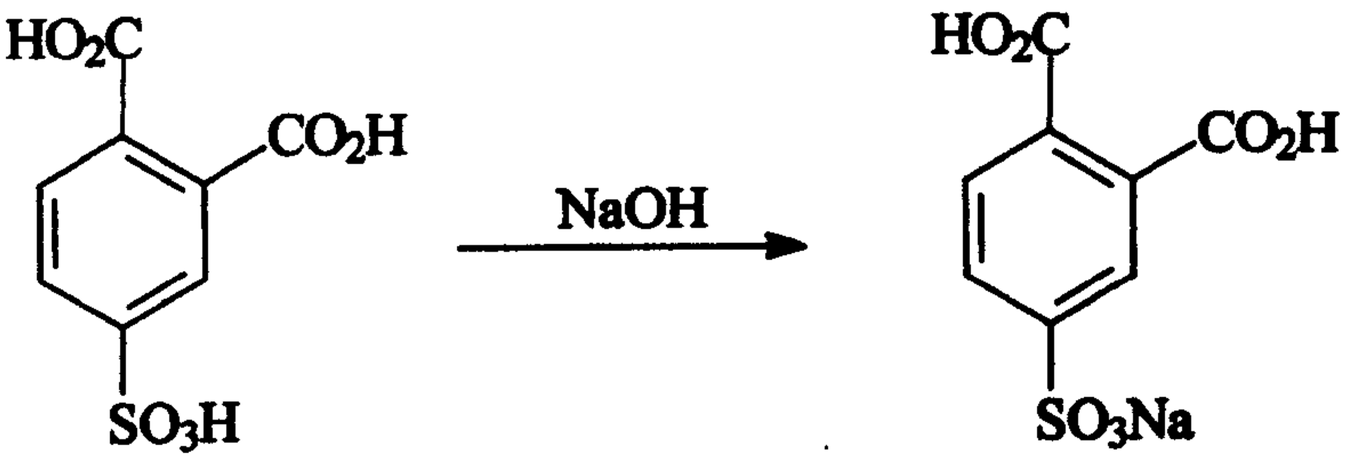

Scheme 8: Neutralisation of 4-Sulfophthalic acid

The 4SPA was supplied in the acid form as a 50 Wt% solution in water. Conversion to the sodium salt was desired to increase its ionic properties. 4SPA solution (37 ml) was titrated with a solution of NaOH (1M) and the reaction followed potentiometrically using a Hana instruments 8520 pH meter. An approximate titration was undertaken first. Stopping the reaction after the third point of inflection. This gave a rough indicator as to where neutralisation of the sulfonic acid moiety was complete. The reaction was then repeated and stopped when the first point of inflection had been observed. The water was then removed under vacuum and the product freeze-dried.

The three points of inflection are seen clearly in Graph 12. Elemental microanalytical data and FTIR spectral data were obtained.

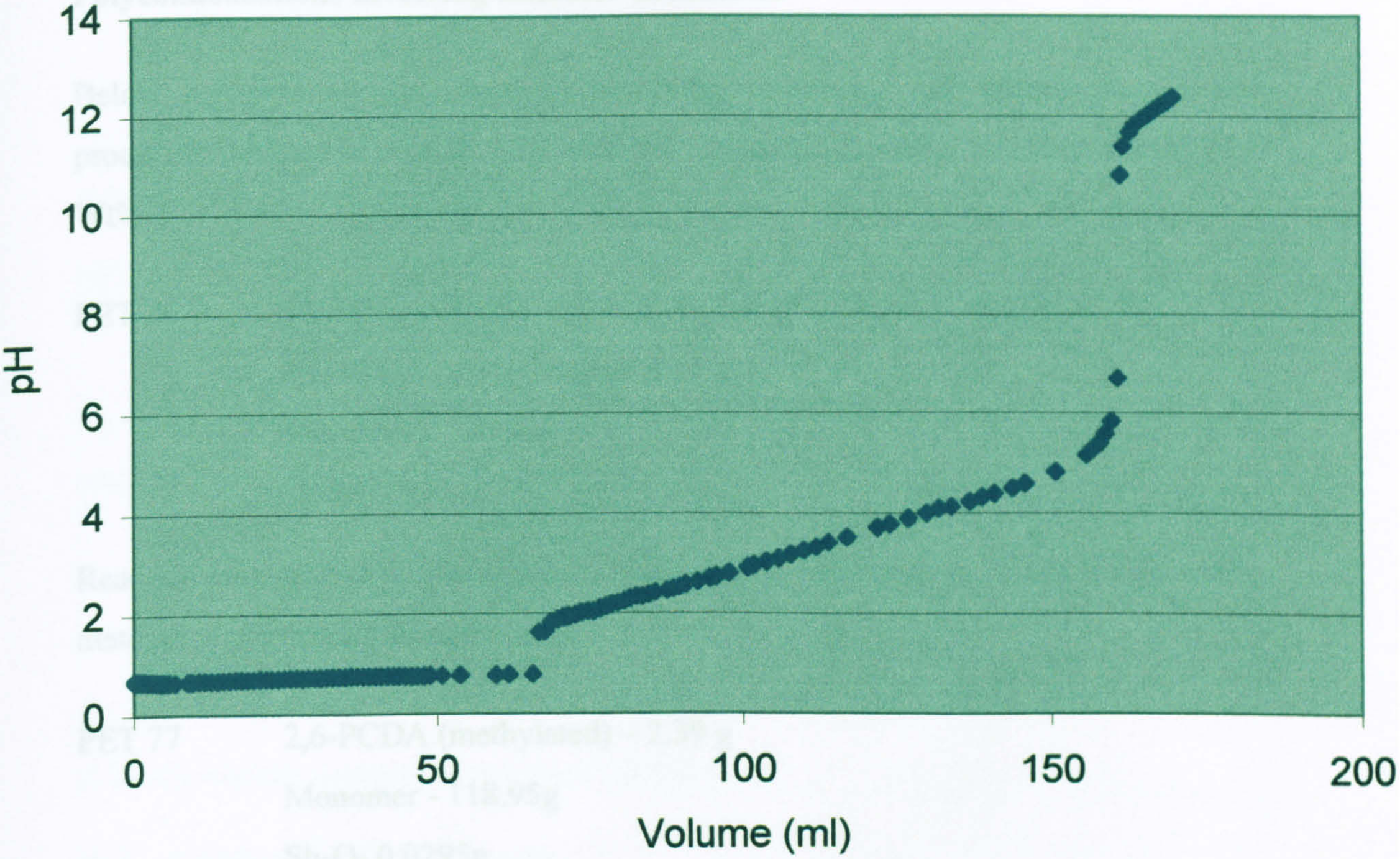

Graph 12: Neutralisation of 4-Sulfophthalic Acid

Microanalytical data (Calculated) C: 35.8% H: 1.9% S: 11.9%

(Found) C: 35.3% H: 1.4% S: 11.9%

FTIR (KBr/cm^{-1}) 3450 (OH), 1710 (Aryl Acid, C=O), 927 (1,2,4-trisubstituted aryl), 895 (1,2,4-trisubstituted aryl) 780 (1,2,4-trisubstituted aryl) 1240 (ionic sulfonate)

Polycondensations involving Ionomer Branchers

Below are detailed the reactions involving ionomers. All follow the general procedure outlined in section 9.3.2 with the ionomeric brancher added at a level of 2 Wt%

PET 76 5 Sulfoisophthalic acid sodium salt (5SIPA,Na) – 4.41g
2,6-PCDA (methylated) – 4.14 g
Monomer - 118.90g
Sb_2O_3 0.0304g

Reaction melt turned purple and then black during the reaction. A black oligomeric material was extruded from the melt.

PET 77 2,6-PCDA (methylated) – 2.39 g
Monomer - 118.95g
Sb_2O_3 0.0295g

Again reaction melt turned purple and then black during the reaction. A black oligomeric material was extruded from the melt.

PET 78 2,6-PCDA – 2.36 g
Monomer - 118.81g
Sb_2O_3 0.0300g

Again reaction melt turned purple and then black during the reaction. A black oligomeric material was extruded from the melt. Rapid evolution of gas was observed during the reaction as well as a strong smell of pyridine.

PET 79 3,5-PCDA – 2.38 g
Monomer - 118.62g
Sb_2O_3 0.0330g

Reaction melt turned purple and then black during the reaction. A black oligomeric material was extruded from the melt.

PET 80 5-SIPA, Na – 4.14 g

Monomer - 118.45g

Sb_2O_3 - 0.0324g

A brittle slightly orange polymer was extruded.

PET 81 2,6-PCDA – 2.38 g

Monomer - 118.62g

Reaction melt turned purple and then black during the reaction. A black oligomeric material was extruded from the melt.

PET 82 4-SPA, Na – 4.24 g

Monomer - 118.15g

Sb_2O_3 - 0.0301g

A brittle slightly orange polymer was extruded.

9.4 Analysis of Polymers

9.4.1 FTIR Spectral Analysis

A pressed disk of KBr was prepared in the normal fashion. Five drops of a 2% solution of the polymer in trifluoroacetic acid (TFA) are applied to the disk and left for 5 minutes to allow the solvent to evaporate. The FTIR spectrum was then recorded in the normal manner.

9.4.2 ^{1}H NMR Spectral and End-group Analysis

For NMR spectral analysis to be possible a suitable deuterated, or non-hydrogen-containing solvent had to be found for the polymers. Due to the polymers extreme insolubility, a search for a suitable solvent was initiated. Solubility of the polymer is also vital for end-group analysis, which has the added problem of requiring the solvent to be miscible with, yet non-reactive to the titrand used in the process.

Solubility of PET

Samples of ICI PET (0.2 g each), were placed in round-bottomed flasks, and subjected to a number of conditions and in a selection of solvents; the experiments are outlined in Table 30 - Table 35.

Solvent	Vol. of Solvent (ml)	Temperature (°C)	Dissolution Time (hr)	Dissolved ?
1,1,2,2-TCE	50	RT	0.5	✗
		25	+ 0.33	✗
		60	+ 0.5	✗
		110	+ 1.25	✗
		147	+ 1	✓

Table 30: Solubility of PET in TCE

At 147 °C the polymer dissolved. It stayed in solution indefinitely.

Solvent	Vol. of Solvent (ml)	Temperature (°C)	Dissolution Time (hr)	Dissolved ?
aniline	10	RT	1	✗
		80	+ 1	✗
	+ 90	150	+ 1	✗
	+ 50	150	+ 1	✗
		190	+ 1	✗
nitrobenzene	20	190	0.5	✓

Table 31: Solubility of PET in Aniline & Nitrobenzene

Although the polymer dissolved in nitrobenzene, it precipitated out on cooling.

Solvent	Vol. of Solvent (ml)	Temperature (°C)	Dissolution Time (hr)	Dissolved ?
benzyl alcohol	20	RT	0.5	✗
		80	+ 1	✗
	+ 30	110	+ 1	✗
	+ 30	150	+ 1	✗
	+ 40	180	+ 1	✗
	+ 40	190	+ 1	✗
	+ 40	210	+ 1	✗

Table 32: Solubility of PET in Benzyl Alcohol

At 210 °C the polymer did not dissolve, but formed a suspension.

Solvent	Vol. of Solvent	Temperature	Dissolution	Dissolved

	(ml)	(°C)	Time (hr)	?
benzyl acetone	50	RT	0.5	✗
		40	+ 0.5	✗
		100	+ 0.5	✗
		180	+ 1	✗
		235	+ 1	✗

Table 33: Solubility of PET in Benzyl Acetone

Solvent	Vol. of Solvent (ml)	Temperature (°C)	Dissolution Time (hr)	Dissolved ?
benzyl acetate/ acetone	25/25	200	2	✗
	25/25	240	2	✗
benzyl alcohol /nitrobenzene	25/25	200	2	✓
benzyl acetate/ benzyl alcohol	25/25	110	1	✗
nitrobenzene/ *o*- dichlorobenzene	15/15	230	+ 2	✗
benzyl alcohol/ *o*- dichlorobenzene	25/25	180	2	✗
	+ 25/25	250	+ 2	✗
	+ 25/25	250	+ 2	✓
ethyl benzoic acid	50	200	2	✗
p-chlorotoluene	50	200	2	✗
benzyl alcohol	100	250	3	✗
	+ 150	250	3	✗
	+ 50	250	3	✓
o-cresol	40	90	2.5	✓

Table 34: Further PET Solubility Tests

The benzyl alcohol/nitrobenzene mixture dissolved the polymer but it precipitated back out on cooling.

Solvent	Vol. of Solvent (ml)	Temperature (°C)	Dissolution Time (hr)	Dissolved ?
benzyl acetate	50	RT	0.5	✗
		40	+ 0.5	✗
		100	+ 0.5	✗
		130	+ 1	✗
		210	+ 1	✗

Table 35: Solubility of PET in Benzyl Acetate

The benzyl alcohol/ *o*-dichlorobenzene mixture dissolved the polymer but, again, the polymer precipitated on cooling.

The benzyl alcohol solution also precipitated out polymer on cooling.

The polymer stayed dissolved in *o*-cresol on cooling.

NMR Spectral Analysis

None of the above solvents were found to be useful for NMR analysis. However after conversations with colleagues in the IRC in Polymer Science, at Durham, it was decided to use a mixture of TFA and chloroform-*d* as a solvent (1:9).

End-group Analysis

Once suitable solvents were found, end-group analysis was carried out on selected polymers via the following procedure.

End-group Analysis Procedure

In order to detect the end-groups on PET the hydroxyl termini must be converted to carboxyl groups. This can be achieved by reaction with succinic anhydride as detailed by Conix.[67]

Reaction of PET with Succinic Anhydride

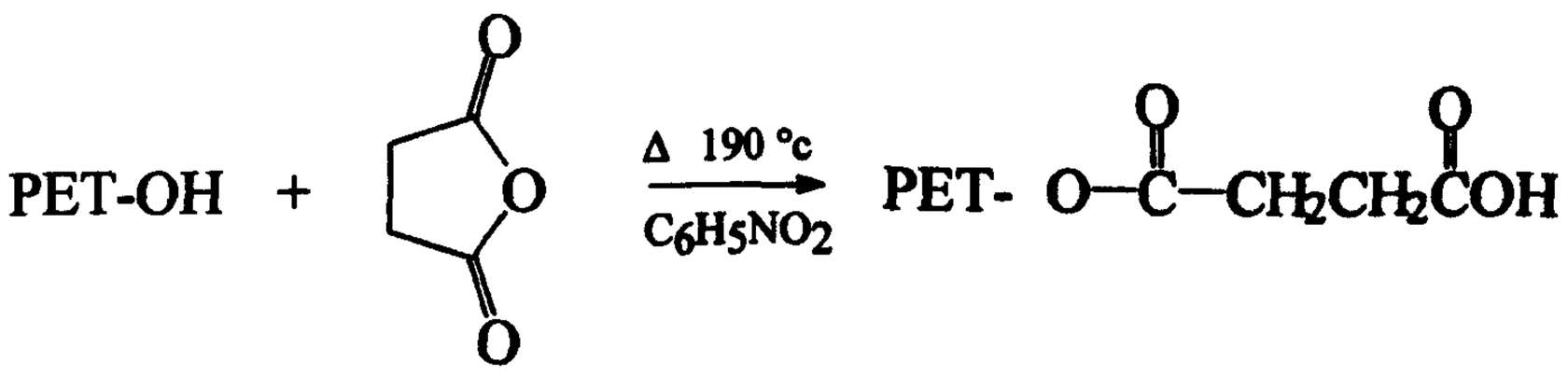

Scheme 9:Reaction of PET with Succinic Anhydride

Succinic anhydride (200 mg, 2 mmol) was dissolved, in freshly distilled nitrobenzene (20 ml). PET (1 g) and pyridine (1 g, 12.6 mmol) were added and the mixture stirred at 190 °C for 1 hour.

When the solution went clear the solution was cooled and while still warm poured into acetone/water (200 ml, 9:1). A fine white precipitate was formed.

The precipitate was washed with acetone (5x20 ml, to remove unreacted anhydride) and vacuum dried at room temperature to constant weight.

An FTIR spectrum of the polymer showed the following bands: -

FTIR (Cast film/cm^{-1}) 3550 (OH), 2970 (aliphatic C-H), 1725 (ester carbonyl), 820 (1,4-disubstituted aryl)

Attempted Potentiometric Titration of End-groups in TCE

Potentiometric titrations were carried out on the converted polymer. The polymer (0.2 g, ICI) was dissolved in TCE (50 ml), by heating to 147 °C for 2 hrs.
Titration of this solution with sodium hydroxide (0.1 molar) failed as the TCE and water where not miscible.

Further titrations were attempted using a solution of sodium hydroxide in TCE. Unfortunately the base degraded the TCE.

Titrations with tetrabutyl ammonium hydroxide, an organic soluble base were also attempted. However, this base is highly air sensitive and quickly degraded.

Attempted Potentiometric Titration of End-groups in BnOH

Potentiometric titrations were carried out on the converted polymer. A sample of ICI's PET (0.2 g), was dissolved in BnOH (50 ml) by heating to 220 °C for 3 hours. The solution was then rapidly cooled to 20 °C in a water bath (for 6-7 seconds). It was then poured into dichloromethane (DCM) (50 ml). The flask was washed out with benzyl alcohol (5 ml). The polymer stayed in solution for half an hour before precipitating out.
If titration was initiated immediately then this would not matter, however repeats of this experiment all failed to get the polymer to dissolve.

Potentiometric Titration of End-groups using o-Cresol/Chloroform

Potentiometric titrations were carried out on the converted polymer. The polymer (0.2 g) was heated to 100 °C in an *o*-cresol/chloroform mix (50 ml, 67:20), until dissolved (~30 min).

Ethanolic sodium hydroxide (5 ml, 0.0615 M) was added to the solution, which was then titrated with ethanolic HCl (0.0531 M)

Both sodium hydroxide and hydrochloric acid solutions were freshly prepared, and the HCl solution was standardised by titration with NaOH (ethanolic, 0.0615 M).

The progress of the reaction was followed by potentiometrically using a Hana Instruments 8520 pH meter.

End-group Conversion Reactions

A list of all the polymers converted using succinic anhydride is shown in Table 36.

Polymer	Mass of Polymer added (g)	Mass of converted polymer recovered (g)
PET ICI	1.0451	1.0410
PET 3	1.0211	0.9982
PET 4	1.0012	0.9875
PET 15	1.0517	1.0125
PET 16	1.0020	0.9875
PET 17	1.0656	1.0625
PET 21	1.0621	1.0385
PET 21	1.0073	0.9864
PET 27	1.0024	0.9610
PET 31	1.0051	0.97
PET 38	1.1051	1.0498
PET 39	1.0305	1.0174
PET 40	1.0098	0.8846
PET 41	1.0520	1.0376
PET 42	1.0259	0.9772
PET 43	1.0632	1.0345
PET 44	1.0052	0.594
PET 45	0.9963	0.3763
PET 46	1.0331	0.5239
PET 50	1.0254	0.9884
PET 52	1.0355	0.9189
PET 54	1.0891	0.9987
PET 55	1.0366	0.9378

Table 36: Summary of PET Conversion reactions

End-group Analysis

The end-group analysis reactions are summarised in Table 38. An example of how this data is calculated and how additional parameters are obtained from it can be found in Appendix 2 (page 159)

Benzoic Acid Model Study

This is a model study of the conversion reaction. Initially terephthalic acid was to be used, however it was found that this would not dissolve in *o*-cresol and so benzoic acid was used instead.

Benzoic acid (0.0310g) was dissolved in o-cresol/chloroform mix (67:20, 20ml). Ethanolic sodium hydroxide (0.0615 M, 5 ml) was added to the solution, which was then titrated with ethanolic hydrochloric acid (0.0531 M) yielding the data shown

Table 37

Vol. HCl (ml)	pH of solution	Vol. HCl (ml)	pH of solution
0.0	8.9	5.0	6.3
0.5	8.9	5.5	5.9
1.0	8.65	6.0	3.9
1.5	8.15	6.6	3.4
2.1	7.75	7.0	2.8
2.5	7.1	7.5	2.8
3.0	7.35	8.1	2.6
3.5	7.05	8.5	2.4
4.0	6.9	9.0	2.1
4.5	6.5	9.5	1.9

Table 37: Model End-group Analysis Data for Benzoic Acid

Summary of End-group Reactions

Test	Mass (g)	No of end-groups, E (/10^6 g)
PET ICI	1.0410	74
PET 3	0.9982	206
PET 4	0.9875	78
PET 15	1.0125	190
PET 16	0.9875	208
PET 17	1.0625	273
PET 21	0.9864	143
PET 27	0.9610	113
PET 31	0.97	212
PET 38	1.0498	269
PET 39	1.0174	151
PET 40	0.8818	174
PET 41	1.0376	329
PET 42	0.9772	184
PET 43	1.0345	270
PET 44	0.594	160
PET 45	0.376	1263
PET 46	0.5239	1017
PET 50	0.9884	109
PET 52	0.9189	109
PET 54	0.9884	300
PET 55	0.9378	207

Table 38: Summary of End-group Reactions

9.4.3 Solution Viscosity

A water tank equipped with a heater and circulator was set up. The thermostat was set at 25°C. Standard test solutions of the polymer in trifluoroacetic acid (TFA) were produced from an original, containing polymer (1 g) in TFA (50 ml, 2 Wt%), by serial dilution to give 2, 1, ½, and ¼ Wt% solutions.

Viscosity measurement was carried out using an Ubbelohde viscometer (Figure 18, nominal constant 0.00999 m^2/s^2). The viscometer was filled first with pure solvent, and placed in the water bath. After equilibrating for 5 minutes, tube c was closed off and vacuum applied to tube b. The solvent was drawn to above point x, where the vacuum was released. Opening tube c allows excess solution to drain back into the reservoir. This leaves the end of the capillary open or suspended. The solution then falls, under gravity, back into the reservoir. The time it takes to fall between x and y

is recorded, t_o. There is no back-pressure exerted on the solution and the volume of the liquid in the reservoir at no time influences the flow time. This is a feature of this kind of suspended level viscometer.

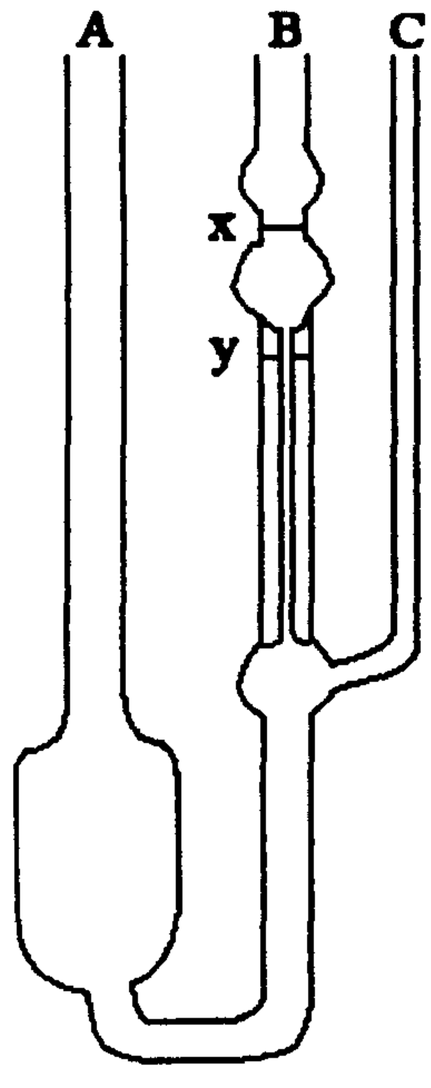

Figure 18: Ubbelohde Viscometer

The fall of the solvent was timed three times to ensure an accurate reading, and then the process was repeated using solutions ¼ through to 2 Wt%. The lowest concentration was used first to ensure that if any remained in the viscometer after rinsing out that it would not adversely effect the results of the next concentration run.

A summary of all the flow-time data is given in tables Table 39 and Table 40. Any changes to the basic procedure are noted below.

Polymer code	Flow time (sec)				
	TFA	C/8	C/4	C/2	C
ICI	66	77	93	118	166
PET 1	67	77	84	102	145
PET 3	67	73	80	96	132
PET 4	67	74	82	102	142
PET 5	-	-	-	-	-
PET 6	-	-	-	-	-
PET 7	66	76	90	112	167
PET 7	-	-	-	-	-

Table 39: Summary of Flow Time Data Used to Compute Solution Viscosity Part A

Polymer code	Flow time (sec)				
	TFA	C/8	C/4	C/2	C
PET 13	67	71	76	86	112
PET 14	67	70	73	83	106
PET 15	67	76	87	112	170
PET 16	67	74	80	96	128
PET 17	67	74	83	104	149
PET 22	114	-	-	-	-
PET 23	114	-	-	-	-
PET 27	67	77	87	114	156
PET 29	67	72	90	79	126
PET 31	66	75	86	109	168
PET 33	64	74	88	121	189
PET 34	64	74	85	118	180
PET 35	64	68	71	77	83
PET 38	65	70	75	87	117
PET 39	65	75	85	110	186
PET 40	65	75	89	104	174
PET 41	66	77	91	118	179
PET 42	69	75	86	105	157
PET 43	66	71	76	82	95
PET 44	66	75	88	113	165
PET 45	67	66	67	70	77
PET 46	67	72	72	73	80
PET 49	66	75	83	103	156
PET 50	66	76	88	117	159
PET 52	67	69	71	80	99
PET 53	66	67	67	80	80
PET 54	67	71	76	87	106
PET 55	67	70	73	89	97
PET 57	64	74	85	88	107
PET 58	64	67	73	78	88
PET 59	64	-	-	-	-
PET 60	64	71	79	95	131
PET 61	64	67	71	78	85
PET 62	64	67	71	73	85
PET 63	64	68	71	78	85
PET 64	64	68	71	75	85
PET 65	64	68	70	76	86
PET 66	64	68	70	74	84

Table 40: Summary of Flow Time Data Used to Compute Solution Viscosity Part B

PET 22, 23

A second viscometer, (Nominal constant 0.009616 cs/s) was used in these experiments.

On examination of polymer solutions, gel was found to be present and so these experiments were abandoned

PET 5, 6

On examination of the polymer solutions gel was found to be present and so these experiments were abandoned. PET 5 was 100% gelled, whereas PET 6 was only 3 % gelled.

PET 7

Two samples of the polymer were dissolved. One of them showed no signs of gel. The other did (~ 0.5%). This shows non-uniformity throughout the sample.

PET 59

Polymer would not dissolve in TFA – formed a brown sludge/emulsion.

PET 67-75

Some of the polymer did not dissolve leaving microgels in the solution.

PET 80, 82

In the case of these polymers, samples were dissolved in both TFA and *o*-chlorophenol (OCP) so that the viscosity could be observed in the salt form and with protonation. The sample in OCP dissolved leaving insoluble crystal structures. Elemental analysis revealed these to be unreacted 5-SIPA, Na and 4-SPA, Na respectively.

Microanalysis data	(Calculated)	C: 36.2% H: 0.8% S 12.1%
	(5-SIPA, Na Found)	C: 35.7% H: 1.7% S 11.7%
	(4-SPA, Na Found)	C: 35.5% H: 1.8% S 11.4%

9.4.4 Differential Scanning Calorimetry (DSC)

DSC analysis was carried out on selected polymers using a Mettler TA 4000 differential scanning calorimeter. In each case approximately 10 mg of polymer was sealed into an aluminium pan. The pan was placed in the heating chamber of the apparatus on a heat sensor. A reference pan, containing an indium sample was placed alongside it on a separate sensor. The DSC was taken through a pre-set temperature programme from –20 to 300 °C at a rate of 20 K per minute. The apparatus records the specific heat and energies of transition.

The salient features of this data are presented in Table 41.

Code	Sample Mass (mg)	T_g (°C)	T_c (°C)	T_m (°C)
PET ICI	11.3	78.1	169.0	253.4
PET 4	18.3	73.1	132.3	258.9
PET 16	12.5	73.8	127.1	258.3
PET 17	18.8	75.0	125.8	260.3
PET 27	10.9	72.8	134.7	254.5
PET 31	11.5	73.3	134.8	251.9
PET 38	10.9	73.0	129.4	258.5
PET 39	10.9	74.8	144.0	254.7
PET 40	10.4	72.4	133.4	254.7
PET 41	14.4	72.9	138.7	251.8
PET 42	10.6	73.4	138.7	256.1
PET 43	15.8	70.8	113.2	256.5
PET 44	12.2	68.7	134.8	255.8
PET 52	16.8	70.3	112.9	257.2
PET 55	12.8	67.4	116.5	246.2
PET 61	10.5	67.1	114.3	244.1
PET 62	11.2	67.5	116.1	247.5
PET 63	10.1	68.3	116.1	247.5
PET 64	10.4	67.2	115.0	245.5
PET 65	11.5	66.0	112.4	242.7
PET 66	10.9	69.4	124.6	244.9

Table 41: Summary of DSC Thermal Transitions for selected PET Samples

9.4.5 Light Scattering

Light scattering experiments were carried out using a Malvern 4700 light scattering instrument, equipped with a variable power (1-150 mW) 488 nm argon laser. Polymer solutions were placed in a vat of xylene held at constant 25 °C. The laser was directed at the cells and the scattering from the solution measured by a photomultiplier tube (PM). The PM was mounted on a mechanical arm and so can be moved round the sample to measure the scattering at various angles (10 -150°). The photomultiplier passes the data on to a correlator and thence to a computer which can calculate the molecular weight and radius of gyration of the sample.

Standard test solutions of the polymer firstly in a mixture of TFA and chloroform (initially 1:9 and then 1:1 as described below) and then pure TFA were produced to give solutions of 1, 0.8, 0.6, 0.4, and 0.2 Wt%. These were then filtered 15 times through a 0.22 μm polyvinylidene difluoride filter, to remove any dust particles, into 'Buchard' cells. These cells are made of quartz and are perfectly rounded. The TFA and chloroform were both freshly distilled and filtered before use.

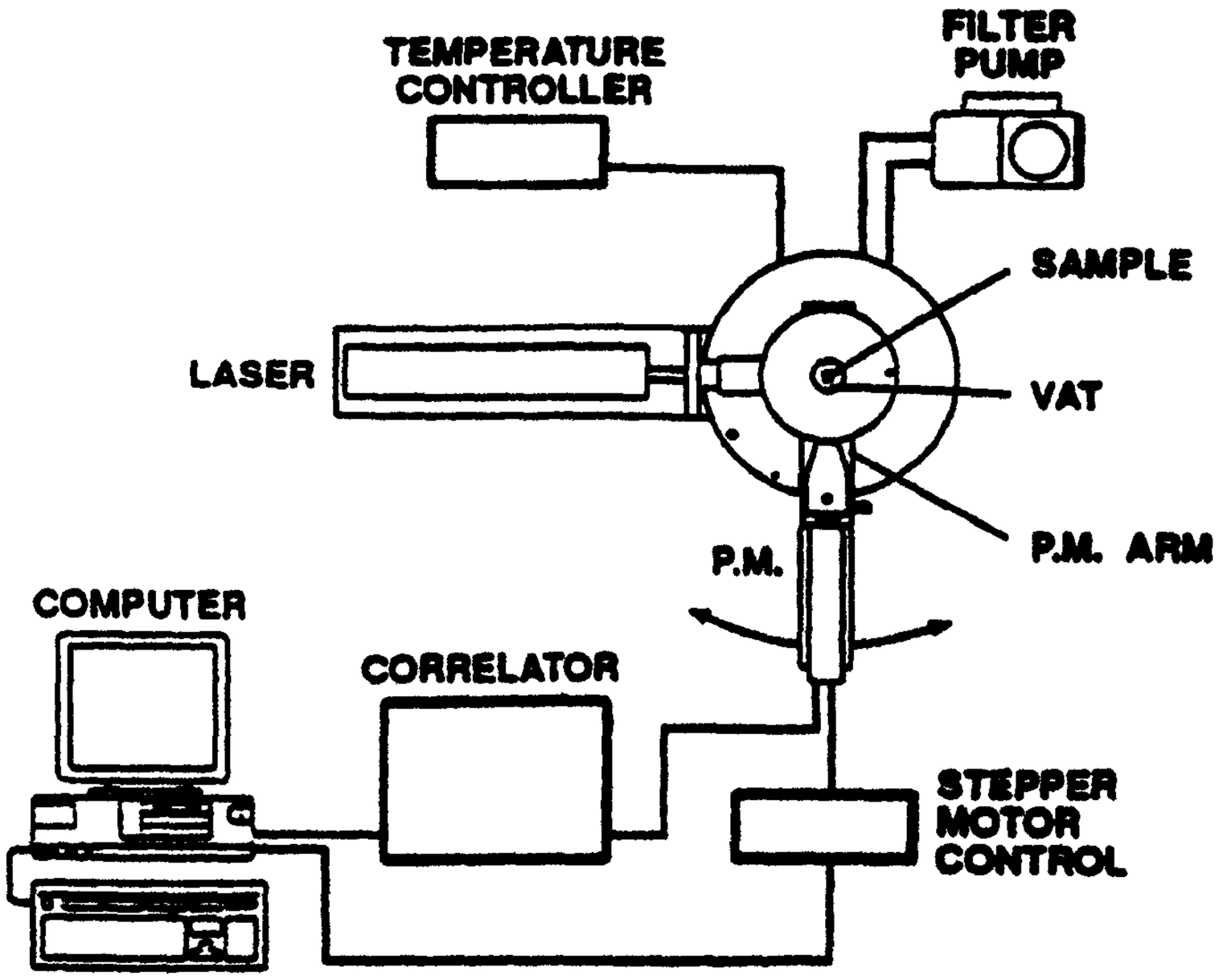

Figure 19: Malvern 4700 Light Scattering Equipment

Initial Experiments

Initial experiments were carried out using solutions of polymer in firstly a 1:9 TFA/chloroform mix and then a 1:1 TFA/chloroform mix, gathering data at 21 points between 30 and 150°. Light scattering observed from these solutions was not enough to proceed with the experiment (samples gave the same scattering as the standard). Further experiments were carried out using pure TFA and at a fixed angle (90°). These experiments are detailed below.

Light Scattering Experiments Using Pure TFA as Solvent at 488 nm and 90°

The results of the light scattering experiments following the above procedure but using pure TFA as solvent and a fixed angle scan of 90° are shown in tables 42 - 49

	PET ICI		PET 4	
Rough solution concentration (% wt/v)	Accurate concentration (g/ml)	Intensity of scattering, I (Kc/s)	Accurate concentration (g/ml)	Intensity of scattering, I (Kc/s)
Standard	-	25.5	-	26
1	0.0108	31.0	0.0101	32.00
0.8	0.0081	28.9	0.0081	37.60
0.6	0.0062	27.5	0.0060	32.30
0.4	0.0041	25.2	0.0041	23.50
0.2	0.0022	22.3	0.0020	20.50
0.0	-	14.9	-	14.9

Table 42: Light Scattering of PET ICI and PET 4 in Pure TFA

	PET 27		PET 31	
Rough solution concentration (% wt/v)	Accurate concentration (g/ml)	Intensity of scattering, I (Kc/s)	Accurate concentration (g/ml)	Intensity of scattering, I (Kc/s)
Standard	-	25.5	-	25.3
1	0.0113	44.2	0.0130	130.9
0.8	0.0084	38	0.0080	105.7
0.6	0.0065	34	0.0062	93
0.4	0.0045	28.2	0.0040	75.7
0.2	0.0027	23.3	0.0020	50
0.0	-	13.5	-	14.8

Table 43: Light Scattering of PET 27 and PET 31 in Pure TFA

	PET 16		PET 44	
Rough solution concentration (% wt/v)	Accurate concentration (g/ml)	Intensity of scattering, I (Kc/s)	Accurate concentration (g/ml)	Intensity of scattering, I (Kc/s)
Standard	-	25.5	-	25.4
1	0.0118	107	0.0112	165.3
0.8	0.0081	92.6	0.0079	163.7
0.6	0.0067	86.8	0.0060	157
0.4	0.0051	78.9	0.0049	152.8
0.2	0.0030	60.1	0.0024	113
0.0	-	14.9	-	13.5

Table 44: Light Scattering of PET 16 and PET 44 in Pure TFA

	PET 43		PET 17	
Rough solution concentration (% wt/v)	Accurate concentration (g/ml)	Intensity of scattering, I (Kc/s)	Accurate concentration (g/ml)	Intensity of scattering, I (Kc/s)
Standard	-	26.1	-	25.3
1	0.0099	72.2	0.0103	118.1
0.8	0.0080	63.3	0.0080	105.7
0.6	0.0059	61.8	0.0061	89
0.4	0.0044	53.6	0.0044	75.7
0.2	0.0023	37.7	0.0019	50
0.0	-	13.8	-	14.9

Table 45: Light Scattering of PET 43 and PET 17 in Pure TFA

	PET 39		PET 38	
Rough solution concentration (% wt/v)	Accurate concentration (g/ml)	Intensity of scattering, I (Kc/s)	Accurate concentration (g/ml)	Intensity of scattering, I (Kc/s)
Standard	-	25.4	-	25.5
1	0.0103	159.4	0.01088	105.6
0.8	0.008	170.9	0.00849	97.7
0.6	0.0060	168.8	0.00693	86.8
0.4	0.0048	139.4	0.00468	75.9
0.2	0.0030	120	0.00298	64.9
0.0	-	13.3	-	13.5

Table 46: Light Scattering of PET 39 and PET 38 in Pure TFA

	PET 42		PET 55	
Rough solution concentration (% wt/v)	Accurate concentration (g/ml)	Intensity of scattering, I (Kc/s)	Accurate concentration (g/ml)	Intensity of scattering, I (Kc/s)
Standard	-	26.1	-	30.3
1	0.0111	133.6	0.01000	103.5
0.8	0.0083	122.6	0.00804	93
0.6	0.0063	122.3	0.00629	73.6
0.4	0.0043	107	0.00500	66.7
0.2	0.0026	84.7	0.00228	48
0.0	-	13.5	-	16.1

Table 47: Light Scattering of PET 42 and PET 55 in Pure TFA

	PET 52		PET 41	
Rough solution concentration (% wt/v)	Accurate concentration (g/ml)	Intensity of scattering, I (Kc/s)	Accurate concentration (g/ml)	Intensity of scattering, I (Kc/s)
Standard	-	25.3	-	25.9
1	0.0099	68.9	0.01044	177.7
0.8	0.0083	64	0.00847	176
0.6	0.0060	55	0.00674	172.9
0.4	0.0048	45.3	0.00477	154.5
0.2	0.0028	36.3	0.00202	109.5
0.0	-	13	-	14.1

Table 48: Light Scattering of PET 52 and PET 41 in Pure TFA

	PET 40		PET 15	
Rough solution concentration (% wt/v)	Accurate concentration (g/ml)	Intensity of scattering, I (Kc/s)	Accurate concentration (g/ml)	Intensity of scattering, I (Kc/s)
Standard	-	25.7	-	25.3
1	0.0107	161.1	0.0101	118
0.8	0.0081	165.9	0.0081	151.2
0.6	0.0064	161.9	0.0060	172.1
0.4	0.0047	145.9	0.0041	180.4
0.2	0.0021	108.8	0.0020	188.1
0.0	-	14.2	-	13.8

Table 49: Light Scattering of PET 40 and PET 15 in Pure TFA

Further Light Scattering experiments at 633 nm

Due to mechanical failure of the 488 nm argon-ion laser, a 633 nm helium-neon laser was used for the final batch of experiments. These experiments followed the same procedure as before and the results are summarised in Tables 50 -54.

	PET 45		PET 46	
Rough solution concentration (% wt/v)	Accurate concentration (g/ml)	Intensity of scattering, I (Kc/s)	Accurate concentration (g/ml)	Intensity of scattering, I (Kc/s)
Standard	-	30	-	30
1	0.0099	70.1	0.0105	65.0
0.8	0.0081	68.9	0.0084	60.0
0.6	0.0061	60.8	0.0060	54.1
0.4	0.0041	55.0	0.0040	46.4
0.2	0.0020	45.0	0.0023	38.8
0.0	-	20	-	20

Table 50: Light Scattering data for PET 45 and PET 46 in Pure TFA

	PET 61		PET 62	
Rough solution concentration (% wt/v)	Accurate concentration (g/ml)	Intensity of scattering, I (Kc/s)	Accurate concentration (g/ml)	Intensity of scattering, I (Kc/s)
Standard	-	30	-	30
1	0.0113	60.8	0.0101	59.6
0.8	0.0085	59.9	0.0083	56.3
0.6	0.0066	55.9	0.0061	50.7
0.4	0.0043	53.9	0.0047	47.5
0.2	0.0021	43.3	0.0021	45.0
0.0	-	20	-	20

Table 51: Light Scattering data for PET 61 and PET 61 in Pure TFA

	PET 63		PET 64	
Rough solution concentration (% wt/v)	Accurate concentration (g/ml)	Intensity of scattering, I (Kc/s)	Accurate concentration (g/ml)	Intensity of scattering, I (Kc/s)
Standard	-	30	-	30
1	0.0101	60.7	0.0143	110.0
0.8	0.0084	59.6	0.0083	105.0
0.6	0.0061	54.8	0.0062	98.2
0.4	0.0039	52.9	0.0044	91.2
0.2	0.0022	39.6	0.0022	82.3
0.0	-	20	-	20

Table 52: Light Scattering data for PET 63 and PET 64 in Pure TFA

	PET 65		PET 66	
Rough solution concentration (% wt/v)	Accurate concentration (g/ml)	Intensity of scattering, I (Kc/s)	Accurate concentration (g/ml)	Intensity of scattering, I (Kc/s)
Standard	-	30	-	30
1	0.0099	115.1	0.0106	50.9
0.8	0.0081	106.9	0.0081	52.0
0.6	0.0061	99.3	0.0060	55.5
0.4	0.0041	91.2	0.0043	50.9
0.2	0.0020	85.6	0.0021	43.3
0.0	-	20	-	20

Table 53: Light Scattering data for PET 65 and PET 66 in Pure TFA

	PET 35	
Rough solution concentration (% wt/v)	Accurate concentration (g/ml)	Intensity of scattering, I (Kc/s)
Standard	-	30
1	0.0100	175.1
0.8	0.0080	166.3
0.6	0.0059	159.3
0.4	0.0041	151.2
0.2	0.0023	145.4
0.0	-	20

Table 54: Light Scattering data for PET 35 in Pure TFA

9.4.6 Determination of dn/dc

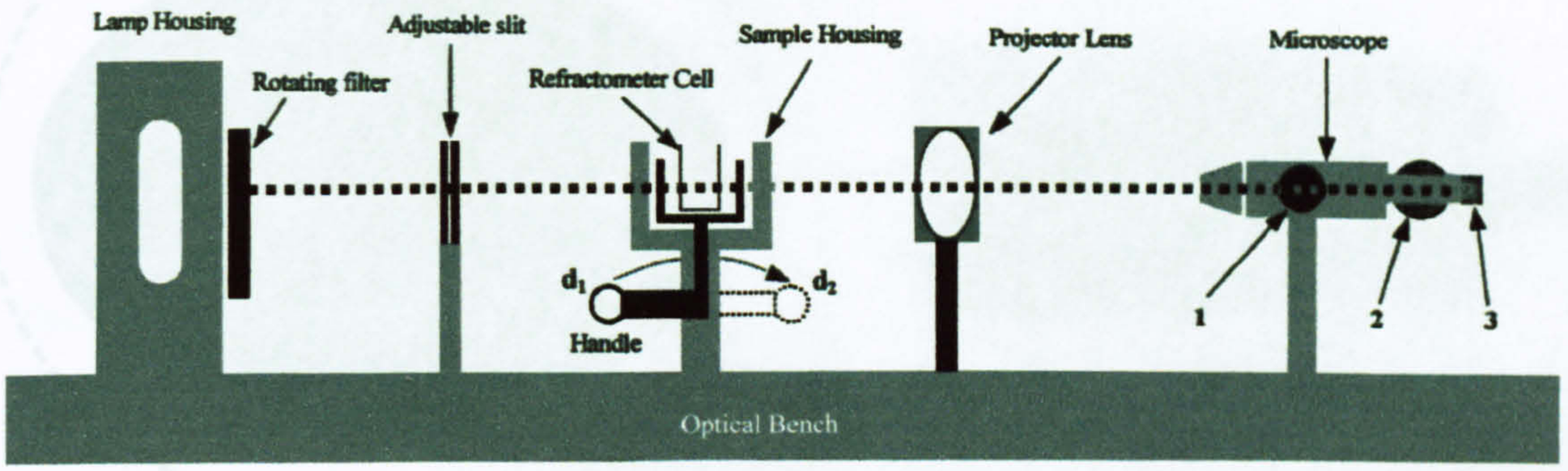

Figure 20: Differential Refractometer Set-up

To measure dn/dc, Δn (the difference in refractive index between a solution and its solvent) must be determined for a series of solution concentrations. The range of concentrations to be probed depends on the extent to which higher concentrations displace the slit image line (since higher concentrations will shift the line off the scale). Six solutions ranging from 0.1875 to 3.0000% w/v polymer were prepared.

Before taking any solution readings, the solvent zero reading was obtained.

First the lamp was switched on and allowed to equilibrate for 15 minutes.
The desired wavelength was selected by rotating the filter (*e.g.* 488nm).
The handle was set at position d_1, (see above). This put the solvent compartment closest to the lamp and the solution compartment closest to the microscope.
The cell was flushed through with solvent several times and then both compartments of the refractometer were filled with solvent (~ 1 ml) and the compartments sealed.

Knob (1) was used to focus the microscope vertical slit image, the crosshair within the microscope was focussed using knob (3).

Knob (2) was used to set the crosshair so that it was aligned exactly down the centre of the slit image. The reading was then noted as d_1 the deviation of the beam through the solvent in the forward direction.

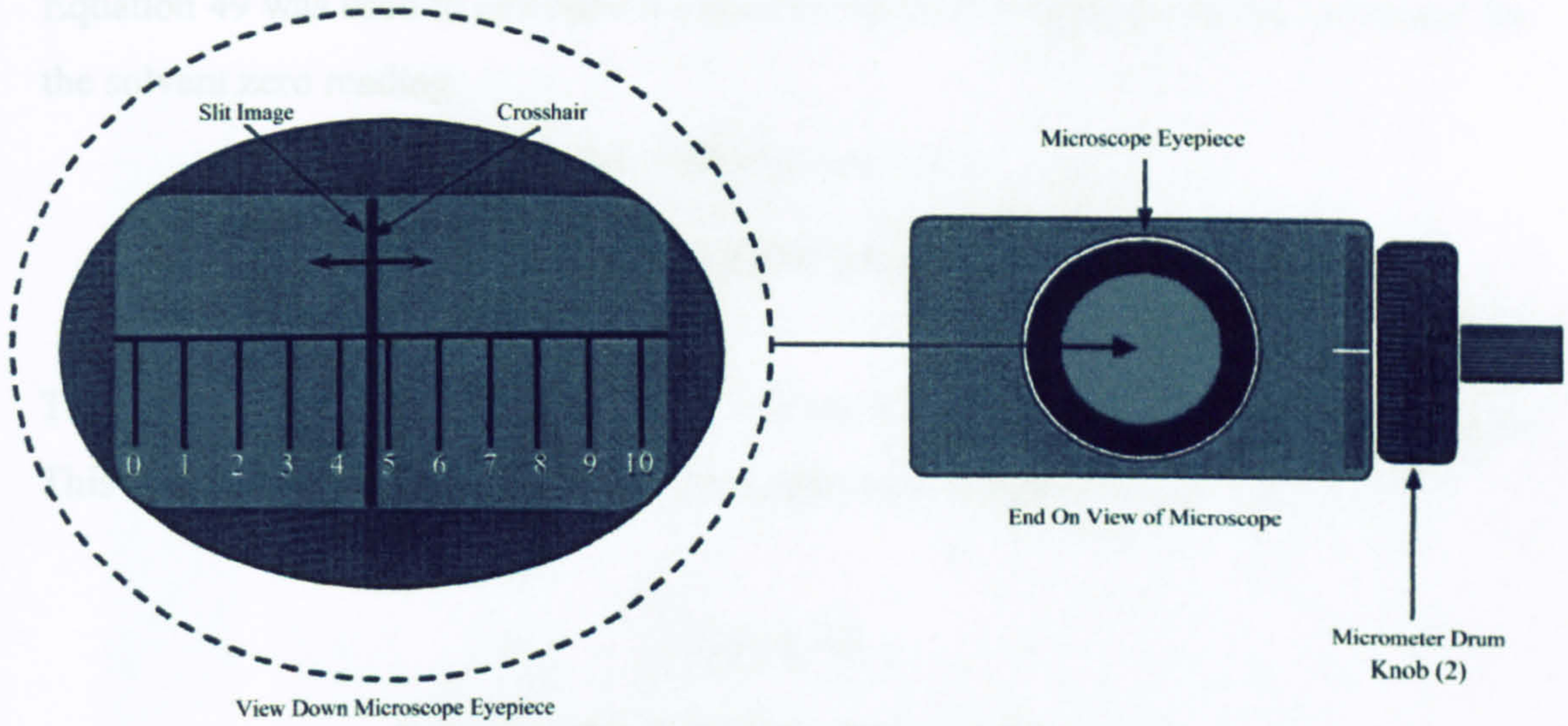

Figure 21: Taking Refractometer Readings

For example (see Figure 21), looking down the microscope eyepiece, the main scale reads between 4 and 5 (once crossbars aligned).

Then to obtain figures after the decimal place, the reading from the micrometer drum is 63, with an estimate for the third decimal place of 2.

Therefore the value obtained for $\mathbf{d_1}$ is 4.622.

The drum was displaced and the alignment procedure repeated twice. The values were then averaged. The handle was rotated to position d_2 (Figure 21) and the above procedures repeated to give d_2 the deviation of the beam through the solvent in the reverse direction.

$$\text{Solvent zero reading} = (d_2' - d_1')$$

Equation 48: Solvent Zero reading

This procedure was repeated replacing one of the solvent cells with each of the polymer solutions in turn. Leaving them for 5 -10 minutes to equilibrate before any measurements were taken. This gives the values, d_1 and d_2 for each solution.

Equation 49 was used to calculate a value for the total displacement Δd, corrected for the solvent zero reading.

$$\Delta d = (d_2 - d_1) - (d_2' - d_1')$$

Equation 49: Total Displacement

The refractive index difference, Δn is calculated using the calibration constant, k. This is specific for the apparatus at a particular wavelength.

$$\Delta n = k \Delta d$$

Equation 50: Refractive Index Difference

This gives Δn for each concentration. A plot of Δn versus concentration gives dn/dc as the gradient of the graph.

The entire procedure was repeated twice to give three values for dn/dc which were than averaged. Initially this procedure was carried out for PET ICI in 1:1 TFA:chloroform. However, this procedure was found to give an inadequate change in refractive index with concentration and with the mixed solvent system, there is the possibility of selective sorption of one or other solvent to the polymer required. This means that for accurate results the polymer solutions should be at a constant chemical potential. Dialysis experiments to this end, resulted in the polymer precipitating out of solution. Therefore, dn/dc could not be measured at constant chemical potential. Later dn/dc measurements were taken for PET ICI in pure TFA, HFIP and TCA. These results are summarised in Tables 55 -58. Due to mechanical failure of the 488 nm laser, dn/dc measurements were also taken in pure TFA at 633 nm to allow further experiments to be carried out using a replacement laser of that wavelength. These results are shown in Table 59

Table 55: Differential Refractometer Data for ICI PET in $CHCl_3$/TFA 1:1

Solution	λ (nm)	d1					d2					d2 - d1	Δd (d2-d1)-(d'2-d'1)	Δn	error
		1	2	3	Average	error	1	2	3	Average	error				
Solvent															
$CHCl_3$/TFA	488	5.033	5.013	5.045	**5.030**	0.016	5.467	5.442	5.463	**5.457**	0.013	0.4270	-	-	-
1:1	488	5.000	5.050	5.050	**5.033**	0.029	5.485	5.420	5.485	**5.463**	0.038	0.4300	-	-	-
	488	5.053	5.057	5.046	**5.052**	0.006	5.370	5.375	5.369	**5.371**	0.003	0.3193	-	-	-
										d'2-d'1	**488**	**0.4270**	**±**	**0.0210**	
											488	**0.4300**	**±**	**0.0473**	
											488	**0.3193**	**±**	**0.0064**	
Solutions															
Concentration															
(g/ml)	488	5.000	5.020	5.045	**5.022**	0.023	5.458	5.439	5.415	**5.437**	0.022	0.416	-0.011	-1.066E-05	-3.537E-05
1.875	488	5.023	5.050	4.985	**5.019**	0.033	5.41	5.43	5.415	**5.418**	0.010	0.399	-0.031	-2.916E-05	-5.498E-05
	488	4.967	5.037	5.010	**5.005**	0.035	5.455	5.423	5.44	**5.439**	0.016	0.435	0.115	1.085E-04	3.699E-05
	488	4.775	4.753	4.765	**4.765**	0.011	5.693	5.643	5.645	**5.660**	0.028	0.896	0.469	4.412E-04	3.528E-05
3.75	488	4.748	4.770	4.787	**4.768**	0.020	5.67	5.67	5.69	**5.677**	0.012	0.908	0.478	4.499E-04	4.978E-05
	488	4.790	4.777	4.765	**4.777**	0.013	5.665	5.665	5.667	**5.666**	0.001	0.888	0.569	5.352E-04	1.520E-05
	488	4.517	4.523	4.503	**4.514**	0.010	5.944	5.955	5.947	**5.951**	0.006	1.437	1.010	9.497E-04	2.617E-05
7.5	488	4.491	4.490	4.490	**4.490**	0.001	5.934	5.92	5.96	**5.938**	0.020	1.448	1.018	9.572E-04	5.024E-05
	488	4.545	4.505	4.493	**4.514**	0.027	5.965	5.93	5.92	**5.938**	0.024	1.424	1.105	1.039E-03	3.733E-05
	488	4.260	4.265	4.237	**4.254**	0.015	6.18	6.157	6.187	**6.175**	0.016	1.921	1.494	1.405E-03	3.441E-05
15	488	4.245	4.217	4.209	**4.224**	0.019	6.185	6.157	6.173	**6.172**	0.014	1.948	1.518	1.428E-03	5.352E-05
	488	4.221	4.213	4.223	**4.219**	0.005	6.147	6.16	6.17	**6.159**	0.012	1.940	1.621	1.524E-03	2.499E-05
	488	3.943	3.900	3.878	**3.907**	0.033	6.53	6.53	6.55	**6.537**	0.012	2.630	2.203	2.072E-03	4.794E-05
30	488	3.870	3.867	3.869	**3.869**	0.002	6.553	6.538	6.545	**6.545**	0.008	2.677	2.247	2.113E-03	5.377E-05
	488	3.832	3.903	3.872	**3.869**	0.036	6.549	6.535	6.575	**6.553**	0.020	2.684	2.365	2.224E-03	4.970E-05

Table 56: Differential Refractometer Data for ICI PET in Pure TCA

Solution	λ (nm)	d1					d2					d2 - d1	Δd (d2-d1)-(d'2-d'1)	Δn	error
		1	2	3	Average	error	1	2	3	Average	error				
Solvent															
Pure	488	4.698	4.687	4.690	4.692	0.006	4.284	4.293	4.304	4.294	0.010	-0.398	-	-	-
DCA	488	4.432	4.48	4.509	4.474	0.039	4.257	4.232	4.263	4.251	0.016	-0.223	-	-	-
	488	4.577	4.550	4.550	4.559	0.016	4.200	4.230	4.250	4.227	0.025	-0.332	-	-	-
										d'2-d'1	**488**	-0.398	±	0.012	
											488	-0.223	±	0.042	
											488	-0.332	±	0.030	
Solutions															
Concentration															
(g/ml)	488	4.477	4.474	4.477	**4.476**	0.002	4.424	4.405	4.419	**4.416**	0.010	-0.060	0.338	3.179E-04	1.501E-05
5.44	488	4.672	4.682	4.664	**4.673**	0.009	4.410	4.425	4.419	**4.418**	0.008	-0.255	-0.032	-2.979E-05	-4.123E-05
	488	4.495	4.470	4.475	**4.480**	0.013	4.376	4.360	4.355	**4.364**	0.011	-0.116	0.216	2.032E-04	3.232E-05
	488	4.601	4.601	4.598	**4.600**	0.002	4.118	4.119	4.151	**4.129**	0.019	-0.471	-0.073	-6.835E-05	-2.080E-05
10.74	488	4.834	4.840	4.840	**4.838**	0.003	4.282	4.260	4.290	**4.277**	0.016	-0.561	-0.338	-3.176E-04	-4.267E-05
	488	4.763	4.773	4.800	**4.779**	0.019	4.160	4.172	4.159	**4.164**	0.007	-0.615	-0.283	-2.659E-04	-3.405E-05
	488	4.752	4.672	4.655	**4.693**	0.052	4.260	4.258	4.253	**4.256**	0.004	-0.438	-0.040	-3.715E-05	-5.003E-05
15.13	488	4.692	4.763	4.750	**4.735**	0.038	4.280	4.296	4.271	**4.282**	0.013	-0.453	-0.230	-2.160E-04	-5.470E-05
	488	4.73	4.720	4.738	**4.729**	0.009	4.296	4.290	4.290	**4.292**	0.003	-0.437	-0.105	-9.877E-05	-2.932E-05
	488	4.689	4.696	4.712	**4.699**	0.012	4.069	4.091	4.139	**4.100**	0.036	-0.599	-0.201	-1.894E-04	-3.716E-05
19.76	488	4.839	4.835	4.840	**4.838**	0.003	4.144	4.185	4.150	**4.160**	0.022	-0.678	-0.455	-4.283E-04	-4.530E-05
	488	4.76	4.772	4.778	**4.770**	0.009	4.130	4.161	4.136	**4.142**	0.016	-0.628	-0.295	-2.778E-04	-3.322E-05
	488	4.94	4.912	4.941	**4.931**	0.016	4.028	4.049	4.062	**4.046**	0.017	-0.885	-0.487	-4.578E-04	-2.565E-05
29.37	488	5.001	4.999	4.999	**5.000**	0.001	4.063	4.070	4.063	**4.065**	0.004	-0.934	-0.711	-6.691E-04	-4.097E-05
	488	4.968	4.992	5.013	**4.991**	0.023	4.047	4.030	4.050	**4.042**	0.011	-0.949	-0.616	-5.797E-04	-3.730E-05

Table 57: Differential Refractometer Data for ICI PET in Pure TFA

Solution	λ (nm)	d1					d2					d2 - d1	Δd (d2-d1)-(d'2-d'1)	Δn	error
		1	2	3	Average	error	1	2	3	Average	error				
Solvent															
Pure	488	5.120	5.105	5.205	**5.143**	0.054	4.691	4.694	4.710	**4.698**	0.010	-0.445	-	-	-
TFA	488	5.173	5.194	5.200	**5.189**	0.014	4.670	4.705	4.670	**4.682**	0.020	-0.507	-	-	-
	488	5.177	5.182	5.208	**5.189**	0.017	4.708	4.720	4.717	**4.715**	0.006	-0.474	-	-	-
										d'2-d'1	**488**	**-0.445**	**±**	**0.055**	
											488	**-0.507**	**±**	**0.025**	
											488	**-0.474**	**±**	**0.018**	
Solutions															
Concentration															
(g/ml)	488	4.758	4.792	4.777	**4.776**	0.017	5.141	5.136	5.116	**5.131**	0.013	0.355	0.800	7.528E-04	5.559E-05
5.05	488	4.863	4.881	4.899	**4.881**	0.018	5.044	5.050	5.050	**5.048**	0.003	0.167	0.674	6.343E-04	2.908E-05
	488	4.888	4.903	4.903	**4.898**	0.009	5.108	5.116	5.119	**5.114**	0.006	0.216	0.690	6.493E-04	1.960E-05
	488	4.511	4.512	4.505	**4.509**	0.004	5.418	5.437	5.429	**5.428**	0.010	0.919	1.364	1.283E-03	5.288E-05
9.91	488	4.518	4.524	4.522	**4.521**	0.003	5.412	5.413	5.420	**5.415**	0.004	0.894	1.401	1.318E-03	2.458E-05
	488	4.500	4.517	4.510	**4.509**	0.009	5.410	5.412	5.410	**5.411**	0.001	0.902	1.376	1.294E-03	1.959E-05
	488	4.089	4.091	4.081	**4.087**	0.005	5.803	5.806	5.813	**5.810**	0.005	1.723	2.168	2.039E-03	5.299E-05
15.1	488	4.110	4.101	4.104	**4.105**	0.005	5.840	5.850	5.849	**5.846**	0.006	1.741	2.249	2.115E-03	2.622E-05
	488	4.102	4.114	4.099	**4.105**	0.008	5.820	5.835	5.827	**5.827**	0.008	1.722	2.196	2.066E-03	2.199E-05
	488	3.845	3.840	3.843	**3.843**	0.003	6.087	6.105	6.114	**6.102**	0.014	2.259	2.704	2.544E-03	5.466E-05
20.02	488	3.787	3.794	3.804	**3.795**	0.009	6.070	6.084	6.069	**6.074**	0.008	2.279	2.787	2.621E-03	2.871E-05
	488	3.800	3.799	3.790	**3.796**	0.006	6.102	6.128	6.123	**6.118**	0.014	2.321	2.795	2.629E-03	2.518E-05
	488	3.033	3.041	3.020	**3.031**	0.011	6.749	6.777	6.779	**6.768**	0.017	3.737	4.182	3.934E-03	5.805E-05
29.72	488	3.074	3.062	3.062	**3.066**	0.007	6.560	6.576	6.575	**6.570**	0.009	3.504	4.012	3.773E-03	3.131E-05
	488	3.029	3.029	3.029	**3.029**	0.000	6.782	6.783	6.806	**6.790**	0.014	3.761	4.235	3.984E-03	2.843E-05

Table 58: Differential Refractometer Data for ICI PET in Pure HFIP

Solution	λ (nm)	d1					d2					d2 - d1	Δd (d2-d1)-(d'2-d'1)	Δn	error
		1	2	3	Average	error	1	2	3	Average	error				
Solvent															
Pure	488	5.149	5.144	5.146	**5.146**	0.003	4.755	4.767	4.777	**4.766**	0.011	-0.380	-	-	-
HFIP	488	5.160	5.176	5.159	**5.165**	0.010	4.738	4.748	4.759	**4.748**	0.011	-0.417	-	-	-
	488	5.196	5.190	5.193	**5.193**	0.003	4.810	4.816	4.810	**4.812**	0.003	-0.381	-	-	-
										d'2-d'1	**488**	-0.380	±	0.011	
											488	-0.417	±	0.014	
											488	-0.381	±	0.005	
Solutions															
Concentration															
(g/ml)	488	4.827	4.837	4.844	**4.836**	0.009	4.980	4.993	4.992	**4.988**	0.007	0.152	0.532	5.007E-04	1.649E-05
4.99	488	4.873	4.869	4.884	**4.875**	0.008	5.075	5.070	5.089	**5.078**	0.010	0.203	0.619	5.826E-04	1.955E-05
	488	4.839	4.851	4.855	**4.848**	0.008	5.040	5.062	5.083	**5.062**	0.022	0.213	0.594	5.590E-04	2.343E-05
	488	4.544	4.582	4.578	**4.568**	0.021	5.400	5.403	5.413	**5.405**	0.007	0.837	1.217	1.145E-03	2.812E-05
9.70	488	4.501	4.444	4.489	**4.478**	0.030	5.369	5.370	5.390	**5.376**	0.012	0.898	1.315	1.237E-03	3.734E-05
	488	4.495	4.510	4.495	**4.500**	0.009	5.399	5.412	5.407	**5.406**	0.007	0.906	1.287	1.211E-03	2.009E-05
	488	4.054	4.075	4.089	**4.073**	0.018	5.687	5.705	5.720	**5.713**	0.011	1.640	2.020	1.900E-03	3.433E-05
14.99	488	4.179	4.164	4.168	**4.170**	0.008	5.709	5.727	5.709	**5.715**	0.010	1.545	1.961	1.845E-03	3.129E-05
	488	4.099	4.130	4.132	**4.120**	0.019	5.689	5.702	5.689	**5.693**	0.008	1.573	1.954	1.838E-03	3.191E-05
	488	3.842	3.817	3.801	**3.820**	0.021	6.027	6.079	6.093	**6.066**	0.035	2.246	2.626	2.470E-03	5.225E-05
20.79	488	3.645	3.649	3.640	**3.645**	0.005	6.037	6.049	6.052	**6.046**	0.008	2.401	2.818	2.651E-03	3.998E-05
	488	3.652	3.682	3.670	**3.668**	0.015	6.050	6.070	6.065	**6.062**	0.010	2.394	2.775	2.610E-03	4.026E-05
	488	3.151	3.140	3.144	**3.145**	0.006	6.660	6.689	6.682	**6.677**	0.015	3.532	3.912	3.680E-03	5.420E-05
30.56	488	2.992	3.002	3.000	**2.998**	0.005	6.643	6.628	6.661	**6.644**	0.017	3.646	4.063	3.821E-03	5.694E-05
	488	3.127	3.130	3.129	**3.129**	0.002	6.667	6.636	6.660	**6.654**	0.016	3.526	3.907	3.675E-03	5.331E-05

Table 59: Differential Refractometer Data for ICI PET in Pure TFA at 633nm

Solution	λ (nm)	d1					d2					d2 - d1	Δd (d2-d1)-(d'2-d'1)	Δn	error
		1	2	3	Average	error	1	2	3	Average	error				
Solvent															
Pure	633	5.172	5.177	5.182	**5.177**	0.005	4.811	4.802	4.820	**4.811**	0.009	-0.366	-	-	-
TFA	633	5.251	5.249	5.251	**5.250**	0.001	4.775	4.777	4.793	**4.782**	0.010	-0.469	-	-	-
	633	5.154	5.159	5.162	**5.158**	0.004	4.760	4.779	4.758	**4.766**	0.012	-0.393	-	-	-
										d'2-d'1	**633**	-0.366	±	0.010	
											633	-0.469	±	0.010	
											633	-0.393	±	0.012	
Solutions															
Concentration															
(g/ml)	633	4.512	4.514	4.520	**4.515**	0.004	5.560	5.564	5.561	**5.562**	0.002	1.046	1.412	1.319E-03	2.120E-05
5.02	633	4.501	4.483	4.506	**4.497**	0.012	5.561	5.558	5.540	**5.553**	0.011	1.056	1.525	1.424E-03	2.684E-05
	633	4.510	4.511	4.516	**4.512**	0.003	5.503	5.520	5.529	**5.517**	0.013	1.005	1.398	1.305E-03	2.497E-05
	633	3.704	3.714	3.713	**3.710**	0.006	6.140	6.130	6.145	**6.138**	0.008	2.428	2.794	2.609E-03	3.864E-05
10.10	633	3.711	3.713	3.713	**3.712**	0.001	6.220	6.216	6.213	**6.216**	0.004	2.504	2.973	2.776E-03	3.995E-05
	633	3.689	3.689	3.707	**3.695**	0.010	6.169	6.144	6.119	**6.144**	0.025	2.449	2.842	2.654E-03	4.625E-05
	633	2.942	2.974	2.963	**2.960**	0.016	6.910	6.900	6.914	**6.907**	0.010	3.947	4.313	4.028E-03	5.968E-05
15.36	633	2.940	2.951	2.945	**2.945**	0.006	6.894	6.906	6.911	**6.904**	0.009	3.958	4.427	4.134E-03	5.917E-05
	633	2.973	2.981	2.960	**2.971**	0.011	6.919	6.918	6.914	**6.917**	0.003	3.946	4.338	4.051E-03	5.853E-05
	633	2.299	2.259	2.210	**2.256**	0.045	7.673	7.694	7.690	**7.686**	0.011	5.430	5.796	5.412E-03	8.734E-05
20.28	633	2.225	2.250	2.223	**2.233**	0.015	7.648	7.650	7.659	**7.652**	0.006	5.420	5.888	5.499E-03	7.868E-05
	633	2.267	2.260	2.264	**2.264**	0.004	7.749	7.756	7.751	**7.752**	0.004	5.488	5.881	5.492E-03	7.757E-05
	633	0.698	0.700	0.694	**0.697**	0.003	9.277	9.270	9.274	**9.274**	0.004	8.576	8.942	8.350E-03	1.169E-04
30.33	633	0.653	0.671	0.691	**0.672**	0.019	9.333	9.362	9.356	**9.350**	0.015	8.679	9.147	8.542E-03	1.216E-04
	633	0.732	0.712	0.684	**0.709**	0.024	9.302	9.339	9.324	**9.322**	0.019	8.612	9.005	8.409E-03	1.212E-04

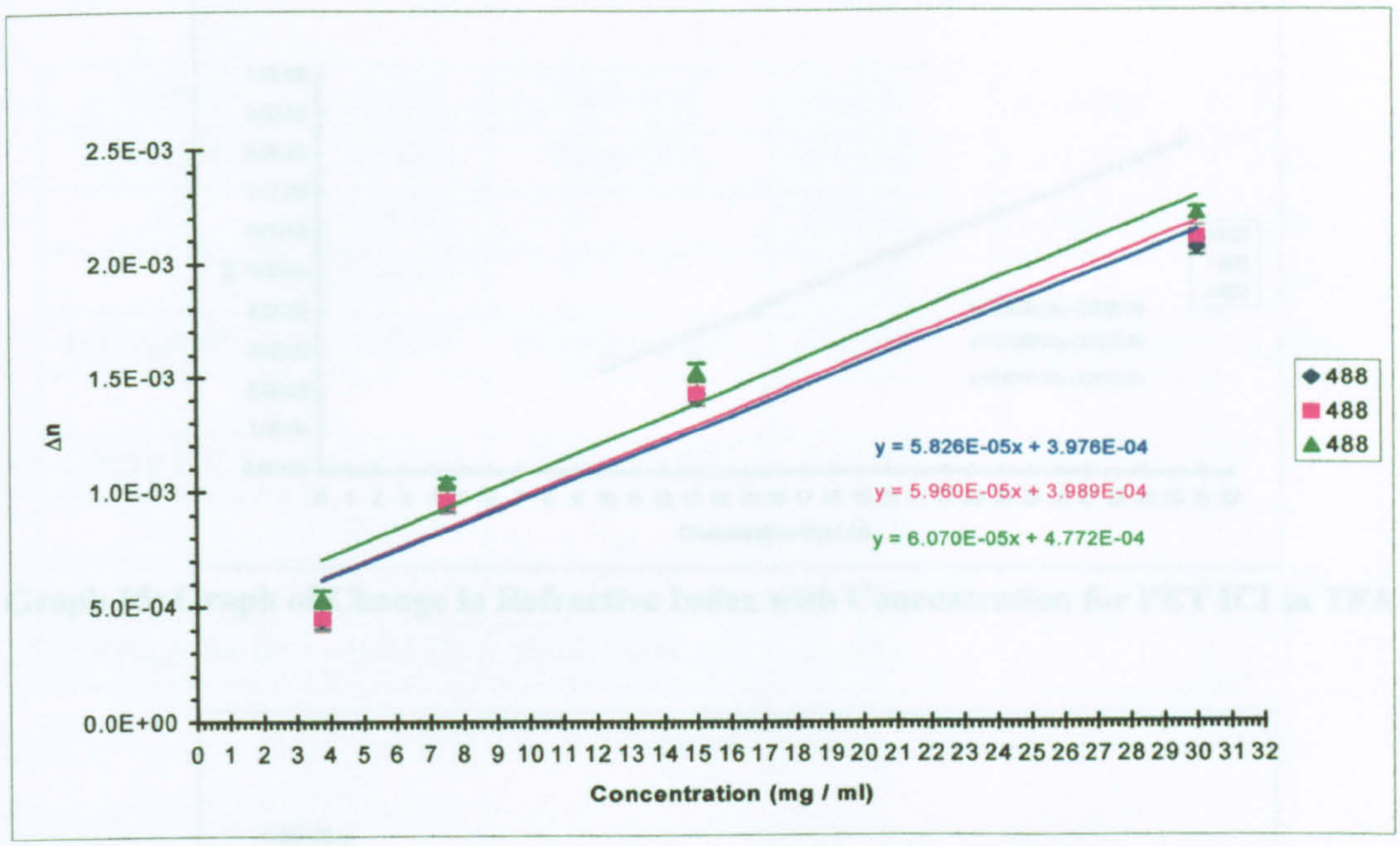

Graph 13: Graph of Change in Refractive Index with Concentration of PET ICI in $CHCl_3$:TFA 1:1

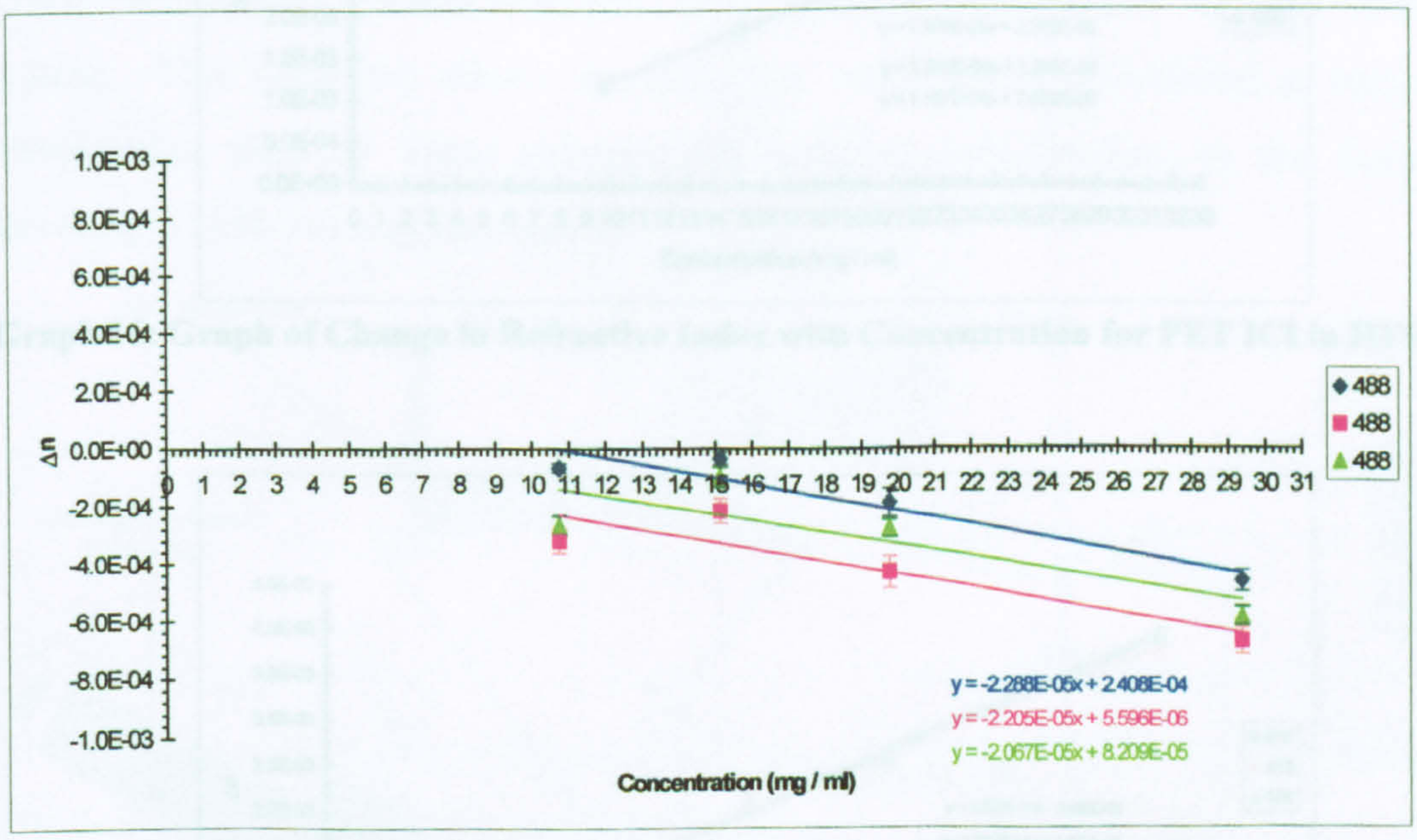

Graph 14: Graph of Change in Refractive Index with Concentration for PET ICI in DCA

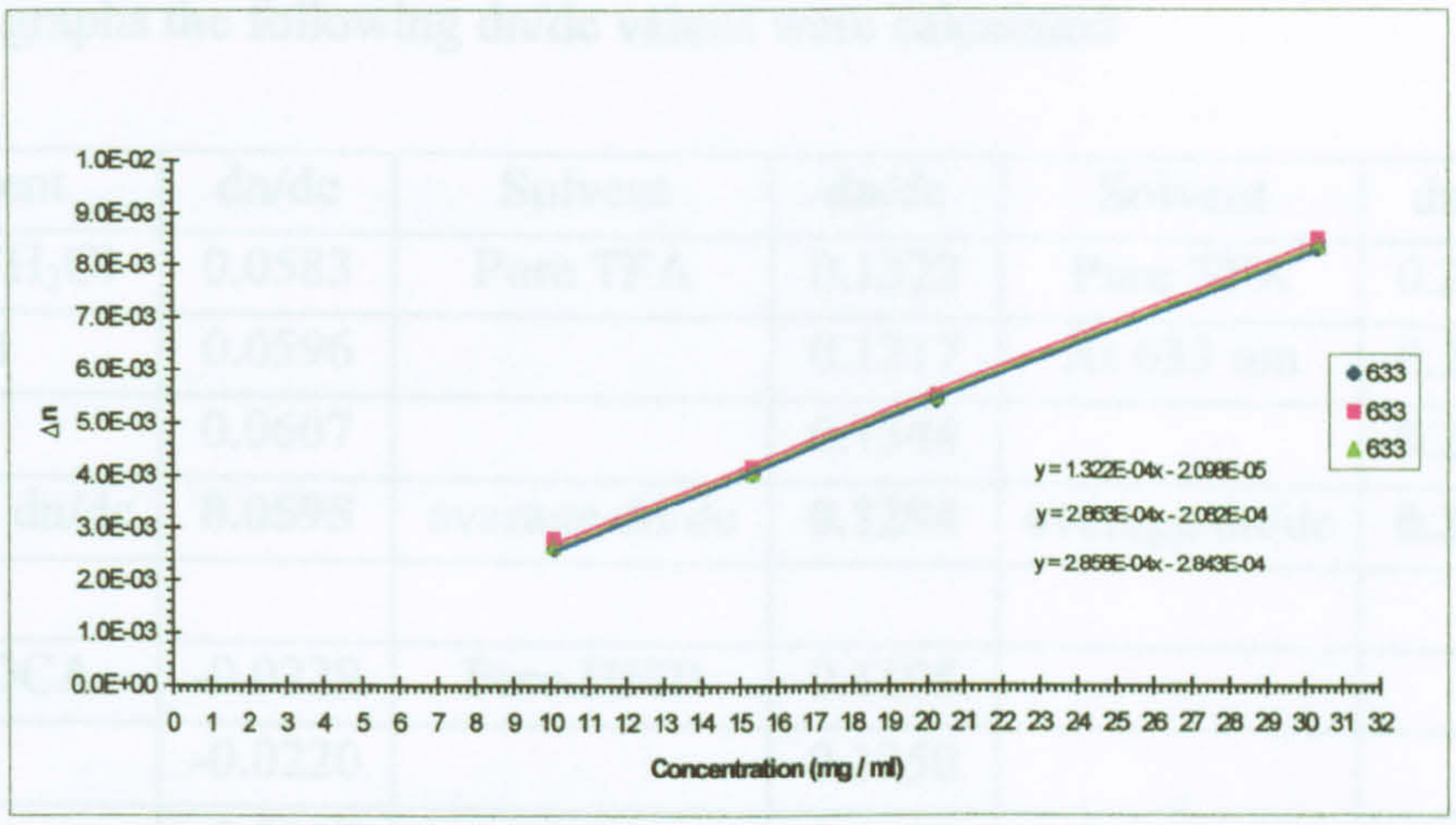

Graph 15: Graph of Change in Refractive Index with Concentration for PET ICI in TFA

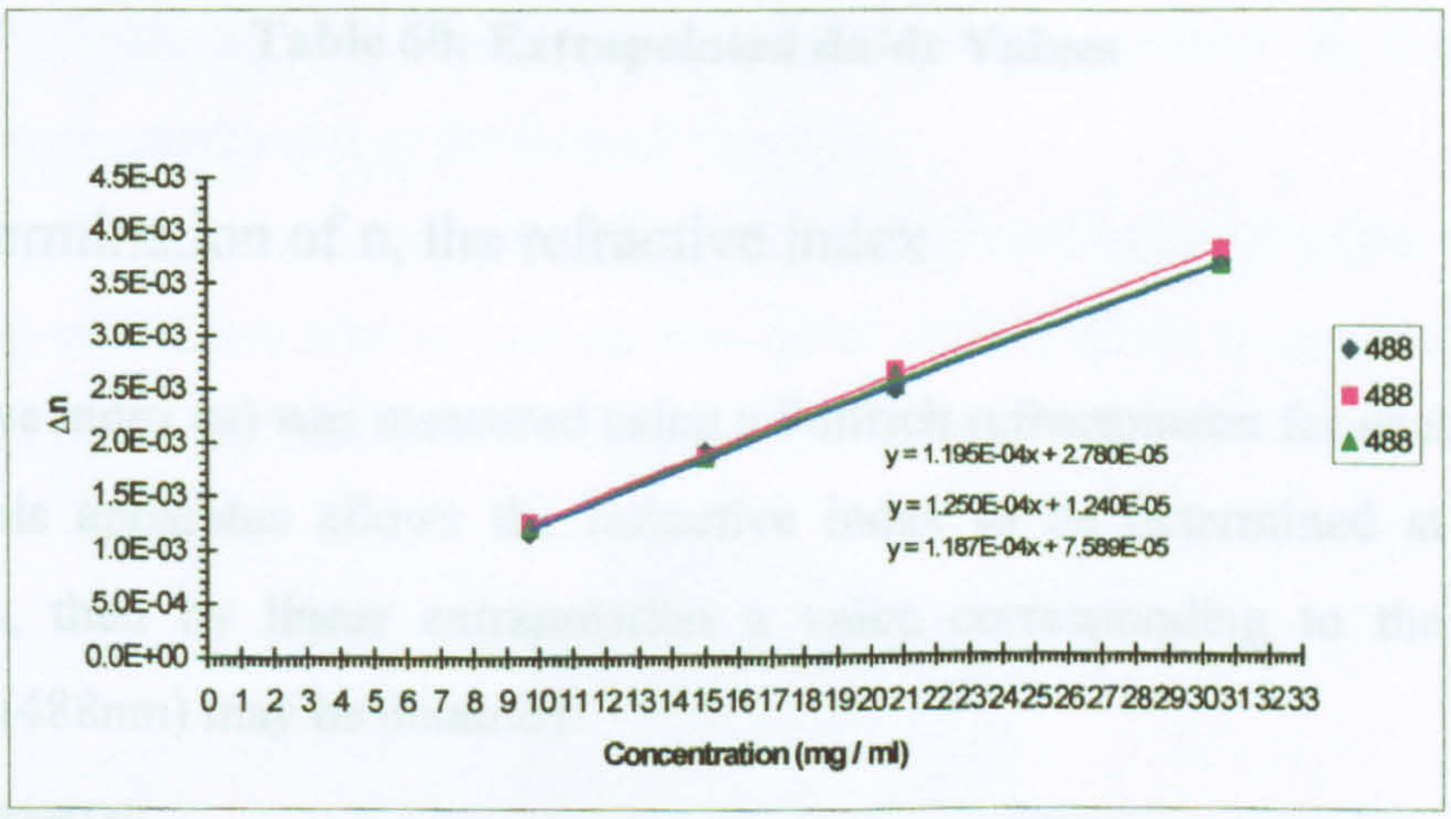

Graph 16: Graph of Change in Refractive Index with Concentration for PET ICI in HFIP

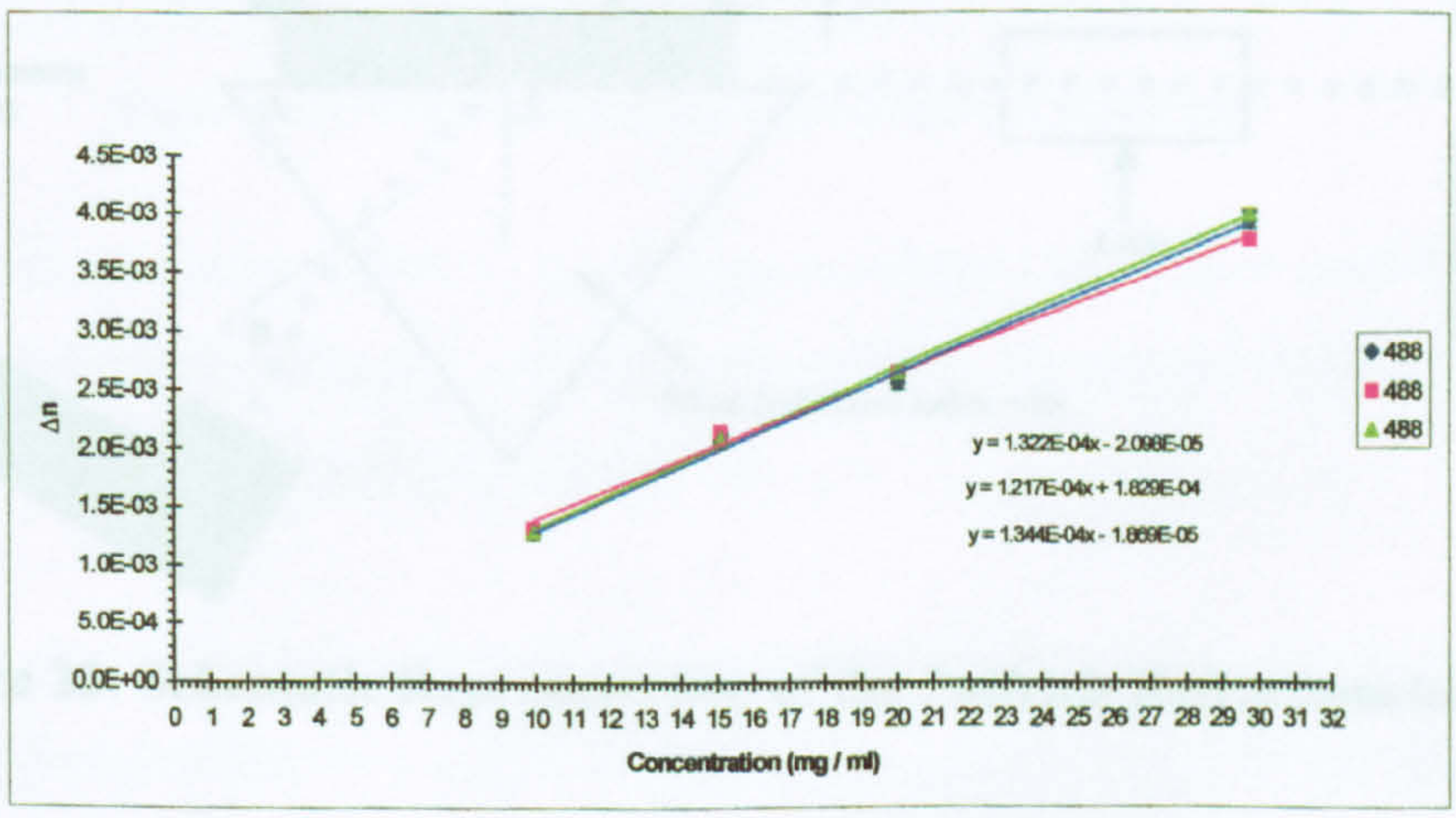

Graph 17: Graph of Change in Refractive Index with Concentration for PET ICI in TFA at 633 nm

From these graphs the following dn/dc values were calculated

Solvent	dn/dc	Solvent	dn/dc	Solvent	dn/dc
TFA:CH_3Cl	0.0583	Pure TFA	0.1322	Pure TFA	0.2845
1:1	0.0596		0.1217	At 633 nm	0.2863
	0.0607		0.1344		0.2858
average dn/dc	**0.0595**	average dn/dc	**0.1294**	average dn/dc	**0.2855**
Pure DCA	-0.0229	Pure HFIP	0.1195		
	-0.0220		0.1250		
	-0.0207		0.1187		
average dn/dc	**-0.0219**	average dn/dc	**0.1211**		

Table 60: Extrapolated dn/dc Values

9.4.7 Determination of n, the refractive index

The refractive index (n) was measured using a Pulfrich refractometer for each solvent system. This apparatus allows the refractive index to be determined at various wavelengths, then by linear extrapolation a value corresponding to the desired wavelength (488nm) may be obtained.

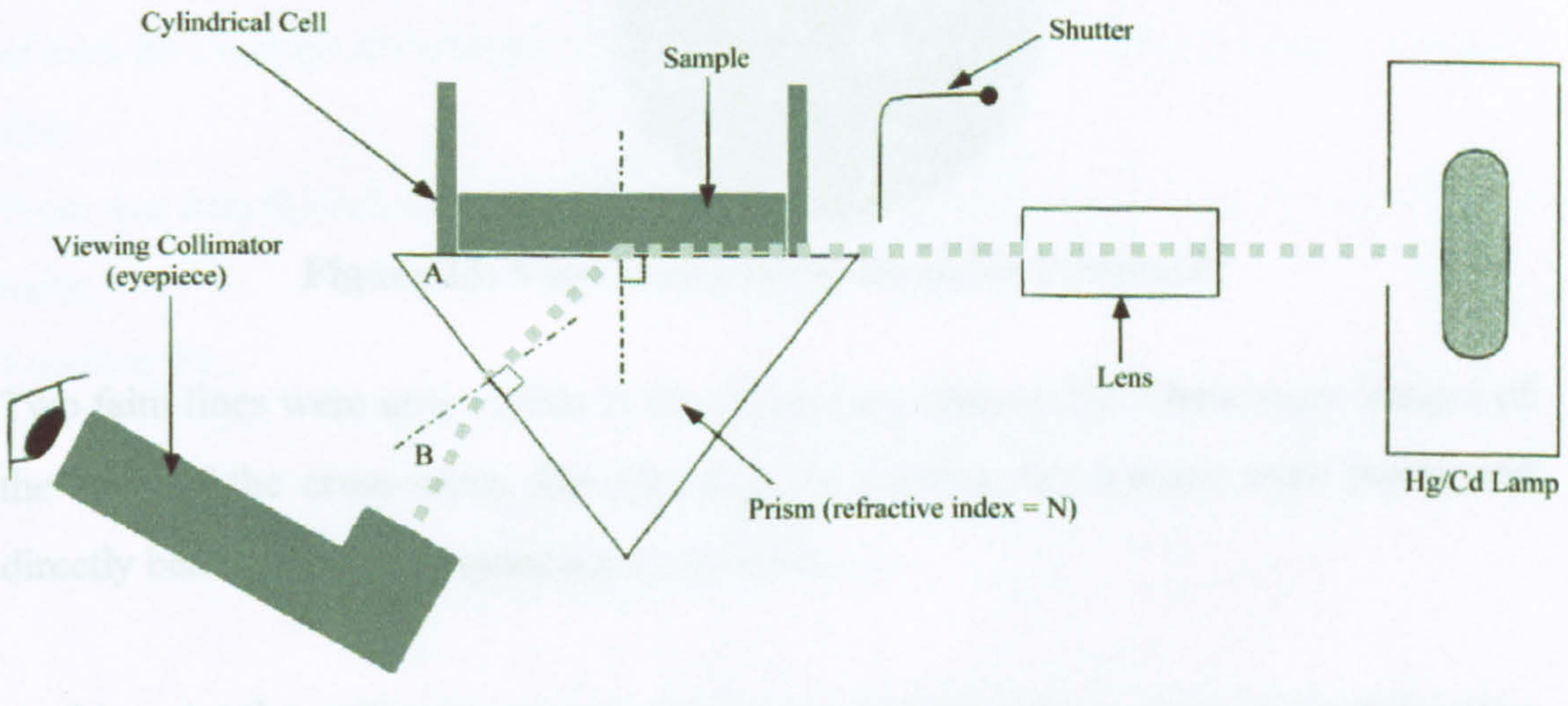

Figure 22: Schematic Representation of the Pulfrich Refractometer

PROCEDURE

Each time a measurement is to be taken, two readings must be determined

1. The angle of the normal to the emergent face of the prism
2. The angle of the emergent beam from the lamp

Determination of the normal:

This was achieved by illuminating inside the apparatus with a standard small 1.5V bulb (not the Na or Hg/Cd lamp), this illuminated the circular scales, and the eyepiece. The viewing collimator (eyepiece) was then moved to a position approximately perpendicular to the face of the prism.

Looking down the eyepiece, two cross-wires and a circle with a small recess could be seen. As the collimator was moved up and down, a brighter area appeared in the recess. At this point the collimator was fixed in position.

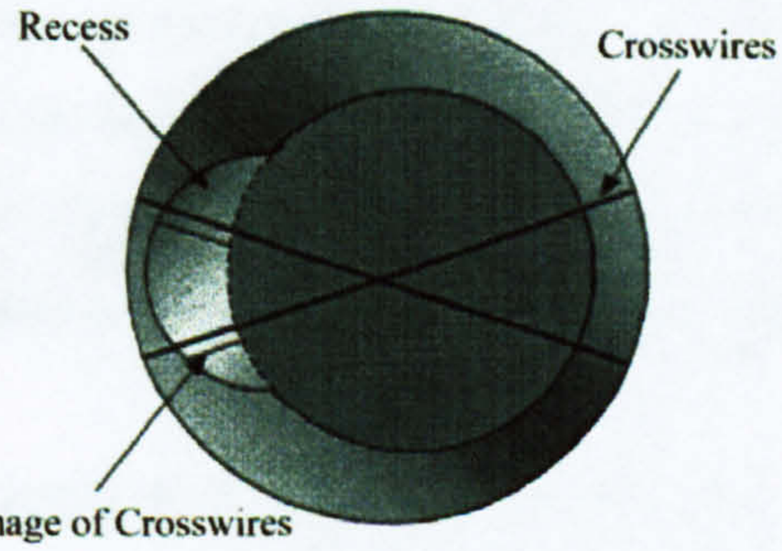

Figure 23: View Down the Collimator (eyepiece)

Two faint lines were now visible in the recess (see **Figure 23**). These were images of the ends of the cross-wires. By adjusting the vernier, the images were positioned directly beneath the corresponding cross-wires.

At this point the collimator was in the exact position of the normal of the refracting face of the prism, and readings of the angles (a, b and c), defining this position, were taken. From these three readings the normal was simply calculated as: -

$$a + c - b$$

Having obtained the normal, the light was switched off and a Hg/Cd lamp was

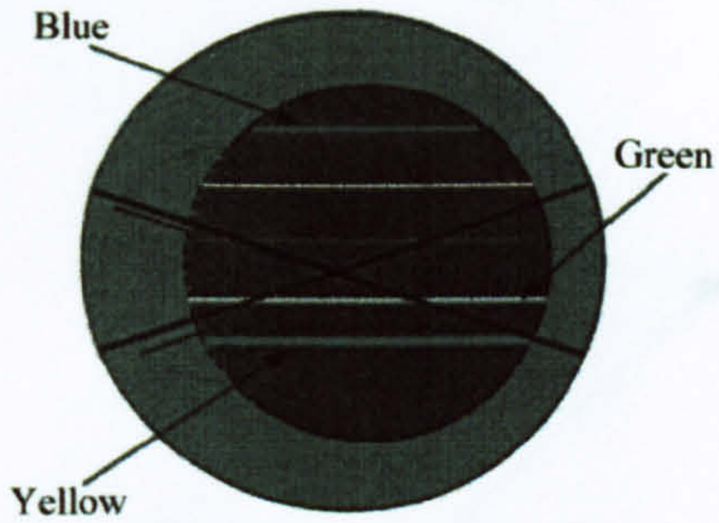

Figure 24: Hg/Cd Border Lines Viewed Down Eyepeice

switched on to allow determination of the refractive index of the sample. The solvent used in earlier light scattering experiments was then introduced to the cylindrical cell above the prism, and a temperature-controlled lid was set on top. The temperature controller was set at 25 °C and the apparatus was left for 10 –15 minutes to equilibrate.

The collimator was moved and focused until the distinct borderlines of the lamp are visible (see Figure 24). Three of these lines were chosen to investigate (yellow, 579.1 nm green 546.1 nm and blue 435.8 nm). The cross wires were placed on the bottom of each line and the three angles a, b, and c were recorded as with the normal for each line.

From this data the refractive index for the solvent was calculated for each wavelength using

Equation 51.

$$n = (\sin A\sqrt{N^2 - \sin^2 B}) + \cos A \sin B$$

Equation 51: Refractive Index

Plots of refractive index against $1/\lambda^2$ gave straight lines and the refractive indices at the wavelength of interest (488 nm) were determined for each solvent (Graphs 18 – 20).

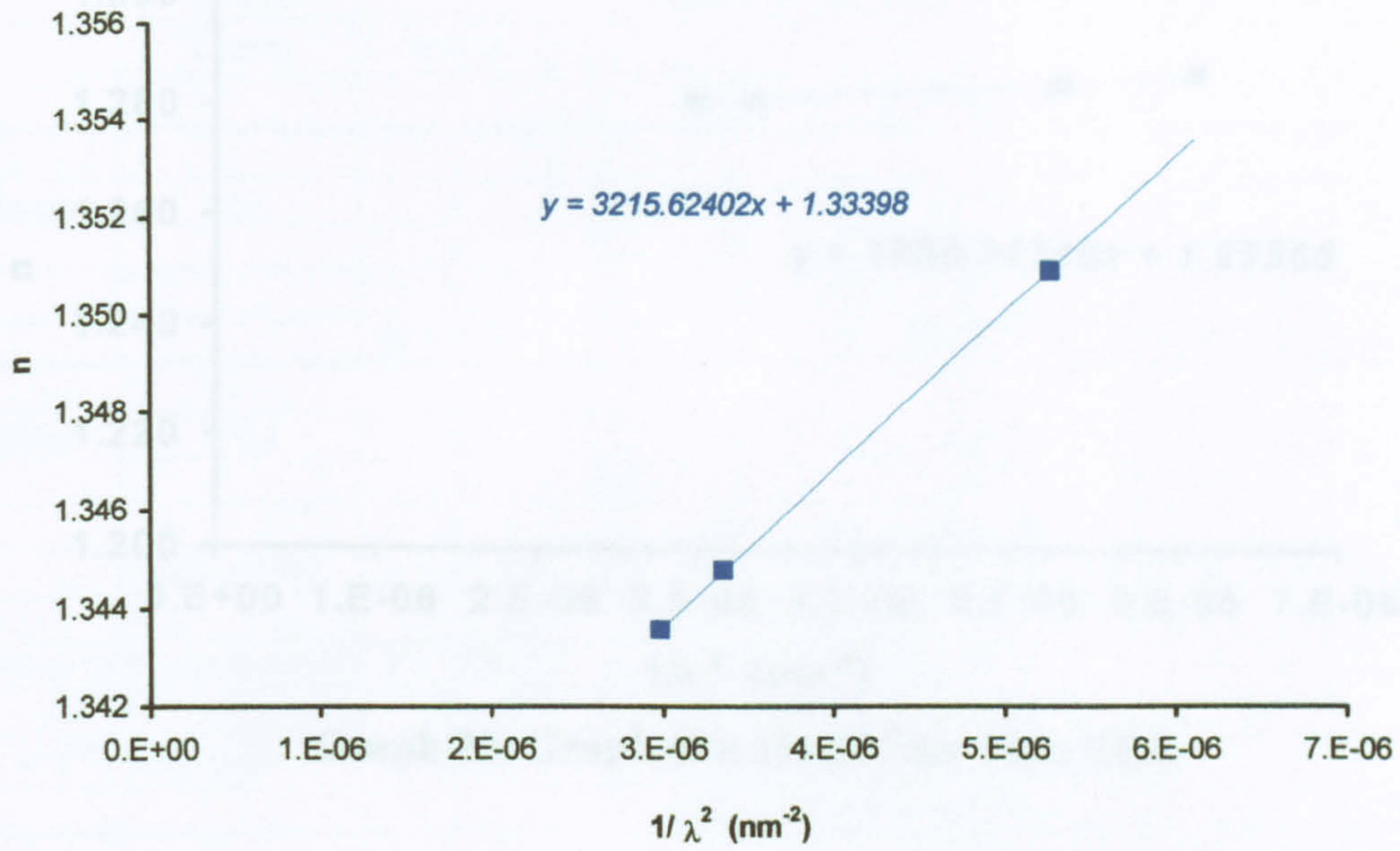

Graph 18: Graph of n vrs $1/\lambda^2$ for 1:1 TFA:CH_3Cl

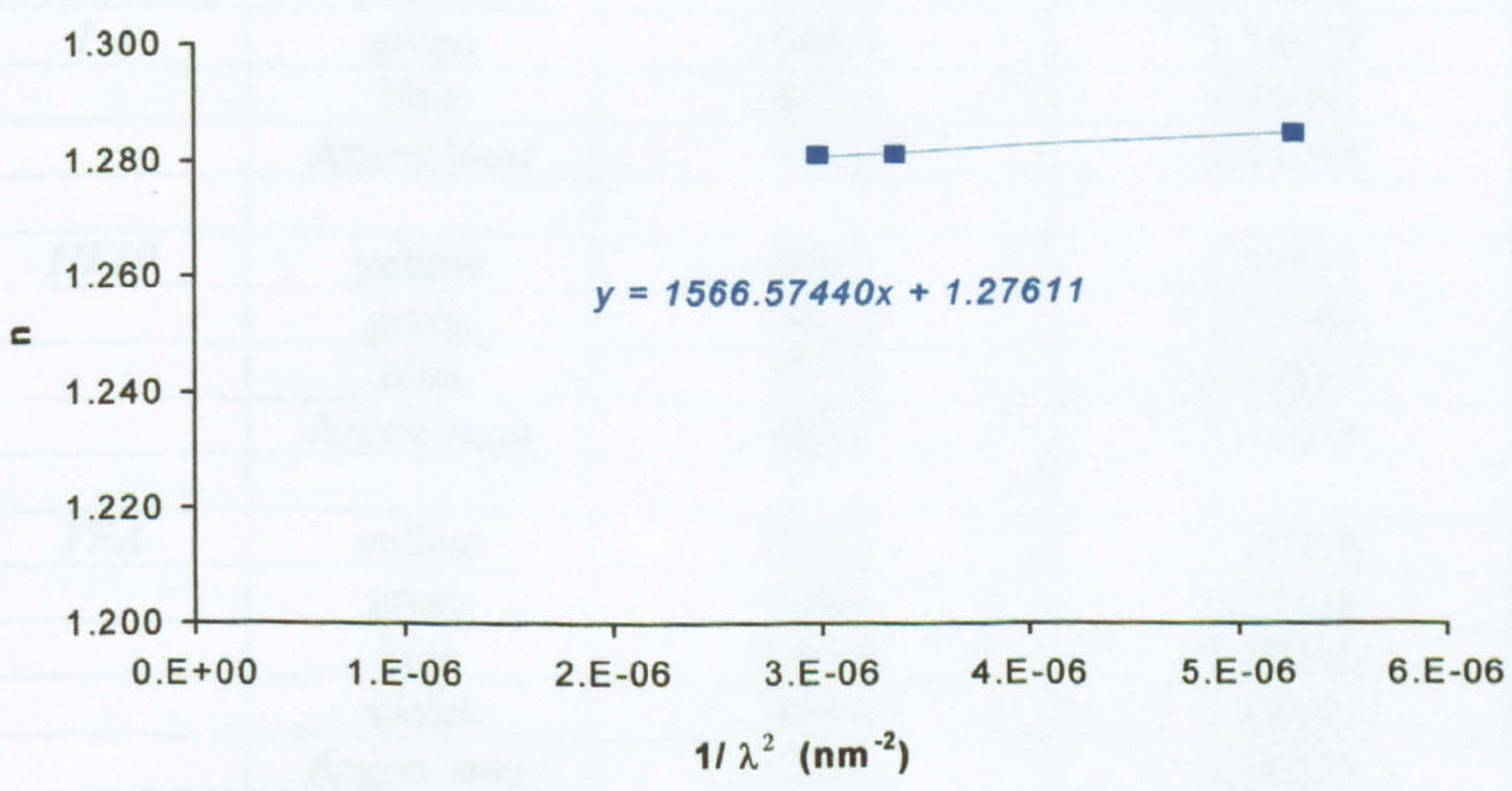

Graph 19: Graph of n vrs $1/\lambda^2$ for HFIP

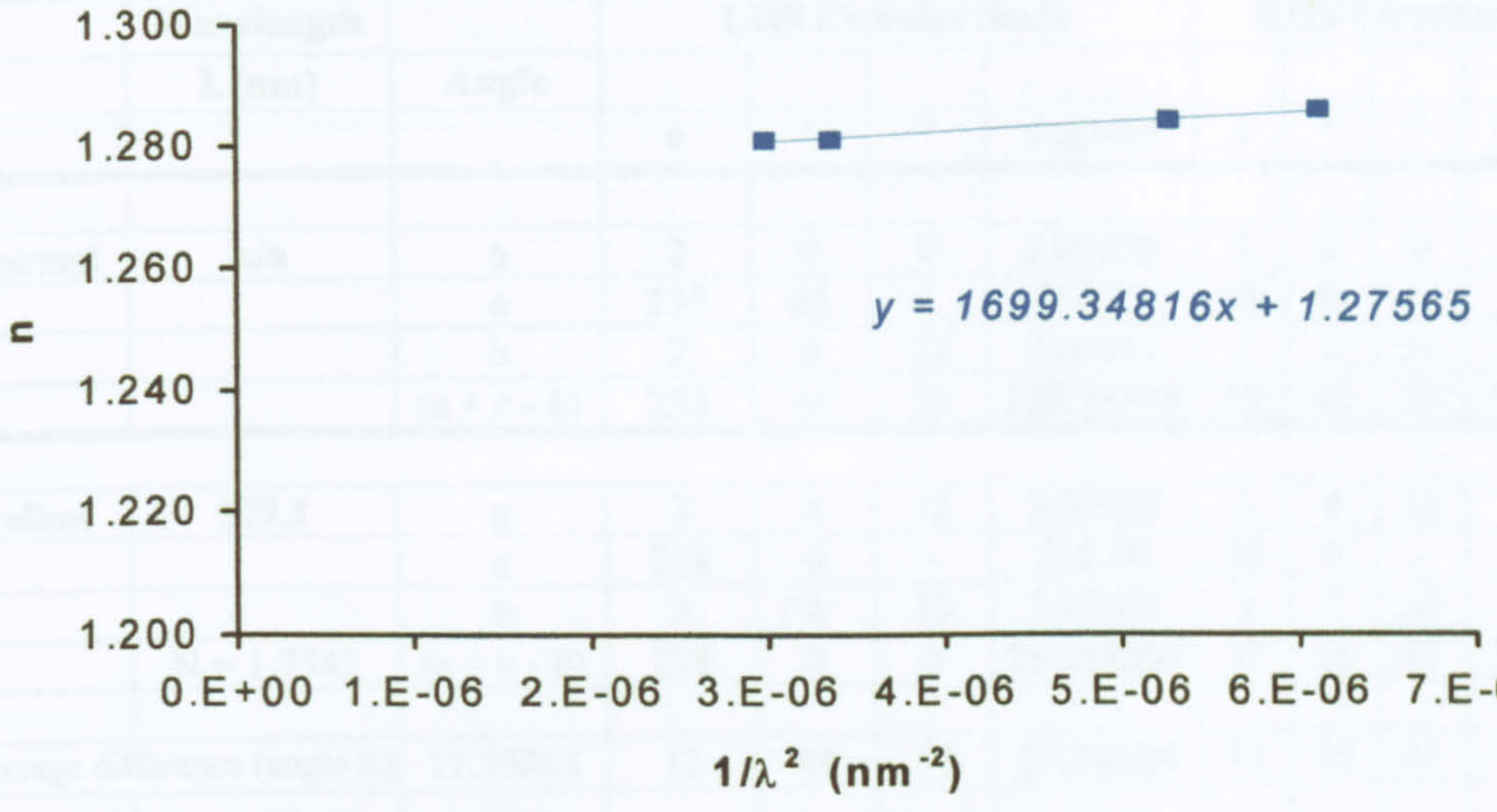

Graph 20: Graph of n vrs $1/\lambda^2$ for Pure TFA

The calculated refractive indices are summarised in Table 61.

Solution		Wavelength λ (nm)	Refractive Index, *n*
TFA:CHCl₃	yellow	579.1	1.34356
1:1	green	546.1	1.34477
	blue	435.8	1.35091
	Argon laser	488.0	1.34748
HFIP	yellow	579.1	1.27511
	green	546.1	1.27501
	blue	435.8	1.27817
	Argon laser	488.0	1.27658
TFA	yellow	579.1	1.28099
	green	546.1	1.28111
	blue	435.8	1.28440
	violet	404.7	1.28621
	Argon laser	488	1.28279
	Helium-Neon	633	1.27989

Table 61: Calculated Refractive Indices.

The angles found for each border line and the normal for the various solvent systems are summarised in Tables 62 - 64.

	Wavelength		LHS Circular Scale				RHS Circular Scale			
	λ (nm)	Angle								
			o	'	"	degrees	o	'	"	degrees
normal	n/a	a	2	0	0	2.00000	2	0	0	2.00000
		c	235	45	-	235.75	55	45	-	55.75
		b	2	0	22	2.00611	2	2	31	2.04194
		(a + c - b)	235	44	38	**235.74389**	55	42	29	**55.70806**
yellow	579.1	a	3	4	13	3.07028	3	4	13	3.07028
		c	218	0	-	218.00	38	0	-	38.00
		b	3	4	13	3.07028	3	7	25	3.12361
	N = 1.7542	(a + c - b)	218	0	0	**218.00000**	37	56	48	**37.94667**
Average difference (angle B)		**17.75264**	17	44	38	**17.74389**	17	45	41	**17.76139**
n, at 579.1nm (yellow) =		**1.34356**		(from eqtn 1)		**1.64849**				
				(from eqtn 2)		**1.34356**				
green	546.1	a	3	7	25	3.12361	3	7	25	3.12361
		c	217	45	-	217.75	37	45	-	37.75
		b	3	10	46	3.17944	3	15	10	3.25278
	N = 1.75947	(a + c - b)	217	41	39	**217.69417**	37	37	15	**37.62083**
Average difference (angle B)		**18.06847**	18	2	59	**18.04972**	18	5	14	**18.08722**
n, at 546.1nm (green) =		**1.34477**		(from eqtn 1)		**1.65494**				
				(from eqtn 2)		**1.34477**				
blue	435.8	a	3	15	10	3.25278	3	15	10	3.25278
		c	216	0	-	216.00	36	0	-	36.00
		b	3	22	23	3.37306	3	25	22	3.42278
	N = 1.78878	(a + c - b)	215	52	47	**215.87972**	35	49	48	**35.83000**
Average difference (angle B)		**19.87111**	19	51	51	**19.86417**	19	52	41	**19.87806**
n, at 435.8nm (blue) =		**1.35091**		(from eqtn 1)		**1.69084**				
				(from eqtn 2)		**1.35091**				

Table 62: Experimental Angles of Border Lines and Normal TFA:CH_3Cl 1:1 System

	Wavelength		LHS Circular Scale				RHS Circular Scale			
	λ (nm)	Angle								
			o	'	"	degrees	o	'	"	degrees
normal	**n/a**	a	2	0	0	2.00000	2	0	0	2.00000
		c	235	45	-	235.75	55	45	-	55.75
		b	2	1	48	2.03000	2	2	39	2.04417
		(a + c - b)	235	43	12	**235.72000**	55	42	21	**55.70583**
yellow	**579.1**	a	2	2	39	2.04417	2	2	39	2.04417
		c	212	30	-	212.50	32	30	-	32.50
		b	2	14	7	2.23528	2	15	3	2.25083
	N = 1.7542	(a + c - b)	212	18	32	**212.30889**	32	17	36	**32.29333**
Average difference (angle B)		**23.41181**	23	24	40	**23.41111**	23	24	45	**23.41250**
n, at 579.1nm (yellow) =		**1.28099**		(from eqtn 1)		**1.67835**				
				(from eqtn 2)		**1.28099**				
green	**546.1**	a	3	18	5	3.30139	3	18	5	3.30139
		c	212	0	-	212.00	32	0	-	32.00
		b	3	23	25	3.39028	3	25	24	3.42333
	N = 1.75947	(a + c - b)	211	54	40	**211.91111**	31	52	41	**31.87806**
Average difference (angle B)		**23.81833**	23	48	32	**23.80889**	23	49	40	**23.82778**
n, at 546.1nm (green) =		**1.28111**		(from eqtn 1)		**1.68497**				
				(from eqtn 2)		**1.28111**				
blue	**435.8**	a	2	15	41	2.26139	2	15	41	2.26139
		c	210	0	-	210.00	30		-	30.00
		b	2	23	14	2.38722	2	24	8	2.40222
	N = 1.78878	(a + c - b)	209	52	27	**209.87417**	29	51	33	**29.85917**
Average difference (angle B)		**25.84625**	25	50	45	**25.84583**	25	50	48	**25.84667**
n, at 435.8nm (blue) =		**1.28440**		(from eqtn 1)		**1.72038**				
				(from eqtn 2)		**1.28440**				

Table 63: Experimental Angles of Border Lines and Normal for TFA System

	Wavelength		LHS Circular Scale				RHS Circular Scale			
	λ (nm)	Angle								
			o	'	"	degrees	o	'	"	degrees
normal	**n/a**	a	2	0	0	2.00000	2	0	0	2.00000
		c	235	45	-	235.75	55	45	-	55.75
		b	2	1	48	2.03000	2	2	39	2.04417
		(a + c - b)	235	43	12	**235.72000**	55	42	21	**55.70583**
yellow	**579.1**	a	3	10	25	3.17361	3	10	25	3.17361
		c	212	0	-	212.00	32	0	-	32.00
		b	3	23	33	3.39250	3	23	53	3.39806
	N = 1.7542	(a + c - b)	211	46	52	**211.78111**	31	46	32	**31.77556**
Average difference (angle B)		**23.93458**	23	56	20	**23.93889**	23	55	49	**23.93028**
n, at 579.1nm (yellow) =		**1.27511**		(from eqtn 1)		**1.68083**				
				(from eqtn 2)		**1.27511**				
green	**546.1**	a	3	23	53	3.39806	3	23	53	3.39806
		c	211	30	-	211.50	31	30	-	31.50
		b	3	32	53	3.54806	3	32	30	3.54167
	N = 1.75947	(a + c - b)	211	20	60	**211.35000**	31	21	23	**31.35639**
Average difference (angle B)		**24.35972**	24	22	12	**24.37000**	24	20	58	**24.34944**
n, at 546.1nm (green) =		**1.27501**		(from eqtn 1)		**1.68750**				
				(from eqtn 2)		**1.27501**				
blue	**435.8**	a	3	32	5	3.53472	3	32	5	3.53472
		c	209	30	-	209.50	29	30	-	29.50
		b	3	42	15	3.70417	3	44	5	3.73472
	N = 1.78878	(a + c - b)	209	19	50	**209.33056**	29	17	60	**29.30000**
Average difference (angle B)		**26.39764**	26	23	22	**26.38944**	26	24	21	**26.40583**
n, at 435.8nm (blue) =		**1.27817**		(from eqtn 1)		**1.72280**				
				(from eqtn 2)		**1.27817**				

Table 64: Experimental Angles of Border Lines and Normal HFIP System

9.4.8 Melt Viscosity Measurement

The melt viscosity and oscillation curves of selected samples were obtained by means of a TA Instruments CSL^2 500 Carri-Med controlled stress rheometer. Samples were prepared by hot pressing into 2 cm diameter, 500 μm thick disks of polymer using a Graseby Specac constant thickness film-maker at 240 °C for 10 minutes under 10 tonnes of pressure. Samples were then quenched in cold water.

Experiments were carried out at 260 °C. Melt viscosity was recorded using a 10-point program at shear rates of 0.2 –1 s^{-1}. Oscillation was recorded using a 21-point program at angular frequencies of 1 –100 π s^{-1}. This provided two plots, from which the Newtonian melt viscosity and the elastic/loss moduli at 100 π s^{-1} were obtained. The Newtonian melt viscosity was found by extrapolation of the flow curve to zero shear rate and the elastic/loss moduli were recorded straight from the graph. Each experiment was carried out in triplicate and the mean values obtained. The results of which are shown in Table 65.

Code	Melt Visc. (Pa.s)	Elastic Modulus (G′, Pa)	Loss Modulus (G″, Pa)
PET ICI	60	580	2565
PET 4	80	610	2575
PET 15	140	1680	7120
PET 16	120	1265	4375
PET 17	90	1070	3000
PET 27	80	595	1630
PET 31	130	850	4080
PET 38	65	700	1550
PET 39	170	1150	7550
PET 40	260	1150	7860
PET 41	205	3300	12830
PET 42	160	2460	7540
PET 43	70	650	635
PET 44	360	2100	7900
PET 52	20	620	630
PET 55	15	590	230
PET 61	~0	1650	290
PET 62	~0	1740	190
PET 63	~0	1590	215
PET 64	5	1435	350
PET 65	5	1280	300
PET 66	10	990	1100

Table 65: Melt Rheology Data

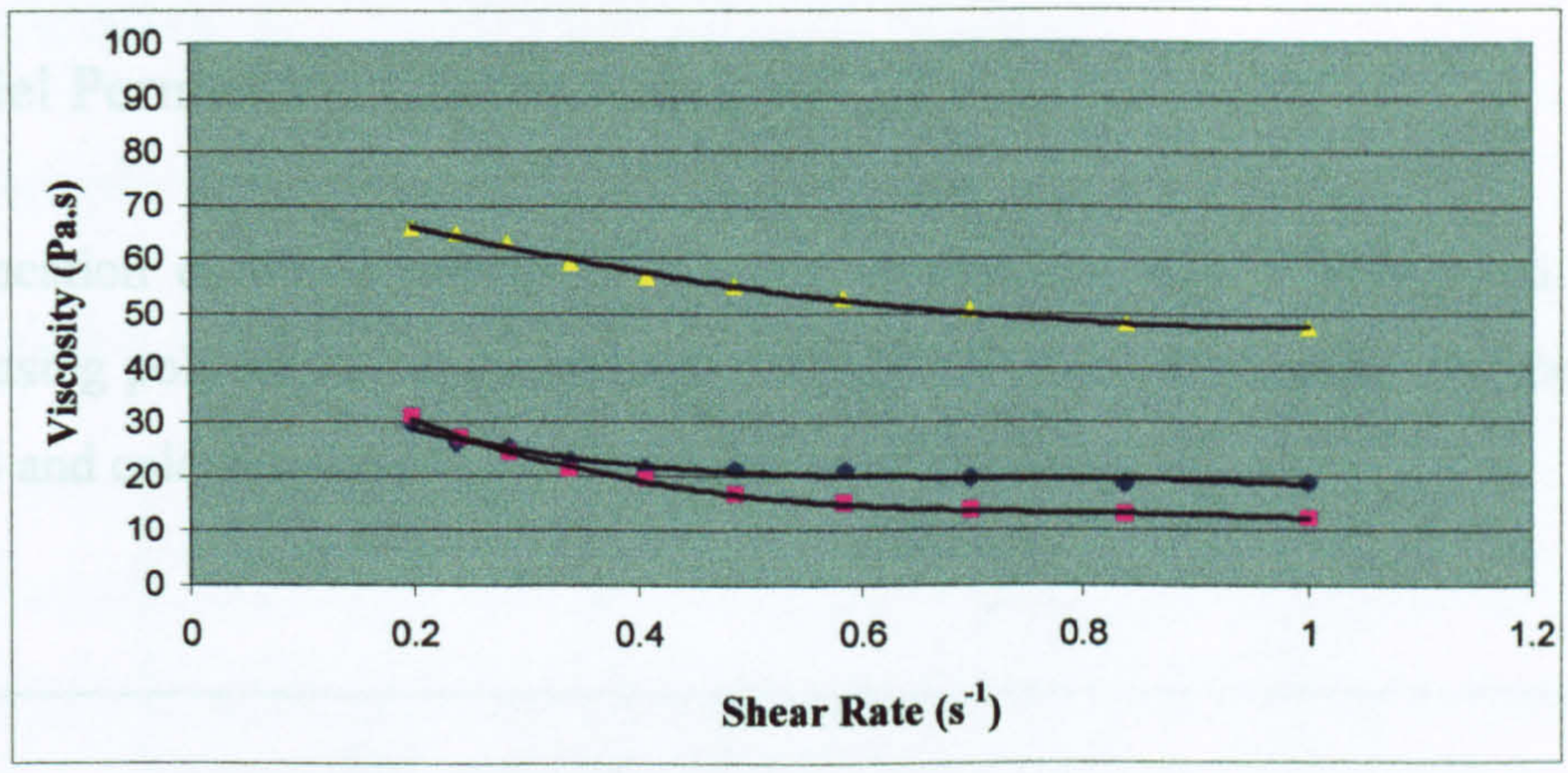

Graph 21: Typical Flow Curve, ICI PET

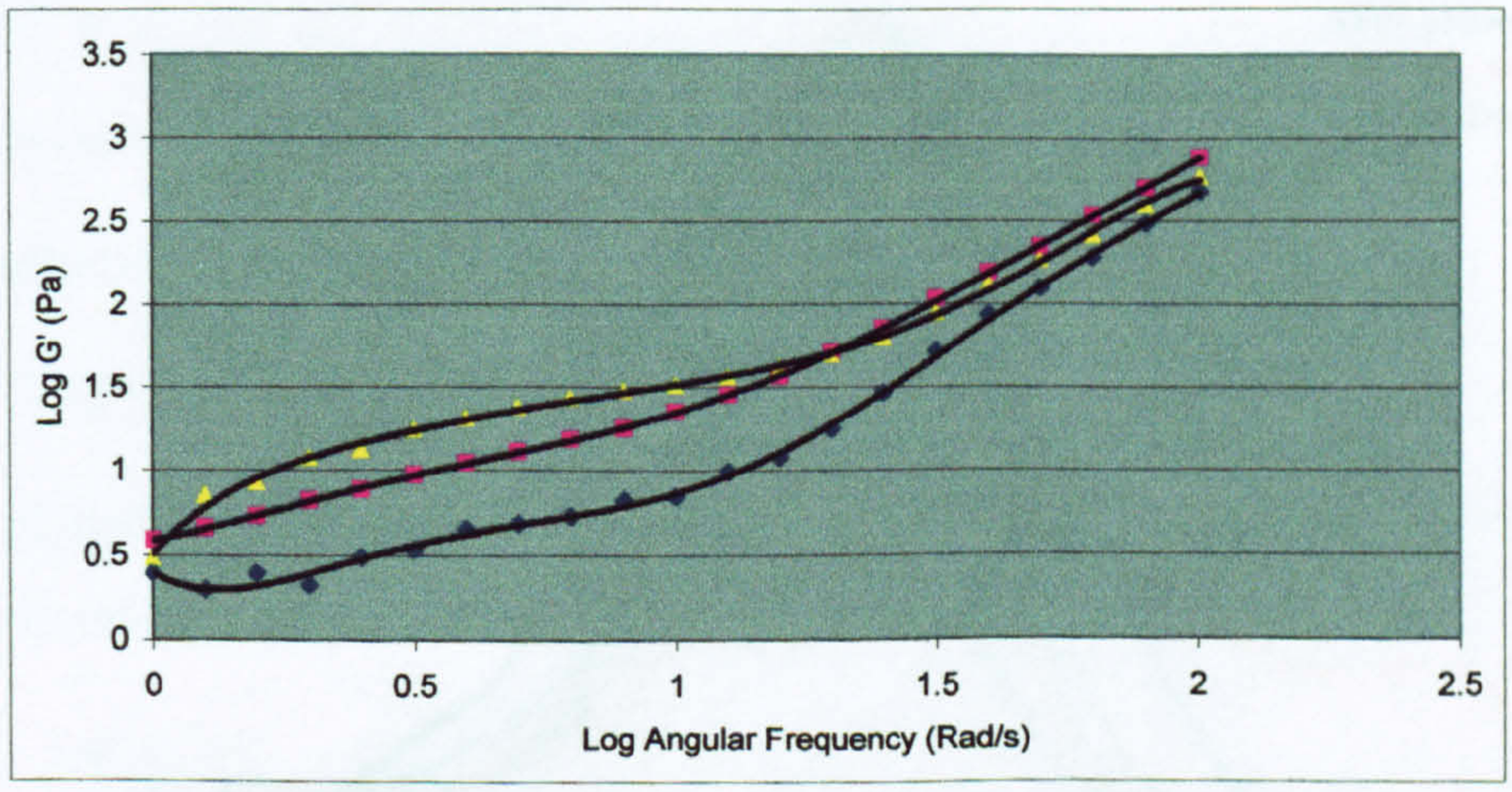

Graph 22: Typical Elastic Modulus vs Angular Frequency Plot, ICI PET

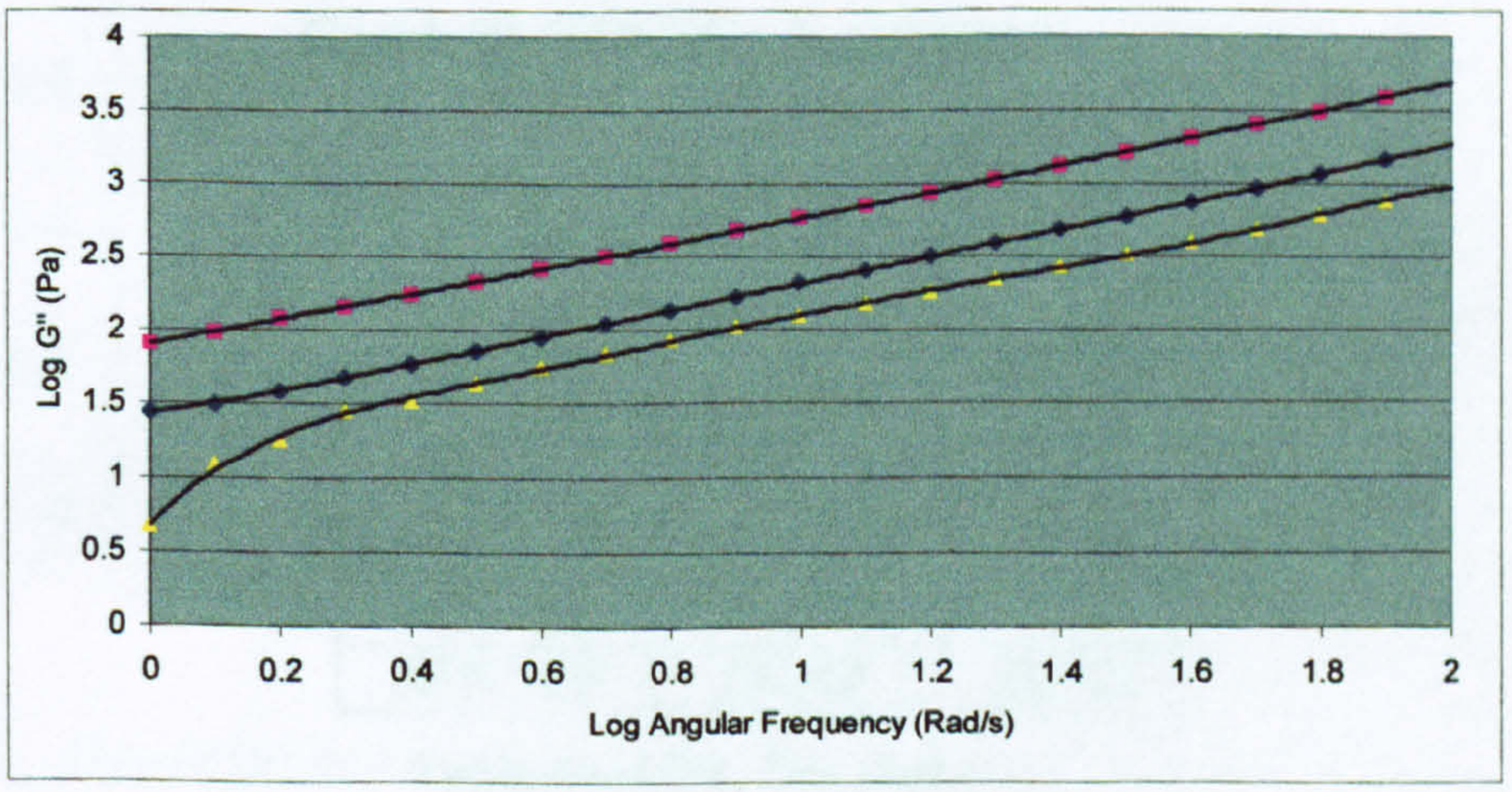

Graph 23: Typical Loss Modulus vs Angular Frequency Plot, ICI PET

9.4.9 Gel Permeation Chromatography

Gel permeation chromatography (GPC) was carried out at ICI Wilton on 6 key samples using polystyrene as the internal standard. The chromatograms are shown in Graph 24 and calculated molecular weight data in Table 66.

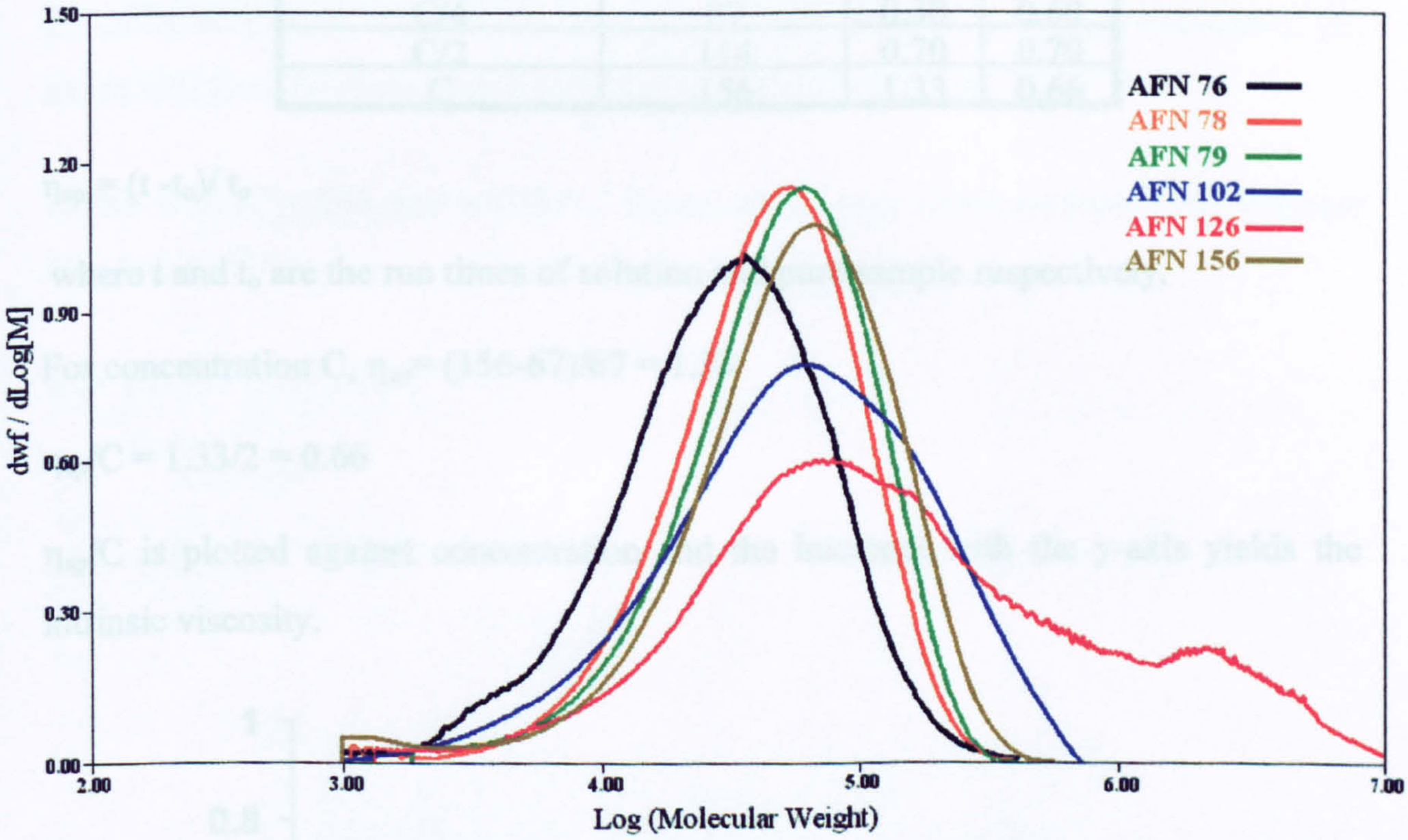

Graph 24: GPC $\overline{M}w$ distributions

Code	$\overline{M}w$	$\overline{M}n$
AFN 76	38800	17800
AFN 78	52800	27900
AFN 79	59000	31400
AFN 102	89700	28100
AFN 126	568800	42200
AFN 156	69100	26400

Table 66: GPC $\overline{M}w$ Data

10 Appendix 1

10.1 Sample calculation of intrinsic viscosity

This calculation is based on data from Polymer PET 27

Concentration	Run time (s)	η_{sp}	η_{sp}/C
TFA	67	-	-
C/8	77	0.15	0.60
C/4	87	0.30	0.60
C/2	114	0.70	0.70
C	156	1.33	0.66

$\eta_{sp} = (t - t_o)/ t_o$

where t and t_o are the run times of solution and pure sample respectively.

For concentration C, $\eta_{sp}= (156-67)/67 = 1.33$

$\eta_{sp}/C = 1.33/2 = 0.66$

η_{sp}/C is plotted against concentration and the intercept with the y-axis yields the intrinsic viscosity.

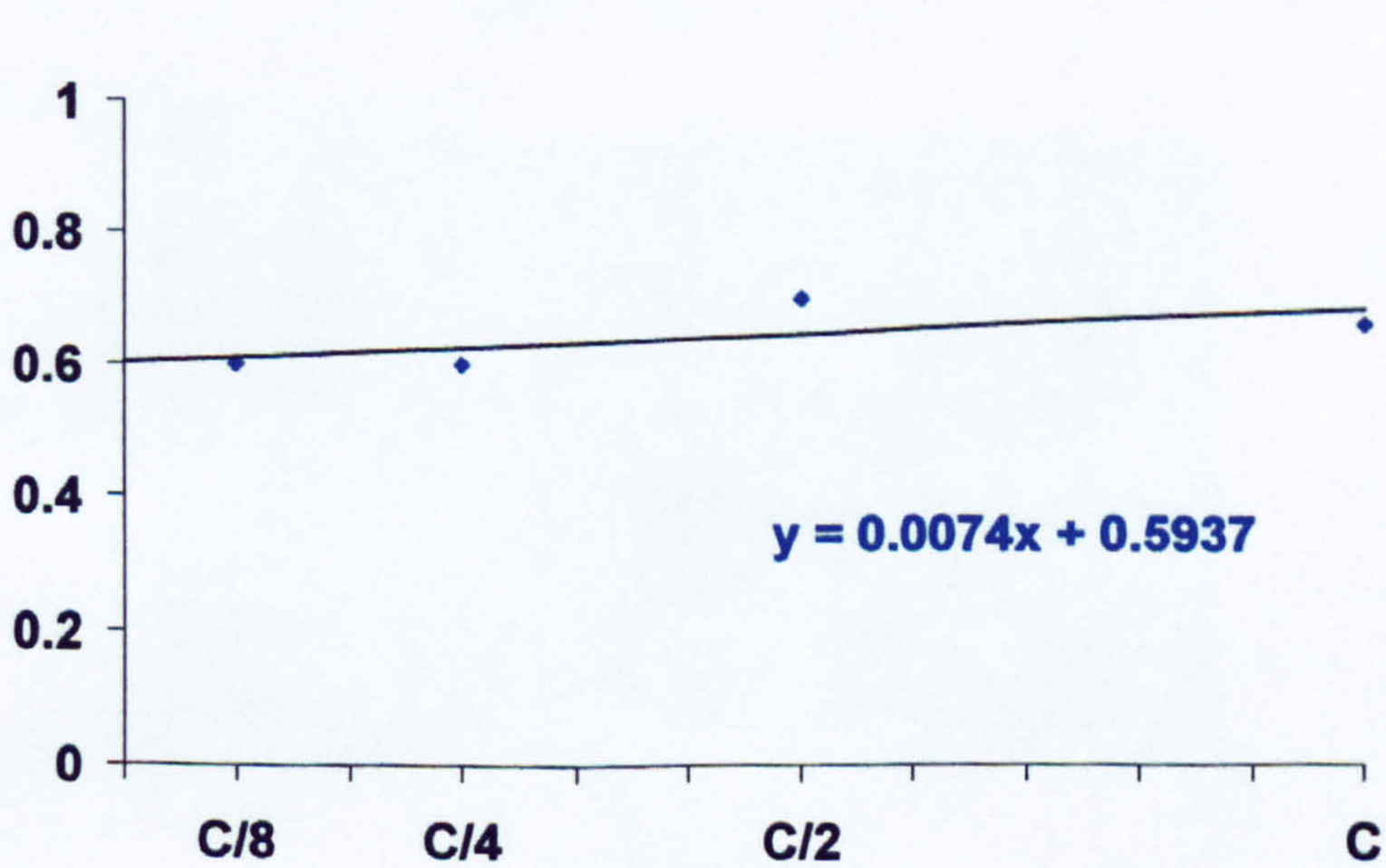

Graph 25: Intrinsic Viscosity, PET 27 (linear 'monomer')

The intrinsic viscosity can then be used in the Mark-Houwink equation, to calculate the molecular weight (viscosity average) of the polymer. This relationship applies only to linear polymers and so this method cannot be used to establish the molecular weights of the branched polymers.

$$[\eta] = K'M_v^{a}$$

K' and a are constants for a particular polymer/solvent system, and can be established by calibrating with fractions of known molecular weight, and once calculated, [η] alone will give the molecular weight for an unknown fraction.

In this case K' = 140, and a = 0.64. These values were obtained from 'The Polymer Handbook'.[89]

$M_v = [(0.5937 \times 10^5)/140]^{1/0.64}$

$= 12750$

$M_v \sim 13000$ D

11 Appendix 2

11.1 Calculation of Number of End-Groups (E) of PET 31 from End-Group Analysis Data

The end-groups of PET 31 were converted to carboxylic acid groups *via* the method outlined in section 9.4.2 (page 120). The polymer was then dissolved in *o*-cresol, and the solution made alkaline with ethanolic sodium hydroxide. The solution was back-titrated potentiometrically with ethanolic HCl. The resultant pH curve was used to calculate the number of end-groups on the polymer by means of the formula:-

$$E_t = (1000 \times V \times M)/m$$

Equation 52: Total Number of Polymer End-groups

Where V is the volume of HCl (ml) required to react with all the end-groups of the polymer.

M is the Molarity of HCl used

and m is the mass of polymer (grams)

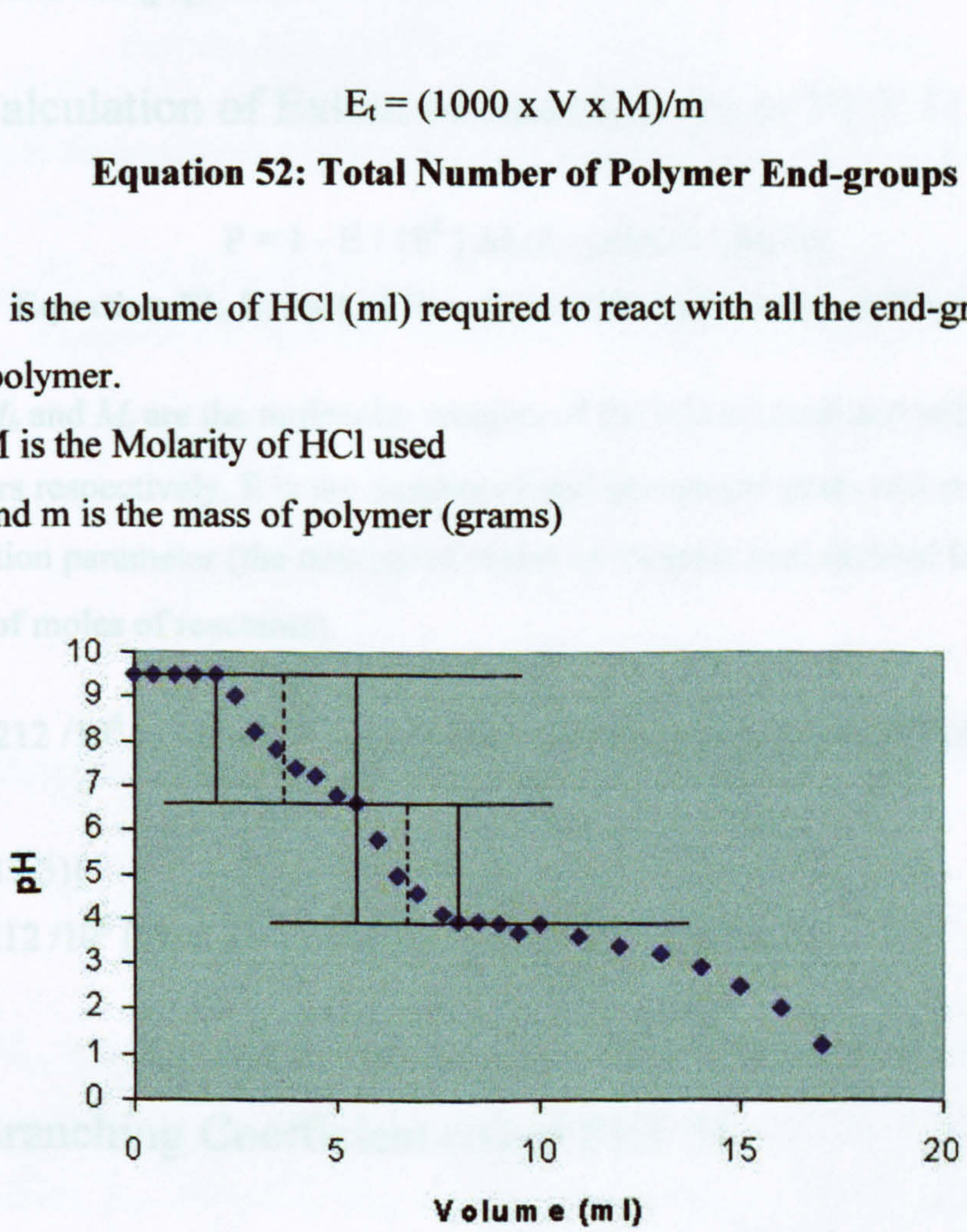

Graph 26: Graph of pH vs volume of HCl added for polymer PET 31

The graph contains two points of inflection; these correspond to the neutralisation of all the excess base and the neutralisation of the end-groups respectively. The difference in these two values gives the volume required to react with the end-groups alone. The total number of end-groups is calculated from Equation 52.

$$E_t = (1000 \times 4 \times 0.0513)/0.97$$
$$= 212 /10^6 \text{ g}$$

From this value other calculations can be made in accordance with the methods laid out in section 4.6 (page 35).

11.2 Calculation of Extent of Reaction (P) of PET 31

$$P = 1 - E / 10^6 [M_b/2 - \rho(M_b/2 - M_t/3)]$$

Equation 53: Extent of Reaction, with Trifunctional Brancher

Where M_b and M_t are the molecular weights of the bifunctional and trifunctional monomers respectively, E is the number of end-groups per gram and ρ is the composition parameter (the number of moles of trimesic acid divided by the total number of moles of reactants).

$P = 1 - 212 /10^6 [1358.43/2 - \{(3x0.004713)/(3x0.004713+2x0.087351)\}(1358.43/2 - 159.12/3)]$

$= 1 - 212 /10^6 [1358.43/2 - 0.0749 (1358.43/2 - 159.12/3)]$

$= 0.87$

11.3 Branching Coefficient (α) of PET 31

$$\alpha = P\rho / 1 - P(1-\rho)$$

Equation 54: Branching Coefficient

$\alpha = 0.87(0.0749) / 1 - 0.87(1-0.0749)$

$= 0.33$

11.4 Number Average Degree of Polymerisation ($\bar{X}_n$) of PET 31

$$\bar{X}_n = (3 - \rho) / (3 - \rho - 3p)$$

Equation 55: Number-average Degree of Polymerisation

$$\bar{X}_n = (3 - 0.0749) / (3 - 0.0749 - 3[0.87])$$
$$= 8.96$$

11.5 Number Average Molecular Weight ($\bar{M}_n$) of PET 31

$$\bar{M}_n = \bar{X}_n M_o = (3M_b + \rho(2M_t - 3M_b)) / (3 - \rho - 3p)$$

Equation 56: Number-average Molecular Weight

where M_o is the molecular weight of the average monomeric unit, as defined below.

$$M_o = (M_b N_b + M_t N_t) / (N_b + N_t) = (3M_b + \rho(2M_t - 3M_b)) / (3 - \rho)$$

Equation 57: Average Molecular weight of Monomeric Unit

$$M_o = (3x1358.43 + \rho(2x159.12 - 3x1358.43)) / (3 - 0.0749)$$
$$= 1297.029$$
$$\bar{M}_n = 8.96x1297.029$$
$$= 11600$$

11.6 Weight Average Molecular Weight of PET 31

$$\bar{M}_w = \bar{M}_{w,o} + [p f_{n,o} \bar{M}_o^2] / (\bar{M}_{n,o}[1 - p(\bar{f}_{w,o} - 1)])$$

Equation 58: Weight-average Molecular Weight

Where $\bar{M}_{w,o} = M_b W_b + M_t W_t + M_m W_m$, is the weight-average molecular mass of the initial monomers and $f_{w,o} = 2\rho_b + 3\rho_t + \rho_m$, is the weight-average functionality of the same mixture, $f_{n,o} = 2(N_b/(N_t+N_b)) + 3(N_t/(N_t+N_b))$ and W_b, W_t, and W_m are the initial weight fractions of mono-, bi- and trifunctional monomers respectively. $\bar{M}_{n,o}$ is the number average molecular mass of the initial monomeric mixture.

$$\bar{M}_w = 1350.897 + [0.87x2.051 (1297.029)^2] / (1268.627[1 - 0.87 (2.07 - 1)])$$
$$= 35500$$

11.7 Number Average Branching Density ($\overline{B}_n$) of PET 31

$$\overline{B}_n = 2\rho / (3 - \rho - 3p)$$

Equation 59: Number-average Branching Density

$$\overline{B}_n = 0.0047/((0.0047+0.087)-(3*0.0047/2 + 0.087)* 0.87)$$

$$= 0.46$$

11.8 Weight Average Branching Density ($\overline{B}_w$) of PET 31

$$\overline{B}_w = 3\overline{B}_n\overline{M}_w / 2\overline{M}_n$$

Equation 60: Weight-average Branching Density

$$\overline{B}_w = 3(0.46x35500) / (2x11600)$$

$$= 0.022$$

11.9 Intrinsic (Inherent) Viscosity of PET 31

$$\log\eta_o = -12.96 + 3.54\log\overline{M}_w + 0.25\log\overline{B}_w$$

Equation 61: Intrinsic Viscosity Expressions

$$\log\eta_o = -12.96 + 3.54\log(35500) + 0.25(0.022)$$

$$= -12.96 + 16.11 + 0.0055$$

$$= 3.16$$

$$\eta_o = 1440 \text{ poise}$$

11.10 Viscosity Average Molecular Weight of PET 31

$$[\eta] = K' \overline{M}_v^{a}$$

Equation 62: Mark-Houwink Equation

Where K' and *a* are constants for a particular polymer/solvent system (in this case K'= 140 and a = 0.64)

$$[0.56x10^5] = 140\ \overline{M}_v^{0.64}$$

$$\overline{M}_v^{0.64} = [0.56]/140$$

$$\overline{M}_v = (400)^{1/0.64}$$

$$\overline{M}_v = 11600$$

12 Appendix 3

12.1 Synthesis of Bis(2- hydroxy ethyl)terephthalate (BHET)

Due to diminished stocks of BHET, originally supplied by ICI, a method of synthesising sufficient quantities of this feedstock had to be established to finish this programme of work.

Thus dimethyl terephthalate, DMT, (600 g), was crushed and placed in a 5 litre open necked flask with ground glass joint along with ethylene glycol, EG, (1918 g) and manganese acetate (200 ppm, 0.24 g). A metal stirrer was inserted and a reactor lid clamped on. The flask was then heated to 140 °C. Once the contents were molten the flask was stirred by means of the overhead stirrer. The temperature was slowly increased to 220 °C over 2 hours, whilst monitoring the volume of methanol evolved. After all the methanol was distilled off (198 ml) the molten product was allowed to cool and water (3 litres) was added and the mixture stirred for 10 minutes (to break-up the product). Half of the mixture was removed and a further two litres of water added to each portion. Each section of product was stirred at 2000 rpm for 1 hour. The mixtures were then filtered and washed with water (6 x500ml). It was then dried on a freeze drier.

Once dry ^{1}H and ^{13}C NMR spectra were obtained using TFA/$CDCl_3$ 1:10 mixture.

^{1}H NMR ($CDCl_3$/270 MHz): δ8.2 (4H, s, aryl), δ4.9 (2H, s, (CO)$OCH_2C\underline{H}_2O$ $C\underline{H}_2CH_2O(CO)$), δ4.8 (4H, s, (CO)$OC\underline{H}_2CH_2OH$), δ4.7 (4H, s, (CO)$OCH_2C\underline{H}_2OH$), δ4.1 (<1H, s, $C\underline{H}_3O(CO)Ph$)

^{13}C NMR ($CDCl_3$/270 MHz): δ170 ($\underline{C}O$), δ134.1 (*p*-aryl), δ133.9 ($CH_3O(CO)\underline{Ar}$), δ130.8 (*m*-aryl), δ66 ((CO)$O\underline{C}H_2CH_2OH$), δ65.2 ((CO)$OCH_2\underline{C}H_2OH$), δ64.8 ((CO)$O\underline{C}H_2CH_2O(CO)$ from dimer), δ64.1 ($\underline{C}H_3O(CO)Ar$)

References

1 Treloar, R.G., *Introduction to Polymer Science*, Wykeham Publications, Chichester, UK, (1970)

2 Flory, P.J., *Principles of Polymer Chemistry*, Cornell University Press, Ithaca, USA (1953)

3 Tomalia, D.A., Baker, J., Dewald, R., Hall, M., Kallos, G., Martin, S., Roeck, J., Ryder,J., Smith, P., *Polym. J.*, **17**, 117, (1985)

4 Cowie, J.M.G., *Polymers: Chemistry & Physics of Modern Materials*, 2nd Edition, Blackie Academic & Professional, Glasgow, UK, (1991), Chapter 2, p26 -51

5 Billmeyer, F.W., *Textbook of Polymer Science*, 3rd Edition, Wiley, New York, USA, (1984), Chapter 2, p25 - 48

6 Carothers, W.H., *J.Am. Chem. Soc.*, **51**, 2548, (1929)

7 Flory, P.J., *Chem. Rev.*, **39**, 137, (1946)

8 Flory, P.J., *Principles of Polymer Chemistry*, Cornell University Press, Ithaca, USA, (1953), Chapter 3

9 Flory, P.J., *J. Am. Chem. Soc.*, **61**, 3334, (1939)

10 Amass, A.J., *Polymer*, **20**, 515, (1979)

11 Flory, P.J., *High Molecular Weight Organic Compounds*, Vol. 6, interscience, New York, USA, p211-283, (1949)

12 Flory, P.J., *J. Am. Chem. Soc.*, **63**, 3083, (1941)

13 Flory, P.J., *J. Am. Chem. Soc.*, **63**, 3091, (1941)

14 Flory, P.J., *J. Am. Chem. Soc.*, **63**, 3096, (1941)

15 ICI, *How Much do You Know About the Films Industry?*, Product Information Leaflet, Wilton, UK

16 ICI, *The Chemistry and Technology of Polyester Polymer*, Information Booklet, Wilton, UK

17 Carothers, W.H., Arvin, J.A., *J.Am. Chem. Soc.*, **51**, 2560 (1929)

18 Carothers, W.H., *Chem. Revs*, **8**, 353 (1931)

19 Carothers, W.H., van Natta, F.J., *J.Am. Chem. Soc.*, **55**, 2560 (1933)

20 Whinfield, J.R., Dickson, J.T., *British Pat. 578,079*, (1941)

21 Moncrieff, R.W., Man-made Fibres, 6th Edition, Newnes-Butterworth, London, UK, (1975), Chapter 24, p434 - 481

22 Stevenson, R.W., Nettleton, H. R.,*J. Polym. Sci. (A-1)*, **6**, 889, (1968)

23 Challa, G., *Makromol Chem.*, **38**, 105, 123, 138, (1960)

24 Campanelli, J.R., Kamal, M.R., Cooper, D.G., *J. Appl. Polym. Sci.*, **54**, 1731, (1994)

25 Campanelli, J.R., Kamal, M.R., Cooper, D.G., *J. Appl. Polym. Sci.*, **53**, 985, (1994)

26 Tomita, K., *Polymer*, **14**, 50, (1973)

27 Yoshioka, T., Sato, T., Okuwaki, A., *J. Appl. Polym. Sci*, **52**, 1353, (1994)

28 Kao, C., Cheng, W., Wan, B., *J. Appl. Polym. Sci*, **70**, 1939, (1998)

29 Shah, T.H., Bhatty, J.I., Gamlen, G.A., *Polymer*, **25**, 1333, (1984)

30 Tomita, K., *Polymer*, **17**, 221, (1976)

31 Apicella, B., Di Serio, M., Fiocca, L., Po, R., Santacesaria, E., *J. Appl. Polym. Sci.*, **69**, 2423, (1998)

32 Tomita, K., Ida, H, *Polymer*, **14**, 55, (1973)

33 Tomita, K., Ida, H, *Polymer*, **16**, 185, (1975)

34 Gamlen, G.A., Shah, T.H., Bhatty, J.I., *Thermochimica Acta*, **106**, 105, (1986)

35 Stevenson, R.W., Nettleton, H.R., *J. Polym Sci. A-1*, **6**, 889, (1968)

36 Newkome, G.R., *J. Org. Chem.*, **50**, 2003, (1985)

37 Tomalia, D.A., Naylar, A.M., Goddard III, W.A., *Angew. Chem. Int. Ed. Engl.*, **29**, 138, (1990)

38 Haddleton, D.M., Hardeep, S., Taylor, P.C., Yeates, S.G., *J. C. S., Perkin 1*, **7**, 649, (1996)

39 Wooley, K.L., Hawker, C.J., Pochan, J.M., Fréchet, M.J.M, *Macromolecules*, **26**, 1514, (1993)

40 Mourney, T.H., Turner, S.R., Rubinstein, M., Fréchet , J.M.J, Hawker, C.J.,

Wooley, K.L., *Macromolecules*, **25**, 2401, (1992)

41 Hawker, C.J., Wooley, K.L., Fréchet , J.M.J , *J. Am. Chem. Soc.*, **115**, 4375, (1993)

42 Newkome, G.R., Young, J.K., Baker, G.R., Potter, R.L., Audoly, L., Cooper, D., Weis, C.D., Morris K, Johnson, C.S., *Macromolecules*, **26**, 2394, (1993)

43 Kim, Y.H., Webster, O.W., *J. Am. Chem. Soc.*, **112**, 4592, (1990)

44 Tomalia, D.A., Hall, V.B.M, Hedstrand, D.M., *Macromolecules*, **20**, 1164, (1987)

45 Hawker, C.J., Fréchet, J.M.J., *J. Am. Chem. Soc.*, **112**, 7638, (1990)

46 Hunt B.J., Holding S.R., *Size Exclusion Chromatography*, Black & Son Ltd, London, UK, (1989), Chapter 1, p 3 – 12

47 Cowie, J.M.G., *Polymers: Chemistry & Physics of Modern Materials*, 2nd Edition, Blackie Academic & Professional, London, UK, (1991), Chapter 9, p195

48 Billmeyer, F.W., *Textbook of Polymer Science*, 3rd Edition, Wiley, New York, USA, (1984), Chapter 8, p191

49 Billmeyer, F.W., *Textbook of Polymer Science*, 3rd Edition, Wiley, New York, USA, (1984), Chapter 11 - 12, p301 -307, 340

50 Zimm, B.H., Stockmayer, W.H., *J. Chem. Phys.*, **17**, 1301, (1949)

51 Zimm, B.H., Kilb, R.W., *J. Polym. Sci.*, 37, 19, (1959)

52 Bohdanecký, M., Kovár, J., *Viscosity of Polymer Solutions*, Elsevier Scientific, Amsterdam, The Netherlands, (1982), Chap 1 - 3, p1 - 23, 87 - 94, 133 - 154, 166 - 210

53 Tompa, H., *Polymer Solutions*, London Butterworths Scientific, London, UK, (1956), Chapter 4 & 9, p 75 - 121, & 263 - 290

54 Cowie, J.M.G., *Polymers: Chemistry & Physics of Modern Materials*, 2nd Edition, Blackie Academic & Professional, Glasgow, UK, (1991), Chapter 9, p207 - 210

55 Staudinger, H., Heuer, W., *Ber. Dtsch. Chem. Ges.* B, **63**, 222-234 (1930)

56 Billmeyer, F.W., *Textbook of Polymer Science*, 3rd Edition, Wiley, New York,

USA, (1984), Chapter 9, p242 - 243

57 Billmeyer, F.W., *Textbook of Polymer Science*, 3rd Edition, Wiley, New York, USA, (1984), Chapter 8, p198 - 202

58 Cowie, J.M.G., *Polymers: Chemistry & Physics of Modern Materials*, 2nd Edition, Blackie Academic & Professional, Glasgow, UK, (1991), Chapter 9, p196-202

59 Kratochvil, P., *Classical Light Scattering from Polymer Solutions*, Polymer Science Library 3, Elsevier Scientific , Amsterdam, The Netherlands, (1987), Chapter 1, p7-58, Chapter 3, p113-115, Chapter 4, p145-182

60 Buchard, W., *Applied Fibre Science, Vol 1*, Academic Press, New York, USA, (1978), Chapter 10, p382-420

61 Tyndall, J., *Phil. Mag.*, **37**, 384, (1809)

62 Rayleigh, J.W., *Phil. Mag.*, **41**, 107, 274, 447, (1871)

63 Debye, P., *J. Appl. Phys.*, **15**, 338, (1944)

64 Debye, P., *J. Phys. Colloid. Chem.*, **51**, 18, (1947)

65 Zimm, B.H., *J. Chem. Phys.*, **16**, 1093, (1948)

66 Zimm, B.H., *J. Chem. Phys.*, **16**, 1099, (1948)

67 Conix, A., *Makromol. Chem.*, **26**, 226, (1958)

68 Zimmerman, H., Kulbig, C., *Faserforsch. Textiltech.*, **18**, 586, (1966).

69 Stockmayer, W.A., *J. Polym. Sci.*, **9**, 69, (1952)

70 Stockmayer, W.A., J. *Polym. Sci.*, **11**, 424, (1953)

71 Polymer Laboratories Thermal Sciences Division, *DMTA MKII Operators Manual* (Jan 1986), P6 -9

72 Feast, W.J., Stainton, N.M., *J. Mater. Chem.*, **5**(3), 405, (1995).

73 Manaresi , P., Parrini, P., Semeghini, G.L., de Fonasari, E., *Polymer*, **17**, 595, (1976).

74 Busse, W.F. and Langworth, R.J., *J. Polym. Sci.*, **58**, 48, (1962)

75 Fujimoto, T., Narukawa, H., Nagasawa, M., *Macromolecules*, **3**, 57, (1970)

76 Pannell, J., *Polymer*, **12**, 558, (1971)

77 Peticolas, W.L., *J. Polym. Sci.*, 58, 1405, (1962)

78 Schreiber, M.P., Bagley, E.B., *J. Polym. Sci.*, 58, 29, (1962)

79 Ram, A., Miltz, J., J. *Polm. Sci.: Polymer Symposia, 23rd International Symposium on Macromolecules, Madrid*, **2**, 748, (1974)

80 Manaresi, P., Munari, A., Pilati, F., *Polymer*, **27**, 955, (1986).

81 Stockmayer, W.A.J., *Chem. Phys.*, **11**, 45, (1943).

82 Stockmayer, W.A.J., *Chem. Phys.*, **12**, 125, (1944).

83 Stockmayer, W.A.J., *Polym. Sci.*, **11**, 424, (1953).

84 Munari, A., Pezzin, G., Pilati, F., Manaresi , P., *Rheol. Acta*, **28**, 29, (1989).

85 Rosu, R.F., Shanks, R.A., Bhattacharya S.N., *Polym. Internat.*, **42**, 267, (1997).

86 Jaykannan, M., Ramakrishnan, S., *J. Polym. Sci. A: Polym. Chem.*, **36**, 309, (1998)

87 Thompson, C.B., *Polycondensation Rig Standard Operating Procedure*, (1995)

88 Payne, K., Eves, M.E., ICI Polycondensation Rig Standard operating Procedure, RTM102, (1996)

89 Brandrup, J., Immergut, E.H., *The Polymer Handbook 2nd Edition*, Wiley Interscience, New York, USA (1975), IV- 25